Modelling the northern hemisphere and Antarctic ice sheet changes through the last glacial cycle

by

Brendan Coutts (Brendan Campion)
B.Sc (Hons)

Submitted in fulfilment of the requirements
for the degree of
Doctor of Philosophy

University of Tasmania
May 1999

For Mateus

"Ice is nice."

M.P.French

Declaration

This thesis contains no material which has been accepted for a degree or diploma by the University or any other institution, except by way of background information and duly acknowledged in the thesis, and to the best of my knowledge and belief no material previously published or written by another person except where due acknowledgement is made in the text of the thesis.

Brendan Coutts

Authority of Access

This thesis may be made available for loan and limited copying in accordance with the Copyright act 1968.

Brendan Coutts

Abstract

In order to gain a proper understanding of the present state of the Earth's cryosphere in relation to its environment, it is desirable to have a sound knowledge of the glacial history which led to the present conditions. In this study, the ice sheets of the northern hemisphere and the Antarctic are modelled through the last glacial cycle in order to gain some understanding of both present and palaeo environments. The results of the energy balance model of Budd and Rayner (1993), which was driven by orbital variations in radiation as well as internal climate and ice sheet feedbacks, provides the shape of the time series of primary climate forcing for global ice sheet modelling. The amplitude of the climate forcing comes from matching palaeo-reconstructions of ice margins, sea level, temperature and accumulation rate. The ice sheet model is coupled to an ice shelf model and includes isostatic adjustment of the bedrock as well as simple thermodynamics.

Results for the northern hemisphere modelling indicated that forcing with a maximum temperature change of about -13°C at the southern margin of the ice sheets leads to ice sheet extents in general agreement with palaeo-observations. This temperature change is representative of the ablation region over the ice margin where there is a sharp contrast between temperature changes over land and the much larger changes over the interior of the ice sheet. Ice sheet extent is also found to be dependent on the initial bed topography, but is found to be weakly dependent on changes to the sea level and the base accumulation distribution outside the ice sheet 'elevation-desert' effect. The existence and extent of a large ice shelf in the Arctic Ocean however, is found to be strongly dependent on the net accumulation rate. An estimate of eustatic sea level change through the last glacial cycle based on the modelling of the northern hemisphere ice sheets also agrees reasonably well with other sea level change reconstructions. The timing and extent of the 'fresh water pulse' from the maximum rate of deglaciation

exhibits some correspondence with the initiation of the Younger Dryas cooling episode.

The Antarctic is shown to be sensitive to changes in sea level and accumulation rate, and it is found that these influences have largely opposing effects. While the sea level change strongly influences ice thickness in regions of significant basal sliding, variation in the accumulation rate offsets this effect and there is little modelled grounding line movement during the glacial cycle. This leads to only a small net contribution to post glacial maximum sea level change from the Antarctic, in the order of 1m. The West Antarctic region is very sensitive to the sliding parameterisation and grounding line dynamics and consequently the results are not as robust as those for East Antarctica. The derived present state of the ice sheet shows that in central East Antarctica, there is $\sim$20% positive mass balance still remaining, whereas nearer the coast the ice sheet is closer to balance. It is concluded that prior to the onset of recent anthropogenic influences, the net Antarctic mass balance was near to zero with only a very small positive net balance contributing slightly towards sea level lowering.

Acknowledgements

Firstly, I gratefully acknowledge the Antarctic CRC for providing the scholarship without which, this study could never have been undertaken. Even with this assistance however, there were many times when I seriously doubted that this thesis would be completed, but this was apparently not the case for my supervisor, Professor Bill Budd. While I am constantly amazed at the volume of his knowledge and am immensely grateful for that fraction which he was able to pass on to me, I am equally thankful for his enormous patience and encouragement. In the face of what so often seemed to me to be cause for despair, Bill was always calm, non-judgemental and positive and somehow I always left his office feeling more confident than I had been when I entered. I will also never understand how he managed to be so constantly busy and yet always available.

My thanks also go to my other supervisor, Dr. Roland Warner. Without his advice and assistance with all my modelling problems, my task would have been much more difficult. Although my time under her supervision was short, I am extremely grateful to Dr. Catherine Ritz, who allowed me to study with her in Grenoble. My time there was pivotal to the completion of this thesis.

To many of the staff and students, past and present, at IASOS I am also grateful. Particularly I would like to thank Dr.'s Rob Massom and Brendan Buckley for gracing me with their own brands of genius, and to Rob for proof reading this thesis. Thanks also to Annie Wong and her ability to understand and share my sometimes cynical view of things. The companionship of my fellow residents of room 310 has made my work environment an enjoyable place and so I am also grateful to Louise, Bernadette, Richard, Irina and Katrina.

Whatever the value of this thesis, I will be able to look back on the time spent on it satisfied that if no profound results lie herein, at least there were some great truths unearthed in my discussions with Justin and Chris O'Connor in various establishments around Hobart. Although the ideas may have been

quickly forgotten, some part of my memory of those times will long resist decay. While no such times were had with my e-friends, the regular communication I enjoyed with M.P. French brightened many a day. For my friendship with Ana, which has been through so much and which I hope will always survive, I am deeply grateful. Thankyou also to Veronica, for so many things, but particularly for tenderly restoring some balance to my life.

It is difficult to describe the debt of gratitude I owe my parents. All I can say is that it is vast and filled with love. My sincerest gratitude also to my beautiful sister Marg for her love and for the happy café hours we spent together. Thanks also to Maryanne, John and Damian, whose support I have always felt, despite the physical distance between us.

Finally, and most importantly, thankyou to Mateus - my greatest teacher.

Supporting publications

Some of the work presented in this thesis appears in a published paper. Where substantial parts of this paper are reproduced in this thesis, it is in all cases my own original contribution to that paper that is transposed.

The paper directly related to this thesis is:

Budd, W.F., **B. Coutts,** and R.C. Warner, Modelling the Antarctic and Northern Hemisphere ice-sheet changes with global climate through the glacial cycle, *Annals of Glaciology*, 27, 153-160, 1998

Contents

List of Figures

List of Tables

Chapter 1

Introduction

Large ice sheets, such as those which presently exist in Greenland and Antarctica, are in many ways removed from our everyday experience. The extreme conditions which prevail there, and their consequent remoteness from more populated areas, limit our direct exposure to these regions and consequently our ability to understand them also suffers due to the scarcity of observations yet available. As well as being spatially removed from these ice sheets, we are also temporally separated from them. Large ice masses react to external influences over periods of the order of many thousands of years, far beyond the experience of our historical records. The slow response times of ice sheets make it difficult to interpret their interaction with the environment. Nevertheless, the influence of the ice sheets on the environment is very significant and for the large changes which occurred over the last glacial cycle, the role of the ice sheets is dominant.

The aim of this thesis is to use ice sheet modelling to simulate the changes of the large ice sheets through the last glacial cycle in a way which matches those observations which are available, and thereby to provide further information on the accompanying climate changes.

1.1 Northern hemisphere

For much of the last 130,000 years, large areas of the high-mid latitudes in the northern hemisphere were covered by massive ice sheets. Although they largely disappeared thousands of years ago, their effects are still being felt in the continued response of the Earth's surface and ocean bed to the now removed

burden of the ice and the corresponding change in water load over the ocean. The contribution of these melted ice sheets to sea level change may be also still being expressed in the Antarctic Ice Sheet's reaction to that change.

The cumulative volume of these now decayed northern hemisphere ice sheets was probably more than that of the present Antarctic and Greenland Ice Sheets combined, and the ice sheets occupied an extensive area of the northern land surface. Most of this region is now ice-free and covered in plant and animal life, and includes densely populated regions of northern North America, Europe and Eurasia. Even in places where there was no ice, conditions were considerably different during the ice age.

Understanding the dramatic environmental changes which occur between ice age conditions and the interglacial conditions which presently exist, is interesting and important for a variety of reasons. Given the prospect of future climate change, particularly the possibility of anthropogenic change due to an enhanced greenhouse effect (Houghton et al. 1996), improving our knowledge of the Earth's climate system and its processes takes on enormous significance. By investigating previous states of the climate system, of which the northern hemisphere ice sheets were a dominant part, we should enhance our understanding of the nature of the climate and of climate change.

Reconstructing past conditions also allows the testing of our ability to model climatic conditions that are significantly different to those of the present (Manabe 1989). If our knowledge of the workings of the climate system is sound enough to allow accurate modelling of the palaeo-environment, we may be more justified in placing some faith in predictions of future conditions based on that knowledge. This is not only the case for the study of the ice sheets themselves, but also for the study of the climate. If reliable reconstructions of palaeo-ice sheet conditions can be obtained, the possibility then exists to use these ice sheet reconstructions as boundary conditions for palaeo-climate modelling with general circulation models.

Despite the magnitude of the difference between glacial and interglacial conditions, it is difficult to establish a single dominant process which caused this change. It appears likely, from the evidence of both the palaeo-record and modelling, that the cycling between ice age and warmer conditions which has

prevailed over the last one and a half million years or so, is primarily driven by radiation changes associated with variations in the Earth's orbit. The response of the climate system to these changes however, is probably the most critical aspect of the extent and nature of the climatic changes. By focussing on the changes which occurred over the last glacial cycle to the cryosphere, particularly the highly variably northern hemisphere ice sheets, it is hoped that some light may also be shed on the nature of the climate changes in general. The nature of glacial cycles may be determined by anything from the composition of the solar system (Muller and MacDonald 1997) to internal climate feedbacks (Budd and Rayner 1990; Budd and Rayner 1993). Such is the holism of the glacial cycle system that investigation of a single component should allow inferences to be made about other aspects of the environment.

The influence of the northern hemisphere ice sheets is still being felt today. Reconstruction of the northern hemisphere glacial ice sheets allows interpretation of the present distribution and makeup of soils in previously iced areas as well as helping to explain and predict the motion of the Earth's surface and ocean bed in response to the past burden of the ice sheets (Fulton and Prest 1987). The present pattern of plant and animal distribution and probably the evolution of some species would have been directed by the change in distribution of ice and associated effects over the last 130,000 years. It is likely that the opening of land bridges due to low sea levels caused by the existence of the large northern hemisphere ice sheets enabled the migration of people into North America across the Bering Strait, into Tasmania from mainland Australia, and elsewhere. The subsequent sea level rise, as particularly the northern hemisphere ice sheets retreated, was a global phenomenon and may still be influencing the state of the Antarctic Ice Sheet, thousands of years after the transient northern ice sheets disappeared.

1.2 Antarctica

The Antarctic continent covers about 10% of the Earth's land surface. More than 70% of the world's freshwater is currently held in the ice sheet there and if it were all to melt, sea level would rise by about 70 metres (Coutts 1992). It is

an intrinsic part of our climate system, closely linked with atmospheric and ocean circulation, sea level, sea ice distribution, the global carbon cycle and the biosphere. Changes to the Antarctic Ice Sheet may cause or result from climate change.

As it is such an important part of the climate system, understanding the state of the Antarctic Ice Sheet is a crucial aspect of the understanding of our environment. With the prospect of future climate warming, there is increasing interest into the potential response of the Antarctic Ice Sheet to climate change (e.g. Coutts (1992), Huybrechts (1992), Budd et al. (1994), Warner and Budd (1998)). However, the future of the ice sheet is constrained by its current state. Before determining the changes which may occur to the ice sheet, ideally that present state should be known. Knowledge of the present state of the ice sheet is also valuable in itself, not just as a point from which to look into the future. Information on the distribution of ice aids our understanding of the current climate, and information on the present rates of change of the ice distribution and bed topography contributes to knowledge of present day sea level change. But just as the present state of the ice sheet must be known to be able to predict its future, that present state itself has been determined by the past evolution of the ice sheet.

While some ablation does occur around the coastal margins of the Antarctic Ice Sheet, net surface ablation may be considered negligible compared to the loss of ice through calving. This is particularly the case when considering glacial conditions when temperatures, and so ablation rates, were generally lower. As the changes in ice mass due to accretion and melt beneath the floating ice shelves are poorly known, mass changes in the ice sheet are considered to have occurred as changes in the rate of ice accumulation due to snowfall and changes in the rate that ice leaves the continent through iceberg calving. The configuration of the ice sheet and its underlying bedrock would have been further affected by variation in ice flow as the ice dynamics responded to changing accumulation rate and sea level. Sea level could have been affected by changes in the Antarctic Ice Sheet itself, and one of the aims of this thesis is to investigate the possible contribution of that ice sheet to sea level change during the last glacial cycle. However, it is thought that the dominant influence

on sea level variation throughout the cycle would have come from cryospheric changes in the northern hemisphere. The relatively global nature of the sea level change caused by the growth and retreat of the northern ice sheets means that the sea level change influencing the northern ice sheets would have been similar to that affecting the Antarctic.

1.3 The modelling approach

Their remoteness in space and time and the slow rate of response of the large ice sheets of the last glacial cycle, including the Antarctic and Greenland Ice Sheets as well as the now non-existent northern hemisphere ice sheets, make simulation by computer models an extremely useful tool in interpreting their evolution. Geomorphological data have been used to estimate the extents and the behaviour of ice sheets in the past, but this approach is dependent on accurate dating which in the case of ^{14}C techniques is primarily available for events which have occurred in perhaps the last 50,000 years - less than half a complete glacial cycle. Physical evidence such as this also suffers from the cyclical nature of ice ages as evidence of earlier times may be overwritten by later glacial advances. Other palaeo-evidence exists, such as the time series obtained from sea sediment and ice cores. Model output may be evaluated in the light of observational evidence but also may be used to assist the interpretation of the palaeo-data. Information provided by ice sheet models concerning cryospheric changes may be relevant to the analysis of ice cores, and modelled ice volume estimates may be similarly valuable to the evaluation of sea sediment cores. In regions where palaeo-evidence is sparse or non-existent, such as in the Arctic Ocean where it is speculated a large ice shelf may have existed during the last glacial cycle (Denton and Hughes 1981), model output may be used to direct future studies. That ice sheet models deal directly with glacial processes, not only outcomes, and that they provide a virtually continuous record (within the constraints of grid spacing and time-step length) further supports the value of a modelling approach to the reconstruction of the palaeo-ice sheets, particularly if performed in conjunction with comparison of the results to the palaeo-record.

In order to investigate the ice sheets of the last glacial cycle and the assumptions which must be made in an attempt to model them, an understanding of the glacial environment is required. The complex interaction of the ice sheets and climate in response to the solar insolation variations which are considered to drive glacial cycles are explored in chapter 2. A further investigation of glacial conditions, particularly that of the ice sheets is made in chapter 3, where the palaeo-record is investigated to allow for interpretation and assessment of model output. The ice sheet model, and its associated isostatic and ice shelf models are described in chapter 4. The boundary conditions and forcing applied to the model for both the northern hemisphere and the Antarctic are then discussed in chapter 5, where the model input data are presented. Chapters 6 and 7 give the results for the northern hemisphere ice sheets and the Antarctic Ice Sheet respectively. The implications of these results are summarised at the end of each chapter and further in the conclusions (chapter 8) where the overall findings of the thesis are brought together and discussed in relation to possible future work and further developments.

Chapter 2

Causes and nature of glacial cycles

Over the last 60 Ma (million years) or the Cenozoic era, the Quaternary period of about the last 1.7 Ma has been the period of perhaps the greatest climatic change (Bradley 1985). The cycling between times of extensive glaciation and those of relatively warm, ice-free conditions has been prevalent during this period and is intrinsic to the environmental variation which has occurred, particularly over the last million years. The primary causes of glacial cycles appear to lie beyond the atmosphere, ice and ocean system, although the resulting climatic state also depends heavily on the complex interaction between the cryosphere and the internal mechanics of the climate system.

2.1 Proposed explanations

In 1864, Croll proposed the theory that glacial cycles might be triggered by variations in the Earth's orbit (Croll 1864). He suggested that although the net radiation received by the Earth as a whole does not vary greatly over time, seasonally the amount of radiation received could vary enough to trigger glaciation. Milankovitch (1941) placed this theory into a more mathematical framework by combining radiative theory and calculations of the Earth's orbit. He found that at critical latitudes (particularly around 65°N) and seasons (northern hemisphere summer), there has been significant variation in the amount of incident radiation and he theorised that glacial cycles occurred in response to these changes.

Various other possible explanations of glacial cycles have been offered. The variation in solar output associated with either sunspots (see Imbrie and Imbrie (1979)) or the gravitational effect of interstellar dust clouds (McCrea 1975) have been considered as potential catalysts. It has also been suggested that the amount of radiation reaching the Earth's surface may have been affected by variations in the Earth's magnetic field, which shields some solar radiation (Wollin et al. 1977), or by volcanic activity and its effect on the transparency of the atmosphere (Bray 1979; Rampino and Self 1992). Other theories have had the source of glacial cycles lying purely within the climate system and depending only on oscillations between modes of atmospheric (Ewing and Donn 1956; Matteucci 1993), or oceanic circulation (Newell 1973). A range of environmental factors which act in response to radiation changes, amplifying and redistributing Milankovitch's radiation signal, have been posed as potential glacial drivers (see Hays et al. (1976), and Section 2.4), many of which appear certainly to be valid. Their roles however, are more as feedbacks to climatic change being fundamentally driven by something else. The evidence from isotopic studies of sea sediment cores (Emiliani (1955), Hays et al. (1976), Imbrie et al. (1984) - see Figure 2.4), ice cores (Jouzel et al. 1987), sea level records (Mesolella et al. 1969; Bloom et al. 1974; Chappell and Shackleton 1986) and various other sources (see Broecker and Denton (1989)) correspond so well with the glacial cycles suggested by the Milankovitch theory that this theory has now become generally accepted as being central to the driving of ice ages (Gallée et al. 1991).

2.2 Milankovitch cycles and orbital radiation changes

Figure 2.1 illustrates the three components of the Earth's orbit which affect the radiation regime, and Figure 2.2 shows the variation in these orbital parameters with time. The eccentricity describes the shape of the orbit, going from nearly circular to an ellipse where there is 20% more radiation received outside the Earth's atmosphere at the time of closest approach (perihelion) than when the Earth-Sun distance is at its greatest (aphelion). The eccentricity cycles are not

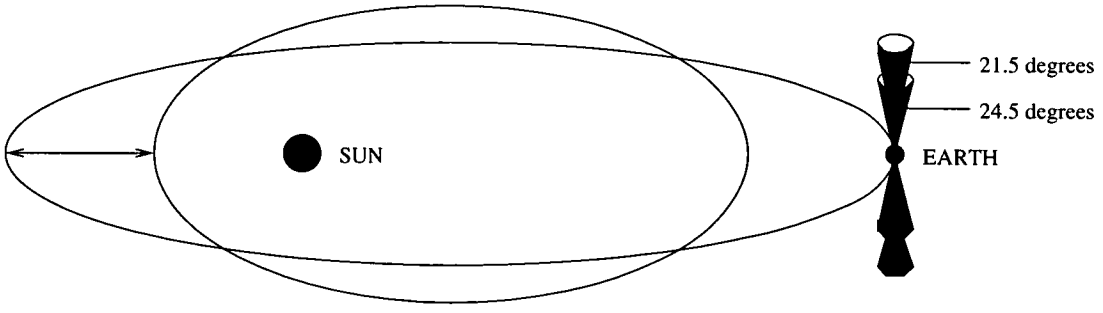

Figure 2.1: Components of the Earth's orbital variation. Eccentricity describes the shape of the Earth's orbit, or how circular it is. The angle of the Earth's spin axis to the Earth's orbital plane gives the obliquity. The orientation of the Earth's spin axis also changes, tracing out a cone in space and giving the precession of the equinoxes. After Broecker and Denton (1990).

perfectly regular but one of these cycles occurs on average about every 95,800 years (Bradley 1985). The obliquity oscillates between about 21.8° and 24.4° as shown, with an average period of 41,000 years. With a period of around 21,700 years, the precession of the equinoxes has the effect of changing the Earth's position on the ecliptic at any one time of year, affecting the distribution of insolation. The result of this perihelion shift is a change in the relative intensity of the seasons as there is variation in the time of year of, for example, maximum and minimum insolation.

Of these three components, it is only the eccentricity which has any effect on the Earth-Sun distance, which helps determine the net annual insolation of the planet. The resultant variation in global annual mean insolation however, is of the order of 0.1% (Berger 1978; Imbrie and Imbrie 1980). This has generally been considered negligible (Schneider and Thompson 1979), but Berger suggests that this small variation could have some climatic effect. However, more extensive variation occurs in the insolation at individual latitudes and at particular times of year. While the net radiation over the whole globe may be considered almost constant throughout the recent era of glacial cycles, the distribution of that radiation over the planet and throughout the year varies substantially with the changes in the Earth's orbit. High radiation in one season is compensated by low radiation in the opposite season from the perihelion effect with the result that the two hemispheres have opposite phases in these

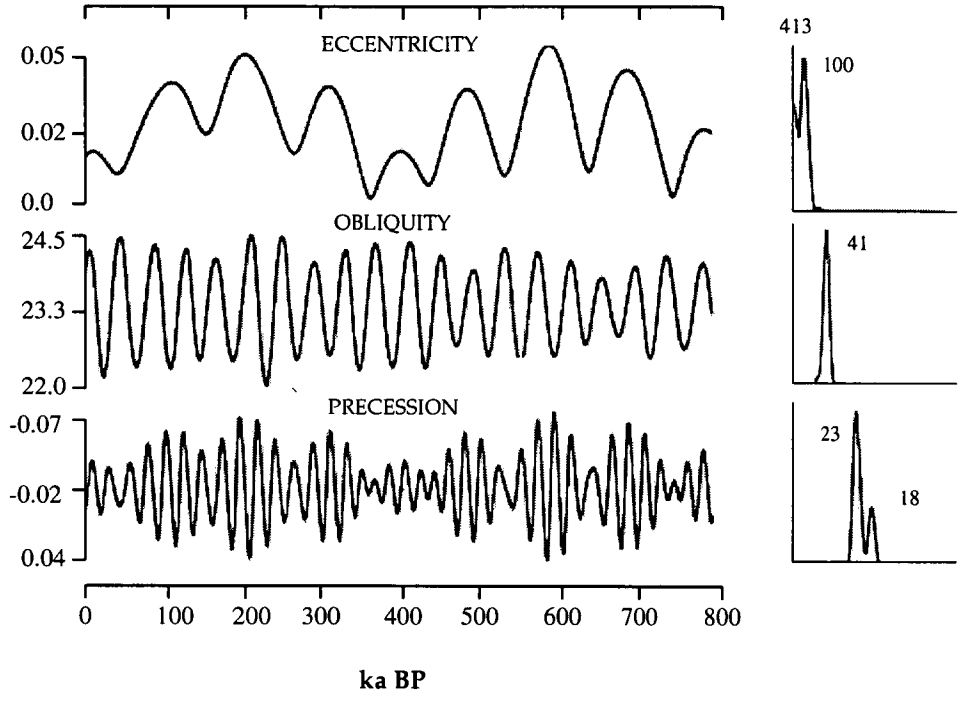

Figure 2.2: Variations in eccentricity, obliquity and precession index over the past 800,000 years according to calculations by Berger (1978). Obliquity is in degrees. The climatic effect of precession is recorded as an index ($\Delta e sin\,\omega$) that is approximately equal to the deviation from its 1950 value of the Earth-Sun distance in June, expressed as a fraction of the semi-major axis of the Earth's orbit. To the right of each time series is shown variance spectra calculated from that time series, indicating the dominant periods (in ka) of significant peaks. Figure taken from Crowley and North (1991).

seasonal anomalies. Changing obliquity has a smaller but out of phase effect at low latitudes compared with its influence towards the poles where increased obliquity leads to a greater difference between summer and winter radiation in both hemispheres. The combined effects of the oscillations in eccentricity and precession are seasonally opposed between the hemispheres. Variations in the separate components of the orbit combine to determine the incident radiation anomaly at any latitude and time. These effects can be calculated to high accuracy (Berger 1978) and are illustrated for summer and total anomalies relative to the present in Figure 2.3 using the data of Vernekar (1972) (from Budd and Rayner (1993)).

From the figure, the periods of the obliquity (~40ka) and the precession of the equinoxes (~20ka) can be seen. The period of the eccentricity (~100ka) is

apparent in the change in amplitude of the precession cycle anomalies which were, for example, larger around 120-100ka BP than for the present. Particularly at lower latitudes, the summer anomalies are largely opposed between hemispheres due to the seasonal influence of the precession and eccentricity. Peaks in the north correspond to troughs in the southern hemisphere and the northern anomalies tend to have been generally more positive than present and the southern more negative due to the present timing of the perihelion around the 5th of January. This hemispheric contrast is less significant close to the poles where the effect of the obliquity brings the hemispheres closer to synchronous in their summer radiation anomalies.

Particularly significant are the large anomalies north of 40°N, especially for summer radiation. It is in these largely continental regions that decreased radiation could cause a lowering of the snowline and the covering in snow of extensive elevated areas. Ice sheets may have been seeded in this way (Brooks 1926; Birchfield et al. 1982), although there has been some debate over how quickly this coverage may have occurred (Fulton and Prest 1987). The relatively low thermal inertia due to the continentality of these latitudes allows for greater response with less delay to radiation extremes than, for example, much of the southern hemisphere where the largely oceanic conditions produce a smaller amplitude of temperature change (Kutzbach and Guetter 1986). The different temperature response time constants of continent and ocean are reflected seasonally as well as over longer (and shorter) time scales. The large amplitude seasonal cycles over land as compared to ocean mean that the long term seasonal anomalies are also larger over land.

The amplitude of the critical summer radiation anomalies around 65°N is about 25 Wm^{-2} (Figure 2.4 (a)). Due to the continentality of these latitudes, there is a strong temperature response to the insolation changes, ranging from cold enough to initiate glaciation to warm enough to prohibit significant ice formation. If the zone were more oceanic, the range of temperature response may not be enough to allow both glacial and interglacial conditions. Similarly, if these critical land masses were much further north or south, the temperature range there may not encompass the extremes required to produce the glacial variation (Weertman 1976). The extreme continentality of Siberia may have

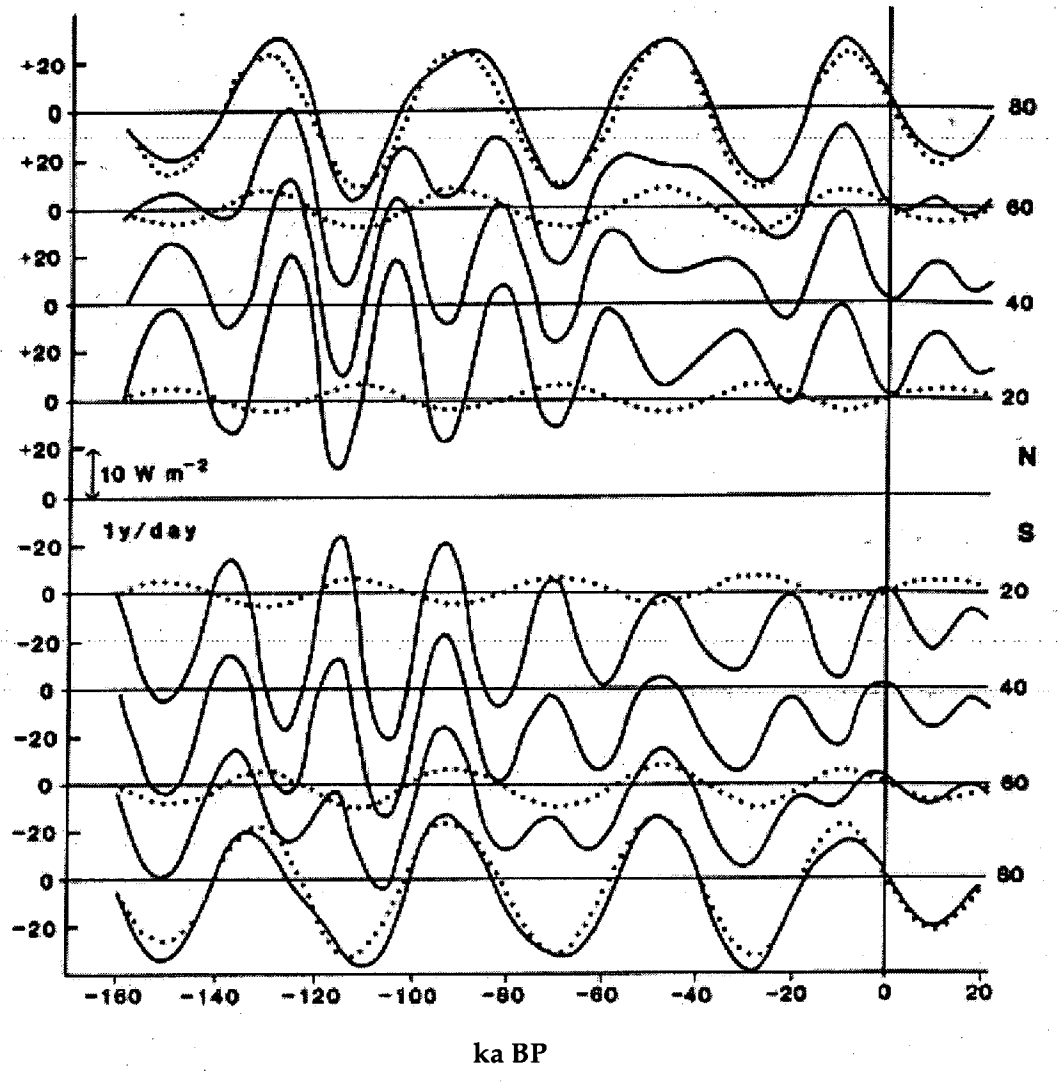

Figure 2.3: Summer half year (-) and total (...) radiation anomalies relative to present (1950) due to variations in the Earth's orbital characteristics. Scales are shown for ly/day and W/m^2 ($1W/m^2 = 2.07ly\,day^{-1}$). Figure taken from Budd and Rayner (1993) (data from Vernekar (1972)).

meant that even in low insolation summers, summer melt may have been too great for severe glaciation to occur there (North et al. 1983).

Not only is the radiation anomaly at a particular latitude important, but also the time of year is significant. Summer radiation anomalies are considered important to glacial mechanisms, as it is in the summer that most ablation takes place. Cold, low insolation summers contribute to the onset of glaciation by determining the capacity of the snow on the ground to remain year round,

strongly influencing the albedo (see Section 2.4.1). Colder summers allow the preservation of snow on the ground over larger areas, the consequent increase in albedo then feeds back to produce colder conditions. Low summer insolation then allows for lower snowlines, as at some locations a 2.4°C change in temperature can lead to an estimated 10° latitude shift in the snowline (Suarez and Held 1976), and ice caps previously confined to isolated peaks may then extend into larger elevated regions (Ledley and Chu 1995). Deglaciation, on the other hand, is associated with summers of increasing insolation (Kutzbach and Guetter 1986).

There have been estimates that as much as 66% of ice sheet ablation is due to direct radiative melting (Braithwaite 1990), suggesting that summer is the most significant ablative period. Studies have shown that the vast majority of ablation occurs in the summer half year with over 80% in the summer months for ice sheets and glaciers at high northern latitudes (Ahlmann 1948; Braithwaite 1993). Indeed, some suggest that the critical period may be even shorter and that it is the summer solstice radiation anomalies which compare best with the isotopic ice volume record (Ledley and Chu (1995) and see Figure 2.4).

2.3 Non-linearities of climate response

While the theory described above does give some qualitative explanation of glacial cycles, fundamental features remain unexplained. Rudimentary studies based on the interaction between incident radiation and a highly parameterised cryosphere have suggested that radiation changes alone could produce ice sheets of the size known to have existed during the last glacial (Calder 1974; Weertman 1976), but these have been dependent on significant assumptions and simplifications (Gribbin 1978; Budd and Smith 1981). Other climate model studies have found that this basic response to incident radiation is not sufficient in itself to be the sole cause of ice ages (Imbrie and Imbrie 1980), although more complex models have had some success (Dong and Valdes 1995).

The relationship between summer radiation at 65°N and glacial cycles is shown in Figure 2.4. Figure 2.4 (a) illustrates the variation in insolation at

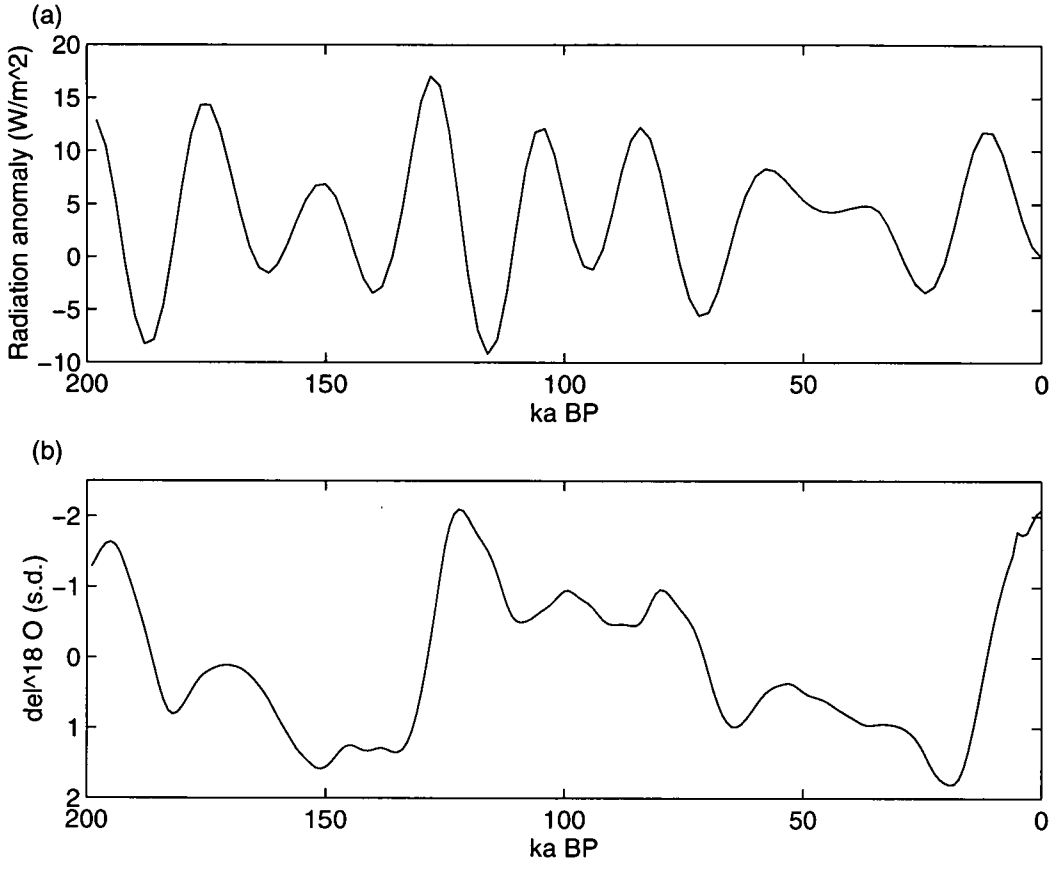

Figure 2.4: (a) Radiation anomalies at 65°N, over the last 200 ka (data from Berger (1978,1979)). (b) $\delta^{18}O$ for the last 200 ka (from Imbrie et al. (1984) and Martinson et al. (1987)). $\delta^{18}O$ is considered to be representative of eustatic sea level and hence of global ice volume. Sea level appears to follow the radiation forcing in a manner indicative of causation. The $\delta^{18}O$ curve is inverted for more easy comparison with the radiation anomaly curve (positive $\delta^{18}O$ corresponds to high ice volume and low sea level).

65°N (Berger 1978; Berger 1979) for the last 200ka, and Figure 2.4 (b) shows $\delta^{18}O$ data from sea sediments (from Imbrie et al. (1984) and Martinson et al. (1987)) which are considered to be representative of changes in eustatic sea level (and global ice volume). The two plots display striking similarities. Increasing radiation largely corresponds to increasing sea level, while decreasing radiation is strongly associated with decreasing sea level. It is evidence such as this which led to general acceptance of Milankovitch-type forcing as being central to the cycling of ice ages. However, also obvious are various non-linearities between the plots.

Compared to present, incident radiation at 65°N was generally higher during the last glacial with three periods of lower than present radiation at ~115ka BP (Before Present), ~75ka BP, and ~25ka BP (Figure 2.4 (a)). The persistence of ice and low temperatures despite the high radiation suggests the influence of some feedback or thermal inertia due to the existence of the ice sheets themselves. According to Budd (1981), there was only one time during the last glacial cycle that radiative conditions alone were extreme enough to induce the growth of ice sheets, all other advances being dependent on prior ice sheet existence. Although the climate is strongly influenced by radiation changes, similar radiation regimes do not necessarily give the same climatic response with, for example, enormous climatic differences between the Last Glacial Maximum (LGM) at around 20ka BP, and present, despite the similarities in the insolation at those times.

While in the past the radiation was generally higher than present in the northern hemisphere, in the south it was generally lower. Despite this, evidence suggests that the southern climate change throughout glacial cycles reflects the radiation patterns of the northern hemisphere rather than those in the south. The influence of some internal climatic feedback to the radiation anomalies is further implied by this global climatic response to radiative forcing in the north. Snowline altitudes appear to have changed uniformly throughout all latitudes and in different regions, regardless of their altitude, continentality or other circumstances (Broecker and Denton 1989; Lowell et al. 1995). Such a globally consistent change in snowline indicates that the changes represented are in the temperature rather than precipitation regime. That there was apparently no north-south gradient in the magnitude of temperature change also suggests that that change was relatively constant at all latitudes, contrary to that which may be expected in a system being driven from the north. However, it was found that changes in sea surface temperatures (sst's) at low latitudes were in fact smaller than those at higher latitudes (CLIMAP 1976; CLIMAP 1981), and it may have been that the growth in Southern Ocean sea ice (Budd and Rayner 1990) and ice shelves (Denton et al. 1986) during glacial times compensated for the lack of influence of the northern ice sheets in high southern latitudes. Differences between sst and snowline data may be attributable to a change in

lapse rate (Gates 1976).

On the scale of orbital variations (10's of thousands of years), the climatic change throughout the climate system may be considered synchronous. However over shorter periods than this, there is some degree of asynchrony. Imbrie et al. (1992) and Imbrie et al. (1993) show that the response of various parts of the climate system are not perfectly in phase with each other and generally lag the radiation anomalies. Some regions and climate components reflect this lag more than others. Even on these shorter time scales however, there is no north-south gradient in the timing or location of response; in fact, there is an apparent tendency for the southern hemisphere to lead the north (Imbrie et al. 1992). The different time constants of different climate components and the various feedback mechanisms through which the radiation signal is transmitted obscure any obvious chain of causality.

There is a clear 100ka periodicity in the $\delta^{18}O$ isotope curve (Imbrie et al. 1993). Higher frequency cycles are also apparent and these are closely related to the obliquity and precessional components of the Earth's orbit, there being an almost linear correlation with the associated radiation anomalies at critical latitudes (Imbrie et al. 1992). However, the 100ka cycle in ice cover and climate cannot be so easily attributed to changes in the eccentricity of the Earth's orbit. The radiation changes due to variation in the obliquity and equinox precession are large compared to those resulting from variation in the eccentricity and changes in the eccentricity can't be expected to directly influence climate as strongly as do these other orbital components (Imbrie et al. 1993).

The role of eccentricity variations in glacial cycles is brought further into question by investigation of a climate record longer than the last few hundred thousand years. Climatic cycles of 100ka appear to have occurred during eras when there was no glaciation (Olsen 1986), but conversely there have been ice age episodes when there was little or no such periodicity in the eccentricity (Mix 1987; Imbrie et al. 1993). Furthermore, over the last million years, the 100ka period apparent in the climate record has become more pronounced while the amplitude of the eccentricity forcing has decreased. In fact, the dominant periodicity in the eccentricity forcing is at around 400ka (see Figure 2.2), but there is no equivalent period apparent in the climate record.

Also characteristic of the 100ka cycle is its sawtooth nature. Long periods of gradually increasing ice volume, followed by relatively abrupt terminations leading into interglacials, have been inferred from sea sediment $\delta^{18}O$ (see Figure 2.4 (b)).

Glacial cycles and their associated climate changes can be seen to be strongly dependent on variations in the Earth's orbit. However, while the connection is obviously strong, its nature is not readily apparent. The paths through which the radiation signal is transported play an important role in determining the climate changes themselves. So, although the cause of glacial cycles may be attributed to orbital variations, the nature of the changes is largely determined by the many feedbacks from all parts of the climate system and in particular by the growth and decay of the ice sheets.

2.4 Climate feedbacks

The radiation signal which drives glacial cycles is propagated through, and influenced by, the entire climate system. In fact, the direct effect of radiation changes on the glacial climate is relatively small compared to the influence of the resulting change in topography, albedo, surface temperatures, sea ice extent and the composition and circulation of the atmosphere and oceans (Hall et al. 1996).

2.4.1 Ice sheets

Ablation and albedo

As mentioned in Section 2.2, ablation plays an important role in the glacial climate. It is considered that ablation is the dominant process in determining ice sheet mass balance changes on glacial scales (Gallée et al. 1992). In fact, rapid ice sheet collapse due to high ablation rates during deglaciation compared to the length of time required for ice sheets to grow, suggests that the natural growth and decay cycle of ice sheets is sawtoothed (Weertman 1964). This may be some part of the source of this shape in the climate record. The rate of ablation also affects the ice sheet surface slopes and so the velocities of ice sheets and clearly plays a large part in determining the size and nature of ice sheets and glaciers where it is prevalent. The extreme latitude and height of the

Surface	Albedo
Dry snow	0.8
Melting snow	0.7
Firn	0.5
Clean ice	0.4
Dirty ice	0.2
Blue ice	$\leq$0.5*
Desert	0.3
Forest	0.15

Table 2.1: Approximate albedos for various surfaces. The generally high albedo of ice and its capacity to appear and disappear relatively quickly from a surface allows ice to significantly affect climate. The blue ice albedo for the Antarctic was estimated by Weller (1968) to be ~0.5 but northern hemisphere values may lower than this. Other values are from Paterson (1994) and Houghton (1985).

Antarctic Ice Sheet however, mean that temperatures are sufficiently cold that surface ablation there is much less significant and so losses through interaction with the ocean, including calving and basal melting, become more important.

Energy used in the surface ablation process comes partly from radiation and partly from the atmosphere. The process of ablation itself therefore tends to enhance the possibility of cooling of the air near the ice surface by directly removing energy from it. Once the ice cover forms, air temperature is reduced by contact with the ice.

Persistence of snow or ice cover is of course heavily dependent on the ablation rate. The fact that snow or ice can form or melt relatively quickly makes glacial extent itself a powerful mechanism for climate change. Table 2.1 shows the approximate albedo's for various surfaces based on data collated by Weller (1968), Paterson (1994) and Houghton (1985). The difference between albedos of iced regions (typically $\sim$ 0.7) and bare land ($\sim$ 0.2) can be so large that the amount of radiation absorbed at that surface may vary dramatically. So, as well as having a vital direct effect on ice sheets, ablation also affects the growth and retreat of ice sheets indirectly through its role in determining ice extent and therefore albedo and therefore the radiation budget in sensitive regions.

The albedo of an ice covered surface may also vary depending on the

nature of the snow or ice surface as determined by the amount of precipitation and ablation and the thickness of the ice. When radiation and temperature increase early in deglaciation, the snowfall fraction of precipitation declines and ablation increases, particularly at the southern margins of the northern hemisphere ice sheets. Together these changes cause snow ageing, melting and the production of darker blue ice resulting in a reduced albedo. The effects can be substantial and may play a significant role in ice sheet decay (Peltier and Marshall 1995). While cold temperatures must prevail in all regions of ice sheet growth, warming at one margin can melt the ice locally, drawing down ice from upstream and so reduce ice thicknesses and volume throughout the ice sheet. However, during the early growth phase of an ice sheet, surface energy processes lead to a negative surface radiative budget which tends to suppress ablation and lead to a net accumulation there (Berger 1993).

The effects of albedo are felt particularly in summer when the incident radiation is greatest and so the potential for change in the amount of radiation absorbed due to albedo changes is greatest. Hence the ice sheet albedo effect for a growing ice sheet tends to enhance the influence of cooler summers, further assisting ice sheet growth (Budd 1981).

The albedo feedback therefore tends to amplify the effects of negative radiation anomalies where conditions allow ice formation. Aspects of the feedback then also resist initial ice sheet decay and large positive radiation anomalies are then required to instigate ice sheet retreat. However, once the ice does begin to retreat, the albedo and associated feedbacks work in reverse and the influence of the high insolation becomes significantly greater, leading to accelerated ice sheet decay.

The amplification of the radiation signal by ice sheet albedo feedback is less important for the Antarctic than for the ice sheets of the northern hemisphere where ice sheet area has varied greatly. The extent to which the Antarctic may have expanded during an ice age is limited since it presently extends close to the edge of the continental shelf around much of the ice margin and the surface mass balance is positive over most of the ice area. The change in albedo due to an expanded Antarctic Ice Sheet during the ice age could only have been secondary compared to the corresponding changes of the northern ice

sheets.

With the climate being affected by the ice sheet albedo effect, it is the area of ice which is important rather than the volume. Ice volume changes will tend to lag changes in ice area with the ice at the ice sheet margins responding more quickly to climate change than the thick ice in the centre. Budd and Rayner (1993) suggest that the apparently earlier response of the southern hemisphere may be explained by the response there to the changed ice area and albedo in the north with the ice volume change lagging by a few thousand years. However, the effects of the reduction in absorbed radiation due to the presence of the ice sheets are greatest at the ice sheets themselves and diminish with distance away from them. While it appears that the larger the ice sheets, the further their cooling influence reaches, this influence may not have extended from the northern hemisphere ice sheets to the southern hemisphere. Climate model studies considering the LGM radiation regime and ice distribution indicate that the existence of the ice sheets significantly lowered temperatures throughout the northern hemisphere, particularly in the vicinity of the ice sheets, but these effects were greatly reduced in the southern hemisphere, where the minimal expansion of the Antarctic and the remoteness from the northern ice sheets did not allow for as much temperature change. Manabe and Broccoli (1985), using a general circulation model (GCM), and Budd and Rayner (1993), using an energy balance model (EBM), indicate that the minimum changes were found in the Southern Ocean but amplification occurred further south over the Antarctic sea ice and continent.

The time constant of ice sheet growth ($\sim$10ka) gives some explanation of the phase delay in the climate response to radiation variations. It also indicates that the amount of time any radiation regime prevails becomes important as it determines the extent to which the ice sheet is able to respond to that regime. Also, the ability of large northern hemisphere ice sheets to extend into regions where the regime is controlled by precession, rather than obliquity (which influences the regime more at high latitudes), may have a significant effect on the nature of the climate change (Ruddiman et al. 1989). Ice sheets influence and are affected by climate. However, since large ice sheets feedback more strongly with their environment, there appears to be a critical ice sheet size

which defines whether the ice sheet is more master or slave of climate (Imbrie et al. 1993).

Therefore, while the ice sheets have the potential to amplify the radiation signal through their albedo feedback, the enhancement does not explain the global nature of the temperature change. Further climatic influence may be exerted by the northern hemisphere ice sheets through connection with other components of the climate. Ocean temperatures, salinity and hence circulation, are affected by meltwater rates from ice sheets, the quantity of icebergs being produced and the extent of the sea ice. Variation in ice sheet structure and flow may have been reflected in oceanic change and from there may have been transmitted to other regions of the planet and climate.

Topography

With ice sheets growing to thicknesses of several kilometres over large distances, their effect on the topography of the land is considerable. The change in topography affects the local ice surface climate as well as having larger scale influence.

The ice sheet surface lapse rate tends to be steeper than the free air lapse rate ($\sim$-6.5°C km^{-1}) due to the development of strong near surface inversions over the inland ice cap regions. Assuming an ice sheet surface lapse rate of -10°C km^{-1}, and that the saturation vapour pressure approximately halves for every 10°C temperature drop, precipitation roughly halves for every kilometre of elevation (Mavrakis 1992). This effect restricts the growth of ice sheets to thicknesses which produce elevations where there is enough accumulation to maintain the mass balance.

While this 'elevation-desert' effect tends to limit the growth of the ice, the temperature change with altitude encourages ice growth and maintenance. As the ice sheets grow to higher altitudes and lower temperatures, ablation will decrease and more of the precipitation will fall as snow, rather than rain. Conversely, as an ice sheet sinks due to isostatic bed depression or is drawn down to lower elevations, higher ablation rates can significantly reduce the albedo of the iced surface, enhancing prospects of further melt.

The growth of the large northern ice sheets caused the pattern of river

drainage to change. There is evidence that increased freshwater flow into the Mediterranean Sea during deglaciation episodes may have led to an altered ocean circulation there, possibly leading eventually to a decrease in precipitation over the Eurasian Ice Sheet (Arkhipov et al. 1995). The damming of inland lakes on the inland margins of the northern ice sheets may have lead to a marine-style margin there, possibly affecting the ice sheet dynamics and providing a moisture source along southern inland ice sheet margins (Hughes 1996).

Regionally and globally, the effect of the changing topography due to waxing and waning ice sheets is felt in the altered atmospheric features and circulation induced by the different surface topography types and shapes.

2.4.2 Atmosphere

CLIMAP (1976) produced maps of the estimates of global sst's in summer and winter for the last glacial maximum (LGM) relative to the present, based primarily on sea sediment records. These data were updated using additional data and revised techniques to produce CLIMAP (1981) maps. The maps also included estimates of sea and land ice changes. These data have been used to provide the basis for lower boundary conditions used in atmospheric GCM's to simulate the LGM climates. Other changes to the climate forcing used for the LGM included reduction in greenhouse gases, the appropriate orbital characteristics and the reduction in sea level. Various such investigations into the nature of the atmosphere in glacial times, employing models of differing sophistication, have been made (e.g. Manabe and Broccoli (1985), Kutzbach and Guetter (1986), Shinn and Barron (1989), Berger (1993), Harrison et al. (1995)). Despite differences between the models and techniques employed, results were often similar, perhaps due to their common usage of CLIMAP (1981) as their source for boundary conditions. Generally, colder and drier conditions were produced and a greater equator-pole temperature gradient led to a more vigorous circulation.

Results indicated that the size of the Laurentide Ice Sheet forced a split in the jet stream, with one branch going north of the ice sheet into the very cold Arctic regions and then carrying cold, dry air into the North Atlantic,

producing low sst's there and encouraging the growth of sea ice. The southern branch directed storms along the sea ice boundary in the North Atlantic and the southern margin of the Laurentide and Eurasian Ice Sheets (Manabe and Broccoli 1985). Planetary wave modification by the Laurentide Ice Sheet also led to increased precipitation further east, along the southern margin of the Eurasian Ice Sheet in eastern Europe and into Russia (Gallée et al. 1992). The blocking caused by the ice sheet tended to force warm air northward into the Yukon Valley, maintaining relatively mild conditions there (Broccoli and Manabe 1987a).

Conditions were generally drier, partly because of the lower temperatures, particularly in the Antarctic (Yiou et al. 1985), but also due to circulation changes (Kapsner et al. 1995) and the ice sheets acting as moisture sinks (Manabe and Broccoli 1985; Broccoli and Manabe 1987b). However, not all regions in the models had precipitation rates less than those of the present day.

Increased snow cover decreased the intensity of the Asian monsoon (Joussaume 1993) and models commonly produced less LGM precipitation in continental interiors, particularly eastern Siberia (e.g. Manabe and Broccoli (1985), Harrison et al. (1995)). Evidence from Greenland and Antarctic ice cores indicates that there was significantly less precipitation at those sites during glacial times, and the general dryness of the atmosphere suggests a reduced transport of latent energy, augmenting the equator-pole energy imbalance and further contributing to a stronger circulation (Manabe and Bryan 1985). However, the location of the mid-latitude depressions along the southern margin of the LGM northern hemisphere ice sheets, particularly those bordering the North Atlantic, compensated a decrease in convective precipitation and supplied moisture to the south east Laurentide and the south west Eurasian Ice Sheets (Hall et al. 1996), sustaining the ice at these latitudes (although low precipitation further south discouraged further expansion (Broccoli and Manabe 1987a)). Furthermore, due to the cold surface temperatures, precipitation in the vicinity of the ice sheets during glacial times was much more likely to fall as snow than for the present day at the same location and, despite a general decrease in precipitation, snowfall may have actually increased (Hall et al. 1996). Colder air temperatures allowed for less

evaporation and ablation, promoting the survival of summer snow, further contributing to ice sheet maintenance (Berger 1993), although these effects would have been partially negated by the dryness of the air.

A dry glacial climate suggests a higher lapse rate, which could contribute to the globally lower snowlines at high altitude glaciers (Broecker and Denton 1990). However, model climates suggest that the lapse rate did not change enough to explain the discrepancy (Hall et al. 1996).

Altered patterns of evaporation and precipitation would have affected ocean salinity and this may have had profound effects on ocean circulation, particularly in the North Atlantic, with the consequences felt across the planet (Broecker et al. 1985). Some authors have also suggested that at the onset of a glacial cycle, the lag in the temperature change of the oceans behind the land would establish a thermal gradient between ocean and land, encouraging the passage of storms over ice fields developing near the ocean (Ruddiman and McIntyre 1981). They argued that the prevailing warm winters and relatively high ocean salinity would discourage extensive sea ice, allowing the oceans to remain warm and open to evaporation, supplying moisture to the landward bound storms and the developing snowfields. However, despite some changes in the circulation of the atmosphere throughout a glacial cycle, in many ways the climate of the LGM is comparable to other palaeo-climates (Rind 1986) and differences occur largely in the amplitude of climatic response rather than in structure (Hall et al. 1996).

The dryness of the glacial climate also affects the global albedo. At low latitudes where presently there is a great deal of vegetation, a reduced precipitation during glacial times may have produced larger areas of desert and savanna (Eyles 1993), further increasing the planetary albedo as these surfaces reflect more radiation than those of denser vegetation. Similar changes in the vegetation at high latitudes may also have occurred (Berger 1993; Harrison et al. 1995), although vegetation changes would have lagged the climate forcing by some time. The tendency towards higher albedo would have been further enhanced as low soil moisture content makes for lighter coloured and more reflective soil (Manabe and Broccoli 1985). Models have been able to reproduce many of the aspects of ice sheet initiation in high northern latitudes by

accounting for changes in albedo due to vegetation and cryospheric changes as well as insolation variation (Gallimore and Kutzbach 1996). Aridity, as well as exposed continental shelves and a more vigorous atmospheric circulation in glacial times may also have led to high atmospheric dust content (Shaw (1989), Figure 2.5) which could have contributed significantly to atmospheric albedo and global temperature change (Harvey 1988). Estimating glacial albedos however, is made difficult by our poor knowledge of cloud cover history. Clouds can be highly reflective and differences in their past distributions could have significantly affected both the planetary albedo (Broccoli and Marciniak 1996) and the influence of surface albedo changes. At present however, models still provide conflicting estimates of cloud distributions during glacial times. It is concluded that although albedo changes for land in ice-free areas may have been significant, by far the most important changes were the changes from ice-free to snow- or ice-covered.

It should be noted that the GCM studies discussed here deal only with the climate since the LGM and not with other periods of the last glacial cycle. They may be further limited by their common use of CLIMAP boundary conditions as others have found that the size of the ice sheets used can substantially affect the modelled atmospheric circulation (Shinn and Barron 1989).

Greenhouse gases

Altered circulation was not the only difference between the glacial atmosphere and that of today. As well as the lower water vapour content of the dry glacial atmosphere, concentrations of other greenhouse gases such as carbon dioxide (CO_2) and methane (CH_4) were also lower (Barnola et al. 1987; Chappellaz et al. 1990). Figure 2.5 shows the variation in concentration of these gases through a glacial cycle and their apparent close relationship with temperature change (after De Angelis et al. (1987), Jouzel et al. (1987), Lorius et al. (1990) and Rampino and Self (1992)).

While the correlation between CO_2, CH_4 and temperature is relatively strong, their relationship is uncertain. CO_2 increases generally with temperature as the climate goes from glacial to interglacial but lags temperature change during periods of glaciation (Barnola et al. 1987), and its phase relationship

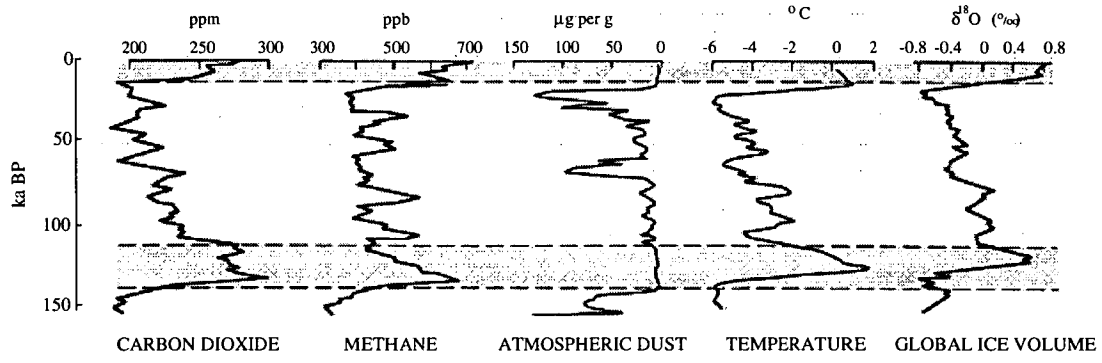

Figure 2.5: Comparison of changes in greenhouse gas concentrations with temperature change through the last glacial cycle (after De Angelis et al. (1987), Jouzel et al. (1987), Lorius et al. (1990), Rampino and Self (1992)). Figure taken from Eyles (1993). Shading indicates interglacial periods.

with temperature is generally not well known. Nevertheless, evidence is strong that lower concentration of greenhouse gases was a significant contributor to the lowering of global temperature during the last ice age, with estimates of CO_2 changes contributing up to 3°C (Eyles 1993) and CH_4 contributing another 30% (Chappellaz et al. 1990), although this could be an overestimate.

The global character of the distribution of these greenhouse gases offers a mechanism for global temperature change which can't be explained by the northern hemisphere ice sheet's direct influence on climate. Various climate models have found that the inclusion of carbon dioxide changes made for better comparison with the palaeo-temperature record in distribution - producing temperature change in low latitudes and the southern hemisphere, and amplitude - as the magnitude of the modelled temperature changes compared better with the record (Ruddiman and Duplessy 1985; Berger 1993). Without accounting for feedbacks such as that of CO_2, some modelled climates had difficulty maintaining the very ice sheets which were driving them (Manabe and Broccoli 1985), although CO_2 forcing alone was found to be capable of producing significant ice sheets in the northern hemisphere (Lindstrom and MacAyeal 1989).

The mechanism through which greenhouse gas concentration in the atmosphere does respond to climate is not well understood. Land based

processes determined by changes in high latitude peatlands (Franzén 1994) or the effect of drainage disruption on methane production (Adams and Petit-Maire 1992) have been suggested, as has volcanic activity under the influence of the loading and unloading of the Earth's mantle by the advancing and retreating ice sheets and their influence on sea level (Caldeira and Rampino 1992). The exposure and flooding of the continental shelves due to sea level change throughout a glacial cycle may also lead to methane being released during deglaciation (Nisbet 1990), although this is dependent on the pre-existence of sea level variation. The ocean's influence was probably more significant and greenhouse gas changes may have been driven by mechanisms such as changes in: ocean temperature and salinity (see Broecker (1992)), the oceans 'biological pump' (Broecker and Peng 1989), carbonate ion concentration in the deep sea (Broecker et al. 1991) or surface ocean (Boyle 1988).

The role of the ocean in the reduction of CO_2 concentration in the atmosphere during glacials has been studied with the use of a carbon cycle ocean model by Heinze et al. (1991). It was concluded that a combination of ocean processes treated in the model could explain the bulk of atmospheric changes seen in the ice cores. Nevertheless, the changes of the land based biosphere should also be kept in mind, particularly with regard to the large area of northern temperate forest which was covered by ice during the glacial periods.

2.4.3 Floating ice

Sea ice

The dependence of the carbon cycle on ocean surface water, particularly that in polar regions, highlights the importance of sea ice distribution (Shaffer and Sarmiento 1995). The influence of sea ice on sst's, salinity (Broecker 1992) and biology (Imbrie et al. 1992) indicates that the ocean's ability to act as a sink for greenhouse gases is strongly dependent on the sea ice distribution.

Sea ice extent is dependent more on summer radiation than winter, and so the low radiation northern hemisphere summers during glaciation would have tended to produce growth in sea ice cover despite the greater winter radiation (Harrison et al. 1995). Sea surface temperatures in the regions of ice sheets are

also strongly influenced by winds, katabatic or otherwise, coming off the continent and so sea ice growth is also dependent on the size of adjacent ice sheets. These winds would also tend to create polynyas, affecting ocean salinity profiles and deep water production. Sea ice also responds and feeds back strongly to temperature variations through its influence on albedo (Budd 1991). The larger area of high albedo in glacial times due to the expanded sea ice extent would have contributed further to atmospheric cooling around the ice sheets.

Sea ice acts as a lid on the ocean, reducing moisture and heat transport between ocean and atmosphere. Insulating the atmosphere from the ocean, the more extensive glacial ice pack could have led to a cooler atmosphere. With sst's lagging the changes in insolation by 1000's of years during the early stages of glaciation (Berger et al. 1996), the main moisture source for feeding of the growing ice sheets would have remained open (Ruddiman and McIntyre 1981). The decrease in sst may have led to an expanded sea ice area, particularly in the North Atlantic (Kutzbach and Guetter 1986), and a reduction in that moisture source poleward of the ice edge, although there is some doubt as to the extent of this moisture cutoff (Hebbeln et al. 1994). While the area of ocean exposed to the atmosphere was at times reduced, the influence of the sea ice on the baroclinic structure of the atmosphere may have caused increased storm activity along the sea ice margin and a resulting increase in precipitation in the regions of the northern hemisphere ice sheets southern margins (Hall et al. 1996). The effects of sea ice expansion on atmospheric moisture were possibly not only local as increased aridity in regions throughout the hemisphere has been attributed to the changes in Arctic sea ice (Honda et al. 1996).

North Atlantic Deep Water (NADW) is sensitive to changes in sea ice distribution in the high latitudes of the North Atlantic (Imbrie et al. 1992). By influencing surface winds, temperature and salinity, sea ice may have contributed to altered NADW circulation during glacial times. The ocean circulation in turn affects global climate, and changes in NADW production would have influenced Antarctic sst's and sea ice although other influences must be invoked to explain the amount of Antarctic sea ice present at the LGM (Crowley 1992). Variations in southern hemisphere radiation would also

influence the sea ice there although Genthon et al. (1987) found that November irradiation changes at 60°S did not have a strong connection to the temperature at Vostok (78.3°S 106.5°E). An expanded Antarctic sea ice region with the resulting albedo feedback would have caused significant temperature change throughout Antarctica and much of the southern hemisphere but that this change could have occurred prior to those in the north seems unlikely if Antarctic sea ice extent was dependent solely on changes in NADW circulation changes.

Budd and Rayner (1990) used a global EBM to study the independent and combined effects on the climate of changes in the orbital radiation regime and the ice cover. It was found that the glacial extension of the northern hemisphere ice cover caused an expansion in Antarctic sea ice areal extent which, through positive feedback, produced much lower temperatures in the latitude band of the sea ice than for the open ocean further north. Following this, Budd and Rayner (1993) showed a simulation of the Antarctic sea ice through the glacial cycle from the combined influence of the northern ice cover and the orbital variations. It was found that Antarctic sea ice extent was more in phase with the northern ice area which slightly lead the changes in the ice volume, although the radiation regime also had some influence.

There is some suggestion that sea ice may have played a more direct role in the inception of the northern marine ice sheets by thickening until grounding and spreading from there (Grosswald 1980). However, others feel that the marine ice sheets are the result of ice spreading from inland (Elverhøi et al. 1993).

Ice shelves

Conditions in glacial times were also conducive to the growth of ice shelves. The lower sst's and less violent ocean movement through expanded sea ice would have produced less melt under ice shelves and so allowed for their expansion (Denton et al. 1986). The albedo of ice shelves is considerably greater than that of sea ice because of the relative continuity of ice shelves through time (no great seasonal changes in extent) and space (no leads). Ice shelf expansion also allows for ice sheet growth as the shelf may ground on high continental shelf points,

particularly as sea level drops, and the ice sheet may then fill in behind. It may even be that ice shelf existence preceded that of their marine ice domes which would have been too unstable to survive were it not for the buttressing shelves (Hughes et al. 1977). Regardless, floating ice shelves during glacial times would have protected the grounded ice just as the embayed ice shelves in Antarctica slow the outflow from the grounded ice there today. The presence of an Arctic ice shelf across the Arctic Ocean would have linked and stabilised the northern hemisphere ice sheets into a single ice sheet-shelf system. Consequently, removal of the ice shelves in conjunction with delayed bedrock uplift may have helped destabilise the grounded ice up stream. Rapid ice sheet collapse resulting from the removal of ice shelves is another glaciological process which would have produced the rapid ice sheet decay and sea level rise typical of glacial terminations. The larger the area covered by ice, the less precipitation returned to the ocean and while changing thickness of floating ice will have little direct effect on sea level, the salinity of the ocean could be affected.

2.4.4 Ocean circulation

Evidence that changes in the production of NADW have produced significant climate change in the North Atlantic region and possibly further afield (Charles and Fairbanks 1992) offers a mechanism through which a climate signal may be amplified and transmitted globally.

Presently, the North Atlantic receives a considerable amount of energy from the Gulf Stream, a warm surface current flowing from low to high latitude. This current is characterised by high salinity and at high latitudes cools and mixes with colder, fresher Arctic water, forming NADW. This deep water then flows southward to the southern hemisphere, mixing with warmer water and eventually joining the Antarctic Circumpolar Current (Broecker and Denton 1990) above the colder Antarctic Bottom Water (AABW). A reduction in this deep water production in the North Atlantic could reduce the northward flow of the warm, saline surface waters and lead to a colder North Atlantic. If NADW production were to slow or stop, the transport of that warmer deep water to the Antarctic would also decrease and this could lead to cooling in the Southern Ocean (Weyl 1968). In this way the southern hemisphere could be linked to

climate changes in the North Atlantic.

The extent to which NADW reaches the Southern Ocean appears also to be dependent on wind stress around the latitudes of Drake Passage (Toggweiler and Samuels 1992). It is suggested that the maximum westerlies in this region migrated northwards in the early stages of the last glaciation and that this migration produced a reduced flow of NADW southward (Imbrie et al. 1992). Migration of the polar front due to the influence of ice sheets and sea ice on the wind field in the North Atlantic may also be crucial in the deep water variability of glacial cycles (Keffer et al. 1988).

There is evidence to support the idea that NADW flow was reduced during glacial times (see Boyle (1995)). Where currently evaporation dominates over meltwater and precipitation input to the North Atlantic, a different circulation pattern may have altered this balance, resulting in a decrease in ocean salinity and density (Broecker and Denton 1989). It appears unlikely that NADW production shutdown entirely and some source areas for that water mass may be affected more than others during circulation changes (Lehman and Keigwin 1992). Meltwater from the Laurentide (Broecker and Denton 1989), European (Schaferneth and Stattegger 1997) and other northern ice sheets would have affected the salinity and so the circulation of NADW (a possible cause of the Younger Dryas cold period (Manabe and Stouffer 1997)). Altered atmospheric circulation during glacial times may also have affected ocean salinity due to changed water vapour transport (Ruddiman et al. 1989).

An altered ocean circulation in the North Atlantic could also have produced cooling in the Arctic Ocean. A consequent reduction in ocean melt and a lower snow line there would have assisted in the preservation of an Arctic ice shelf (Hughes et al. 1977).

Nevertheless, altered ocean circulation in itself only primarily leads to an altered distribution of energy and the amount of net cooling or warming resulting from circulation change alone is limited (Broecker and Denton 1989). The suggested glacial circulatory change can only explain an estimated 30% of the LGM glacial temperature change in Greenland (Charles et al. 1994).

Antarctic Bottom Water is a cold deep water mass whose formation plays a vital role in the distribution of dissolved CO_2 (Budd 1991). Any disruption of

AABW production in glacial times would also then have influenced the carbon cycle at the time (Imbrie et al. 1992) and the temperature of the deep ocean which has some influence on the volume of the oceans and so global sea level. Sea sediment cores and model results indicate that AABW production was higher at the LGM (Fichefet et al. 1994).

Certainly the role of deep ocean circulation appears to have a significant effect on climate on various timescales (Bond et al. 1993) and is an important factor in changes in atmospheric CO_2 levels (Broecker et al. 1985). The nature of the forcing and location of the source are uncertain (Pearce 1997) but results suggest that changes in ocean circulation are partly responsible for the climate teleconnection between the North Atlantic and Antarctica (Bender et al. 1994).

The Bering Strait is a channel through which at present, fresh North Pacific water can mix with North Atlantic waters. The rate of this flow will affect the salinity of the North Atlantic and so can also influence thermohaline circulation (Shaffer and Bendtsen 1994) and sea ice formation (Walin 1985) there. Depending on sea level and possibly the extent of grounded ice, this strait was open and closed at various times during the last glacial cycle, and it is expected that such discreet changes could affect ocean circulation significantly.

2.4.5 Sea level

As ice sheets grow, the accretion of ice on the land corresponds to a decrease in the volume of water remaining in the ocean. This volume change results in eustatic sea level change and will be further influenced by thermal effects as cooler oceans contract and warmer oceans expand with climate change. The altered distribution of mass over the surface of the planet due to ice sheet growth and retreat also influences the Earth's spin axis, in turn giving effective sea level changes of 10's of metres (Bills and James 1996). The isostatic adjustment of the Earth's crust due to the loading and unloading of ice of thicknesses of several kilometres further influences relative sea level during glacial times, with depression in one region being compensated by uplift in others, although relative crustal motions are complicated by lithospheric cooling (Gornitz 1995). Relative sea level will also be affected by the isostatic response of the ocean bed due to the changing water load as eustatic sea level changes in

response to variation in global ice volume.

As well as influencing ocean circulation in the ways discussed in Section 2.4.4, sea level change altered the characteristics and circulation of shallow basins, impacting on the climate of those regions (Hemleben et al. 1996). Broecker (1992) also points out that without invoking coral growth due to sea level rise during deglaciation to compensate for the increase in terrestrial biomass, the change in CO_2 between LGM and present cannot be explained.

In many ways a change in sea level is analogous to a change of the opposite sign to the altitude (or depth) of the land. A lower ocean results in effectively higher altitude and generally colder and drier conditions on land. A sea level change of 100m may correspond to ~0.6 °C temperature change relative to the ocean surface and significantly alter precipitation quantity and pattern. Land tended to be somewhat higher and colder in glacial times due to the sea level change, which fed back positively to ice maintenance, although precipitation would have generally decreased as height above sea level increased. Changing sea level and displacement of atmospheric mass by ice sheets may also have slightly altered the optical depth of the atmosphere, influencing greenhouse capacity, surface pressure and temperature (Manabe and Broccoli 1985).

Lower sea level corresponds to more land being exposed. As the ocean retreats, coast lines advance, and land area expands. The greater continentality of glacial conditions (land area increases by 10% and area of ocean decreases by 3% for a sea level lowering of 100m (Bradley 1985)) influences climate, as the ocean's stabilising influence on temperature and their moisture become more distant to inland regions. Albedo also increases as an area previously covered by water becomes exposed to the more reflective land. Larger areas of land above sea level also allows for the expansion of ice sheets as grounding lines advance further and larger ice sheets can be thus supported. Conversely, rising sea level tends to undermine marine ice sheets as grounding lines are forced to retreat.

With a large component of sea level change being uniform over the planet, sea level is one mechanism which connects the marine margins of the Antarctic Ice Sheet and those of the northern hemisphere with climate. Ice volume changes in the northern hemisphere will be reflected in the Antarctic by changes in grounding line dynamics resulting from sea level change (Denton et al. 1986).

The effective altitude changes will also tend to be global and provide another link for climate change at all latitudes.

2.4.6 Bed response

Just as sea level change alters the effective altitude of an ice sheet, subsidence under the weight of an ice sheet or uplift when ice is unloaded also affects topography. These processes are important, particularly for marine ice sheets, as ice elevation not only influences exposure to heat and moisture but also influences the grounding zone dynamics, as they are affected by water level. As bed response tends to lag the loading and unloading of ice by some thousands of years, bedrock-ice sheet systems can get out of phase with the climate forcing.

The delay in the response of the bed to loading and unloading allows developing ice sheets to rise and spread without immediately sinking to warmer altitudes, and once deglaciation commences well after the sinking has set in, the bed and overlying ice remain at lower altitude and more vulnerable to high ablation. The depression of the bed into the ocean also decreases the amount of ice above floating, increasing sliding, decreasing the thickness and increasing the likelihood of the ice coming afloat. The resulting increased ice flow rate draws down ice from the interior of the ice sheet and the ice sheet diminishes. Early in deglaciation, the delayed response of the bed keeps its ice sheet at low elevations and vulnerable to sea level rise and, as insolation increases, the ablation of increasingly warm summers. With sea level rising faster than bedrock at these times, marine ice sheets tend towards greater buoyancy at their margins and become increasingly unstable. Hughes et al. (1977) propose that in the northern hemisphere, ice spreading seawards tended to end in rapid stream flow as flow was focussed between coastal mountains but landward spreading ice was divergent across inland plains. They argue that the resultant increase in basal melting would have led to increased ice-bed uncoupling and the increased possibility of surging.

The depression of the rock beneath an ice sheet is compensated by uplift in other places, including the ocean floor. Uplift beneath the ocean will contribute to an effective sea level rise, partly offsetting the lowering due to other factors. However, the altered load on the oceanic bed due to eustatic sea

level changes must also be considered.

Bed close to equilibrium under a large ice sheet is also more likely to tend toward an unstable profile than when less depression has occurred. When the bed elevation decreases inland of the grounding line, the ice sheet is more unstable as a small change in sea level can potentially lead to ungrounding of large regions of ice (Weertman 1974). Since an ice sheet is generally thicker inland of the grounding line, more depression takes place there and so the bed profile tends towards greater instability the closer it gets to equilibrium under a load. If warm, melting conditions prevail long enough, this instability may become dominant over its climate forcing and ice sheet melt may overtake radiation forcing.

Deglaciation could be further enhanced if the bed itself begins to shear under the basal stress of a large ice sheet (Peltier and Hyde 1984), producing an effective increase in ice velocity. It is proposed that this could account for up to 90% of the ice velocity (Boulton and Jones 1979) but this hypothesis would need to be substantiated. It has also been proposed that combined with sea level rise and delayed bed response feedbacks, the growth of northern hemisphere ice sheets to a critical size resulting in bed deformation could explain the rapid nature of deglaciation (Imbrie et al. 1993). Several of the recent glacial maxima appear to have involved similar volumes of ice (Broecker and Denton 1990) and it has been suggested that a natural, internal oscillation in the ice sheet-bedrock system may explain the length and shape of the 100ka period in glacial cycles (Denton et al. 1986). Nevertheless, the simulation of a number of glacial cycles in response to orbital forcing with ice sheet albedo feedback and using an ordinary ice sheet model, which was also used to match existing ice sheets, was found by Budd and Smith (1987) to give a reasonable representation of ice volume changes in comparison to sea sediment and ice core records.

Regardless of the influence of bed deformation on ice sheet stability, the erosion of the bed beneath ice sheets may significantly affect bed topography over time (Drewry 1986). Throughout a glacial cycle, changes in bed elevation due to erosion may influence ice sheet elevations at both the base and the surface, with possible consequences on surface climate and grounding lines.

2.5 Sequence of events

2.5.1 Climatic preconditions for recent glacial cycles

Regardless of the orbitally driven Milankovitch radiation anomalies, or any internal feedbacks, it remains that the current climatic regime where glacials follow interglacials at a relatively regular period has not always persisted. This pattern has only emerged in the last several million years and the 100ka period of the recent ice ages has only come to dominance in the last million years (Figure 2.6). Clearly, some longer term influences have been crucial in providing the background from which the recent glacial history has been able to emerge.

The Pleistocene ice sheets may be thought of as the culmination of long global climatic deterioration which began 60 Ma BP (Eyles 1993). The opening of the Tasman Sea and Drake Passage around 40 Ma BP led to the opening of the circum-Antarctic ocean current and the thermal isolation of the Antarctic (Kennett 1982). A continental ice sheet is thought to have formed by about 36 Ma BP and become virtually permanent by 14 Ma. Tectonic uplift during this time further contributed to the climatic deterioration in Antarctica as the Transantarctic Mountains formed, with considerable effect on the climate. Cooling continued and a period of rapid uplift in the Transantarctic Mountains determined that by 2.5 Ma the Antarctic ice sheet had in the main lost its temperate characteristics and become a polar ice sheet (Webb et al. 1984). It is at around this time that the large northern hemisphere ice sheets began to form.

As discussed in Section 2.2, the distribution of land masses is a crucial factor in determining where and whether glaciation may occur. The different location of continental area and the height of the land topography in previous eras may have prevented large ice sheets from forming regardless of other circumstances. A continental topographic distribution similar to that which exists today may be a precondition for the development of large ice sheets. However, it appears that this requirement had been fulfilled for some time prior to the onset of significant glaciation in the northern hemisphere around 2.4 Ma. Although there may have been a small ice cover before this time, there were further requirements for the development of the large Pleistocene ice sheets.

Uplift of the Tibetan Plateau in particular, as well as in the Himalayas

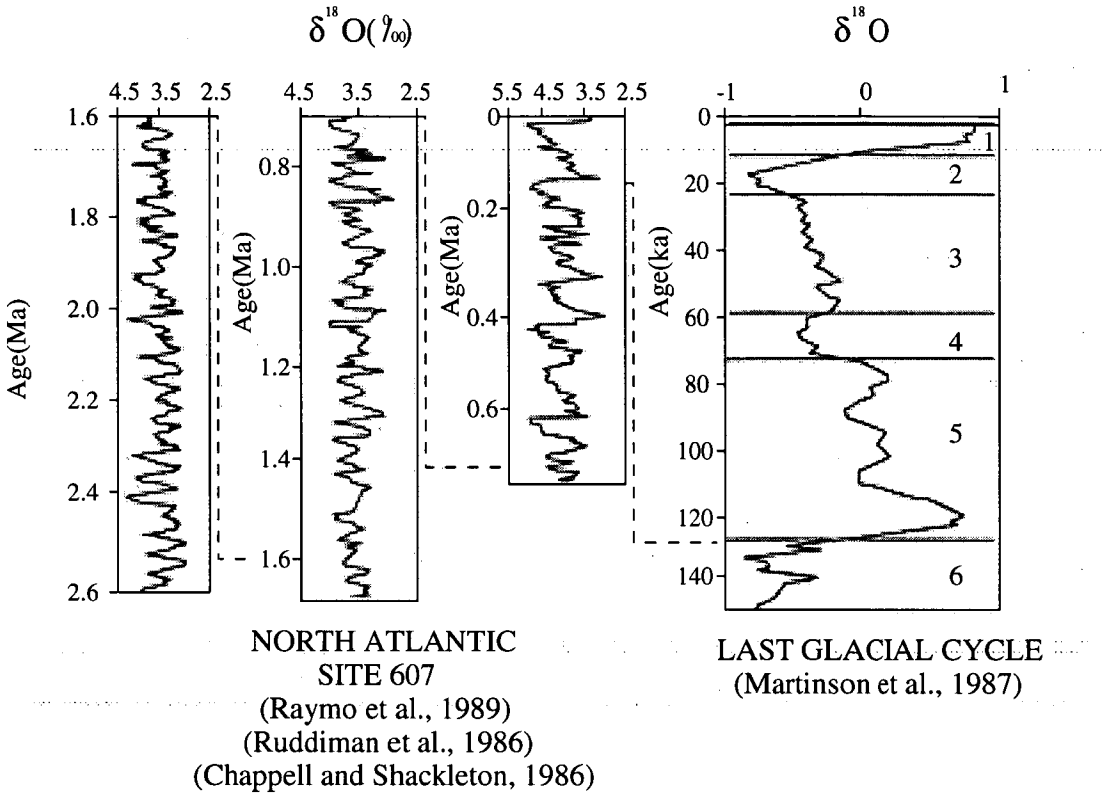

Figure 2.6: Deep sea oxygen isotope records for the last 2.6Ma. The 100ka period in the climatic variation can be seen to emerge only in around the last million years. Compiled from listed sources. Figure taken from Eyles(1993).

and the western Cordilleras in North and South America, is considered to have been important to the late Cenozoic climatic deterioration (Ruddiman and Kutzbach 1989). By altering upper tropospheric waves, this uplift affects the surface climate in middle and high latitudes, leading to longer winters and cooler, moister summers (Eyles 1993). The upwarping of passive margin plateaus around the North Atlantic may also have been a vital pre-condition to the formation of the ice sheets there, as it provided large elevated areas as seeding regions for ice sheet growth (Eyles 1993).

With the widespread uplift came increased chemical weathering, gradually reducing atmospheric CO_2 (Raymo and Ruddiman 1992). Alone, the influence on atmospheric circulation of raised mountains and plateaus probably would not be enough to provide the climatic setting for the growth of large ice sheets (Ruddiman and Kutzbach 1989) and the reduction of atmospheric CO_2 may

have been an important factor also. Progressive cooling of deep water during the emerging glacial cycles of the last 3 Ma indicate that changing NADW production during this time may be another such climatic influence (Dwyer et al. 1995). Tectonic influence on ocean circulation (Crowley 1993), and a strong correlation between increased volcanism and the climate of the last 2 Ma (Kennett and Thunell 1975), also suggest other sources of contribution to the climatic deterioration which ultimately reached a threshold beyond which the large Pleistocene ice sheets could emerge.

2.5.2 Emergence of the 100ka period

Figure 2.6 shows the deep sea oxygen isotope records for the last 2.6 million years, with data from Raymo et al. (1989), Ruddiman et al. (1986), Chappell and Shackleton (1986) and Martinson et al. (1987). It can be seen that prior to about a million years ago, the glacial record was dominated by a period of around 40ka. Since then a 100ka period has emerged and with it an increasing amplitude of ice volume change. At first glance it appears that the influence of eccentricity increases and starts to dominate that of the obliquity cycle. However, over this period the strength of the eccentricity forcing has in fact declined and at no stage was it powerful enough to alone produce the ice volume amplitude apparent in the record. Because of this, the ice sheets themselves with their large time constants have been suggested as the causes behind the regular 100ka period in the glacial climate (Genthon et al. 1987). That there was no such periodicity until the last million years despite the occurrence of glacial cycles since two and half million years ago may be explained, albeit a little circularly, by the smaller size of the earlier ice sheets (Pisias and Moore 1981).

It has been proposed that the 100ka period in the climate record may result from oscillations in the inclination of the Earth's orbit relative to the plane of the solar system, either alone or in concert with the variation in eccentricity (Muller and MacDonald 1997). By periodically moving the Earth's orbit into a cosmic dust cloud, it is suggested that the change in inclination of the orbit could potentially exert enough influence on the climate to produce glacial cycles and there is a good correlation between the timing of glacial cycles

and the change in the angle of the Earth's orbital plane. Muller (1994) argues that this theory can also explain the absence of the 400ka (eccentricity) period from the climate record and the sudden appearance and disappearance of the 100ka period. However, the theory has been fiercely contested (Roush 1997) and more recent modelling studies have been able to reproduce many of these aspects of the climate record while operating within the traditional framework of Milankovitch forcing (Paillard 1998).

The link between eccentricity and the 100ka ice age cycle was placed in a different context by Rial (1995), who found that the 100ka cycle in the isotope record corresponds almost linearly to the 1st time derivative of the eccentricity itself, not the radiation anomalies caused by it at any latitude (Figure 2.7). It is suggested that through its influence on accumulation and ablation rates on ice sheets, the change in eccentricity may be able to dictate the tempo of glacial cycles, although it is not clear that such a mechanism would have sufficient influence. While the process through which this relationship is maintained is not identified, it appears that with amplification via some resonance in the climate, eccentricity is closely tied to the 100ka cycle which dominates the recent glacial record.

It was shown by Budd and Smith (1981) and Budd and Smith (1987) using a three dimensional ice sheet model, forced by orbital variations with ice albedo feedback, that the initial strong 40ka oscillations which develop for small ice sheet growth further develop to about 100ka variations as the ice sheets become larger and able to bridge between two 40ka obliquity cycles. The relative synchrony of the 20ka precession cycle and the 40ka cycle meant that 80ka or 120ka periods developed with larger ice sheets which were only able to reach their full size or decay when the high latitude radiation changes were sufficiently large and in the right phase of obliquity and precession changes.

There is a range of models designed to explain the source of the 100ka period in recent glacial cycles. Imbrie et al. (1993) believe that the most likely explanation lies in some combination of purely internal climate mechanics determined by the inertia of large ice sheets and a non-linear response to some orbital forcing. They also recognise that individual cycles may arise from basically different processes.

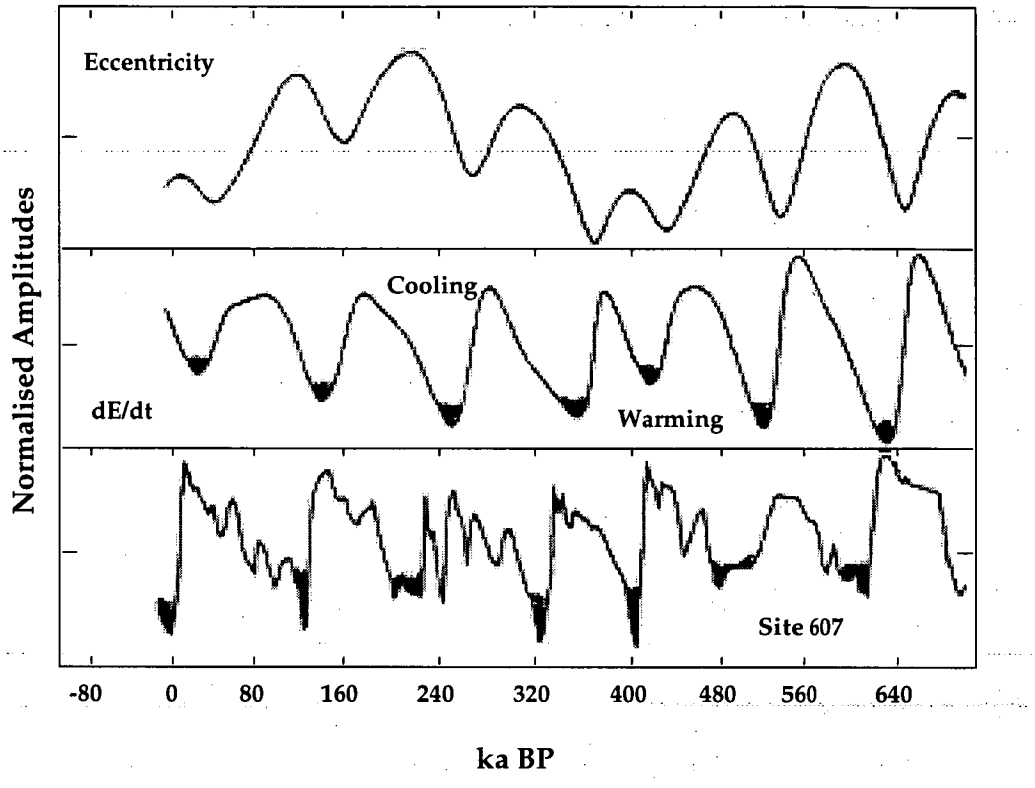

Figure 2.7: Eccentricity (e), $\frac{de}{dt}$ and oxygen isotope curves for the last 700ka. There is a strong suggestion of a relationship between $\frac{de}{dt}$ and glacial terminations. The shading highlights possibly related events. Figure taken from Rial (1995). References for site 607 data are given in Figure 2.6.

2.5.3 Individual ice ages

Given some climatic pre-conditions, it is apparent that the growth and retreat of the Antarctic Ice Sheet and those in the northern hemisphere have been in response to orbital changes and their effect on the distribution of radiation at different latitudes and seasons. However, the variation in insolation alone doesn't explain the extent to which ice sheets and climate change during glacial cycles, nor the global nature of the climate change. Feedbacks internal to the Earth's climate system are required to amplify the local radiation signal and transport it throughout the planet. The path taken by this signal is not clear. Some evidence points to early response in the southern hemisphere but there is a strong suggestion that the entire response is initiated at mid-high northern latitudes. Below is a discussion of the anatomy of an individual glacial cycle,

indicating a possible chronology for the sequence of events.

Glaciation

Decreasing summer radiation at the continental latitudes around 65°N resulted in larger snow fields surviving through the year. Eventually large uplifted areas became snow bound although various methods by which this initial stage of ice sheet growth occurred have been proposed (Flint 1971; Ives et al. 1975). Regardless, the effect was an increase in the surface albedo and a net decrease in absorbed radiation, feeding back to increased cooling and ice sheet growth. The growing ice sheets were fed by moisture from the still uncovered nearby oceans.

An altered precipitation and evaporation regime arising directly from insolation changes may have already affected the thermohaline circulation in the northern North Atlantic, reducing NADW production. The reduction of NADW flow into the Southern Ocean and a related increase in AABW production and sea ice extent may have produced the early southern hemisphere response, although Southern Ocean sea ice extent was probably also being driven by radiation changes there. The influence of southern waters on equatorial climate activated the early low latitude response. As the northern ice sheets became larger, their influence became more widespread and atmospheric and oceanic circulation changes resulted. Altered temperatures and winds produced more sea ice in the North Atlantic, increasing the albedo in that region. Migration of the polar front due to the changed wind pattern and increased influx of meltwater from the ice sheets into the North Atlantic further reduced thermohaline circulation and NADW production there, causing a further cooling in the North Atlantic.

Largely due to the changed oceanic circumstances, atmospheric greenhouse gas concentration decreased, cooling the Earth's surface at all latitudes. With further cooling the ice sheets grew and sea level decreased in response to thermal as well as eustatic effects. The lower sea level allowed marine ice sheets to advance further and produced à relative cooling on the ice sheets as altitude above sea level increased.

A generally drier climate and exposed continental shelves in conjunction with a stronger atmospheric circulation drew greater amounts of dust into the

atmosphere with a consequent possible further reduction in planetary albedo. While there was generally less precipitation, its distribution and increased propensity to fall as snow allowed for maintenance of the ice sheets.

Deglaciation

The inertia generated in the climate system by the large, slow-responding ice sheets meant that glacial conditions could survive positive radiation anomalies if these radiation changes were small enough or did not persist for too long. Large anomalies were required to overcome the stable ice age climate and trigger deglaciation to a full interglacial.

By the time of maximum glaciation, the bed was approaching its maximum depression and the ice sheet base was near its lowest altitude. When temperatures began to increase due to orbital considerations, the southern margin of the ice sheet was at its most vulnerable. Increased ablation and lower rates of solid precipitation at the southern margin caused the albedo to decrease. The increased melting there and higher ice flow rates drew down ice from the interior and the entire ice sheet was brought to lower elevations as the bedrock response was slow to react to the reduced load.

In some locations the changes to the bed may have given rise to high sliding rates and combined with increased buoyancy due to sea level rise, flow rates increased further, ice sheets thinned and volume decreased. Again the slow bed response was critical as the thinning inland ice became more buoyant and could more easily come afloat as the bed there remained depressed. Increased ablation of buttressing ice shelves from pinning points would have further destabilised marine ice domes in the Arctic (Hughes et al. 1977).

Changes in wind patterns, sea surface temperatures, sea level, continental meltwater and sea ice allowed NADW production to resume, and ocean and atmosphere circulations returned to interglacial conditions, affecting the carbon cycle. Greenhouse gas concentration in the atmosphere increased almost simultaneously with ice volume decrease and this further contributed to deglacial warming.

In the Antarctic, the higher sea level combined with the bedrock depression and increased precipitation at the end of the glacial drove the ice

sheet's response as temperatures there remained cold enough for the precipitation to fall as snow while surface ablation remained insignificant.

2.6 Summary

That glacial cycles are initiated by changes in insolation caused by variations in the Earth's orbit is almost certain. Correlation between radiation and climate change indicates that a connection must exist. However the nature of the connection is not clear as the variations in insolation in themselves are not enough to produce the observed terrestrial changes. Of the internal mechanisms which amplify and redistribute the radiation signal, the ice sheets and sea ice of the northern hemisphere and the Antarctic play a major part.

The role of the ice sheets in the climate of ice ages is central and critical. The difference between the size to which ice sheets grow in full glacial conditions, compared to the interglacial state is perhaps the dominant change in landscape over the period. Their control over atmospheric circulation and content as well as that of the ocean, influence the climate throughout the planet. The growth and decay of the ice sheets affects the hydrological cycle, lithosphere and biosphere as well as the radiation budget. However, while the importance of the ice sheets to the climate of glacial cycles is apparent, the exact nature of their influence is not clear. Much of the character of glacial cycles remains unknown. There is debate about the cause and mechanisms behind the 100ka period in the record and about the early response in the southern hemisphere and the tropics. The response of the glacial climate to Milankovitch forcing is not completely understood.

Knowing that ice sheets are driven by influences such as solid precipitation, ablation, melting, isostasy and sea level, and by estimating the range of possible values these factors may have had over the last glacial cycle, the ice sheets of that time may be modelled in relative isolation from the processes which produced those conditions. Palaeo-evidence has allowed some reconstruction of glacial cycles and their ice sheets. By attempting to reproduce that reconstruction with an ice sheet model, the conditions required to produce those palaeo-ice sheets can be inversely determined.

Chapter 3

Reconstructions of glacial conditions

In order to assess modelled reconstructions and to assist in estimating the influence of the palaeo-climate forcing, knowledge of the distribution of ice through the ice age until the present is required. The palaeo-distribution of ice is investigated, particularly in the time since the LGM. Due to dating difficulties associated with older events and the overwriting effect of the last glacial advance on evidence for earlier, generally less extensive ice sheet margins, the period since the LGM is reconstructed more readily than earlier stages in the glacial cycle. In many ways this most recent period has also been the most influential in producing present conditions. It is therefore the period from the LGM through the last deglaciation which must be understood as well as possible to allow the most useful comparison with model output.

Even for the period since the LGM however, dating difficulties arise. The most useful method of dating for studies of late Quaternary climatic fluctuations is radiocarbon dating (Bradley 1985). However, even within the range of this technique ($\sim$ 50ka) there is a variety of problems which may lead to inaccuracies. Sample contamination can occur in various ways, some of which are difficult to detect. In photosynthetic dependent samples, the influence of fractionation effects must also be considered as, due to isotopic fractionation, the plant ^{14}C content is lower than that of the atmosphere which leads to misleading results. The strength of this effect is different for different organisms and accurate dating requires that the effect is considered, although it is not always clear whether this has been done (Bradley 1985). Radiocarbon dating

operates under the assumption that atmospheric ^{14}C levels have remained constant through the period in question. This has been found not to be the case, with raw radiocarbon dates diverging from calibrated tree ring dates by 1000 years over the last 6000 years (Klein et al. 1982). The timing of reconstructions described here then cannot be considered exact, and precision must decrease markedly as age increases, particularly beyond the range of radiocarbon dating. Nevertheless, the evidence is presented here for comparison with later model results. Perhaps through modelling these events via the broad physical processes which caused them, further light may be shed on glacial chronologies.

By using a dynamic ice sheet model reacting to and (in part) influencing the climate, a reconstruction of the change of ice distribution through time can be made, but also the state of ice sheet mass balance may be assessed. Hence, knowledge of the present mass balance of the Antarctic Ice Sheet is also investigated.

Glacial sea level change is to a large extent dependent on the amount of ice (above buoyancy) which was stored and released from the ice sheets. Finding a record of the change in sea level through the last ice age gives some further indication of the timing and magnitude of ice sheet advances and retreats.

3.1 Ice sheet reconstructions

To assist in the interpretation of the text, Figure 3.1 shows the locations of places in the northern hemisphere mentioned in the text here and in Chapter 6, and Figure 3.2 shows the locations of places in the southern hemisphere mentioned in the text here, and in Chapter 7.

3.1.1 Greenland Ice Sheet

The Greenland Ice Sheet is the largest remaining northern hemisphere ice sheet and, compared to the other large northern hemisphere ice masses, remained the least variable (in percentage terms) throughout the last ice age.

Presently the thickness at the ice divide is around 3.2 km and model reconstructions estimate that this thickness varied by only about 200m during the last glacial cycle (Letréguilly et al. 1991; Abe-Ouchi et al. 1994) with low

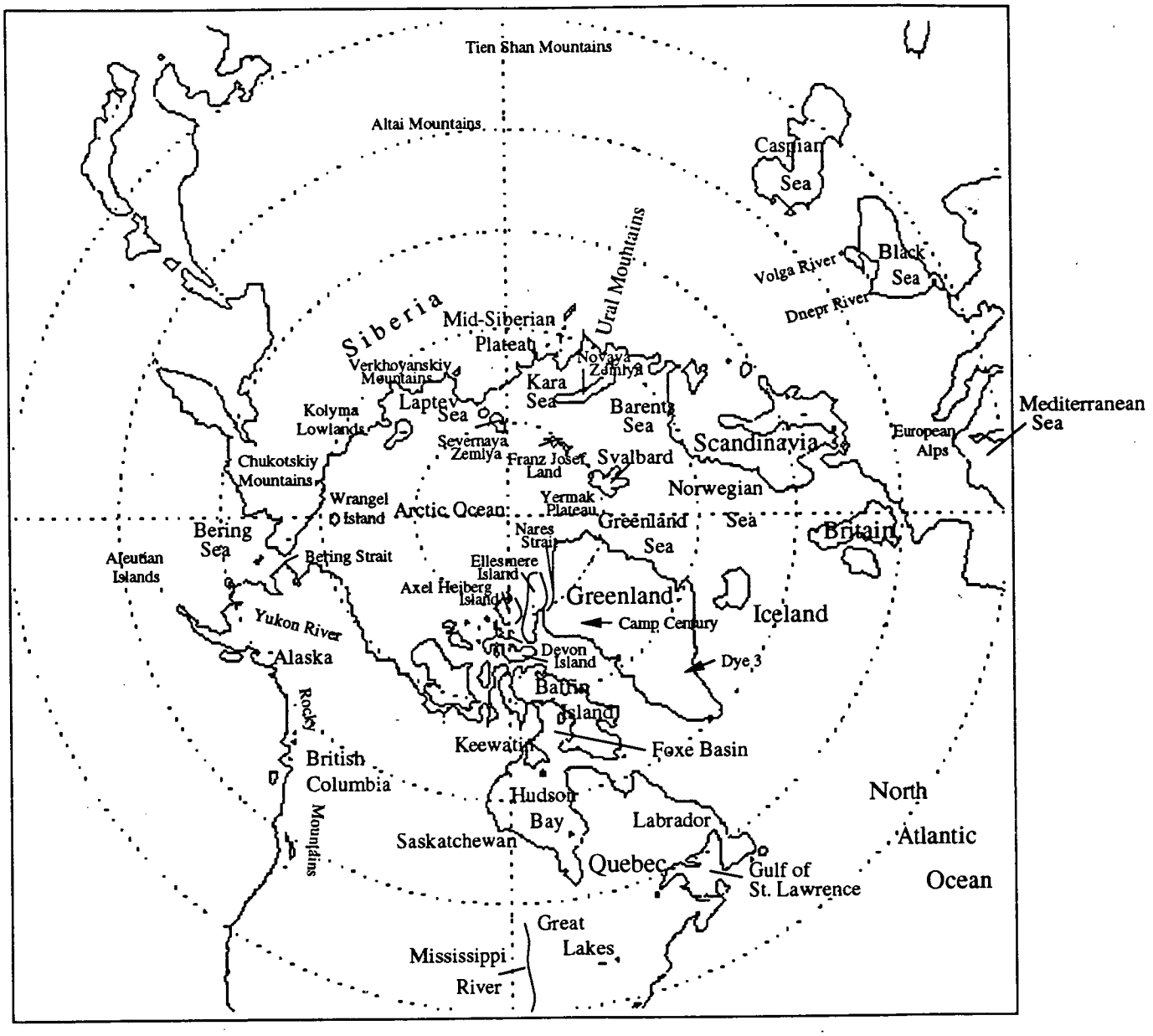

Figure 3.1: Northen hemisphere locations discussed in the text.

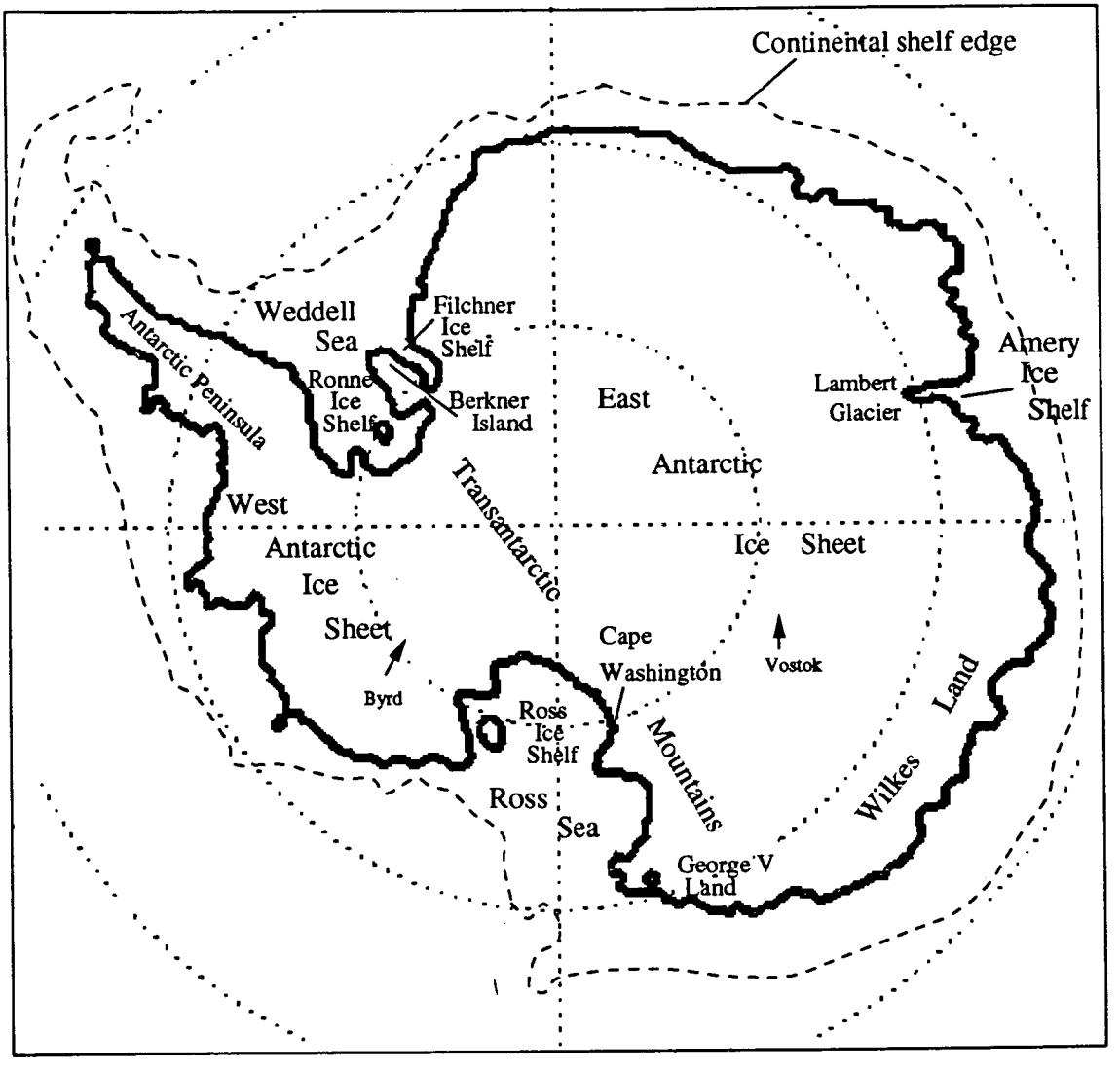

Figure 3.2: Antarctic locations discussed in the text.

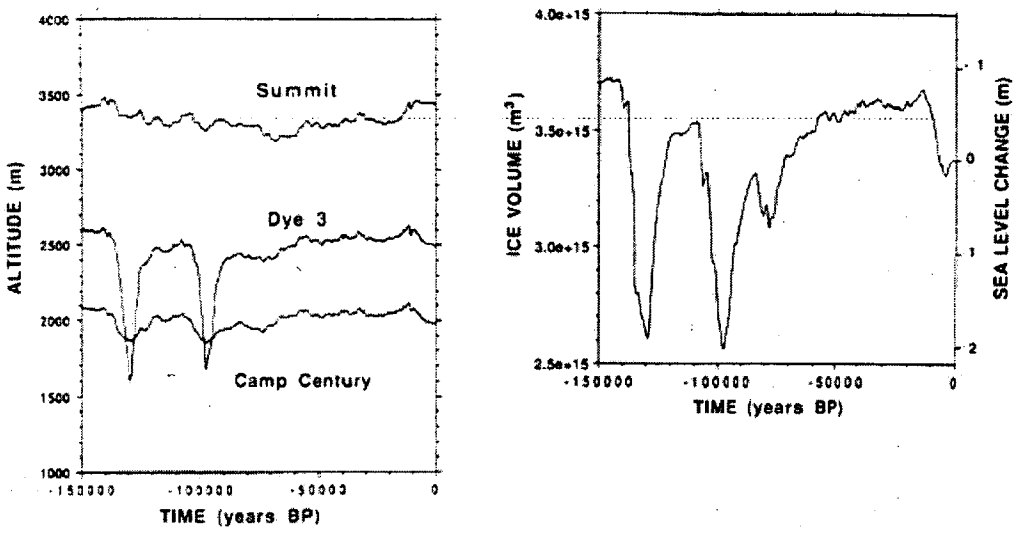

Figure 3.3: The modelling reconstruction of the Greenland Ice Sheet through the last 150ka of Létreguilly (1991). The plot on the left gives the ice thickness change for Summit, Dye 3 and Camp Century locations. The right plot shows the modelled ice volume changes.

thicknesses and elevations in central Greenland corresponding to glacial maxima due to low accumulation at these times. Figure 3.3 shows the change in ice thickness at three Greenland locations and the change in ice volume in Greenland over the last 150ka as modelled by Letréguilly et al. (1991).

The general stability of the ice sheet is supported by evidence of little major grounding line migration through the last glacial cycle in the east (Funder et al. 1994) and elsewhere (England 1985). The minor variation in ice thickness would only have allowed for similarly small oscillations in the bedrock height, in the order of 50m.

Regionally however, it appears that ice thickness in Greenland has varied more significantly during the ice age as the texture and chemistry at the bottom of the Camp Century and Dye-3 ice cores suggest that there may have been complete deglaciation there at the last interglacial (Koerner 1989), a result supported in part by the modelling of Letréguilly et al. (1991) who found that increased ablation at lower altitudes during isotopic substages 5e and 5c may have reduced the ice sheet thickness in the south west, contributing more than a

metre to sea level.

The extent of the connection between Greenland and the northern Canadian islands at maximum glaciation is unclear. Some have suggested that the ice margin at the LGM extended from north west Greenland to Ellesmere Island (Andersen 1981; Grosswald 1988), although there is evidence to suggest that there was no ice ridge in Nares Strait (England 1985).

Nevertheless, in comparison to the other large northern hemisphere ice masses, the Greenland Ice Sheet changed little during the ice age. It persisted through the last interglacial and into the current one and its contribution to change in sea level and the global environment was much less significant than that of the more variable ice sheets.

3.1.2 Laurentide and Cordilleran Ice Sheets

The Laurentide Ice Sheet, located in the north east of North America, was the largest of the transient ice masses of the last glacial cycle and held a large percentage of that transient ice. Although an enormous amount of data is required to complete the picture, reasonable geological reconstructions of ice sheet extent at the LGM and through the deglaciation have been made. Prior to the LGM however, reconstruction becomes less reliable. The limits of carbon dating and the effect of the last glacial advance in overwriting previous evidence render understanding of glacial extents earlier in the glacial cycle difficult (Clark et al. 1993).

As the last interglacial came to a close, iced regions began to appear and expand in northern Canada. It is thought that ice developed in Quebec and on Baffin Island, probably early in isotopic stage 5 (St.Onge 1987). From these source regions and later another in Keewatin, it appears that ice sheets expanded and by 116ka BP had developed across Quebec and Labrador and from Baffin Island across northern Canada (Andrews and Barry 1978), until around twenty thousand years after inception a large Laurentide Ice Sheet covered most of Canada east of British Columbia (Vincent and Prest 1987).

Figure 3.4 illustrates estimated glacial extent in various regions of the Laurentide and Cordilleran Ice Sheets during the last glacial cycle. For some regions where the data are ambiguous, an alternative reconstruction is shown.

According to this reconstruction, following the post interglacial growth the Laurentide Ice Sheet retreated and possibly disappeared in most regions, remaining only in northern Quebec and on Baffin Island and along the ice sheets northern margin (Boulton and Clark 1990). In fact the northern margin of the ice sheet may have reached its maximum extent for the glacial cycle at this time, in the early Wisconsinan, before retreating to a relatively stable state until the LGM when another, less significant advance occurred. There was mid Wisconsinan advance in Quebec and Keewatin and probably also westward into Saskatchewan and through the area south of Hudson Bay. It is unclear whether or not Hudson Bay was ice covered at this time (Dredge and Thorliefson 1987).

In the Rocky Mountains in the west, major ice advance may have been more limited with possibly only two periods of significant ice cap development. The Clark et al. (1993) reconstruction suggests that the Cordilleran Ice Sheet grew to one maximum around 80 ka BP, lasting only ten or twenty thousand years before retreating to where it existed only as remnant glaciers until readvancing in the build-up to the LGM. Although reconstructions of the LGM in North America commonly suggest some junction between the Laurentide and Cordilleran Ice Sheets, whether the ice sheets coalesced and to what extent is uncertain (Mayewski et al. 1981).

Other margins of the Laurentide Ice Sheet during the LGM are not exactly known, leaving the possibility of larger or smaller reconstructions (e.g. Hughes et al. (1981)). Establishing glacial extents is further complicated as the timing of the LGM was not necessarily synchronous between different latitudes. While the lobes on the southern inland margin reached their last glacial maximum extent at around 20ka BP (Ham and Attig 1996), it may have occurred sometime later at the northern extreme of the ice sheet (Clark et al. 1993). Nevertheless, in general the area occupied by the LGM Laurentide ice sheet is well established and reconstructions differ in the detail of the ice extent and in the ice thickness which is less easily estimated from geographical evidence.

Estimates of the thickness of the LGM Laurentide Ice Sheet have varied significantly, although reconstructions based on the deformation of the Earth and the bed depression residue from the Laurentide Ice Sheet exhibit reasonable agreement in their reconstructions of LGM thickness (Tushingham and Peltier

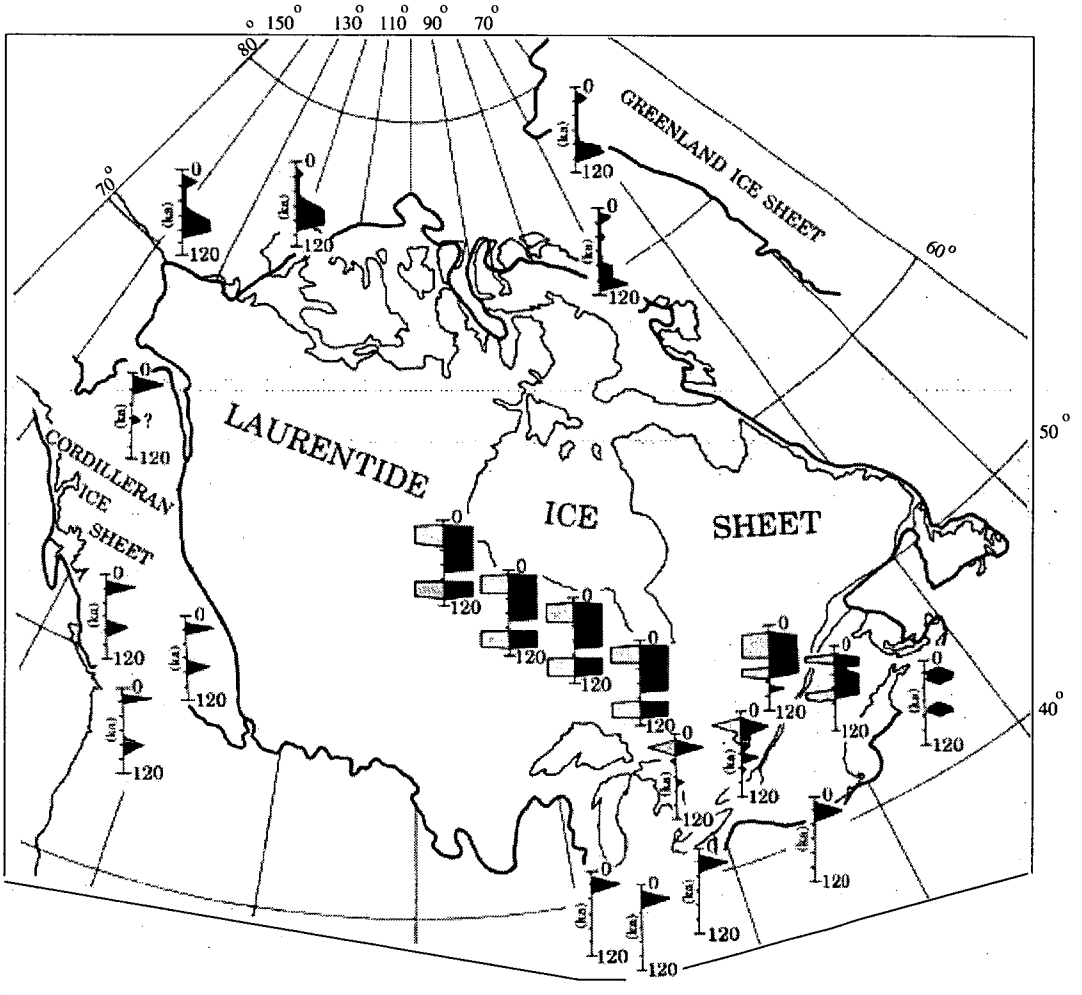

Figure 3.4: Reconstruction of the glacial histories of the Laurentide and Cordilleran Ice Sheets. The extent of glaciation at various locations is shown for the period of the last 120 ka. In some regions an alternative, and generally less extensive reconstruction is shown. Figure taken from Clark et al. (1993).

1991; Clark et al. 1994), which are not dissimilar to those shown in Figure 3.7, although these estimates are dependent on knowledge of the timing and duration of the ice cover - information which is still not well known.

Dyke and Prest (1987) presented a description of Laurentide deglaciation from the LGM, based on their collation of available field evidence. This is summarised as follows. Early signs of deglaciation following the LGM appeared in various regions at around 21ka BP. Initial retreat of the ice sheet was slow, and ice loss contributed to a thinning of the ice rather than a large change in extent. Retreat accelerated after about 13ka BP however, particularly in the inland regions in the south and west. While the collapse was not a simple continuous process, there being several readvances amongst the general retreat, by about 8ka BP, the ice sheet had reduced to 3 major domes in Quebec, Keewatin and Foxe Basin, with Hudson Bay ice free. These domes continued to retreat, with the Foxe dome reducing to small individual domes on the northern Canadian islands. Deglaciation had concluded by 6-7ka BP, leaving a similar distribution of ice to that which exists today - small ice caps on Baffin Island and some of the other northern islands.

3.1.3 Eurasian Ice Sheet

Britain, Scandinavia and Barents Sea

Glaciation in northern Europe following the last interglacial may have commenced slightly later than that in North America (although the evidence is not well dated) but it is thought that by mid isotopic stage 5d, having been initiated in highlands such as the northern Norwegian mountains, ice had spread across Scandinavia and into northern Europe (Mangerud 1991). Recession probably occurred in stages 5c and 5a, but a substantial ice sheet may have persisted into stage 4 when the Eurasian Ice Sheet began to grow towards a maximum at the LGM (Forsström 1996). Climatic oscillations occurred during this time and the growth may not have been continuous, with the likelihood of various minor retreats and readvances and a significant minimum achieved between 30ka and 40ka BP (Baumann et al. 1995).

It appears likely that glaciation occurred in the North Sea joining the

British and Scandinavian Ice Sheets, although this connection was probably brief, occurring just before the onset of the post LGM deglaciation (Sejrup et al. 1994). Maximum thicknesses of the major ice domes in the Eurasian Ice Sheet have been estimated as around 1500m or more in Britain (Hughes et al. 1981; Lambeck 1993), and over 3000m in Scandinavia (Grosswald 1993).

Figure 3.5 illustrates in broad brush strokes the pattern of deglaciation of the western Eurasian Ice Sheet after the LGM, according to a reconstruction by Elverhøi et al. (1993). Reaching its maximum extent between 22ka BP and 18ka BP, ice in Britain retreated quickly to the mountains in western Scotland where it may have survived until around 10ka BP (Lambeck 1993). According to some, the highly marine Barents Ice Sheet also retreated early, separating from the Scandinavian Ice Sheet around 13ka BP (Punkari 1995). Others feel that separation may have been later and less well defined (see Figure 3.6), before continuing to retreat towards the north and west and being lost in the western margin of the ice sheet over Novaya Zemlya and the Kara Sea and in the ice cap in Svalbard. The Scandinavian Ice Sheet was probably in retreat by 15ka BP (Lehman et al. 1991) and continued to retreat northwards into the Norwegian mountains, persisting until after 9ka BP (Andersen 1981).

Glacial advance and retreat in Iceland appears to follow a similar pattern to that in Scandinavia (Eiriksson et al. 1997), at least until the last maximum, which occurred late in Iceland, probably around 10ka BP and lasted only until about 9ka BP (Sigmundsson 1991). Retreat was probably also complete in Svalbard by 9ka BP, although it may have commenced earlier, around 14.5ka BP (Andersen et al. 1996).

Barents and Kara Seas

While some authors consider the glaciations in the Barents and Kara Seas to have formed relatively independent ice domes (Hughes et al. 1981), others suggest that there was a single dominant ice cap in the Barents-Kara region at the LGM (Grosswald 1993).

Grosswald (1980) interpreted geomorphological evidence as indicating that the Barents-Kara Ice Sheet formed initially as a marine ice sheet before spreading southward and inland. The limited evidence available for pre-LGM

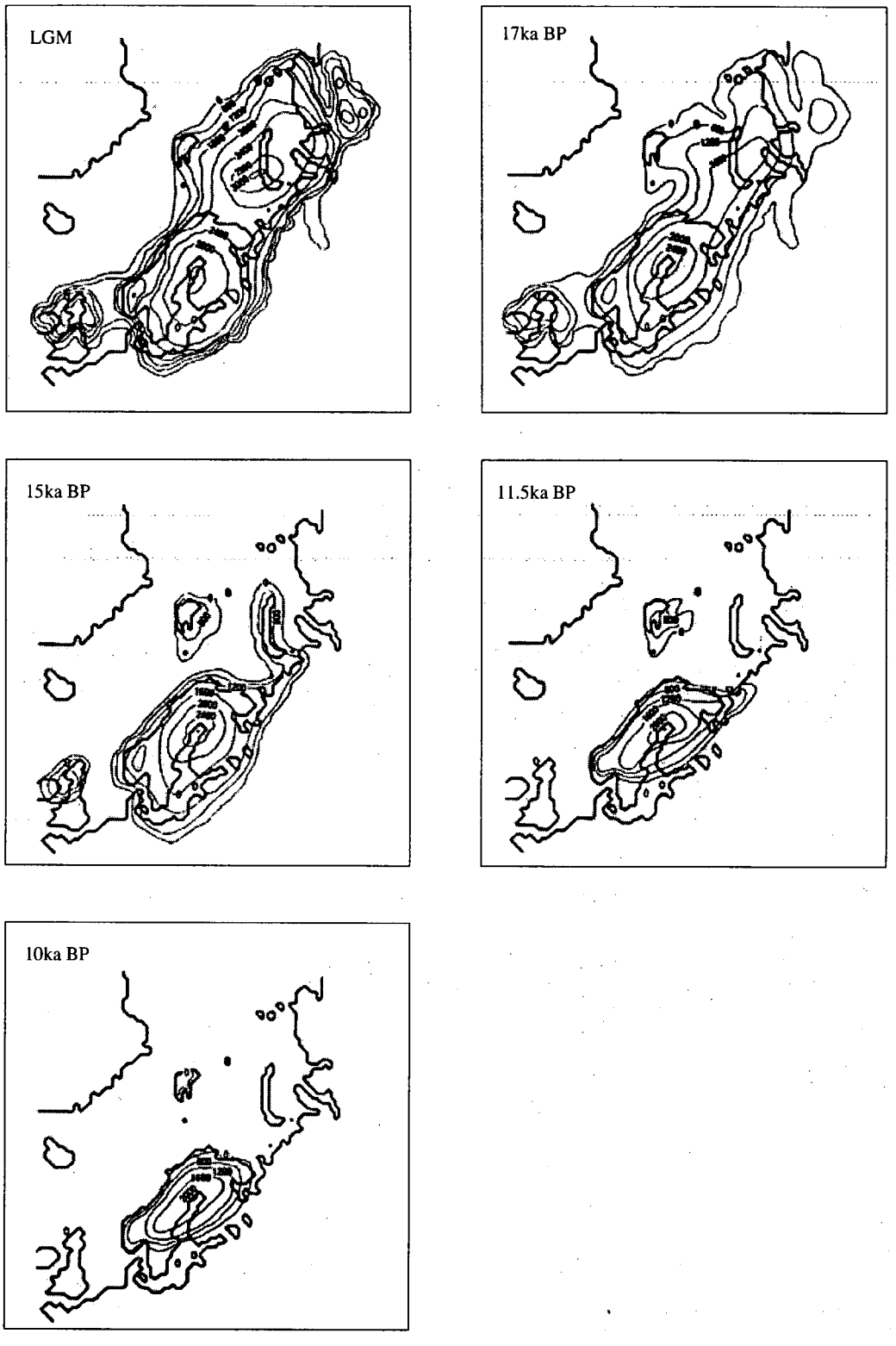

Figure 3.5: Deglaciation of the ice sheet in western Eurasia according to Elverhøi et al. (1993). The contours give estimated ice thickness in metres. Tentative timings for the stages are shown.

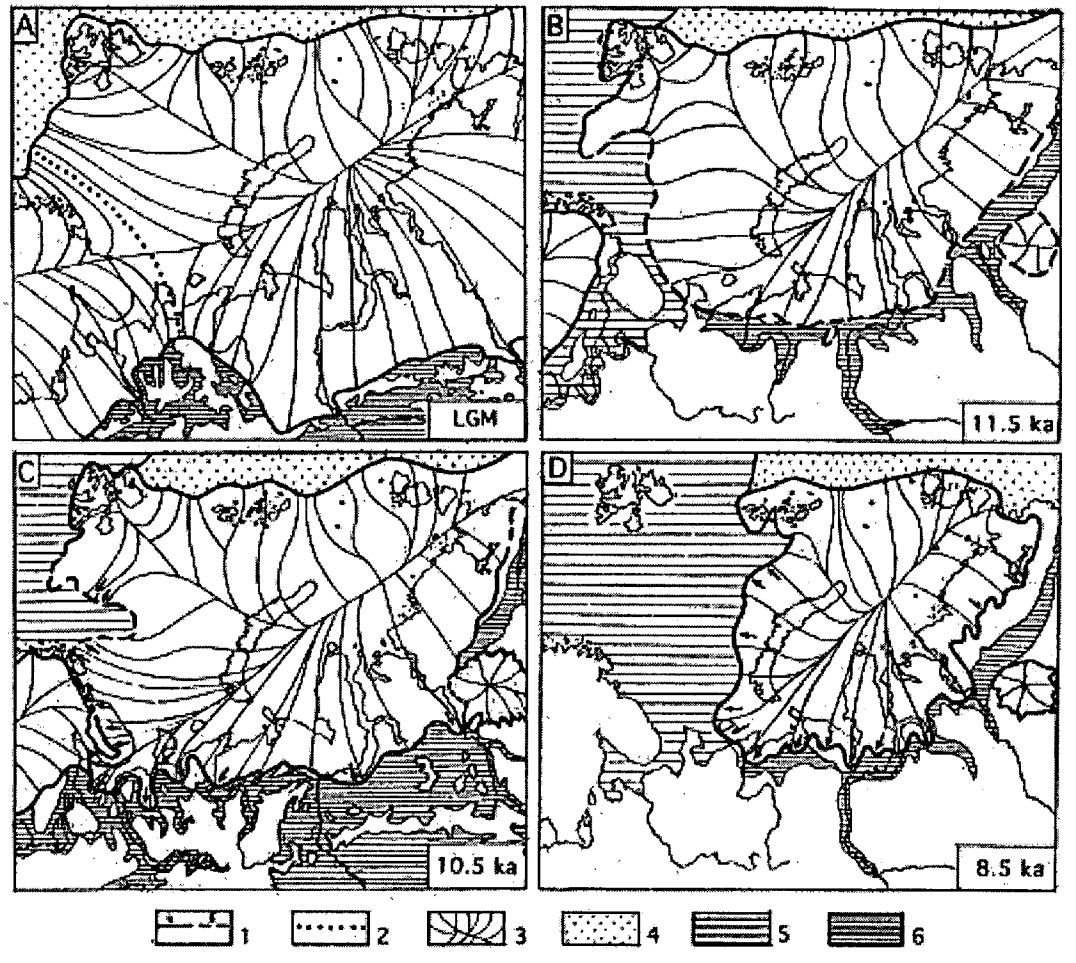

Figure 3.6: Deglaciation of the Barents-Kara ice sheet according to Grosswald (1993). The ice sheet margin (1), established (solid) and assumed (dashed) is shown, as is the LGM boundary with the Scandinavian Ice Sheet (2), inferred ice flowlines (3), floating ice shelves (4), open ocean (5) and proglacial lakes (6).

glacial activity in the region indicates that early Weichselian advance was significant and almost as extensive as at the LGM. Subsequent retreat and readvance probably followed a similar pattern to the fluctuations in Europe, with maximum extent being reached around 18-20ka BP (Andersen 1981).

Figure 3.6 shows the retreat of the Barents-Kara Ice Sheet according to Grosswald (1993). After disconnecting from the Scandinavian Ice Sheet the retreat continued eastward with the final ice dome in the Kara Sea not disappearing until after 8.5ka BP, and possibly not until after the other major ice domes had decayed (Grosswald and Hughes 1995). Other authors however

suggest that retreat may have been earlier and more dramatic (Lambeck 1995).

3.1.4 Siberian Ice Sheet

The extent of glaciation east of the Barents-Kara Ice Sheet to eastern Siberia and the Bering Strait is highly contentious (Biryukov et al. 1988; Hughes 1998). Reconstructions have generally indicated the growth of glaciers and ice caps in the mountains of eastern Siberia (Hughes et al. 1981; Grosswald and Hughes 1995) but the suggested size and interconnectedness of these ice caps varies. Geomorphological and relative sea level evidence have also suggested the existence of a large marine ice sheet in northern Siberia extending northward to the edge of the continental shelf (Peltier 1994; Hughes 1998) although again there is dispute over the extent. In the east, the Siberian Ice Sheet may have reached across the Bering Sea and beyond the present location of the mouth of the Yukon (Hughes 1998) (with implications for the Bering Strait land bridge (Hughes and Hughes)). In the south, some reconstructions have it joining with the glaciated Verkhoyanskiy and Chukotskiya Mountains. Further south, evidence for expanded glacial extent has been found in mountain ranges such as the Himalayas and the European Alps, although the timing of the glaciations may have been somewhat different to that of the large northern ice sheets, particularly in the more remote ranges (Sharma and Owen 1996). Like the Barents-Kara Ice Sheet, the Eastern Siberian ice sheet might have originally developed as a marine ice sheet in the north before spreading southward and establishing a continental presence (Grosswald 1980).

With so little known about the glaciation in this region, the history of deglaciation is all the more difficult to establish. However, using the sea level change during the period of deglaciation since the LGM as a constraint, Peltier (1994) suggested that deglaciation in the region was complete by 14ka BP.

3.1.5 Arctic

The reconstruction of individual northern hemisphere ice sheets discussed above produces an almost continuous band of ice around the arctic ocean at the LGM. With the Bering Strait closed due to the low sea level, only the narrow gap

between Greenland and Britain prevented the complete enclosure of the Arctic Ocean.

There is some suggestion that the Arctic Ocean itself was covered by a huge ice shelf (see Hughes et al. (1977), Denton and Hughes (1981), Grosswald and Hughes (1995)), connecting all the surrounding land and marine based ice sheets into a single dynamic system where northward draining ice from the ice sheets fed this ice shelf which in turn flowed into the North Atlantic. The ice shelf itself may have been necessary to the survival of the ice sheets and may have allowed the northern, marine margins of ice sheets to retreat later than the southern terrestrial margins (Hughes et al. 1977). Evidence of an abiotic Arctic Ocean between 33 ka BP and 13 ka BP (Jones et al. 1994) also supports the possibility of an Arctic Ocean covered by an ice sheet. Chappell and Shackleton (1986) suggested that such an ice shelf could explain discrepancies between relative sea level data and isotopic estimates of sea level change, by influencing the isotopic composition of the ocean without affecting sea level. They also indicated however that evidence from deep-sea cores in the Arctic (Markussen et al. 1985) did not support this theory.

Figure 3.7 illustrates such a unified system. Deep plough marks on the southern Yermak Plateau illustrate the flow of a thick ice shelf or ice bergs caught up in such an ice shelf (Vogt et al. 1994) and a pattern of glacial Arctic ice flow found by Bischof and Darby (1997) not compatible with present day ocean currents but which follows closely the surface slope of the ice shelf in the figure may be further evidence of the flow of an Arctic ice shelf.

The dynamic similarity between the present West Antarctic Ice Sheet and this Arctic Ice Sheet of the LGM has been pointed out by Grosswald and Hughes (1995). It is interesting to speculate as to how close to a complete grounding this Arctic ice shelf may have come.

Given that the existence of an Arctic ice shelf is not established, obviously estimating the timing of its retreat is very difficult. However Hughes et al. (1977) suggest that recession into the Norwegian Sea commenced around 14ka BP. Significant ice masses remain today in Greenland, on Ellesmere, Baffin, Axel Heiberg and Devon Islands of North America as well as in Iceland, Svalbard, Novaya Zemlya, Severnaya Zemlya and some smaller Arctic islands.

Figure 3.7: Reconstruction of the northern hemisphere ice sheets at the LGM according to Grosswald (1988). Explanation of the key: 1 - open ocean, 2 - emerged continental shelves, 3 - ice sheets, 4 - floating ice shelves, 5 - ice dammed and other meltwater lakes, 6 - ice shelf grounding lines, 7 - major spillways, 8 - pradolinas (Urstromtäler) and direction of water flow. The heavy shaded line gives the present continental outline.

3.1.6 Antarctica

Evidence from sea sediments suggest an ice sheet has existed in some form in Antarctica for millions of years (Kennett 1977; Crowley and North 1991). While much of the glacial change in ice distribution in the northern hemisphere occurred as the appearance and disappearance of large ice sheets, in the Antarctic an ice sheet was extant at the onset of the last glacial cycle. Although in comparison to the size of the ice sheet, variations in the ice sheet mass were probably relatively small, changes in the Antarctic cryosphere through the glacial cycle may have significantly contributed to sea level and climate change.

There is some evidence that conditions warmer than present during the last interglacial may for a brief period have corresponded to a sea level higher than present by as much as 6m (Harmon et al. 1981; Neumann and Hearty 1996). Given that ice core evidence exists for warmer temperatures (Barnola et al. 1991; Dome-F Ice Core Research Group 1998) and the speculation that the West Antarctic Ice Sheet may be inherently unstable (Weertman 1974), it is possible that a collapsed West Antarctic Ice Sheet could account for the sea level high. Some consider that warmer temperatures would not produce this effect (Bentley 1997) and with ice core records from the West Antarctic not reaching back to the last interglacial, the source of any interglacial sea level high remains unclear. Regardless, West Antarctic ice cores do establish the existence of an ice sheet there not long after the Eemian interglacial (Epstein et al. 1970) so the configuration of the Antarctic Ice Sheet can be considered to have remained fundamentally unchanged throughout the cycle, with a large East Antarctic ice sheet and a smaller, marine based West Antarctic Ice Sheet. Changes to the cryosphere during the cycle affected the thickness and extents of these ice masses without altering that basic structure.

From correlation with the glaciers in South America, some idea of the state of the Antarctic Ice Sheet prior to the LGM can be estimated, and it is believed that a minor maximum was attained at around 70ka BP (Mercer 1978), before a more recent maximum at the LGM, about 20ka BP.

Last Glacial Maximum

Depending on the bedrock topography and the ice dynamics, decreasing sea level allowed grounding lines to advance to varying extents during the ice age. The continental shelf edge defines the potential limits of the ice sheet and in East Antarctica, except in the main outflow regions of the glaciers and ice shelves, the ice sheet is currently grounded to very nearly the edge of the continental shelf. Therefore, in most of the East Antarctic, lower palaeo-sea levels would not have induced much expansion and LGM extents are estimated to correspond approximately to the present 200m isobath (Goodwin 1995) around the majority of the eastern margin. With the western edge of the East Antarctic ice sheet well constrained by the Trans Antarctic Mountains, the only opportunity for areal expansion in the east was in the Lambert Basin and over the small distance to the continental shelf edge. East Antarctica was then restricted to relatively small changes in thickness with estimates of maximum change in thickness and elevation being around 150m (Huybrechts 1992), primarily in response to accumulation change.

In the west however, present grounding lines are generally a long way south of the continental shelf edge, particularly in the Ross and Weddell Seas. This allows the possibility of there having been a significantly advanced grounding line at the LGM, compared to present. There has been much debate over the position of LGM grounding lines in the West Antarctic, with some authors tentatively favouring a grounding line in the Ross Sea at the edge of the continental shelf (Stuiver et al. 1981), although evidence of this advance may have been caused by a previous glaciation. Others suggest that the ice sheet was grounded to a point some distance south of the continental shelf edge, possibly not far from the present position (Drewry 1979; World Atlas of Snow and Ice Resources 1997). There is a possibility that changes in accumulation may dominate in the West Antarctic as well as the East as evidence from the Byrd ice core suggests that the ice there was thinner at the LGM than it is now (Raynaud and Whillans 1982), possibly due to variation in the accumulation rate. Certainly percentage changes in accumulation rates will have a larger effect at lower elevations where accumulation rates are higher than in central

East Antarctica, for example. Nevertheless, the weight of evidence supports an LGM grounding line in the eastern Ross Sea in the region of Cape Washington (Licht et al. 1996). Westward of there, palaeo-grounding line positions are less well known, although they are considered to be well short of the continental shelf edge (Licht et al. 1996).

Despite the evidence from Byrd mentioned above, it is also considered that the thickness of the ice in the Ross and Weddell Seas would have increased as the grounding line advanced and the ice slowed. However, how much thicker the ice became there is difficult to estimate and various profiles are possible (McInnes and Budd (1984), Denton et al. (1989) and see Figure 3.8 and Figure 3.9).

Contrasting interpretations of the grounding line position at the last glacial maximum exist also for reconstructions in the Weddell Sea. The scarcity of radiometric dates has made it difficult to determine the extent of glaciation at the LGM in the Weddell Sea region and any attempt is dependent on the untested assumption that evidence of the most recent glaciation there was produced at the LGM (Bentley and Anderson 1998). Employing this assumption, Bentley and Anderson (1998) found that the grounding line in the Weddell Sea advanced northward and eastward from the Antarctic Peninsula during the last glacial cycle until ice was grounded to the edge of the continental shelf by the LGM. This effect has also been reproduced by models and advance like this has been commonly regarded as the main source of the Antarctic's contribution to sea level lowering during that period (Huybrechts 1992).

However, due to the uncertainty in defining LGM grounding lines in the West Antarctic, 'large' and 'small' reconstructions are often shown together, illustrating the possible extremes in the extent of grounded ice. An example of this is shown in Figure 3.8 and Figure 3.9 from the World Atlas of Snow and Ice Resources (1997). The reconstructions show significant differences in the West Antarctic, with one indicating ice was grounded to the continental shelf edge at the LGM and the other exhibiting a grounding line only slightly more advanced than present in the Ross Sea and only significantly advanced in capturing Berkner Island in the Weddell Sea.

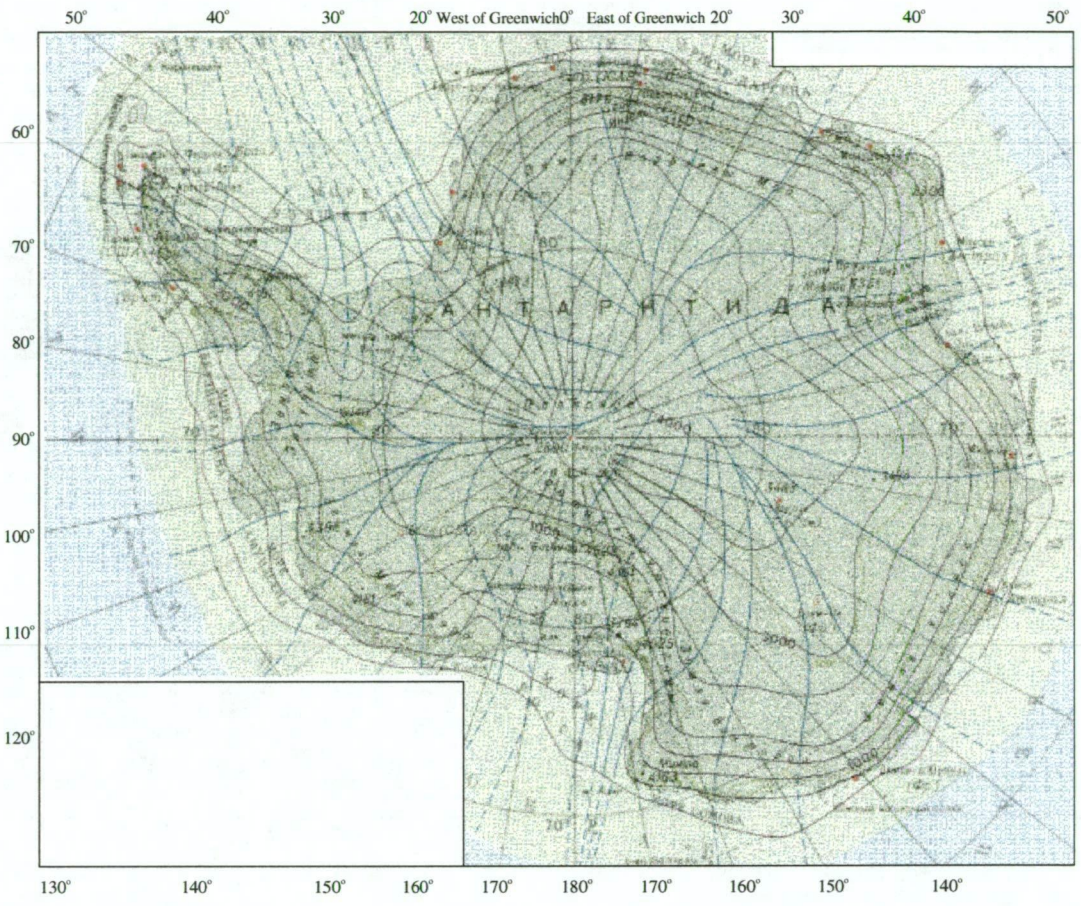

Figure 3.8: Maximum Antarctic reconstruction for the LGM according to the World Atlas of Snow and Ice Resources (1997). Proposed LGM elevation contours are in black and overlie a map of the elevations for the present Antarctic (green contours).

Deglaciation

According to Tushingham and Peltier (1991), deglaciation following the LGM commenced in Antarctica at the time of the maximum rate of deglaciation in the northern hemisphere, around 9ka BP by their estimates. This 'late' deglaciation (relative to that of the northern hemisphere) is supported by an overview o the Antarctic glacial history since the LGM by Ingólfsson et al. (1998) who found that most deglaciation occurred ~10-8ka but continued to some degree until 5ka BP. The delayed response of the isostatic rebound beneath the refloated ice shelves could also lead to later grounding line advance.

Steady state simulations of the Antarctic under various conditions have

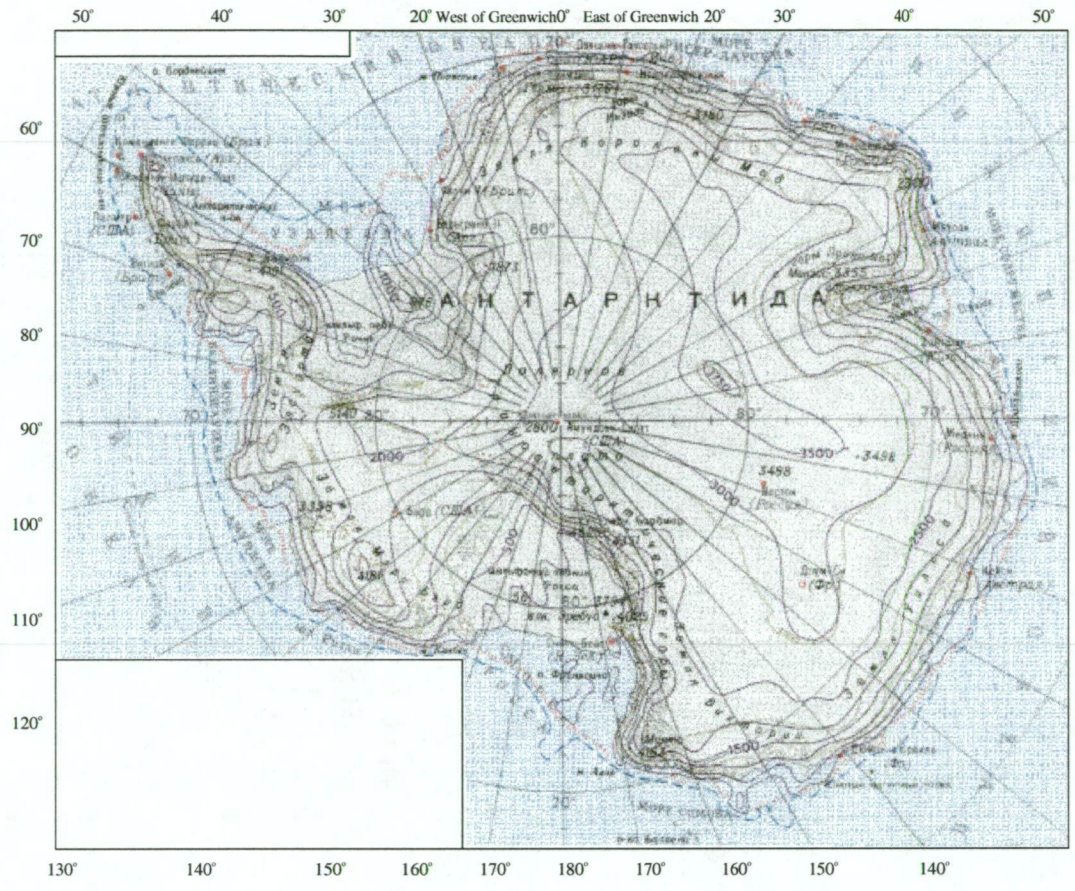

Figure 3.9: Minimum Antarctic reconstruction for the LGM according to the World Atlas of Snow and Ice Resources (1997). Proposed LGM elevation contours are in black and overlie a map of the elevations for the present Antarctic (green contours).

produced reasonable reconstructions of the present distribution of ice in Antarctica (Budd and Smith 1982; Oerlemans 1982; Coutts 1992). The Oerlemans model, which did not include basal sliding was used for simulations with sea level change. It was found that while grounding line advance occurred in the Ross and Weddell Seas for a sea level lowering of 100m, 600m of sea level rise was then required to refloat the ice there. Huybrechts (1990) and Huybrechts (1992) used a three-dimensional, thermomechanically coupled ice sheet-ice shelf model to simulate the behaviour of the Antarctic Ice Sheet through the last glacial cycle. Using temperature and sea level forcing, he found that due primarily to ungrounding in the Ross and Weddell Seas, the Antarctic contributed 12-15m to the sea level rise since the LGM. This was substantially

less than had been found by others (Nakada and Lambeck 1988; Tushingham and Peltier 1991), implying that more ice must have been held in the northern hemisphere ice sheets than had been thought. By forcing the ice sheet through the ice age cycle, the present state of balance of the ice sheet could also be investigated and it was found that while some regions were approaching a state of balance others were still responding to the changes in climate since the ice age.

Present Antarctic

Mass balance

The present state of the mass balance of the Antarctic is very poorly known. While estimates of the present values for fields such as ice thickness are available, it is estimated that the state of balance of the ice can only be calculated to ±20% (Warrick and Oerlemans 1990), or perhaps worse (Budd and Smith 1985; Budd and Jenssen 1989). More extensive measurements of ice velocities could improve this precision (Budd and Warner 1996) and there is the prospect of a better understanding of the state of balance of the Antarctic through direct measurement of elevation change via satellite (Wingham et al. 1998).

Nevertheless, Morgan and Jacka (1981) summarised mass flux estimates of the state of balance in East Antarctica, and while the values varied widely, all estimates were positive, indicating that the East Antarctic Ice Sheet is becoming thicker. Goodwin (1995) estimated that the Antarctic is in a state of slightly positive mass balance, but in summarising other studies found little agreement in the sign of the mass balance, with some authors calculating that the Antarctic mass is increasing and some that it is decreasing. Recent assessment of the net surface mass balance of the Antarctic however, suggests that these other studies may have underestimated the accumulation rate in Antarctica (Vaughan et al. in press). While still inconclusive, it appears that the best estimate of the state of balance of the ice sheet is that it is close to balance, perhaps slightly positive.

Figure 3.10 shows the balance velocities for the Antarctic Ice Sheet. While the accuracy of balance velocity calculations has limitations (Budd and Warner

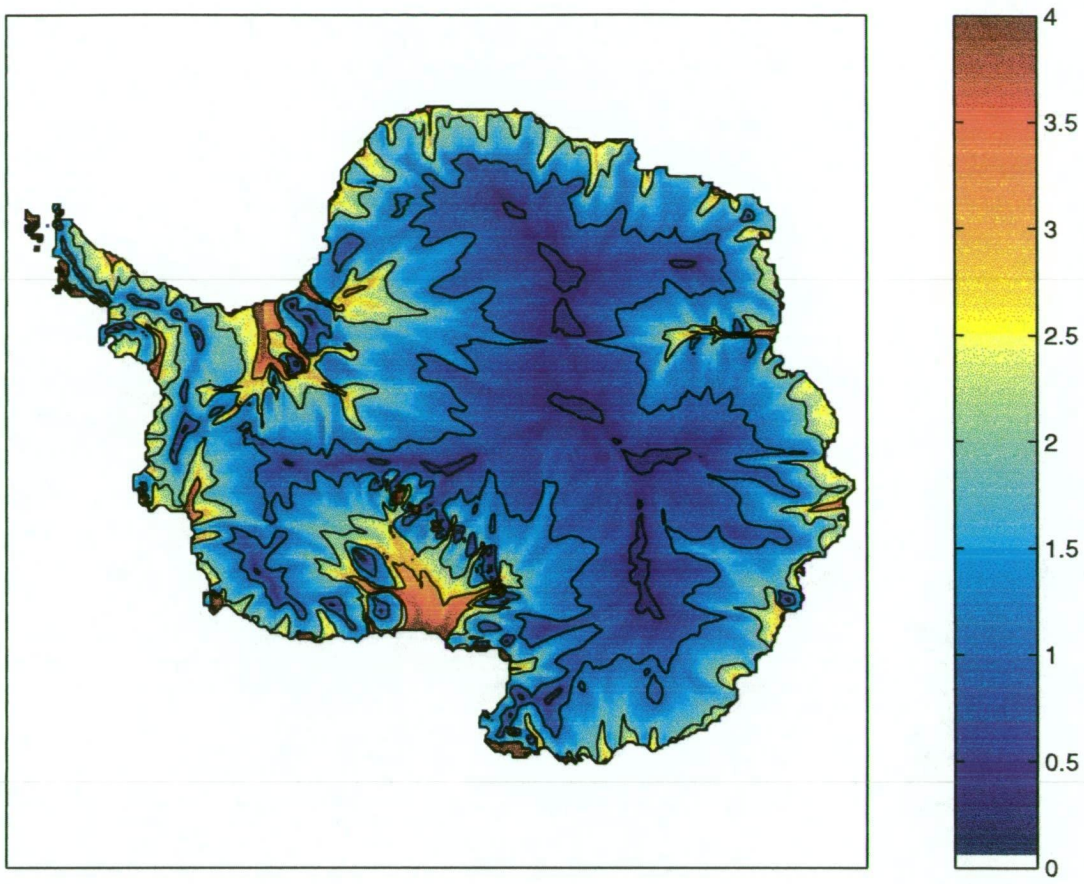

Figure 3.10: Antarctic balance velocities ($log(m\,a^{-1})$). Contours are at $2m\,a^{-1}$, $10m\,a^{-1}$, $100m\,a^{-1}$ and $1000m\,a^{-1}$.

1996), comparisons between balance and observed velocities suggest that in some coastal regions at least, the Antarctic is close to balance (Budd and Smith 1985). Observations in some parts of the West Antarctic Ice Sheet suggest that the ice thickness may be increasing in some locations and thinning in others but even if these estimates are accurate, their validity in long-term application is not established (Thomas et al. 1988; Wingham et al. 1998).

Ice and bedrock distribution

Figure 3.11 and Figure 3.12 show the present ice thickness and elevation distributions for the Antarctic respectively. The data comes from Budd and Jenssen (1989) who digitised the SPRI Map folio (Drewry 1983). The morphological division of the two ice sheets, East and West (defined by the

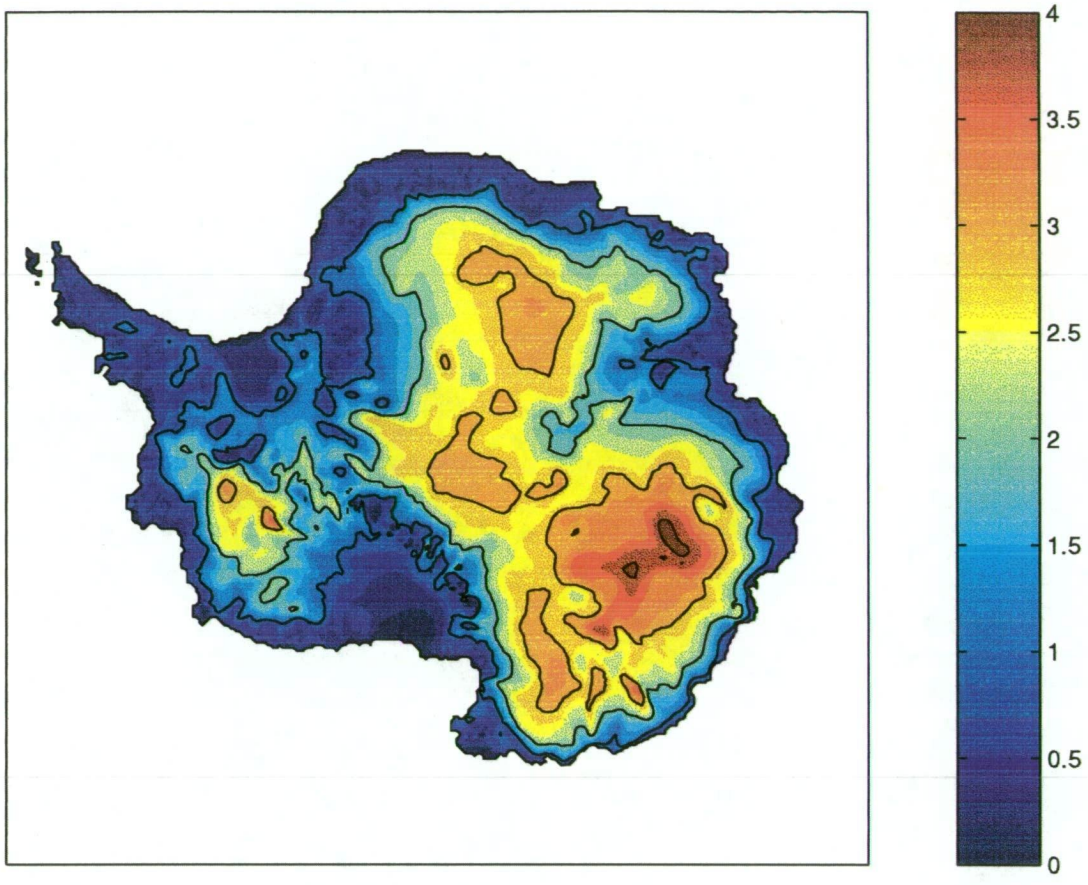

Figure 3.11: Present Antarctic ice thickness distribution (Budd and Jenssen 1989). Contours are at 1km intervals.

Transantarctic mountains and the eastern side of the Ronne-Filchner Ice Shelf) is obvious, with large areas of thick ice and high elevations in the East contrasting with more localised regions of thick ice amongst generally thinner ice in the West, where the surface elevations tended to be lower.

Figure 3.13 shows the present bed topography in the Antarctic (also from the data digitised (to 20km resolution) by Budd and Jenssen (1989) from the SPRI Map folio). Much of this bed is depressed due to the ice load (see Figure 3.11) on it and in some places would be up to 1000 metres higher if allowed to rebound to an ice-free steady state. Relaxing the bedrock in such a way would result in much of the bed in East Antarctica currently below sea level rising to become above sea level. However in West Antarctica, most of the bed would remain below sea level, making the West Antarctic Ice Sheet strongly

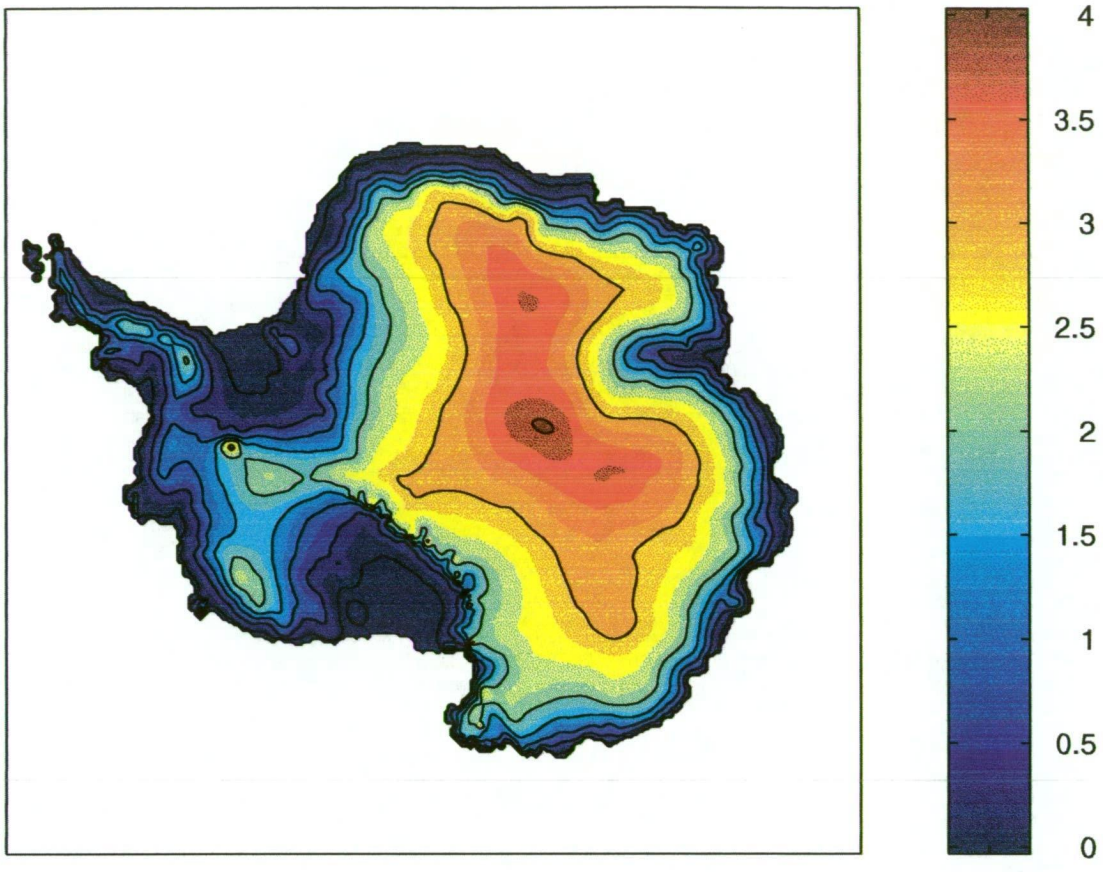

Figure 3.12: Present Antarctic ice elevation distribution (Budd and Jenssen 1989). Contours are at 0km, 100m, 500m, 1km, 1.5km, 2km and 3km.

marine and possibly susceptible to collapse (Weertman 1974). Also of note is the depth of water and topography beneath the Ross and Ronne-Filchner Ice Shelves where the ice may have advanced during the glacial cycle and retreated after the glacial maximum. Residual bed uplift beneath the ice shelves following the retreat of the ice since the glacial maximum may be responsible for present grounding line advance, leading to ice thickening in some sub ice shelf regions (Greischer and Bentley 1980).

3.1.7 Previous modelling reconstructions

Northern hemisphere

The modelling of the ice sheets of the northern hemisphere through the last glacial cycle has often been approached with individual ice sheets being

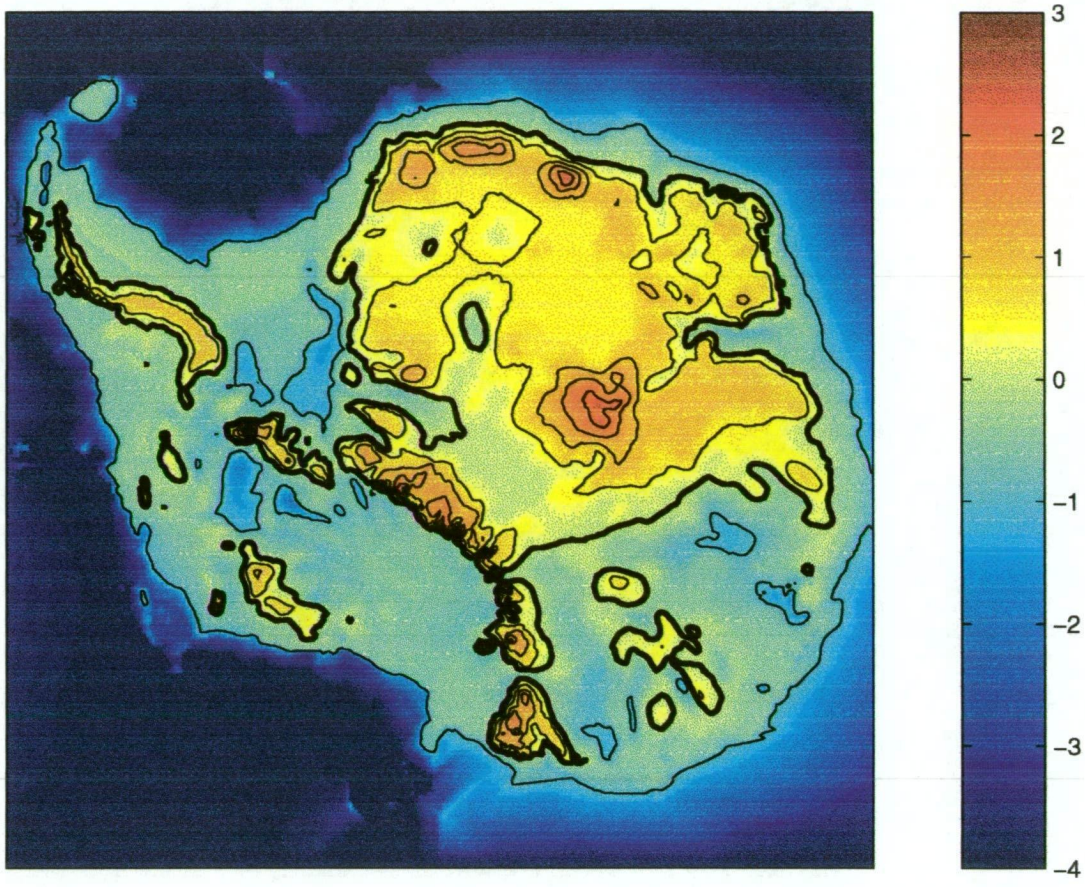

Figure 3.13: Present Antarctic bedrock elevation (Budd and Jenssen 1989). Thin contours are at -1km and every 500m from 500m. Sea level is shown as a thick contour.

modelled in isolation. Modelled reconstructions of the Greenland Ice Sheet (Letréguilly et al. 1991; Huybrechts 1994; Fabre et al. 1995; Greve 1997), the Laurentide Ice Sheet (Budd and Smith 1981; Budd and Smith 1987) and the ice sheets of Eurasia (Letréguilly and Ritz 1993; Siegert and Dowdeswell 1995; Grosswald and Hughes 1995) for ice age conditions have been performed. Some studies have modelled larger portions of the northern hemisphere but still through separate approaches to individual regions (Deblonde et al. 1992; Peltier and Marshall 1995).

Comprehensive models of the grounded ice sheets of the entire northern hemisphere include the steady state simulations of Huybrechts and T'siobbel (1995) and the ice age cycle reconstruction of Marsiat (1995), Greve

(unpublished) and Calov and Marsiat (1998). These, however do not include floating ice calculations and the issue of the likelihood and importance of an Arctic ice shelf was not addressed. Lindstrom and MacAyeal (1989) and Lindstrom (1990) included shelf dynamics when modelling the Eurasian and Siberian Ice Sheets, and found that their equilibrium reconstructions did in fact produce a thick and extensive Arctic ice shelf connecting the northern hemisphere ice sheets.

The northern hemisphere models generally produced results in reasonable agreement with observations except in Siberia and into Alaska where generally too much ice accumulated, although observations in this region are perhaps the least reliable.

The use of more sophisticated Energy Balance Models to generate climatic conditions influencing the modelled ice sheets did in some cases produce LGM ice sheets in good agreement with observations (e.g. Peltier and Marshall (1995)) and Siberian ice in these cases were generally less extensive. However this was not always so (Deblonde et al. 1992) and even when the maximum reconstructions were good, other comparisons with observation, such as during deglaciation, were not so successful and any advantage gained from coupling to an EBM is not obvious with simple parameterisations ultimately doing equally well, if not better.

Antarctic

The first attempt to dynamically model the Antarctic Ice Sheet and its ice shelves was made by Oerlemans (1982). Without accounting for basal sliding and using a simple diagnostic approach to the modelling of floating ice, this model was able to produce a reasonable match to the present Antarctic in many regions. The model exhibited a strong response to sea level lowering, with a sea level decrease of 100m resulting in extensive grounding. For this ice then to unground required a subsequent sea level rise of 600m.

Budd and Smith (1982) investigated the ability of an ice sheet model (similar to that they used for their investigation of the northern hemisphere ice sheets, in particular, the Laurentide Ice Sheet) to represent the Antarctic ice sheet but importantly included basal sliding. Their model also dealt with

floating ice but with ice shelf creep rate dependent only on the ice thickness. They pointed out that a thorough treatment of ice shelf dynamics required horizontal stress integrations.

A more sophisticated approach to modelling the Antarctic ice sheet was performed by Huybrechts (1990) and Huybrechts (1992). He used a three dimensional, thermomechanical model which included a more rigorous treatment of grounded ice flow as well as floating dynamics. Using observed climate and sea level records to supply forcing, this model was run through an entire glacial cycle.

Although it is recognised that there could be significant interaction between ice sheets in both hemispheres (Denton et al. 1986), there has been little attempt to model this cryospheric system as a whole. Zweck (1997) used an ice sheet model similar to that used in this report to establish values for isostatic parameters and lithospheric rigidity by modelling the deglaciation of primarily the Laurentide and Fennoscandian Ice Sheets. He used these values to then model the Antarctic Ice Sheet, and particularly the isostastatic response to changes in that ice sheet through a glacial cycle. His interest was more in the response of the bed than in that of the cryosphere.

This study is an investigation into the behaviour of the ice of the northern hemisphere and that of the Antarctic through the last glacial cycle through the use of an ice sheet model which includes sliding, dynamic ice shelves, isostatic response and simple thermodynamics. The modelling of each hemiphere is performed in isolation but the influences of the ice sheets on global sea level, climate and other ice sheets are also considered.

3.2 Sea level

Reconstructions of sea level change over the last glacial cycle have been based on evidence of relative sea level change such as in raised beaches (Chappell et al. 1996), free air gravity anomalies, observed non-tidal acceleration of the Earth and geomorphological data on ice sheet extents (Tushingham and Peltier 1991; Peltier 1994). Oxygen isotope ratios from sea sediment cores allow estimation of change in oceanic volume (Imbrie et al. 1984). The precision of

isotopic estimates has been brought into question however, as it has been found that the relationship between ocean and sediment isotope values is temperature dependent (Chappell and Shackleton 1986). Furthermore, it was also shown that the sea sediment $\delta^{18}O$ record was unreliable due to the mean isotope depletion changing with time (Mix and Ruddiman 1984). As ice sheets grow, changing climate and increasing ice sheet elevation encourage the formation of isotopically light ice at the expense of isotopically heavier ice which passes into the ocean, biasing the sea sediment record. The accuracy of sea level change estimates based on the evidence of raised beaches is also difficult to assess. As the beaches only form during periods of constant sea level, only certain periods through the glacial cycle are represented. That these records are of relative sea level also contributes to uncertainty, as the relative tectonic motion of the land there must also be estimated. Relative sea level changes will effectively be different at different locations and establishing a global relative sea level pattern is problematic. Sea level curves based on geomorphological evidence of ice sheet extent are limited by their ability to estimate ice thickness and bed depression (which is dependent on the ice distribution and the duration of the ice sheet). Some models have combined several of these data sources to reconstruct sea level change (Tushingham and Peltier 1991; Peltier 1994). However, these models may have suffered from their dependence on carbon dating, the precision of which has been questioned, and their failure to allow for variation in the Earth's spin axis may also have lead to some error (Bills and James 1996).

There has been considerable variation in sea level change estimates based on these various methods. Denton et al. (1986) estimated that sea level must have varied by an amount between 127m and 163m from the LGM to present based on ice sheet reconstructions. Others have suggested that the range of maximum sea level change is more likely between 115m and 150m (Nakada and Lambeck 1988). Chappell et al. (1996) compared the $\delta^{18}O$ record to that of raised beaches from several sites to produce the reconstruction shown in Figure 3.14. There is an apparent sawtooth nature in the sea level change shown in this figure. It should be noted however that the interpretation of isotope anomalies which contributed to this reconstruction were based on the assumption that the isotope distribution in the ice sheets was in equilibrium

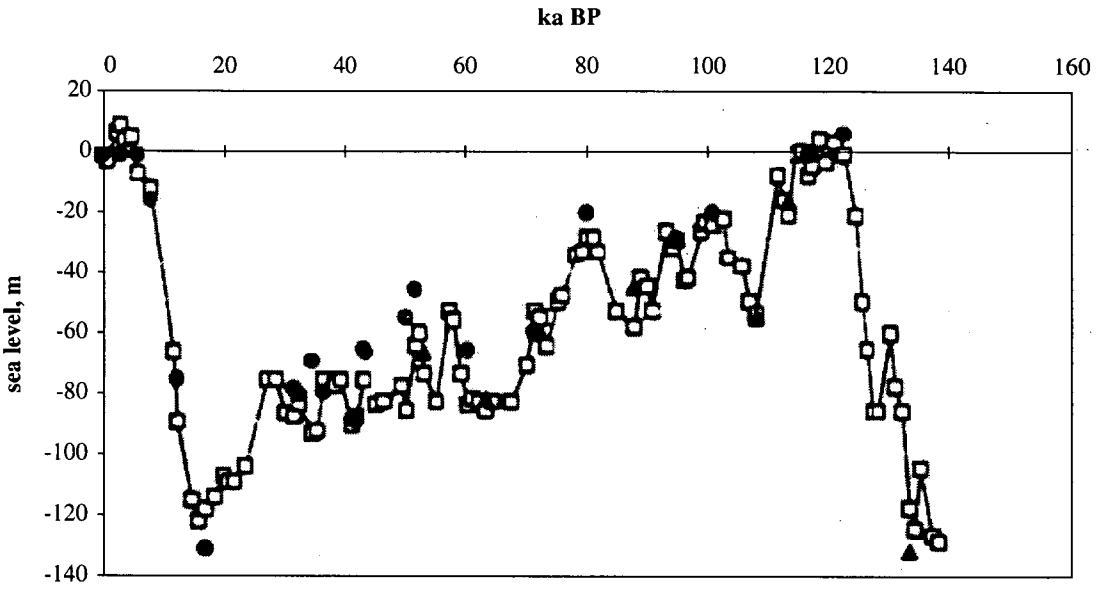

Figure 3.14: Sea level change through the last glacial cycle according to Chappell et al. (1996). The black dots are data from Huon Peninsula (New Guinea) coral terraces. The white squares are from $\delta^{18}O$ data. The black triangles are undated sea levels from the Huon Peninsula.

through the glacial cycle. This was probably not the case as there would have been a greater isotopic depletion in the ice sheets later in the glacial cycle when they were thicker and higher. Failure to allow for this effect tends to increase the sawtoothed nature of the reconstruction.

According to this curve, sea level can be seen to increase from more than 120m below the present level to a peak during the Holocene, before decreasing again over the last ~5ka to present. A Holocene relative sea level peak followed by a decrease in relative sea level to present was also suggested for various regions by Clark et al. (1978). They estimated mid-Holocene relative sea level peaks may have been 2-4 m above present sea level. It was found that regions above sea level which had previously been ice covered experienced a decrease in relative sea level throughout the Holocene, while the oceanic regions surrounding the locations of the former ice sheets experienced an increase in relative sea level.

3.3 Younger Dryas

While records such as the sea level curve shown in Figure 3.14 exhibit relatively constant change from LGM to the Holocene, other high resolution records show that the progression from glacial maximum conditions was not monotonic. Ice core records show that post glacial maximum warming was interrupted and returned to almost glacial levels for ~1000 years (Dansgaard et al. 1993; Mayewski et al. 1996). While the cold episode is considered to have occurred ~12ka BP, the cooling appears in some records to have commenced as early as ~14.5ka BP. This Younger Dryas episode was apparently strongest in the North Atlantic region, although its influences were felt worldwide (Denton and Hendy 1994). Also characterised by changes in the surface ocean circulation (Lehman and Keigwin 1992), possible causes for the cold reversal are an influx of freshwater into the North Atlantic due to altered ice drainage patterns or an increase in the melt rate from northern ice sheets. There is evidence of meltwater pulses into the North Atlantic Ocean at ~14-13ka BP and again at and ~11-10ka BP (Fairbanks 1989).

3.4 Summary

The palaeo-record of ice extents and thicknesses and their change through time based on observation has been investigated. This may be used to evaluate the model reconstructions discussed in chapters 6 and 7. The ability of the model to reproduce observed reconstructions will be dependent on the nature of the forcing and so that forcing will be constrained by the need of the model to match the palaeo-record. This will allow certain aspects of the glacial climate to be estimated.

Evidence of ice sheet margins and thicknesses prior to the LGM is sparse and imprecise. The most reliable evidence to be compared to model output is from the LGM until present. During this time there was enormous retreat of the northern hemisphere ice sheets, except that of Greenland, which remained intact. In the Antarctic, there was probably some amount of grounding line retreat, particularly in the West Antarctic and the embayments currently

occupied by the Ross and Ronne-Filchner Ice Shelves. It is likely that ice thickness changes in West Antarctica were also strongly influenced by variation in the accumulation rate. In East Antarctica, ice thickness and surface elevation were driven primarily by accumulation change.

The modelled Antarctic Ice Sheet may also be compared to what is known of the existing ice sheet. The distribution of ice is reasonably well known in Antarctica but the state of mass balance of the ice sheet is not. From the evidence available it appears that for much of the coastal margin the Antarctic Ice Sheet is within 10 or 20 percent of balance. Overall the ice sheet may be in a state of slight positive mass balance.

Although the amplitude of variation in sea level during the glacial cycle is not well known, a value in the range 120m - 150m appears a reasonable estimate. Modelling the ice sheet changes through the last glacial cycle will allow an estimate of the eustatic sea level changes which occurred to be made and allowing for isostatic effects, this may be compared to observations. Some reconstructions of postglacial sea level indicate that a sea level high was reached during the Holocene, following which sea level has decreased to its present level.

While the climate since the LGM is generally characterised by warming, the Younger Dryas cold episode appears to have occurred between ~14.5-11 ka BP. This may have been initiated by an influx of cold water into the North Atlantic Ocean from the melting northern hemisphere ice sheets.

Chapter 4

The ice sheet model

An ice sheet model similar to, but developed from that described by Coutts (1992) and Mavrakis (1992) is employed in this study. The characteristics of this model are discussed here. Minor differences between the model used to model the northern hemisphere ice sheets and that used to model the Antarctic ice sheet are pointed out.

In modelling the ice sheet dynamics, internal deformation of the ice and basal sliding are considered. The ice sheet model is coupled to an ice shelf model which includes the dynamics of floating ice, allowing the modelling of an ice sheet-ice shelf system. A simple approach is taken to the temperature dependence of the ice flow for both grounded and floating ice. The isostatic response of the bedrock to changes in the overlying ice and sea water load is also modelled. Ice enters the ice sheet-ice shelf system as solid precipitation. The precipitation rate is considered to decrease with altitude and this effect is reproduced in the model through an 'elevation-desert effect'. Ice may be removed from the modelled system through calving, ocean melt, and ablation. The grounding line is not fixed, but rather is calculated within the model, and it is found that while the grounding line may be influenced by changes in sea level, the exact nature of this influence is complex.

4.1 Ice dynamics

Given an ice and mass balance distribution, and assuming incompressibility, the change in ice thickness at a point is determined by the mass balance and the divergence of the flux which is dependent on the horizontal velocity field.

Changes in mass for an ice sheet are assumed to be described by the continuity equation:

$$\frac{\partial D}{\partial t} = \nabla.\vec{F} + M \tag{4.1}$$

Where D is the ice thickness, t is time and M is the mass balance (accumulation-melt). $\nabla.\vec{F}$ is the flux divergence where the flux is given by:

$$\vec{F} = \vec{v}D \tag{4.2}$$

where $\vec{v}$ is the depth averaged ice velocity.

For grounded ice the velocity consists of two components, that due to the internal deformation of the ice and that due to the sliding of the ice over its bed. These components of the velocity must be found separately and summed, providing the total velocity for calculation of the flux divergence. The velocities of floating ice shelves are found using different dynamics again.

4.1.1 Deformation velocity

In order to find the flux divergence in equation 4.1, horizontal velocities must be calculated. By considering ice as a polycrystalline solid, Glen found a flow law for the creep of polycrystalline ice (Glen 1955). This flow law relates the shear strain rate ($\dot{\epsilon}_{ij} = \frac{1}{2}\left(\frac{\partial v_i}{\partial x_j} + \frac{\partial v_j}{\partial x_i}\right)$) to the applied shear stress. For flow in the x and y directions respectively, it may be expressed as:

$$\dot{\epsilon}_{xz} = k_d \tau^{n-1} \tau_{xz} \tag{4.3}$$

$$\dot{\epsilon}_{yz} = k_d \tau^{n-1} \tau_{yz} \tag{4.4}$$

where $\dot{\epsilon_{xz}}$ and $\dot{\epsilon_{yz}}$ are the strain rates and k_d is a temperature dependent factor which is discussed later. The value of the exponent n varies over large changes in stress, but in ice sheets shear stresses generally do not exceed 2 bar (200kPa) and for this range, a value of $n = 3$ is generally considered appropriate (Jezek et al. 1989). τ is the effective shear stress and τ_{xz} and τ_{yz} are the driving stress components.

Hutter (1983) shows that for grounded ice, because longitudinal strain rate variations are small compared to changes in the vertical, a 'shallow ice approximation' is possible. By considering the longitudinal strain rates to be negligible compared to shear strain rates, the pressure gradient caused by the ice surface slope must be balanced by the horizontal and transverse shear stresses. By further assuming that the transverse shear may be neglected for grounded ice sheets, the driving stresses for ice deformation may be expressed as:

$$\tau_{xz}(z) = -\rho g(S - z)\frac{\partial S}{\partial x} \tag{4.5}$$

$$\tau_{yz}(z) = -\rho g(S - z)\frac{\partial S}{\partial y} \tag{4.6}$$

where $\tau_{xz}(z)$ and $\tau_{yz}(z)$ are respectively the horizontal shear stresses in the x and y directions at height z. ρ is the ice density, g the acceleration due to gravity, and S is the surface elevation. The change of S with horizontal distance is the surface slope. The use of the slope itself here, rather than the sine of the slope, is considered valid where the slope is small and the mean slope is calculated over distances an order of magnitude greater than the ice depth (Souchez and Lorraine 1991). Some modelling of the Antarctic was done at a resolution of 20km, only ~5 times the magnitude of the thickest Antarctic ice. However, the surface slopes in these areas of thick ice tend to be slight and constant over large areas allowing this assumption to remain valid (D. Jenssen pers.com). Where the slopes are higher and more spatially variable the ice tends to be thinner, satisfying the above requirement.

The relationship between strain rate and velocity may be approximated by $\dot{\epsilon}_{xz} = \frac{1}{2}\left(\frac{\partial v_x}{\partial z}\right)$. This enables the calculation of deformation velocity at any height in the ice, by integrating equations 4.3 and 4.4 with respect to height:

$$v_{def}(z) = -2(\rho g)^3[\nabla(S).\nabla(S)]\nabla(S)\int_{S-D}^{z} k_d(T(z))(S - z)^3 dz \tag{4.7}$$

The -ve sign indicates that the flow is in the direction of decreasing surface height.

The dependence of the factor k_d on temperature is strong. As the warmest part of the ice sheet is in the basal layers, that is where the deformation is most

significantly affected by the ice temperature and where most deformation occurs. This effect is produced to some extent by the cubic nature of the flow law employed. However, by considering the basal temperature only, a convenient approximation of the effect of temperature on ice deformation can be made. This simplifies equation 4.7 and means that velocity and temperature profiles need not be calculated for every ice layer. Horizontal velocities calculated for each ice layer but dependent on the ice temperature and shear stress at the base of the ice can then be found. By further integrating these velocities over the ice thickness and dividing by that thickness, an expression for the depth averaged velocity results:

$$v_{def_x} = -\frac{2}{5} k_d (\rho g)^3 D^4 \left[\left(\frac{\partial S}{\partial x} \right)^2 + \left(\frac{\partial S}{\partial y} \right)^2 \right] \frac{\partial S}{\partial x} \tag{4.8}$$

$$v_{def_y} = -\frac{2}{5} k_d (\rho g)^3 D^4 \left[\left(\frac{\partial S}{\partial x} \right)^2 + \left(\frac{\partial S}{\partial y} \right)^2 \right] \frac{\partial S}{\partial y} \tag{4.9}$$

4.1.2 Sliding velocity

Establishing a general theoretical description of the basal sliding of ice has been made difficult by the scarcity of reliable data. Information from the base of ice sheets and glaciers is scarce and not necessarily reliable (Paterson 1981). Significant inaccuracy has also been found in laboratory experiments (Weertman 1979). Nevertheless, sliding mechanisms such as regelation and enhanced plastic flow have been proposed (Weertman 1957) and validated (Kamb and LaChappelle 1964), and some empirical relationships between sliding and large scale, measurable parameters have been established. Most of these are of the form (Paterson 1994):

$$v_{sliding} = k_s \frac{\tau_b^p}{N^q} \tag{4.10}$$

where N is the effective normal pressure, k_s is dependent on ice temperature and also on bed roughness (Paterson 1994). As the nature of the bedrock surface is generally poorly known however, k_s is here considered to vary with basal temperature only (see Section 4.1.4) and bed roughness is considered constant. From laboratory tests Budd et al. (1979) found that q=1 and that p

varies depending on the normal load. τ_b is the basal shear stress, given (in the x direction) by:

$$\tau_{b_x} = \rho g D \frac{\partial S}{\partial x} \tag{4.11}$$

Following the work of Budd et al. (1979) and McInnes and Budd (1984), who successfully modelled the behaviour of surging glaciers, a sliding velocity relationship has been developed for use in the present ice sheet model.

$$v_{sliding} = k_s \left(\frac{\tau_b}{(s_1 + z_* + s_2 z_*^2)^2} \right) \tag{4.12}$$

where z_* is the thickness of ice above the thickness which just allows buoyancy. This thickness above buoyancy is given by:

$$z_* = -0.02\frac{\rho_i}{\rho_s} + S - \left(1 - \frac{\rho_i}{\rho_s}\right) D \tag{4.13}$$

where $\rho_i (= 910 kg\, m^{-3})$ and $\rho_s (= 1027 kg\, m^{-3})$ are the densities of ice and sea water and S is the surface elevation. The first term on the right hand side of the equation accounts for an extra 20m of thickness due to snow and firn. When equation 4.13 produces negative values, z_* is set to zero.

In equation 4.12, s_1 is a constant $(= 50 m^2)$ which ensures that as z_* approaches zero, sliding velocity does not go to infinity. In reality lateral stresses become significant as the normal load becomes small and the s_1 constant parameterises this effect. The value of $s_2 (= 3.5 \times 10^{-3} m^{-1})$ is chosen to define the normal load where the influence of sliding begins to 'cut off'. It is considered by many (e.g. Huybrechts (1992)) that basal sliding only occurs in the presence of meltwater, which provides a thin film of water between ice and bedrock. In these cases sliding is only permitted when basal temperatures reach the pressure melting point. Shreve (1984), however found that some sliding is possible when the ice rests directly on the bedrock, although this motion will be much slower than for an ice/water/bedrock interface. This is significant because if the basal phase of the ice is considered an 'on/off' switch for sliding, discontinuities in the sliding velocity will arise. While considered to be dependent on basal temperatures (see Section 4.1.4), the sliding velocity calculated here is continuous, although it decreases rapidly when the normal

load becomes large. The s_2 constant helps produce this effect, and largely determines the load where the transition occurs from regions where sliding is dominant, to regions where deformation dominates.

4.1.3 Ice shelf velocity

Mavrakis (1992) found that a simple ice shelf model which matched observed ice shelf velocities was possible if the important features of embayed ice shelves were captured. For the sake of model computation speed, this simple approach is adopted here, with some modifications made to the method employed by Mavrakis. The ice shelf dynamics employed here are a development from those those used in the Antarctic modelling of Budd et al. (1994) and differ from the 'Weertman-type' thinning used by (Budd and Warner 1998).

MacAyeal (1994) shows that for ice shelves the stress equilibrium equation (for flow in the x direction) may be written as:

$$\frac{\partial}{\partial x}(2\bar{\nu}D(2\frac{\partial u}{\partial x}+\frac{\partial v}{\partial y}))+\frac{\partial}{\partial y}(\bar{\nu}D(\frac{\partial u}{\partial y}+\frac{\partial v}{\partial x}))=\rho g D\frac{\partial S}{\partial x} \tag{4.14}$$

where z_s is the ice surface elevation and $\bar{\nu}$ is the depth averaged effective viscosity. $\frac{\partial S}{\partial x}$ is the surface slope which we henceforth call α.

Considering longitudinal strain rate gradients to be small in comparison to the shear strain gradients and ignoring flow across the ice shelf, this reduces to:

$$\frac{\partial}{\partial y}(\bar{\nu}D\frac{\partial u}{\partial y})=\rho g D\alpha \tag{4.15}$$

If the average thickness and slope ($\bar{\alpha}$) are used, and equation 4.15 is integrated across the flow from the centre line (where $\frac{\partial u}{\partial y}=0$), we get:

$$\nu\frac{\partial u}{\partial y}=\rho g\bar{\alpha}(y-y_c) \tag{4.16}$$

where $y-y_c$ gives the distance from the centre of the channel.

Following the ice flow law we take the viscosity, $\nu=(\frac{\partial u}{\partial y})^{-\frac{2}{3}}A^{-\frac{1}{3}}$, where A is a temperature dependent flow factor (see Section 4.1.4). A further integration across the channel yields an expression for the velocity difference from that of the central flowline:

$$u_y - u_{y_c} = \frac{1}{4}A(\rho g\bar{\alpha})^3(y - y_c)^4 \tag{4.17}$$

Maximum velocity is along the central flowline (u_{y_c}), and may be inferred from the assumption that the ice shelf dynamics produce no motion at the side boundary of the ice shelf ($u(2y_c) = u(0) = 0$). An expression for the velocity at a distance y across the ice shelf, depending on channel width and position in the channel, then results:

$$u_y = \frac{1}{4}A(\rho g\bar{\alpha})^3\left(y_c^4 - (y - y_c)^4\right) \tag{4.18}$$

It is considered the velocity of the ice in the ice shelf will not only result from the dynamics of the floating ice, but also from the existing velocity of the ice as it flows into the ice shelf across the grounding line. This 'background' velocity is calculated as an average of the upstream grounded velocities and is added to the floating dynamics velocity (u_y) to give the total velocity at any point on the ice shelf. This approach was found to give a reasonable approximation of observed distributions of velocities across existing ice shelves (Mavrakis 1992). Including the 'background' velocity, equation 4.18 becomes:

$$u_y = \frac{1}{4}A(\rho g\bar{\alpha})^3\left(y_c^4 - (y - y_c)^4\right) + u_g \tag{4.19}$$

where u_g is the velocity at the grounding line entering the ice shelf.

Finding the channel width

It can be seen that the velocity at any point on the ice shelf is dependent on y_c, a measure of the channel width there. The method of calculation of the channel width has been adapted from that described by Mavrakis (1992). The calculation of this channel width is made assuming the velocity is downslope towards the edge of the ice shelf. The slope ($\bar{\alpha}$) is calculated as a weighted mean of the local slope at the point under consideration, and the average slope of the ice shelf to which that point belongs:

$$\bar{\alpha} = \frac{y_c\alpha_s + c_w\alpha_l}{y_c + c_w} \tag{4.20}$$

where s and l subscripts refer respectively to shelf average, and local values. c_w is a constant which determines that as the channel becomes wider, the local slope becomes less significant.

Ice shelf flow is not only affected by the distance to pinning points on either side of the flow but also by the distance to the shelf edge, or obstructions, ahead and behind. If the nearest grounded point ahead of, or to the rear of the flow is closer than the nearest points to the left or right of the flow, the speed of the flow will be reduced (Mavrakis 1992). In determining the channel width then, it is necessary to look in all directions, not only to the left or right of the flow.

For each point on the ice shelf, the effective width of the channel is considered to be defined by a controlling width, an estimate of the distance from the edge to the central flowline, y_c. To find y_c, the grounding line or ice edge points nearest the point in question are found in each of the four quadrants centred in the directions: forward (in the direction of flow), left, right and behind (see Figure 4.1). Grounding line points are initially sought to define the channel margin but if no such point can be found in any quadrant, the nearest shelf edge point is used and taken to be the centre point of the stream.

From these boundary points, the two closest are generally considered to define the flow channel, so that the channel width, $2y_c$, is the smallest of the distances: front-back, front-left, front-right, back-left, back-right or right-left. Front and back shelf margin points are also tested for the side of the flow channel on which they lie. If the minimum distance is between 2 points on the same side of the channel (e.g. right, and the right side of the back quadrant) this distance is ignored and the next shortest distance between two shelf margin points is found. The channel must be defined by two points on opposite sides of the direction of flow.

The channel half-width is then half the distance between these points if both controlling boundary points are grounding line points, or the entire channel width if either or both the boundary points are shelf edge points. For the sake of model stability, an upper limit of $u = 5000m\,a^{-1}$ is set on the ice shelf velocity.

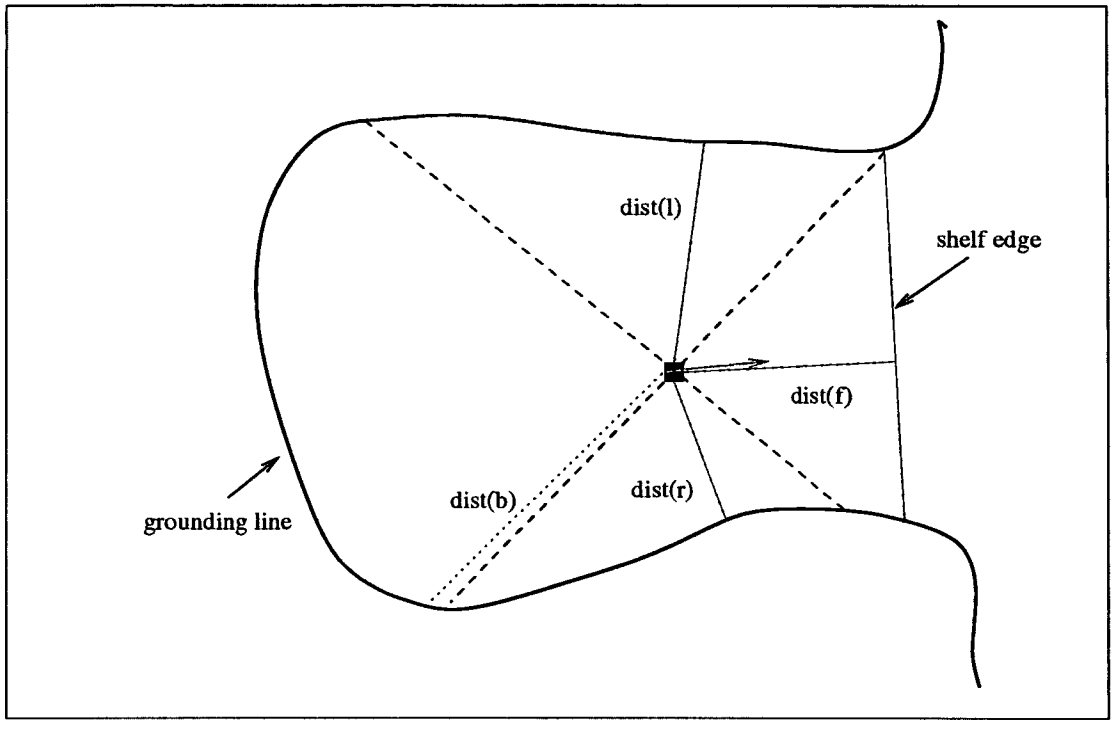

Figure 4.1: Finding the controlling width for ice shelf flow. Distance to the grounding line or shelf edge in the four quadrants (forward (f), behind (b), left (l) and right (r)) are found. The quadrants are defined by the slope determined flow direction (red arrow) at the point being considered. The central flowline is considered to be halfway between the two nearest shelf margin points; in this case, left and right.

4.1.4 Temperature dependence

The factors k_d (equation 4.7), k_s (equation 4.12) and A (equation 4.19) should include a temperature dependence. In fully thermodynamic models (see Huybrechts (1992),Greve (1997)), the temperature is calculated for each level in the ice and the full integral in 4.7, including the change with height of the temperature dependence of the flow, is done. Heat transfer is realistically modelled through the ice in these models, and the internal layer heating caused by ice deformation is also included. Such models are also time dependent and explicitly deal with the advection of temperature. This allows the effects of temperature on deformation rate to be considered through all ice layers. The sliding mechanisms of regelation and enhanced plastic flow are largely dependent either directly on the basal temperature or on whether pressure

melting has been attained, so the inclusion of temperature effects also improves the modelling of basal sliding.

However, to find full temperature and velocity profiles at each grid point is time consuming and considerably reduces model computation speed. As deformation is largely concentrated at the base of the ice and sliding is dependent on basal temperature, a simple velocity-temperature relationship dependent only on the thermal regime at the ice base is employed here. For the purposes of this study, it is felt that computing time is better spent on allowing inclusion of an ice shelf model than in the calculation of full thermodynamics. Uncertainty in the value of the geothermal heat flux, and its spatial variation, also reduces the accuracy of any thermodynamic scheme employed (Budd and Jenssen 1989) and so it was considered the drawback of the computation time requirements of the full thermodynamics outweighed any benefits offered by the scheme.

The calculation of basal temperatures follows from the work of Coutts (1992) who found that the simple thermodynamics work well for steady state conditions, and is discussed in Appendix A. However, the instantaneous reaction to changing surface conditions (accumulation, temperature, slope) caused by the steady state calculation of basal temperatures used in this approach means that the reaction to changes in boundary conditions will be extreme. In reality, the effect of change in temperature at the ice surface will be greatly damped and delayed at the base, especially if the thermal inertia of the bedrock is considered (Ritz 1987), and there is some evidence that there is not significant difference between the results from fully thermodynamic and non-thermodynamic models (Calov and Marsiat 1998).

The dependence of ice motion on the temperature of the ice may be thought of in terms of the activation energy for creep of the ice and can be expressed by an Arrhenius relationship (Budd 1969):

$$V = V_a e^{-Q/RT} \tag{4.21}$$

where V is the velocity, V_a is the velocity independent of temperature, Q is the activation energy, R the gas constant and T the absolute temperature.

For the ranges of stress and temperature which occur at the base of ice masses, a less rigorous but simpler relationship may be sufficient (Lliboutry 1963; Mellor and Smith 1966), and may be written:

$$V = V_0 e^{\eta\theta_b} \tag{4.22}$$

where η is a constant, generally assigned a value of 0.1°C for both sliding and deformation velocities (e.g.Radok et al. (1987)), V_0 is the velocity expected for temperate ice. θ_b is the difference between the base temperature and the pressure melting temperature:

$$\theta_b = T_{base} - T_{pmp} \tag{4.23}$$

where $T_{pmp} = -0.00888D$ and D is the ice thickness in km.

The full, columnar horizontal velocity for grounded ice is then given by:

$$v = (v_{def} + v_{slide})e^{\eta\theta_b} \tag{4.24}$$

The temperature dependence of the flow of floating ice had not been considered in earlier versions of this model. A simple approach to parameterising the effects of temperature on ice shelf flow is included here.

The damping of surface temperature changes is less strong in the ice shelves, which are generally thin enough for surface temperature changes to influence the entire thickness of ice. For the ice shelves it is the average temperature of the entire ice column which influences the rigidity of the ice (Jenssen and Radok 1961) and rate at which the ice flows. Budd and Jacka (1989) show that strain rate changes approximately by a factor of 10 for a 10 °C temperature change. Here the response to change in ice shelf surface temperature is considered to be instantaneous and is accounted for in the A term in the viscosity:

$$A = A_0 10^{\Delta T_{av}/10} \tag{4.25}$$

where A_0 is the initial value for the parameter A. ΔT_{av} is the change in the depth averaged temperature from its initial value. Temperature at the base of the ice shelf may be considered to be constant, and assuming an instantaneous

response to surface temperature change the average temperature change through the ice shelf is considered to be half the surface temperature change:

$$\Delta T_{av} = \Delta T_{surf}/2 \tag{4.26}$$

4.2 Isostatic response

The response of the bedrock to loading and unloading of an overlying burden can feedback significantly to the mass balance of an ice sheet. The depression of bedrock under an increasing load will bring ice lying on that bed to lower elevations where different climatic conditions prevail. The elevation of an ice sheet helps determine the surface temperature, influencing the rate of ablation. The amount of precipitation is also influenced by ice sheet elevation. At the base of the ice sheet, the height of the ice above buoyancy and the position of the grounding line also strongly influence ice sheet dynamics and these factors are largely dependent on bed elevation. Clearly, an adequate representation of the isostatic response to ice sheet evolution is required for the modelling of variable ice sheets such as those of the last glacial cycle. This is particularly the case since the timescale of bed response is long and may be comparable to the timescales of glacial climate change.

Le Meur and Huybrechts (1996) described a variety of possible approaches to the modelling of the deflection of the bed beneath ice sheets. While they found that a comprehensive, physically correct isostatic model is ideal, simpler models also give satisfactory results.

Here it is assumed that the response of the lithosphere is local. Changes in load at one point influence only the directly underlying bed and have no effect on the bed remote from this location. Around ice sheet margins where the load on the bed may vary considerably from point to point, this may be slightly unrealistic but in the interior, where ice thickness is relatively constant, the neglect of any rigidity in the lithosphere is more valid.

While an equilibrium isostatic bed elevation exists for any ice load, it takes considerable time to reach this equilibrium once the load is applied. Following Budd (1981), the rate at which the bedrock elevation approaches its equilibrium

state is considered here to be proportional to the square of the disequilibrium:

$$\frac{\partial B}{\partial t} = -sgn(\phi)a\phi^2 \tag{4.27}$$

where B is the bedrock elevation, t the time, a a constant, and ϕ the extent of the disequilibrium. If $\phi < 0$ the bed is below its equilibrium point and $\frac{\partial B}{\partial t} > 0$ and for $\phi > 0$, $\frac{\partial B}{\partial t} < 0$.

The disequilibrium is dependent on the load and the distance of the bed from equilibrium. It is convenient to find a reference level for the bed to which the equilibrium bed positions can be compared and so the disequilibrium found. For this purpose the bed elevation for a fully rebounded bed with all ice removed is found and denoted B_{ref}. For the northern hemisphere ice sheets, the reference bed is prescribed as described in Chapter 5. For Antarctica, B_{ref} is calculated under the assumption that the present bed is at equilibrium. A fully unloaded (ice-free) and rebounded bed is then calculated. As sea water and ice have different densities, load conditions vary depending on whether the reference bed is above or below sea level and both conditions must be considered.

If the ice is removed, the rebounded bed elevation will be:

$$B_{ref} = b_i D - B \tag{4.28}$$

where b_i is the ratio of the densities of ice ($\rho_i = 910 kg\, m^{-3}$) and mantle ($\rho_m = 3300 kg\, m^{-3}$). If the reference bed is still below sea level ($B_{ref} < 0$) the rebounded bed elevation allowing for the equivalent water load is then found:

$$B_{ref} \rightarrow \frac{B_{ref}}{1 - b_w} \tag{4.29}$$

where b_w is the ratio of sea water density ($\rho_w = 1027 kg\, m^{-3}$) to mantle density.

With the reference bed elevations known, the disequilibrium may be found. For the case when the reference bed is above sea level:

$$\phi = B_{ref} - b_i D - B \tag{4.30}$$

and when B_{ref} is below sea level:

$$\phi = B_{ref} - \frac{b_i D}{1 - b_w} - \frac{B}{1 - b_w} \tag{4.31}$$

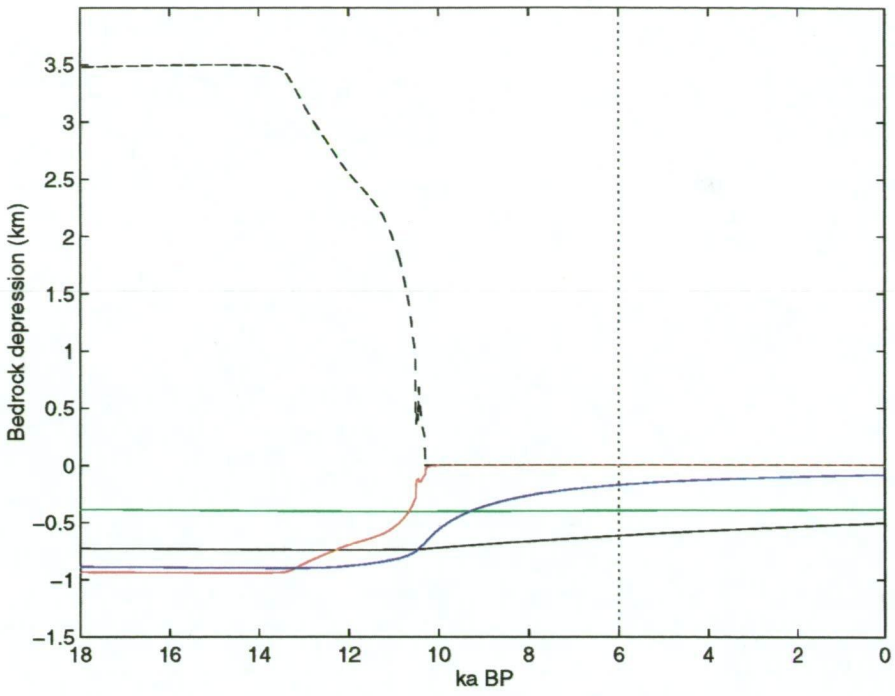

Figure 4.2: Modelled isostatic response beneath the centre of the Laurentide Ice Sheet during deglaciation, for various values of a: red ($a = 1$), blue ($a = 0.001$), solid black ($a = 0.00006$), green ($a = 0.00001$). The dashed black line shows the ice thickness over the location. Uplift rates for the past 6ka based on observation (Walcott 1973) are discussed in the text.

The parameter a in eq. 4.27 was tuned by comparing the results of this isostatic model with the observed uplift rates following the deglaciation of the Laurentide ice sheet. From a modelled glacial cycle, an ice thickness record was obtained for the point where maximum thickness occurred in the Laurentide ice sheet. With a maximum thickness of 3.5km at the LGM, this record was used to calculate the bed response given by eq. 4.27 for various values of a, throughout the cycle and in particular through the deglaciation. The results are shown in Figure 4.2 and may be compared to observations of bedrock uplift. Walcott (1973) estimates that there has been less than $115m$ of uplift at the location of the centre of the Laurentide Ice Sheet in the last 6000 years and that the present rate of uplift there is $1.7 \pm 0.5cm\,a^{-1}$. Employing a value of $a = 6 \times 10^{-5} s^{-1} km^{-1}$, the above isostatic model produces $111m$ of uplift from 6ka BP to present and a present uplift rate of $1.5cm\,a^{-1}$.

Previous versions of this bedrock response model failed to treat the

calculation of the disequilibrium accurately in cases where previously grounded ice comes afloat. This has been corrected in the current model.

Sea level change

Sea level change is effected in the model by altering bedrock elevation. To lower sea level, for example, the bedrock is raised by the amount of sea level change:

$$B_{new} = B_{old} - \Delta sealevel \tag{4.32}$$

and since the ice sheet surface elevation, S is given by $S = B + D$ where D is the ice thickness, it can be seen that sea level change affects the height of the ice surface as well as that of the bed.

4.3 Where the ice goes

The modelled ice sheet gets its ice from accumulation and loses it through ablation, oceanic melting and calving. As soon as the ice melts or calves it is no longer considered by the model.

4.3.1 Ablation

With the liklihood that the northern hemisphere ice sheets would have been strongly affected by the influence of ablation, a method for calculating this influence was developed.

One of the major links between orbitally driven variations in insolation and the growth and retreat of the northern hemisphere ice sheets is through ablation (see Chapter 2). However, while the amount of incident radiation may strongly influence the extent of ablation, this influence may not be direct. There is much evidence that air temperature better represents total ablation than does net incident radiation. Air temperature determines the daily heat flux density and duration of the ablation period as well as being a good proxy for other ablative factors (Ambach 1989; Ruddell 1994). Ablation is strongly concentrated in the summer months, and estimates of total annual ablation may be made based on an average summer temperature T_s, although ideally surface elevation must also be considered as this also impacts on the length of the ablation season

(Paterson 1994). Braithwaite (1993) found that ablation remains similarly focussed in the summer months for different climates and so glacial ablation estimates based on mean summer temperatures may be considered acceptable. Furthermore, it was found that using the mean July-August surface temperature for T_s gave a reasonable representation of ablation (Budd and Smith 1987).

Based on the observations compiled by Budd and Allison (1975), an expression for ablation as a function of mean summer temperatures, latitude and elevation was developed (Budd and Smith 1987). This is simplified by expressing the relationship in terms of temperature rather than elevation and latitude, a conversion made via the moist adiabatic lapse rate of -6.5 °km^{-1}.

$$log_{10}\mu = \frac{(T_0 + T_s)}{7.8} \tag{4.33}$$

where μ is the ablation rate ($m\,a^{-1}$), T_s is the mean July-August surface temperature and T_0 is the temperature at which $\mu = 1m\,a^{-1}$. Note that change in sea level in the model is effectively a change in surface elevation, which in turn alters surface temperatures and so affects ablation.

In reality, the value of T_0 is not constant and will vary depending on the environment (Ruddell 1994). The type of ablation relation expressed in Equation 4.33 has been found to produce results which correspond with the majority of the observed variation of ablation rate with latitude and elevation (Budd and Smith 1981) and remains a good representation of ablation. Various possible values for T_0 were tested. Beginning with the present observed ice distribution, and using a value of $T_0 = -1$°C in a northern hemisphere model run to equilibrium under present climatic conditions (accumulation, temperature and bed distributions are presented in Chapter 5), the ice distribution shown in Figure 4.3 resulted. This was considered a good fit to the current ice distribution and so this value for T_0 was employed for all model runs.

In the Antarctic where temperatures are generally below freezing, ablation does not contribute significantly to the loss of ice from the ice sheet. As glacial temperatures were colder than present, ablation is not considered in the modelling of the Antarctic Ice Sheet.

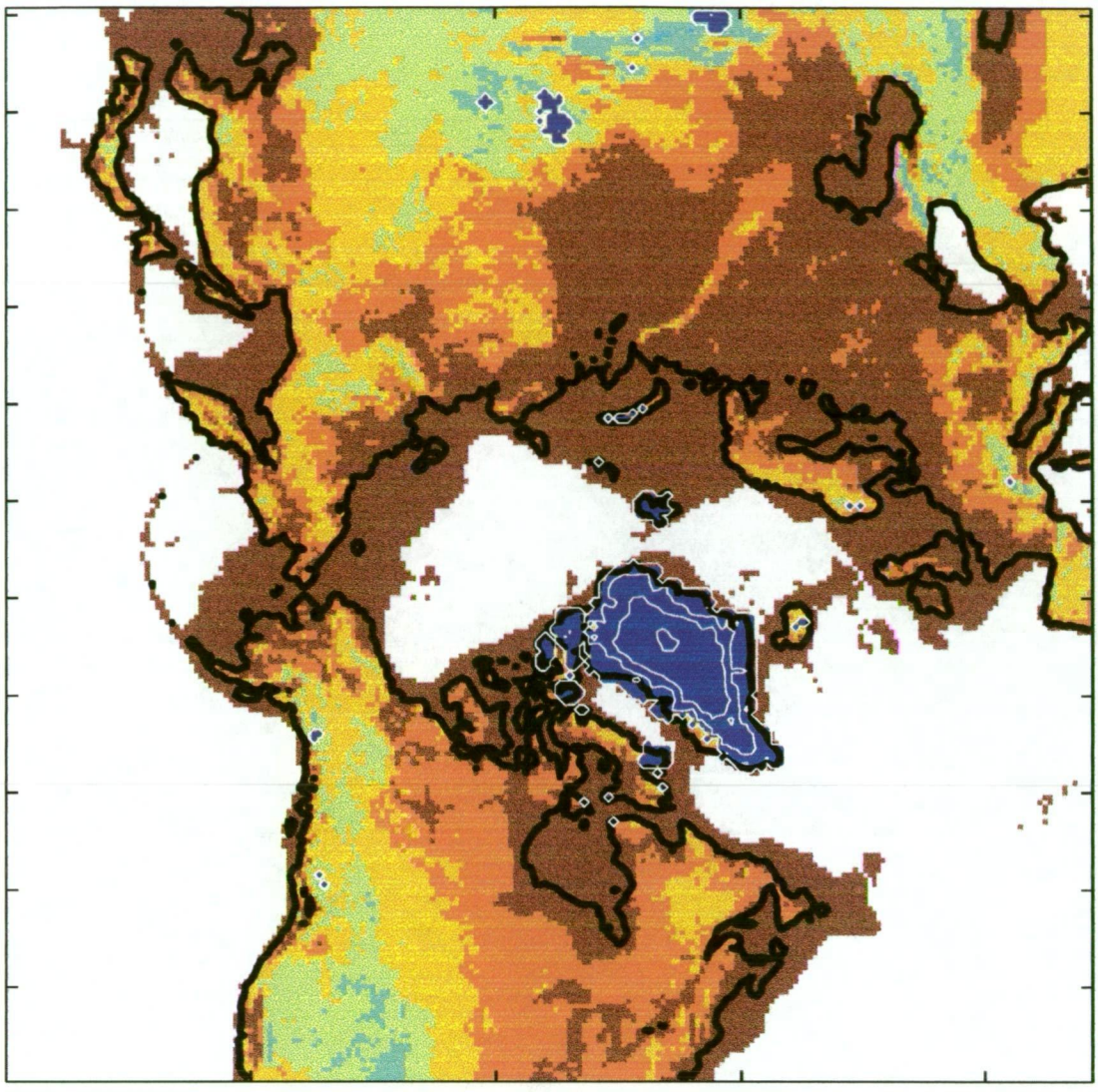

Figure 4.3: Steady state northern hemisphere ice distribution produced by the model for current climate and bed conditions. Land surface elevations are as given in Figure 5.11. Ice covered regions are shown in dark blue. Ice thickness contours are in white, with a contour spacing of 1km.

4.3.2 Oceanic melt

The melting of ice from beneath ice shelves is dependent on ocean temperature and is represented here as increasing with distance away from the pole:

$$M = M_0 + k_{melt}(x - x_0) \tag{4.34}$$

where M is the total oceanic melt and k_{melt} is the rate of increase of the melt rate with distance from the pole. Beyond the distance x_0 (equal to 1400km for the Antarctic and 2400km for the northern hemisphere), k_{melt}=0.004 $m\,a^{-1}km^{-1}$, while within that critical radius the melt rate is considered to be constant with latitude and k_{melt}=0. This rate of increase in melt with latitude is slightly smaller than that estimated from observation of iceberg concentrations by Budd et al. (1980), who found that the melt rate increases approximately linearly with distance from the pole at high southern latitudes, to ensure that ice shelves do not become too large and computationally expensive.

To the latitude dependent melt rate is added a base melt rate, M_0 which is zero for the Antarctic modelling. For the northern hemisphere modelling the value of M_0 varies with the temperature forcing, going from zero when air temperatures are at a minimum and the arctic ocean is insulated by extensive floating ice, to an interglacial maximum of 0.5 $m\,a^{-1}$, in accordance with the laboratory estimates of Russell-Head (1980).

4.3.3 Iceberg calving

Ice is lost from floating ice margins through the calving of icebergs. If ice at the edge of an ice shelf remains thinner than 250m for more than 5 timesteps the ice is removed and considered to have calved off. Once calved, the ice is ignored by the model.

4.4 Elevation-desert effect

While there is no explicit modelling of atmospheric processes in this model, the influence of altitude on atmospheric moisture content and hence precipitation rate is considered. This decrease in the moisture content of the atmosphere as the ice sheet elevation increases and surface temperatures decrease is modelled here by way of an 'elevation-desert' effect. Considering that the saturated water vapour content of the atmosphere approximately halves for a 10 °C temperature decrease and that the temperature decreases about 10 °C for every km of elevation, Budd and Smith (1982) showed that the accumulation rate at some point on an ice sheet may be expressed as:

$$A = A_0 2^{(E_0 - E)} \tag{4.35}$$

where A is the accumulation rate at that point, which has an elevation E. A_0 and E_0 are the reference accumulation rate and reference elevation. It is observed that this effect only occurs above elevations of 1.5km and so this relation is only enforced for elevations above this altitude. Although simple, this relation compares well with the characteristics of existing ice sheets (see Budd and Smith (1982) and Budd and Smith (1987)).

As sea level change influences surface elevation in the model (see Section 4.2) it is apparent that when sea level changes, accumulation rate will also change for regions above 1.5km elevation.

4.5 Grounded to floating transition

The transition from grounded to floating regimes in an ice sheet-ice shelf system may occur gradually as in the case of ice streams, where grounded ice increasingly uncouples from its bed over some distance. Normal stress decreases as the ice thins and becomes more buoyant and lateral stresses and sliding continue to become more significant until the ice is completely afloat. The change in flow regimes may take place more suddenly with a grounding line clearly defining the change from grounded to floating dynamics, but it is generally expected that the ice dynamics will become dominated by basal sliding before becoming afloat and subject to full ice shelf dynamics.

The location of the grounding zone is interrelated with the character of the underlying bedrock, thickness above buoyancy, surface slope and hence ice velocity. Grounding zone location and dynamics are linked with downstream ice shelves whose extent and flow both influence, and are influenced by, the nature of the grounding zone. Advance and retreat of the grounding zone will have a profound effect on the ice sheet and the ability of a model to produce this migration is very important when attempting to model the response to climate change in ice sheets with marine margins.

Here the grounding zone is considered to be defined by the last grounded grid square. These grid squares are treated in the same way as other grounded

points. The downstream floating points however, are considered under different dynamic and numerical regimes. Lestringant (1994) found that in global ice sheet-ice shelf modelling, limited coupling between grounded and floating ice dynamics is acceptable. However, to enable sufficient interaction between grounded and floating ice it is important that the transition between these regimes be as smooth as possible.

4.5.1 Continuity

Numerical stability

The time step length used in the model varies according to the resolution of the model. The continuity equation (eq. 4.1) is essentially an advective equation, and when numerically integrated by a finite difference scheme, is subject to a Courants-Friedrichs-Levy stability criterion which restricts the time step according to the maximum velocity of the ice and the grid spacing. Due to this stability consideration, higher resolution versions of the model require shorter timesteps. For the northern hemisphere, the grid spacing is 50km and timesteps are 2 years. The Antarctic was modelled at 100km and 20km resolutions, which required timesteps of 5 years and 0.5 years respectively.

Non-linear instability is avoided in the model through the use of a staggered grid (see Figure 4.4). Centred differencing may lead to underestimation of slopes, resulting in a miscalculation of the flux divergence (Mavrakis 1992). This effect may allow grid point elevation 'peaks' and 'troughs' to grow unbounded. Through calculating the fluxes midway between grid points, a more reliable evaluation of the flux divergence at the grid points is made, and the solution of the continuity equation remains bounded. It has been noted that non-linear instability may still exist under these circumstances, producing a pattern of alternate peaks and troughs along a line of grid points (Smith 1984). This was not observed in the model used in this study.

To enhance stability then, allowing the use of a larger timestep, a staggered grid is used in the flux calculations for grounded ice. The average thickness and elevation between neighbouring grid points are found and with the slope between the grid points used to calculate velocity and ice flux at these

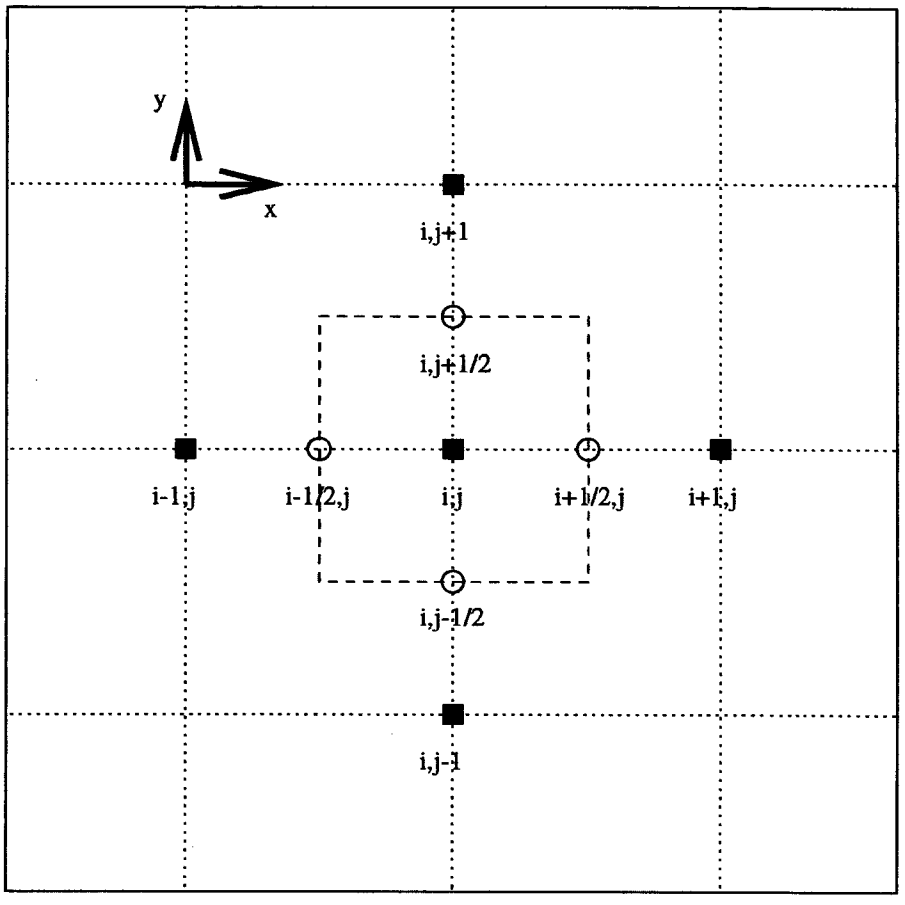

Figure 4.4: Regular and staggered grids. For grounded ice, the slope between grid points and the average ice thickness and elevation between those points are found and used to calculate the velocities and fluxes between the grid points. For floating ice beyond the first floating point, velocities and fluxes are calculated at the grid points. The blue dashed line shows the location of the modelled grounding line if the point (i,j) is grounded and the (i+1,j) is floating.

mid-points. This averaging effectively smoothes the ice and so increases model stability. There are then four flux values which contribute to the calculation of flux divergence at any grid point: either side of the point in the x-direction and either side in the y-direction (Figure 4.4).

For floating ice, where many more calculations are required per grid point than is the case for grounded ice, velocity calculations are made directly at the grid points on the regular grid. Again there are four fluxes contributing to the flux divergence at any point, however these fluxes represent the fluxes through neighbouring grid points themselves and not the mid-points as is the case for

the grounded ice. To ensure the conservation of mass across the grounding line, it is necessary to adjust the flux calculations so that the fluxes into, and out of, the last grounded point are compatible. This had not previously been the case. To allow compatibility with the upstream grounded fluxes, mid-point fluxes are generated for floating ice by interpolation. For example, for fluxes in the x direction for floating ice:

$$fx_{(i+\frac{1}{2},j)} = (fx_{i,j} + fx_{i-1,j})/2 \tag{4.36}$$

where fx is the flux in the x direction and i and j are the grid point coordinates. While this process does not enhance stability (in the way that calculating fluxes on the staggered grid for grounded ice does), flux values do then exist at the mid-points between all grid points.

The transition between regimes is considered to occur half way between the last grounded grid point and the first floating point (see Figure 4.4), so that grounded dynamics determine all the fluxes contributing to the flux divergence at grounded points, but the flux divergence at the first floating point will have some contribution from the grounded ice dynamics. The flux divergence may then be calculated for the entire grid:

$$\nabla f_{(i,j)} = \left(fx_{(i+\frac{1}{2},j)} - fx_{(i-\frac{1}{2},j)} + fy_{(i,j+\frac{1}{2})} - fy_{(i,j-\frac{1}{2})}\right)/grid \tag{4.37}$$

Here, $\nabla f_{(i,j)}$ is the flux divergence at the i,j grid point, and $grid$ is the grid spacing.

4.5.2 Grounding line migration

One of the aims of this thesis is to investigate the nature of the connection between the northern hemisphere ice sheets and the Antarctic ice sheet during the last glacial cycle. This connection may have been partly controlled by sea level change and its influence on ice sheet grounding line positions, and it is possible that sea level change had a significant effect on the extent of the Antarctic ice sheet through the glacial cycle (see Section 3.1.6). Therefore, a preliminary investigation into the nature of grounding line migration in the model, particularly that which occurs in response to sea level change, is made.

The location of the grounding line is determined by the floating criterion for the ice, the ice thickness and the depth of the bed below sea level. Consequently, the grounding line will tend to migrate when grounding, or ungrounding, occurs due to bed elevation changes through isostatic or sea level variation. Grounding or ungrounding of ice near the grounding line may also occur due to thickness changes in the ice in this region.

Sea level change may directly cause grounding line migration by reducing the water gap between floating ice and the bedrock underneath (sea level lowering), until the ice grounds on that underlying bed and the grounding line is advanced. By increasing the buoyancy of grounded ice to the point where that ice comes afloat, sea level rise may also directly produce grounding line retreat.

The influence of sea level change on grounding line migration through its effect on ice dynamics is more complex. Varying sea level will influence the dynamics by directly affecting the surface slopes across the grounding line, but the dominant initial effect of sea level change on the ice velocity is probably through its influence on the thickness of ice above buoyancy which influences the sliding velocity (eq. 4.12). By decreasing the thickness above buoyancy of ice near the grounding line, sea level rise will tend to lead to increased velocities there, which will tend to cause the ice to thin, and possibly unground. On the other hand, sea level lowering will reduce near-grounding line velocities, tending to cause the ice to become thicker. As the ice becomes thicker, the slope at the grounding line will increase and eventually the thicker ice may be advected to the downstream floating ice, causing the ice there to become thicker and possibly grounding. If the ice becomes strongly grounded, the influence of basal sliding is reduced and so the potential response to sea level change is also reduced. Of course, there is no basal sliding beneath floating ice, so once afloat, the ice dynamics are not so strongly directly influenced by changes in sea level.

It appears that in some ways the grounding line may be affected immediately by sea level changes and their affect on ice velocities, but that some changes may take longer as the ice approaches equilibrium with the new sea level. For the case of grounding line retreat, it is the conditions at the last grounded grid point which are significant, whereas grounding line advance is dependent on thickening at the first floating grid point.

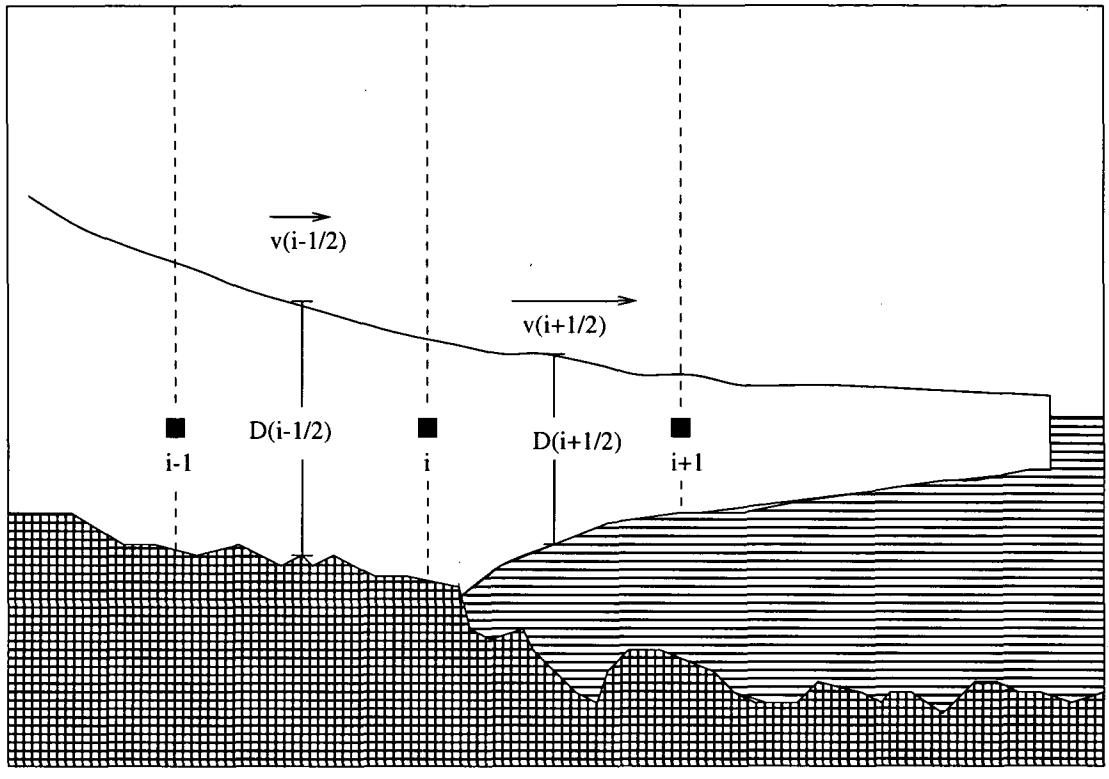

Figure 4.5: Transition from grounded to floating. The ice downstream of the last grounded grid point is generally closer to buoyancy and thinner than the upstream ice (remembering that in the model, the ice at (i+1/2) is considered to be grounded).

Flux divergence at the grounding line

Assuming a constant mass balance, thickness change is controlled by the flux divergence. Figure 4.5 shows a theoretical profile for ice near the grounding line, where flow in only one direction is considered. For a steady state there will be no change in the flux divergence:

$$\Delta(v_{(i-\frac{1}{2})}D_{(i-\frac{1}{2})})) = \Delta(v_{(i+\frac{1}{2})}D_{(i+\frac{1}{2})}) \tag{4.38}$$

The initial effect on the fluxes due to sea level change will be through a change in the velocity, Δv. Looking at the last grounded point (point i in Figure 4.5), for a steady state to be maintained, the ratio of the changes in velocity at the upstream and downstream points must equal the ratio of the downstream and upstream thicknesses at those points:

$$\frac{\Delta v_{i-\frac{1}{2}}}{\Delta v_{i+\frac{1}{2}}} = \frac{D_{i+\frac{1}{2}}}{D_{i-\frac{1}{2}}} \tag{4.39}$$

whereas for ice thickening at the last grounded point, the flux into the point must decrease relative to the flux out of the point:

$$\frac{\Delta v_{i-\frac{1}{2}}}{\Delta v_{i+\frac{1}{2}}} > \frac{D_{i+\frac{1}{2}}}{D_{i-\frac{1}{2}}} \tag{4.40}$$

and for the ice to become thinner:

$$\frac{\Delta v_{i-\frac{1}{2}}}{\Delta v_{i+\frac{1}{2}}} < \frac{D_{i+\frac{1}{2}}}{D_{i-\frac{1}{2}}} \tag{4.41}$$

So, in the case of a sea level rise, for example, if the ratio of the thicknesses at the mid-points $i + 1/2$ and $i - 1/2$ is greater than the ratio of the velocity increases at $i - 1/2$ and $i + 1/2$ resulting from the sea level rise, the ice at the grounded grid point i will tend to become thicker as the flux into the grid point will increase by more than the flux out of the grid point. Although there may be thinning of the ice upstream of this grid point which could subsequently affect the situation at the grounding line, the immediate response at the grounding line under these conditions will be thickening, and stronger grounding, of the ice. Conversely, depending on the thickness and buoyancy profile of the ice, it may be that the grounding line ice would tend to thin, and possibly unground, for sea level down scenarios. Change in flux divergence at the grounding line is subtly dependent on the ice profile and will not always react to sea level change in the same way, or even with the same sign.

Flux divergence at the first floating point

Unless a sea level lowering leads to floating ice being lowered onto the bedrock underneath, change in sea level only directly affects floating ice in the model through the connection of the ice shelf with the grounded ice (the use of grounding line points in the calculation of ice shelf slopes and the addition of average grounding line velocity to the ice shelf velocity), so thickening of the floating ice in response to sea level lowering is dependent on changes at the grounding line being transmitted downstream to that floating ice. A decrease in

sea level will have the immediate effect of reducing the flux into the first floating point by virtue of its influence on thickness above buoyancy, and hence the velocity out of the last grounded point. However, all else being equal, the flux out of the first floating point will remain unchanged, leading to increased flux divergence and a tendency towards thinning rather than the thickening required for grounding line advance. Eventually, if the grounding line ice thickens in response to the sea level lowering, slopes across the grounding line will increase and the flux out of the last grounded point may increase and lead to thickening at the 1st floating point.

This is slightly complicated by the contribution of the grounding line velocity to the that of the ice shelf. Any change in the velocity of the grounded ice will be immediately passed on to the ice shelf (see Section 4.1.3). However, as the ice shelf will generally be thinner than the grounded ice, the flux out of the last grounded point (and into the first floating point) will be more strongly affected by this than will be the flux out of the first floating point. The result under these circumstances would be that this would tend towards thinning at the floating point when sea level went down (and grounding line velocities slowed) and thickening when the sea level came up.

Slope across the grounding line

Sea level change affects surface elevation for grounded ice (see Section 4.2). However, the surface elevation of floating ice remains constant for any sea level (assuming the thickness remains constant), as shown in Figure 4.6. From the figure it can be seen that the slope calculated at the mid-point between the last grounded grid point and its first floating neighbour will be influenced by sea level change. This influence will tend to slow ice leaving the grounding line when sea level rises and accelerate the ice as sea level falls. This is in opposition to the influence of sea level change on the thickness above buoyancy.

The maximum influence sea level change may have on slope through this effect is if the ice at the grounded grid point remains grounded throughout the sea level change. In this case the elevation change at that grounded point will be equal to the change in z_* (which will be equal to the change in sea level) and the change in slope will be:

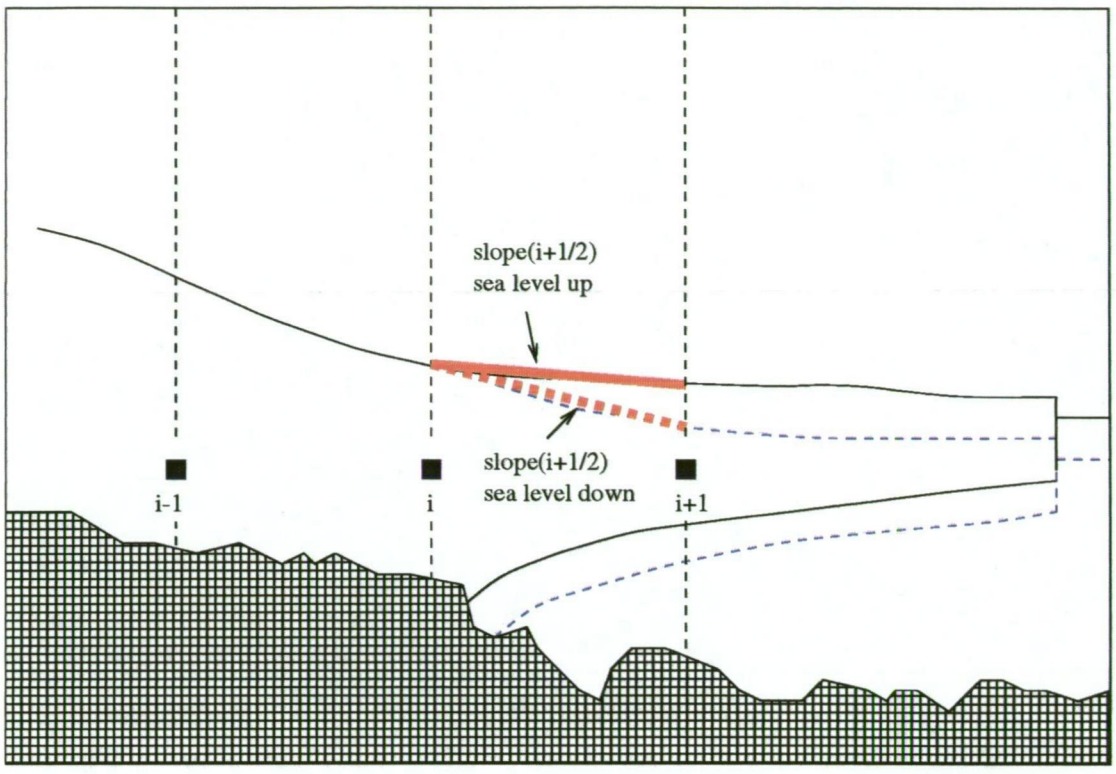

Figure 4.6: When sea level changes, the surface slope across the grounding line changes. Sea level change will also affect the buoyancy of the grounded ice. The ice velocity at the grounding line is affected in opposing ways by these effects.

$$\Delta\alpha = \frac{\Delta z_*}{grid}$$

The influence of the altered slope on sliding velocity will oppose and reduce the influence of the change in load on the sliding velocity (see 4.12), with consequences for the changes in flux across the grounding line and so possibly influencing grounding line migration.

The connection between grounded and floating ice is complex, however Lestringant (1994) indicated that the this type of uncoupled transition between the last grounded point and the first floating point used is valid in principle, although this may not be so for the case of embayed ice shelves such as those modelled here.

Grounding line migration is influenced by sea level change. The relationship however is not linear and sea level change may influence grounding

line dynamics in different and opposing ways so that the response of the grounding line to sea level change may not be easily predicted. Once the influence of changing accumulation rate is included, grounding line changes become even more complicated.

4.6 Model grid

The model data are gridded via a polar stereographic projection. There are 221x221 points in the northern hemisphere grid at a grid spacing of 50km. To enable a large number of runs, most of the model runs for the Antarctic were at a resolution of 100km with a 75x75 grid. Some Antarctic runs were performed on a 281x281 grid at a resolution of 20km.

Projecting data onto a polar stereographic grid produces some distortion in the projected data. The degree of distortion increases with distance from the pole, and at any latitude is given by:

$$k_{lat} = sec^2(\theta/2) \tag{4.42}$$

where k_{lat} is the distortion factor and θ is the co-latitude.

For the Antarctic Ice Sheet, which is largely contained within the 60°S parallel, the effect of this distortion is countered through the use of a standard parallel at 71°S. This enforces a 1:1 correspondence at that latitude. Equatorward of this latitude, distances between points in the projected data will be greater than the distance between those points in reality, and poleward of the standard parallel the projected data will be compressed in comparison to reality, but this distortion is less than 5% (Figure 4.7). The ice sheets in the northern hemisphere extended further towards the equator but were largely contained within the 50°N parallel. Using a standard parallel at 60°N for the northern hemisphere modelling, meant that distortions in the data due to the polar stereographic projection rarely exceeded 5% (Figure 4.7). Considering uncertainties in the accumulation distribution, for example, this degree of discrepancy was considered acceptable.

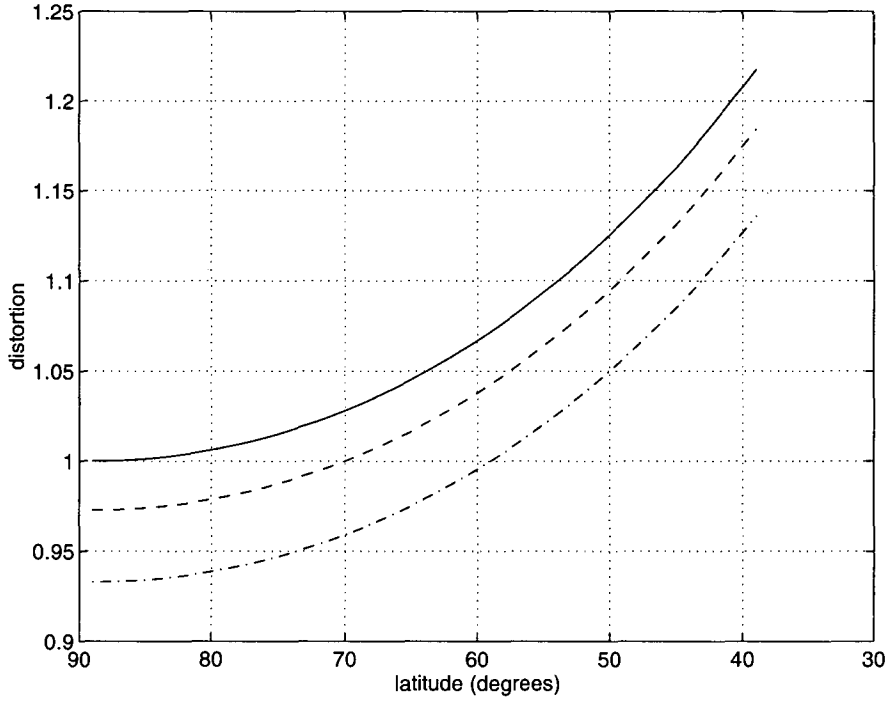

Figure 4.7: Variation of distortion with latitude for a polar stereographic projection. The solid line shows the distortion with the standard parallel at the pole (default). The distortion when the standard parallel is at 71°(–) and 60°(-.) are also shown. It can be seen that when the standard parallel is at 71°, there is less than 5% distortion at latitudes greater than 60°, while when the standard parallel is at 60°, there is less than ~7% distortion for latitudes greater than 50°.

Chapter 5

Data

One of the aims of this project is to gain a better understanding of our present environment by modelling the history of the ice sheets of the northern hemisphere and Antarctic. However, at some point back in time, conditions must be considered to have a negligible effect on producing the present state. Given the apparent relative independence of separate glacial cycles, it is considered convenient to model the Antarctic and northern hemisphere ice sheets from the last interglacial. Initial climatic, topographical, cryospheric and oceanic conditions must therefore be established, from which the model may commence.

The change through time of properties such as ice and bed distribution is calculated by the model. Change in other climatic factors such as sea level, accumulation and temperature is largely dependent on forcing external to the model, although change in these properties is also effected by internal model mechanics.

For all input fields then, initial conditions must be estimated and for some, the nature of their change through time must also be established. The data used in this study are presented here. Any assumptions made in establishing some of the model input are also discussed.

5.1 Temperature

The palaeo-temperature record is still relatively sparse (Peterson et al. 1979; Crowley and North 1991) and imprecise (Webb et al. 1993). Observations have shown however that temperature change over land tends to follow a rather

Latitude Band	Holocene	LGM	Eemian interglacial
5°S - 5°N	0.2	-2.0	0.2
5°N - 15°N	0.3	-2.0	0.2
15°N - 25°N	0.3	-2.0	0.4
25°N - 35°N	0.4	-2.3	0.8
35°N - 45°N	0.8	-5.4	1.6
45°N - 55°N	1.5	-5.4	3.4
55°N - 65°N	2.3	-8.3	4.5
65°N - 75°N	3.0	-11.5	6.2
75°N - 85°N	3.4		6.2

Table 5.1: Zonal palaeo-temperature anomalies (differences from present). Holocene values represent those of the mid-Holocene climatic optimum (6.2-5.3 ka BP). LGM values are from the period 20-18 ka BP and the last interglacial values are from 127-125 ka BP. LGM values are summer temperature anomalies, the others are annual average values. Data are from Borzenkova (1992), and Borzenkova et al. (1992).

uniform zonal pattern, and remains fairly constant with latitude (Stute et al. 1995; Shabalova 1996). This has enabled palaeo-temperature estimates to be made for remote regions where few data have been collected. Table 5.1 shows a latitudinal temperature anomaly (difference from present temperature) reconstruction based on this approach (Borzenkova 1992; Borzenkova et al. 1992). The data used are based on isotopic, palaeo-ecological, palaeontological and lithological studies (Kheshgi and Lapenis 1996).

While Kheshgi and Lapenis (1996) questions the accuracy of these estimates, some other reconstructions agree with them. A similar latitudinal dependence for LGM temperature anomalies was found by Hoffert and Covey (1992). Ekberg et al. (1993) point to simultaneous advance and retreat of the southern lobes of the Laurentide Ice Sheet as evidence that external forcing acted synchronously along the southern margin of the ice sheet. Holocene climatic optimum (Bartlein et al. 1984; COHMAP 1988) and Eemian interglacial (Andrews and Barry 1978) reconstructions also support the Borzenkova distribution. Data for the 75°N - 85°N latitude band is scarce but estimates from the GISP2 ice core at 73°N are that LGM temperatures were on average 15 °C colder than present and may have reached temperatures 21 °C colder than the present temperatures at the site (Cuffey et al. 1995). GCM's

have had some success in reconstructing palaeo-temperatures in agreement with observations (Webb et al. 1987), and modelled temperature reconstructions tend to reflect the above distribution of temperature anomalies also (e.g. Manabe and Broccoli (1985)).

To study the response of the northern hemisphere ice cover to changing climate, it is proposed to examine the magnitude and timing of the temperature changes that give ice sheet advances and retreats which match the pattern derived from glacial geology observations. In particular, a match with the reconstructed ice margin patterns over time is sought through a large number of model runs with different temperature change forcing. Because the ice sheet is most sensitive to the temperatures in the vicinity of the ablation zone near the ice sheet margins, the magnitude of the temperature changes primarily represent the temperature changes in that region.

GCM and EBM studies are limited in their ability to determine the extent of temperature depression at the southern margins of the northern hemisphere ice sheets by their low resolution in comparison to the relatively narrow ablation zone at the margin. In the vicinity of the ice margin, temperatures varied dramatically from over the ice sheet to the ice free region south of the ice sheets. This is apparent in Figure 5.1 which shows a very rapid fall in summer land temperature in the region of the ice sheets southern margins during the ice age, as determined by the EBM study of Budd and Rayner (1990). The temperature depression in the region of the ice sheet margins was found to vary from $\sim$-4°C to $\sim$-28°C as conditions went from ice free in the south to the high, ice covered regions over the ice sheets in the north. The high resolution of the ice sheet model used in this study (50km) in comparison to that of GCM's and EBM's, should allow the ice margins to be better resolved and the temperatures in those zones to be more accurately determined than in these low resolution models.

On the time scale of glacial cycles, it appears that temperature change has been approximately constant at any latitude. Due to simple energy balance considerations and the strong zonal mixing of the atmosphere, global temperature distribution tends to be strongly zonal itself, as seen in Figure 5.3. Through applying a uniform temperature change over the entire grid, the temperature change pattern will be zonal, as required. However, Table 5.1 also

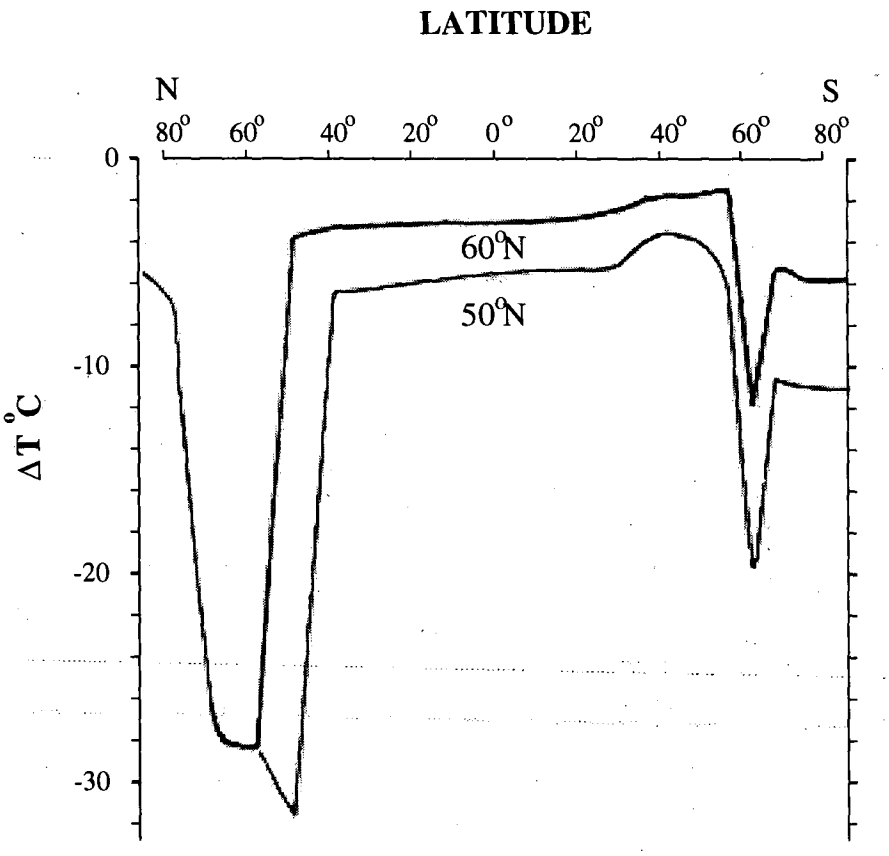

Figure 5.1: The variation of glacial maximum temperature depression with latitude from the EBM study of Budd and Rayner (1990). Shown are summer temperatures over land for simulations with mean land ice limits of 50°N and 60°N. The rapid change in temperature depression in the zone of the northern ice sheet margins (40-50°N and 50-60°N) mean that due to the low resolution of EBM's and GCM's, they cannot accurately determine the temperature depression at the margin.

shows that temperature did not change by the same amount at all latitudes, with the amount of change on average increasing towards the pole - a feature which is not reproduced by the application of a uniform temperature change. Temperature influences the ablation rate very strongly and also the fraction of precipitation which falls as solid. For these purposes it is the temperature at the southern margin of the northern hemisphere ice sheets which is most important to the ice sheet mass balance, as further north ablation will quickly become small. In the model, ablation will follow this pattern whether the temperature change is uniform or latitudinally dependent. As precipitation rates during the

last glacial cycle are not well known, the influence of temperature on the percentage of precipitation which is solid is not considered. The tendency for temperature to decrease towards the pole means that the temperature near the ice sheet margin remains that which is critical to the mass balance of the ice sheet. A pattern of prescribed uniform temperature change throughout the grid therefore remains a valid approach, but the magnitude of the change should be interpreted as applying specifically to the ice sheet margin location.

5.1.1 Temperature change through time

A pattern of temperature change with latitude has been established but a pattern of change through time is also required. Table 5.1 shows temperatures in the latitudes sensitive to ice sheet growth were possibly between 3°C and 6°C warmer than present during the last interglacial, 5°C to perhaps 20°C colder at the LGM and 1°C to 3°C warmer during the mid-Holocene climatic optimum. These values compare well with the findings of Hostetler and Clark (1997) who required temperatures to be between 8°C and 18°C lower than present to maintain LGM mountain glaciers in North America. To force the model however, a more continuous description of temperature change is required. Temperature records from ice cores near both poles (e.g. Lorius et al. (1985), Jouzel et al. (1987)) and from sea sediment cores at various latitudes between (see Imbrie et al. (1993)) illustrate a common qualitative agreement. While the amplitude of the temperature profiles may vary from place to place and relative temperature change in certain periods may not exactly coincide, the relationship between them is strong considering their geographical diversity. The Eemian Interglacial, LGM and mid-Holocene temperature estimates from these records further support the temperature anomaly distribution of Table 5.1, and palaeo-temperature data from other locations (e.g. Guiot et al. (1989), Nikolayev and Mikhalev (1995)) suggest that while the amplitude may vary, the pattern of temperature change with time was global.

The signature periods of orbital variation are clear in the pattern of temperature change, and EBM's, driven by external insolation input together with internal climatic feedbacks (particularly those associated with the ice sheet changes) have been able to produce a pattern of temperature change through

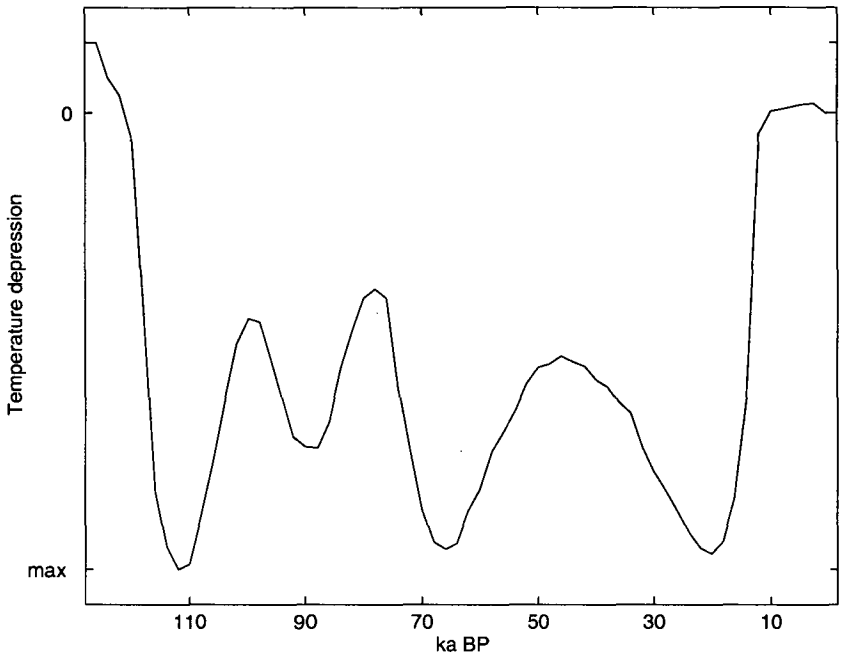

Figure 5.2: Temperature change (difference from present) through the glacial cycle derived from an EBM climatic curve from Budd and Rayner (1993). The present and past interglacial levels are marked, as is the maximum temperature depression.

the last glacial cycle based on physical processes and consistent with proxy temperature records. Budd and Rayner (1993) found that temperature change was dependent on orbital radiation changes and on ice area, and a climate curve based on these findings is shown in Figure 5.2. This curve represents the temperature change forcing used for the modelling of the northern hemisphere ice sheets.

Clearly the present temperature distribution is better known than that of any other time in history, and so it is this distribution which is used as a template. The above pattern of temperature change is uniformly applied to this distribution to produce the palaeo-temperatures for the model. Ablation in the model is calculated based on mean summer temperatures (see Section 4.3.1), specifically the mean July-August temperatures. These present surface temperatures are adjusted by the amount ΔT which can be read from Figure 5.2. The present temperatures come from Gibson et al. (1997) and are shown in Figure 5.3, having been lapsed to sea level with a lapse rate of

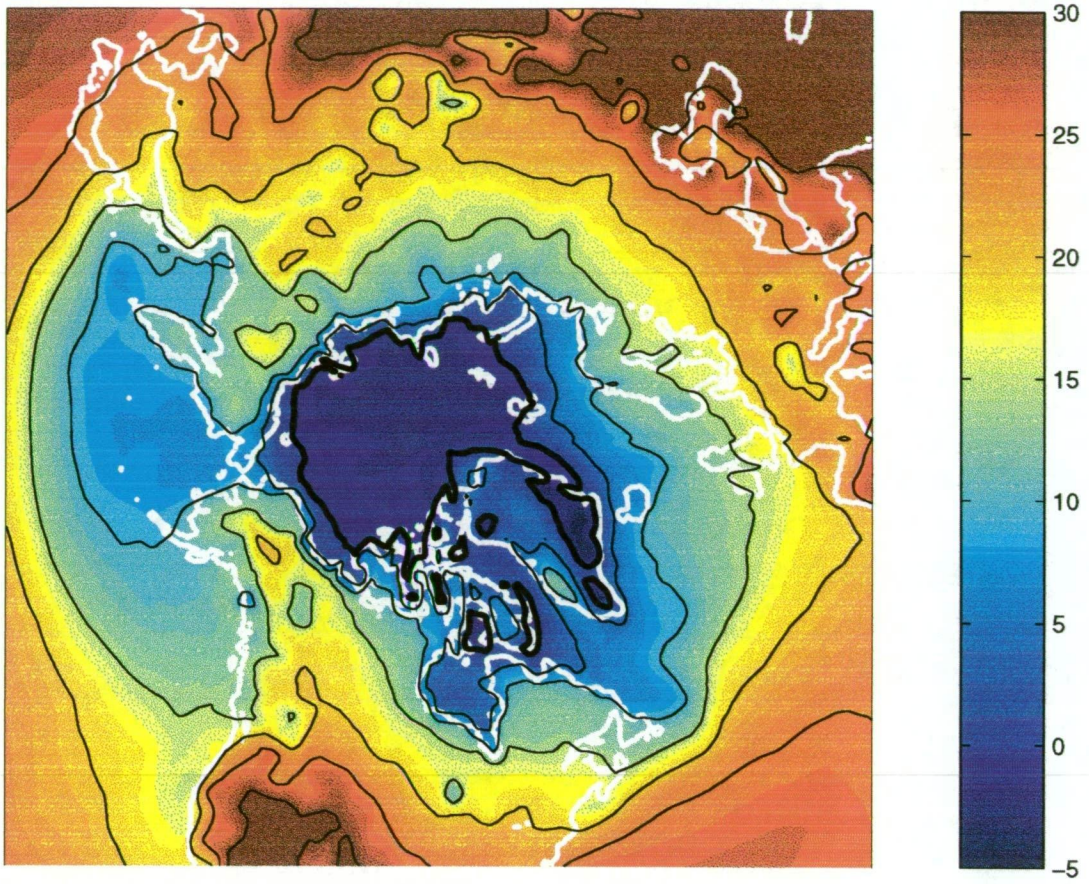

Figure 5.3: ECMWF summer (July-August) temperatures (extrapolated to sea level) averaged over the years 1985-1994. It is the summer temperatures which are required for the ablation calculation used in the model. Contours are every 5°C with a thick contour at 0°C.

$6.5°km^{-1}$.

5.2 Accumulation

5.2.1 Northern hemisphere

Estimation of palaeo-precipitation rates has at times been based on the assumption that precipitation is dependent on air temperature and its influence on the water vapour pressure in the atmosphere (Wigley and Raper 1992; Fabre et al. 1995). While records show that there is some relationship between temperature and precipitation during glacial cycles (e.g. Liu et al. (1995)), it is not simple and clearly other important factors can be involved in determining

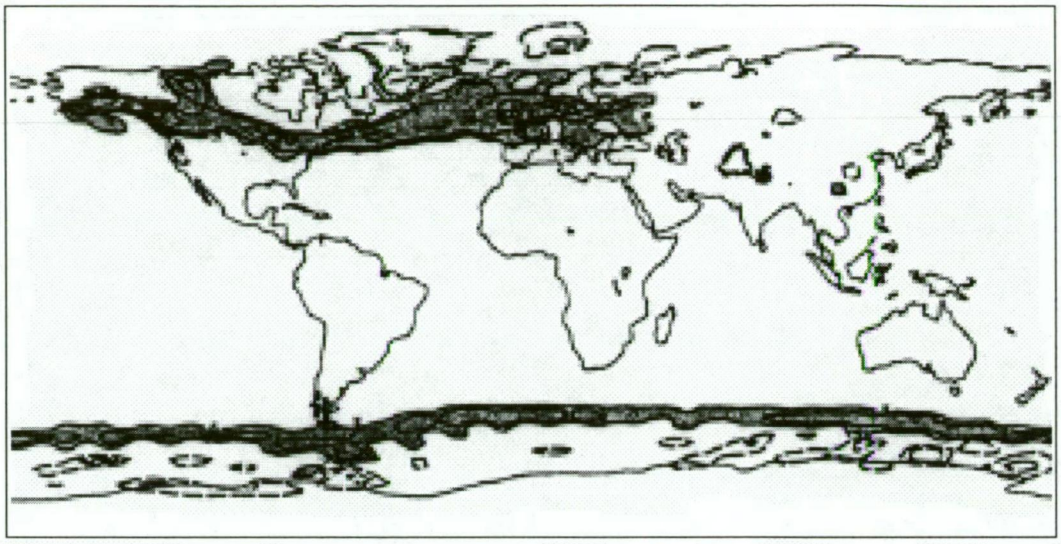

Figure 5.4: Global Climate Model estimate of difference between LGM and present solid precipitation rates (after Hall (1996)). Shading indicates regions where the LGM solid precipitation rate was 0.5 $mm\,day^{-1}$ higher than present.

precipitation rates. Kapsner et al. (1995) found that the precipitation in Greenland through the last ice age was far more dependent on the nature of the circulation of the atmosphere than its temperature. This tended to make precipitation rates variable between regions (Krishnamurthy et al. 1995) and although the glacial atmosphere is thought to have been generally dryer, the distribution of the precipitation and the change of that distribution with time is difficult to reconstruct.

Although their accuracy in reproducing precipitation distributions is questioned (Marsiat 1995; Chen et al. 1995), glacial climate 'snapshots' from GCM's have provided a useful tool in allowing some estimation of glacial precipitation rates, particularly at the LGM. These reconstructions do not well explain changes through time and they are dependent on the accuracy of their boundary conditions, in particular the size and location of ice sheets and floating ice, however they do bear reasonable comparison to the available observations. Also, these models are able to differentiate between solid and liquid precipitation and so the potential contribution to the cryosphere. Figure 5.4 illustrates the difference in solid precipitation between a present control run and

the LGM in the northern hemisphere for one such model (Hall et al. 1996).

This distribution is in many ways similar to the findings of other models (Rind 1986; Broccoli and Manabe 1987a; Broccoli and Manabe 1987b), and shows an increase in the solid precipitation rate for much of the North American and European regions which were thought to be covered by ice sheets. Increased moisture supply to the southern margin of the Laurentide Ice Sheet is also supported by field evidence (Peterson et al. 1979) as is the dryness in Greenland (Meese et al. 1994) and there is also evidence of intermittent high moisture in Western Europe in the palaeo-record (Guiot et al. 1989). The relative dryness across Asia and Siberia is also noticeable.

So although the atmosphere during the last ice age was generally dryer than that of today, in certain important regions, this may not have been the case. Changing atmospheric circulation and temperatures produced different precipitation distributions and types (solid or liquid). While the availability of moisture at certain times was vital to the growth and maintenance of the large northern hemisphere ice sheets, it appears that throughout the glacial cycle the rate of snow and ice accumulation in the sensitive regions may have varied by a factor of two either way. In any case, it has been suggested that changes in precipitation were less important than temperature (and resultant ablation) changes in producing and maintaining ice masses during the ice age (Hostetler and Clark 1997).

Elevation-desert effect

The precipitation rate over ice sheets is strongly dependent on the elevation of the ice sheet surface itself. The significant ice sheet surface elevation changes which may occur during the growth and retreat of an ice sheet will exert great influence on the change in temperature, atmospheric moisture and hence precipitation rate over the ice sheet. The change in precipitation rate with elevation is the dominant influence on precipitation rate for regions where ice sheet surface elevation varies significantly, as was the case for most of the glaciated regions of the northern hemisphere. This 'elevation-desert' effect is modelled interactively in the model used here (see Section 4.4).

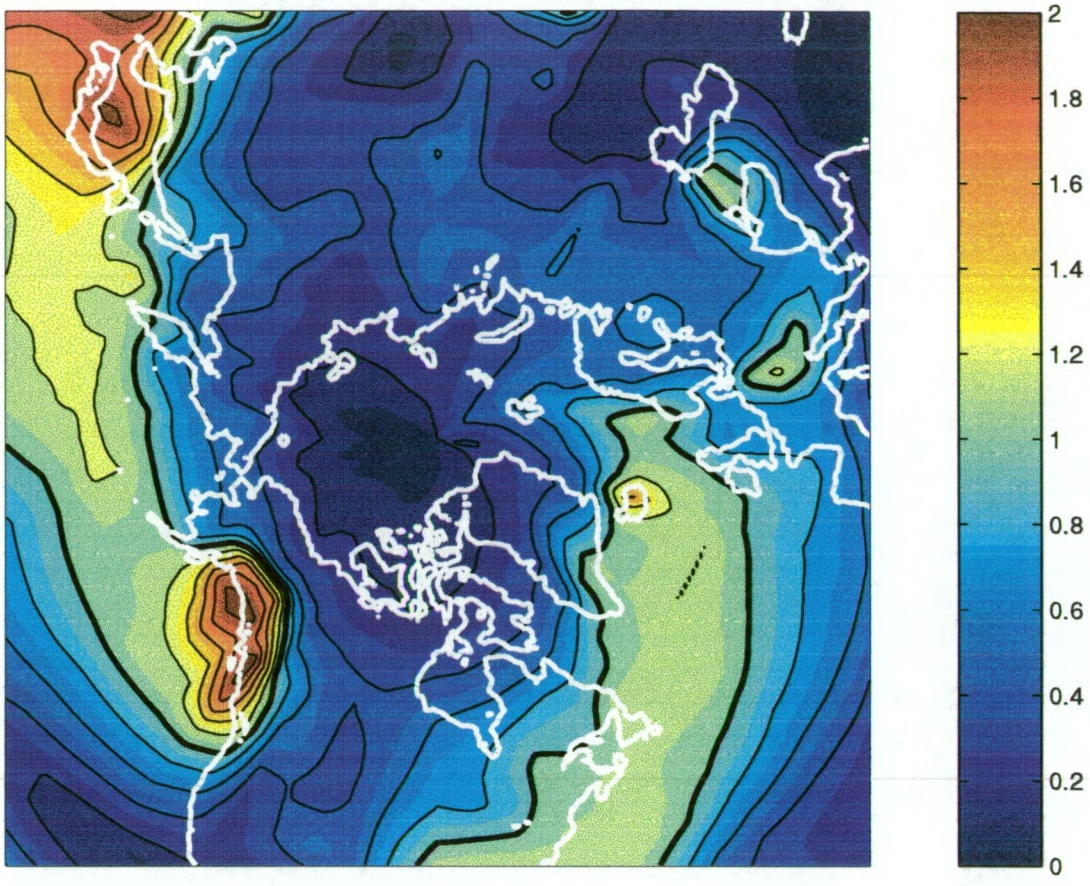

Figure 5.5: The present precipitation distribution ($m\,a^{-1}$) for the northern hemisphere according to Jaeger (1976). The contour interval is 0.2 $m\,a^{-1}$. The 1.0 $m\,a^{-1}$ contour is bold.

Given the uncertainty in palaeo-precipitation distributions, and the dominance of the ablation regime in determining net accumulation, estimates of present day precipitation are considered to be an appropriate source of precipitation data. As the reliability of any precipitation data used would be questionable, this study investigates the sensitivity of the glacial ice sheets to different precipitation regimes rather than attempting to accurately prescribe palaeo-precipitation distributions. With this approach in mind, two types of present day precipitation data are used. The Jaeger data set (Jaeger 1976) supplies an observational set of precipitation data (Figure 5.5) and a climatology from the Melbourne University GCM (Simmonds et al. 1988) offers

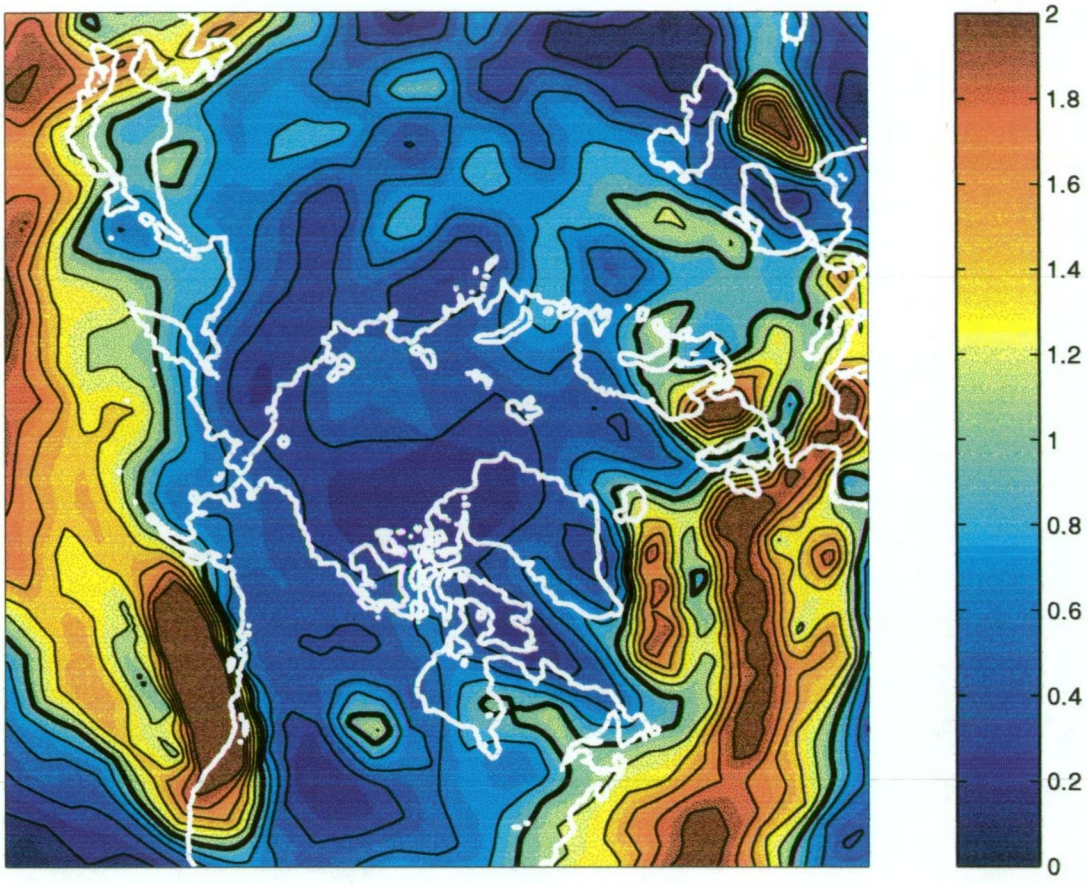

Figure 5.6: The present precipitation distribution ($m\,a^{-1}$) for the northern hemisphere according to a Melbourne University GCM climatology. The contour interval is 0.2 $m\,a^{-1}$. The 1.0 $m\,a^{-1}$ contour is bold.

a set of modelled data for comparison (Figure 5.6). The influence of evaporation and proportion of precipitation which is liquid are not explicitly considered. Sensitivity to precipitation rates is tested by multiplying the precipitation fields by a factor ranging between 0.5 and 2. It is assumed that the effect of evaporation and non-solid precipitation will be contained within these limits.

5.2.2 Antarctic

In the Antarctic, evidence suggests that the climate was less regionally variable and that the changes indicated by the record at Vostok are representative of a large region of the Southern Hemisphere (Jouzel et al. 1987). Because of this, and due to the lack of long term accumulation records from around the

continent, it is considered here that accumulation changed in the same manner throughout Antarctica during the glacial cycle. Once again the glacial climate change curve of Budd and Rayner (1993) is used to describe the change in accumulation rate through time (Figure 5.7). The amplitude of the curve is estimated from the Vostok ice core (Lorius et al. 1989). The Vostok accumulation record is not used here as it is considered that to use similar curves for all the forcing in the model will enable a better comparison of the effects of the respective forcing processes. The shape of this curve is slightly modified from that of the one shown in Figure 5.2. Where the temperature forcing for the northern hemisphere has temperatures at the last interglacial slightly higher than at the present interglacial, the same accumulation rate for the two interglacial states is applied to the Antarctic model. This is in order to facilitate assessment of the influence of the accumulation rate on changes in the ice sheet and to allow multiple consecutive cycles to be easily and seamlessly performed. Given the large uncertainties in the palaeo-accumulation rates this is considered a reasonable adjustment.

The precipitation distribution forced by that record is derived from the dataset described by Budd and Jenssen (1989) (Figure 5.8). All Antarctic precipitation is assumed to be solid and surface melt is assumed to be negligible.

5.3 Sea level

Sea level can change in response to variation in one or more of several factors. Over the last glacial cycle the volume of water in the oceans changed significantly as the volume of ice above buoyancy in the ice sheets and glaciers varied. Following Archimedes Principal, buoyant ice makes no contribution to eustatic sea level. Figure 5.9 shows that where the ice is floating (Figure 5.9(a)) there is no contribution to eustatic sea level, and where ice is grounded above sea level (Figure 5.9(c)) the entire ice thickness affects eustatic sea level, but where ice is grounded below sea level (Figure 5.9(b)) only the thickness above buoyancy affects the eustatic sea level.

The growth and decay of the large northern hemisphere ice sheets in particular and the advance and retreat of more permanent ice masses such as in

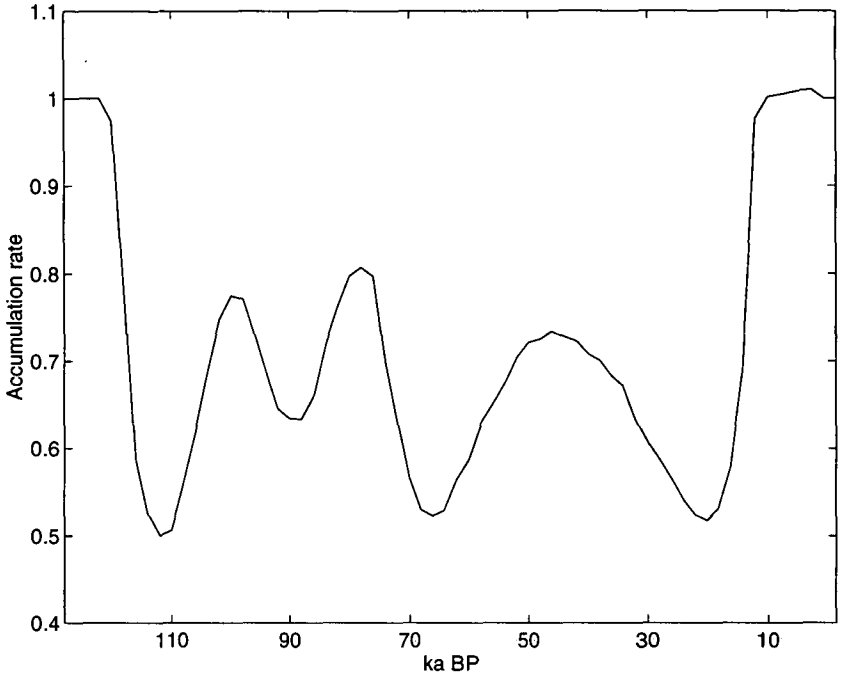

Figure 5.7: Accumulation rate change through the glacial cycle derived from the EBM climatic curve of Budd and Rayner (1993). The accumulation rate is shown as a proportion of its present value.

Antarctica contributed to sea level change in the order of 100 metres. Eustatic sea level is also influenced by change in the temperature of the ocean which causes thermal expansion or contraction. However, throughout a glacial cycle this effect would only have contributed a few metres to sea level change. Relative sea level is further affected by tectonic movement and the isostatic response of the bedrock beneath ice sheets and ocean. Changing loads in one place can cause the bed to lift or sink in places relatively remote from the loading source. Altered ice sheet geometry and eustatic sea level change can simultaneously influence the isostatic response at one location (Lambeck 1997) and relative sea level change will not necessarily be the same in different places. Changes in the distribution of mass throughout the Earth resulted from the growth and retreat of the ice sheets during the last glacial cycle and would have further influenced relative sea level through its affect on the motion of the Earth's spin poles (Bills and James 1996).

A sea level curve is required to drive the modelled ice sheets through the

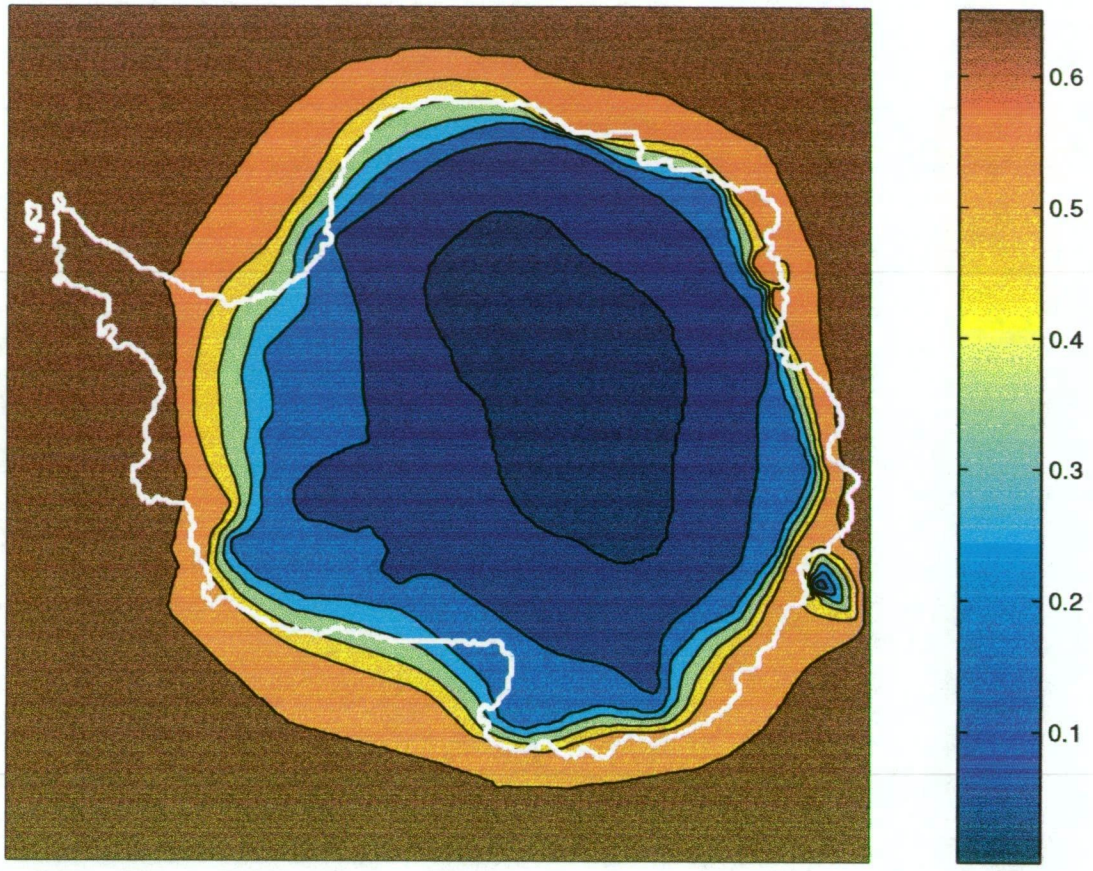

Figure 5.8: The present accumulation distribution ($m\,a^{-1}$) for the Antarctic according to Budd and Jenssen (1989). Contours are at 0.5 $m\,a^{-1}$, 0.1 $m\,a^{-1}$ and then every 0.1 $m\,a^{-1}$.

glacial cycle. Huybrechts (1992) chose to use an idealised sea level curve due to uncertainties in sea level change reconstructions. Given these uncertainties, an estimate for sea level change is obtained from the change in ice volume through the glacial cycle in the EBM results of Budd and Rayner (1993) and is shown in (Figure 5.10). An amplitude of 150m was applied to this as preliminary investigations suggested that the magnitude of sea level change resulting from the northern hemisphere modelling would be of this order. The output of changes in the amount of ice above floating (an estimate of sea level change due to cryospheric variation) can then be compared to this input sea level curve.

Given the relatively global nature of sea level change and for the sake of consistency, the same sea level forcing was applied to the modelling of both

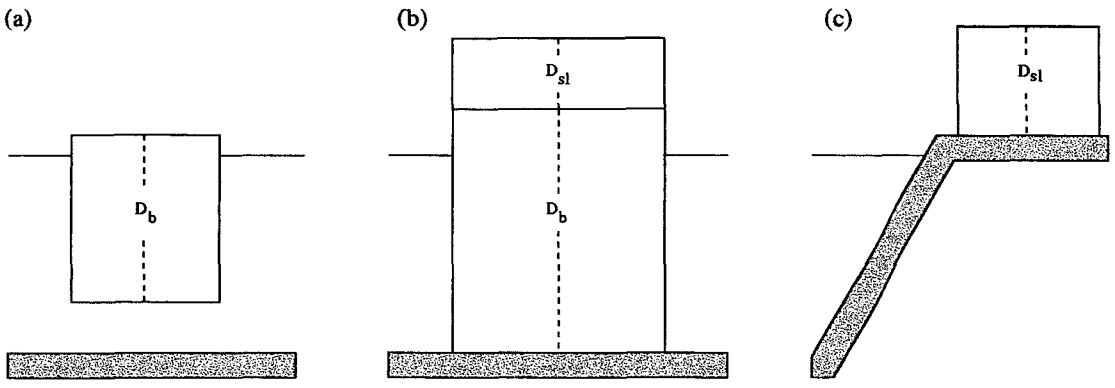

Figure 5.9: The influence of ice buoyancy on eustatic sea level contribution for (a) floating ice, (b) ice grounded below sea level and (c) ice grounded above sea level. Sea level is shown in blue and the green line in (b) delimits the thickness of buoyant ice (D_b) and the thickness of ice which affects eustatic sea level (D_{sl}).

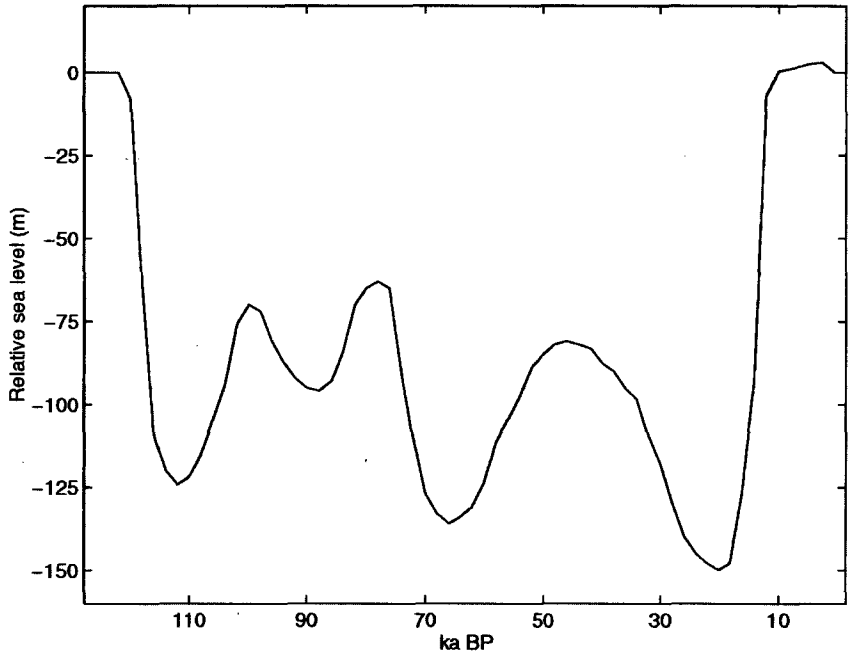

Figure 5.10: Relative sea level change through the glacial cycle derived from the EBM climatic curve of Budd and Rayner (1993). This curve is used as sea level forcing for both the northern hemisphere and Antarctic models.

hemispheres. Hence the sea level curve shown was used for the modelling of both the northern hemisphere and Antarctic Ice Sheets.

5.4 Bed topography

Bedrock in the central regions of areas formerly covered by the ice sheets of the last glacial cycle (e.g. Hudson Bay (Walcott 1973) and the Gulf of Bothnia (Lliboutry 1965)) is observed to be still rising in response to the unloading of ice since the LGM. It is apparent then that an equilibrium elevation for that bedrock in the absence of any load must be higher than the elevations presently observed. Given that we are currently only about 10 ka into this interglacial, and the previous interglacial persisted for somewhat longer than this, it is reasonable to assume that the bedrock at the onset of the last glacial, in the ice free regions of the Northern Hemisphere at least, was probably closer to that ice free equilibrium height. Beyond this rudimentary assessment however, it is difficult to establish a bedrock topography for the last interglacial from observed data.

The approach used here in obtaining a bedrock topography data set to be used as an initial condition for a model run through a glacial cycle was iterative. As a first estimate, the present bed topography was used to represent the bed at the last interglacial and from there the model was run through a glacial cycle to obtain a model estimate of the present bedrock distribution. The difference between present observed bed topography and the modelled 'present' bed was then added to the initial (last interglacial) bed and another glacial cycle modelled from this initial bed condition. This process was repeated until some convergence between observed and modelled present bed distributions was obtained. Following this method, the calculated bedrock for near the end of the last interglacial was produced and is shown in Figure 5.11.

This method should result in a bedrock topography for the modelled present (at the end of the model run) similar to observations. This in itself does not validate the derived initial bedrock topography as there is probably more than one solution which would result in a good fit to present at the end of the run. Raising the surface elevations will tend to produce colder temperatures, less ablation, increased ice growth and so greater bed depression, so raising the original elevations does not necessarily mean that the final elevations will be higher. In fact, through using this method of palaeo-bedrock calculation, any

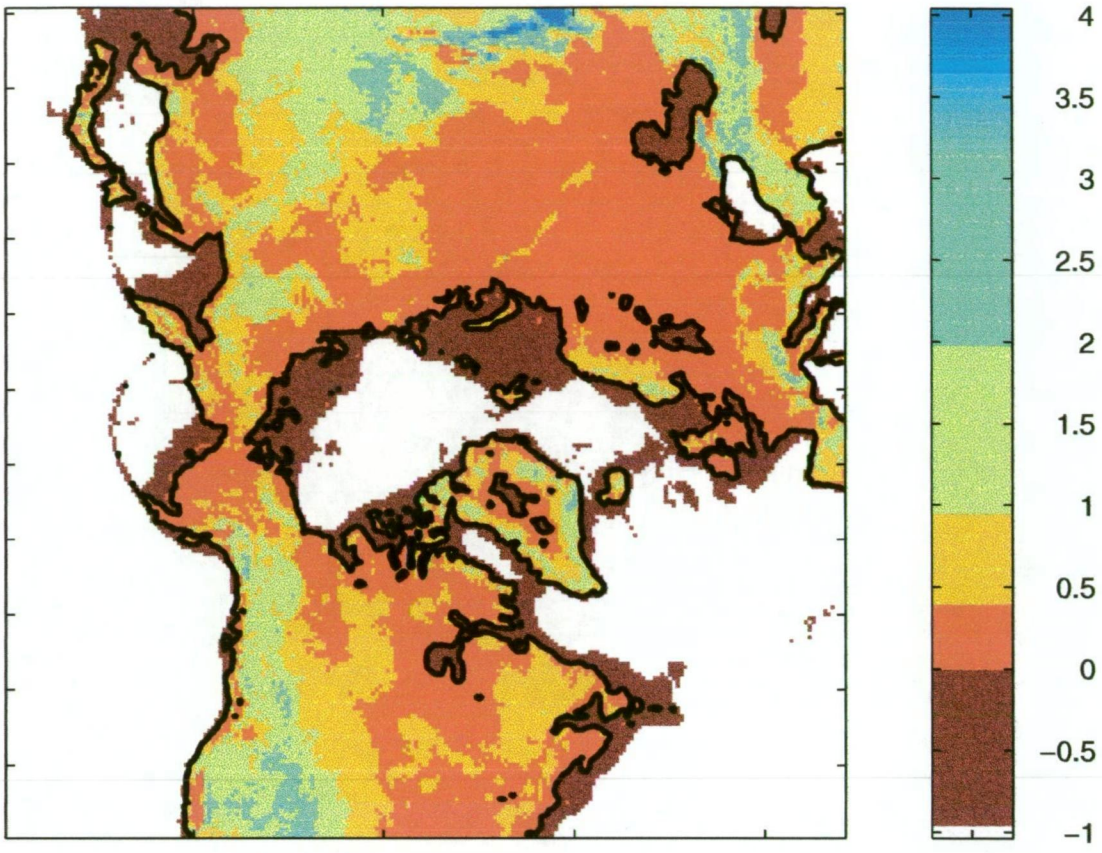

Figure 5.11: Estimated bedrock elevations for the northern hemisphere at the last interglacial. This distribution is used as an initial state for the northern hemisphere model runs. The black contour is sea level. The continental shelf below sea level is shown in brown.

tendency in the model to produce ice in a region could be enhanced. Where ice is initially produced the bed is depressed and so in the following iteration the bed in that region is raised above its previous initial height to colder elevations more likely to produce ice cover (although the decrease of precipitation with elevation inherent in the model will tend to counter this effect). While this may have the effect of producing too much ice in some marginal regions, the raising of the bed for the start of the run is critical for some regions of major glaciations, such as in Hudson Bay. In establishing initial bed conditions, the effects of erosion beneath the ice sheets, which may be in the order of $1 mm\, a^{-1}$ or more (Drewry 1986) were not considered. Uncertainty in the effects of such erosion and in the isostatic equilibrium state of the bed both contributed to

uncertainty in the initial bedrock elevation conditions.

The present day bedrock data comes from the ETOPO 5 bed elevation data set. ETOPO 5 is a dataset of the altitude and bathymetry of the entire world at five-minute resolution produced by the United States National Geophysical Data Center (USNGDC). Beneath Greenland, the bed topography comes from Budd et al. (1982).

5.5 Ice distribution

5.5.1 Northern hemisphere

Just as it was assumed that the bedrock for the northern hemisphere simulation was fully rebounded (except in regions, such as Greenland, which remained ice covered) at the last interglacial, the cryosphere was also taken to be in steady state. To achieve this steady state a model was run under conditions considered to be representative of the last interglacial: present precipitation rate, present sea level, temperatures 2°C warmer than present.

5.5.2 Antarctic

Although the state of West Antarctica during the last interglacial is not well known, it was considered that any imbalance in the Antarctic Ice Sheet at the last interglacial would have had minimal effect on the present state in comparison to the influence of the climatic fluctuations since that time. Nevertheless, at 100km grid resolution it was possible to run the ice sheet model through two glacial cycles to increase the isolation of the final modelled state from applied initial conditions. An initial ice and bed distribution was still required from which the first of these cycles could commence. In the absence of much information about the Antarctic Ice Sheet during the last interglacial, a steady state ice sheet with an elevation distribution approximating that of the present Antarctic was found. This steady state was found for present precipitation rate and sea level and is shown in Figure 5.12. For the higher resolution (20km grid) Antarctic model, time restraints allowed modelling through only one entire glacial cycle and a steady state ice distribution based on

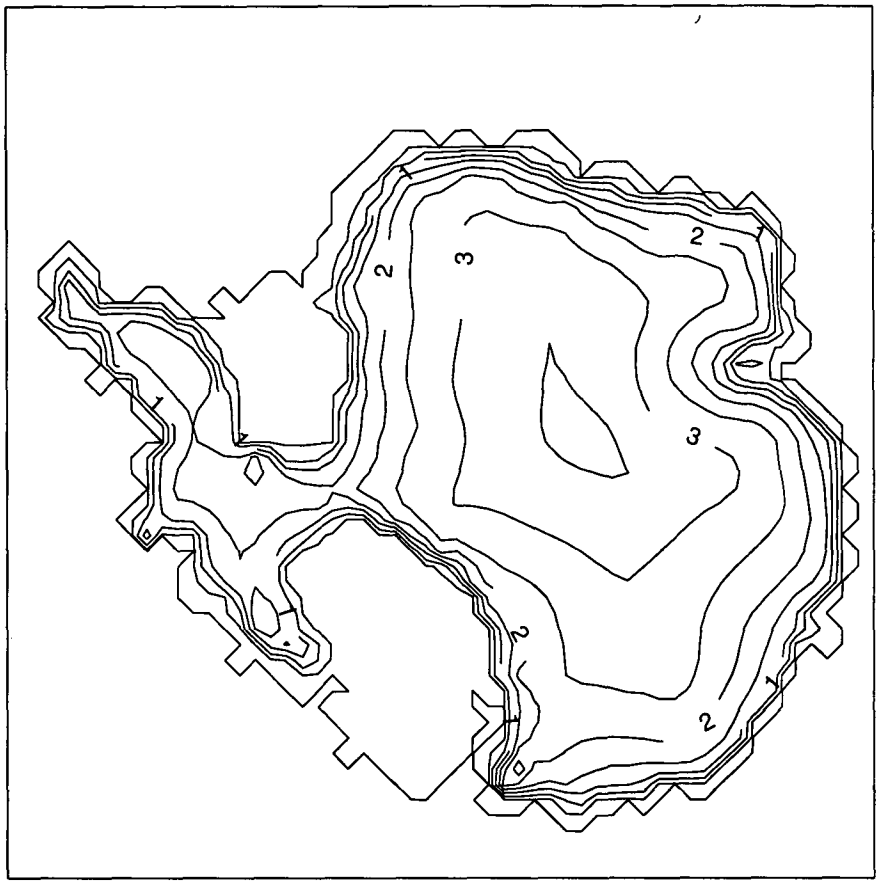

Figure 5.12: Antarctic elevation distribution at the beginning of the modelled last glacial cycle. The contours are at 0m, 100m, 500m, then every 500m.

present conditions was employed to represent the ice sheet at the last interglacial.

5.6 Net Accumulation for the northern hemisphere

Net accumulation in the Northern Hemisphere model is determined by the accumulation and the ablation. Accumulation depends on the initial given precipitation distribution and the surface elevation. Ablation depends on surface temperature which is also determined by surface elevation and the initial temperature distribution. Having established the accumulation and temperature fields, as well as the initial surface elevations, the regions where net

accumulation is positive can be calculated for any value of the temperature depression ΔT. Regions of positive net accumulation for various ΔT's are shown in Figure 5.13. Net accumulation regions for higher temperatures are contained within those for lower temperatures. For the present temperature distribution net accumulation is largely restricted to Greenland, some Arctic islands and a region of the Arctic Ocean, whereas when temperatures were depressed by 20°C there is net positive accumulation to low latitudes and beyond the model domain in some locations.

5.7 Summary

In order to model the ice age ice sheets through a glacial cycle, the climatic conditions which prevailed during that time must be established. Given the uncertainty in our knowledge of past temperatures and precipitation, a range of likely, or possible, values has been estimated for use in sensitivity studies. By using these fields in conjunction with a palaeo-sea level reconstruction to force an ice sheet model through a glacial cycle, a range of glacial responses can be obtained. By comparing these with observed cryospheric changes over the last 130ka, the model results reflect on the influence of those environmental factors and further indicate what values they may have had.

The evidence suggests that a latitudinal pattern of temperature change is reasonable as an approximation of first-order effects. For its change through time the temperature is driven by the influence of variation in the Earth's orbit on insolation and on the climate system's response to those changes. EBM results are used to supply the shape of the climate curves, the amplitude of which can be assessed from observations. There is much uncertainty in the temperature depression at the ice sheet margins at maximum glaciation, but observations suggest that these temperatures were somewhere in the range -5°C to -20°C.

Uncertainty in the precipitation regime and the manner in which it changes during the ice age means that the amount of solid precipitation falling in the region of the northern hemisphere ice sheet margins could have been anything between half and double the present rate. Over the ice sheets

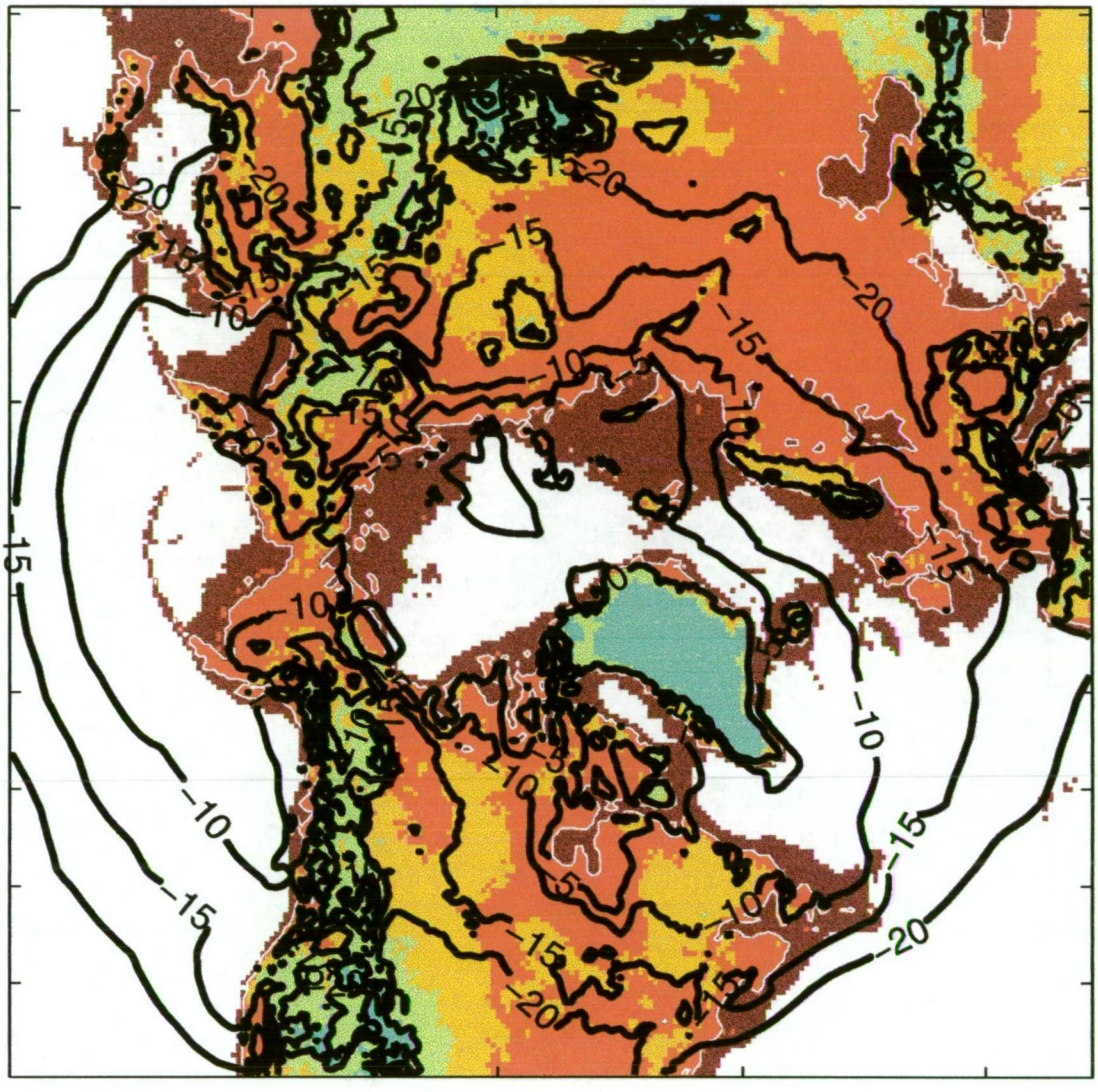

Figure 5.13: Net accumulation zones in the northern hemisphere for various values of temperature depression for the initial bed elevation distribution (representing conditions at the last interglacial). Regions of net accumulation are shown for temperature depressions of: 0°C,5°C,10°C and 20 °C, for the initial northern hemisphere elevations. The sea level contour is shown in white. Other elevations are as for Figure 5.11.

themselves it is expected that the dominant change was that due to the 'elevation-desert effect' which is included interactively in the ice sheet model. The pattern of accumulation in Antarctica is considered to have been more constant throughout the continent but could be expected to change with elevation and temperature.

Our knowledge of the cryospheric conditions and bed surface topography of the last interglacial is limited. Estimates of these conditions were made to supply initial conditions from which the ice sheets of the last glacial cycle could be modelled. Using the northern hemisphere surface elevation estimates and a prescribed precipitation pattern, it was also possible to calculate initial regions of net accumulation for the northern hemisphere for a range of temperature depressions.

Chapter 6

Northern hemisphere ice sheets of the last glacial cycle

Change in global ice volume during the last glacial cycle was primarily controlled by the growth and decay of the ice sheets of the northern hemisphere. Certainly the volume of the Antarctic Ice Sheet may also have varied, as would that of the multitude of smaller glaciers at lower latitudes, but the majority of the change in ice volume and area occurred at latitudes north of 40 °N where the large northern ice sheets existed. An attempt is made to quantify the magnitude of the ice volume changes and the timing of these changes in relation to the corresponding climatic changes.

Establishing distributions of the ice sheets tells us something of the glacial climate, in regions both local to, and remote from the northern ice sheets. Ice distribution is dependent on snowfall and the loss of ice through ablation, melting beneath floating ice and calving (assuming icebergs to be lost to the system) and melting beneath floating ice as well as on the dynamics of the ice. The modelled reconstruction of the northern hemisphere ice sheets of the last glacial cycle, as well as providing an estimate of the state of the cryosphere through the glacial cycle, is effectively an investigation into the conditions required to produce those ice sheets. Hence, the influence on ice distribution of temperature, accumulation rate, sea level change and ocean melt are examined.

Of course, as well as responding to sea level change, the northern ice sheets also dominated eustatic sea level change by locking water into, and releasing it from the grounded ice sheets. The reconstructed glacial ice sheets also provide then an estimate of sea level change. The effects of sea level change

were felt globally and in particular may have been important to changes in the Antarctic Ice Sheet. Furthermore there is the possibility that the nature of the decay of the large northern ice sheets and its influence on the location and timing of the release of significant quantities of fresh water may have influenced ocean circulation (see Chapter 2). This could be another method in which the northern ice sheets transmitted the glacial climate signal globally.

Palaeo-reconstructions of the transient ice sheets of the last glacial cycle are to a large extent instantaneous snapshots of the ice sheets. From geological evidence alone, it is difficult to reconstruct the complete life cycle of an ice sheet and earlier than the LGM, it is difficult to establish much about the ice sheet nature at all. Modelling these ice sheets produces a virtually continuous record of ice distribution which may be compared to observations but which may also serve to suggest likely ice sheet configurations at times and in regions where little is known. Similarly, information on isostatic conditions is also produced. By gaining insight into ice and bed topographies and the conditions required to achieve them, further information on the nature of the glacial climate is obtained.

6.1 Ice sheet margins

Ice margin temperatures at the LGM lie within the range of ~5-20°C according to the palaeo-record (see chapter Chapter 5). It is difficult to determine ice sheet margin temperatures to greater precision than this from EBM and GCM studies as their low resolution only allows the margin temperatures to be placed between those in the interior of the ice sheet and those on the ice free land beyond the ice sheet (see Figure 5.1). These models allow only that the margin temperature depression was between around 6°C and 15°C colder than present at the LGM (Budd et al. 1998). The rapid increase in thickness and elevation inland from the ice margin (e.g. Figure 6.9) means that at the low resolution of climate models and EBM's (the model of Budd and Rayner had a resolution of 1° latitude) the first iced grid point could be more representative of the interior of the ice sheet than the margin. As temperature varies with elevation, the surface climate can change rapidly with distance from the margin and so

defining the position of the ice margin is very sensitive to the resolution of the model. This is particularly so as observations indicate that at times during the last glacial cycle there was a strong temperature gradient immediately south of the northern hemisphere ice sheet margins also (Levesque et al. 1997). The high resolution of this ice sheet model (50km grid) compared to that of EBM's and GCM's allows ice margin temperature to be estimated more precisely by determining the temperature depression which most accurately defines that ice margin. The nature of the change in temperature through the glacial cycle comes from the EBM study of Budd and Rayner (1993) but the amplitude of this curve is determined empirically.

6.1.1 The amplitude of temperature depression

Using a modelled steady state ice distribution representing the distribution at the last interglacial (Figure 6.6 (a)) as an initial state (see Section 5.5.1), the model was run through a single glacial cycle (130ka) for temperature forcing amplitudes (ΔT_{max}) between 5°C and 20°C. Estimates of ice margin temperature at the LGM based on palaeo-evidence and modelling reconstructions lie within this range. The results of the model runs performed here were judged by comparison with ice sheet extents, primarily at the LGM, as estimated from palaeo-evidence.

Figure 6.1 shows the LGM extents of the modelled northern hemisphere ice sheets for ΔT_{max}=-5°C, -10°C, -13°C, -15°C and -20°C and it can be seen that the extents for smaller temperature depressions are contained within the ice extent produced when the temperature change was greater, as may be expected. All these runs commenced from the same initial bed elevation distribution, which was selected on the basis that it would allow something like the present bed to result from a glacial cycle where realistic ice sheets were produced. Hence not all of the results for different ΔT_{max} were attempts to reproduce realistic glacial ice sheets. However, the entire range of results is included here to illustrate the change of ice extent with changing ΔT_{max}.

From a comparison with the reconstruction of LGM ice sheet extent of Grosswald (1988) (Figure 3.7) it appears that application of a maximum temperature depression of -13 °C best approximates the northern hemisphere

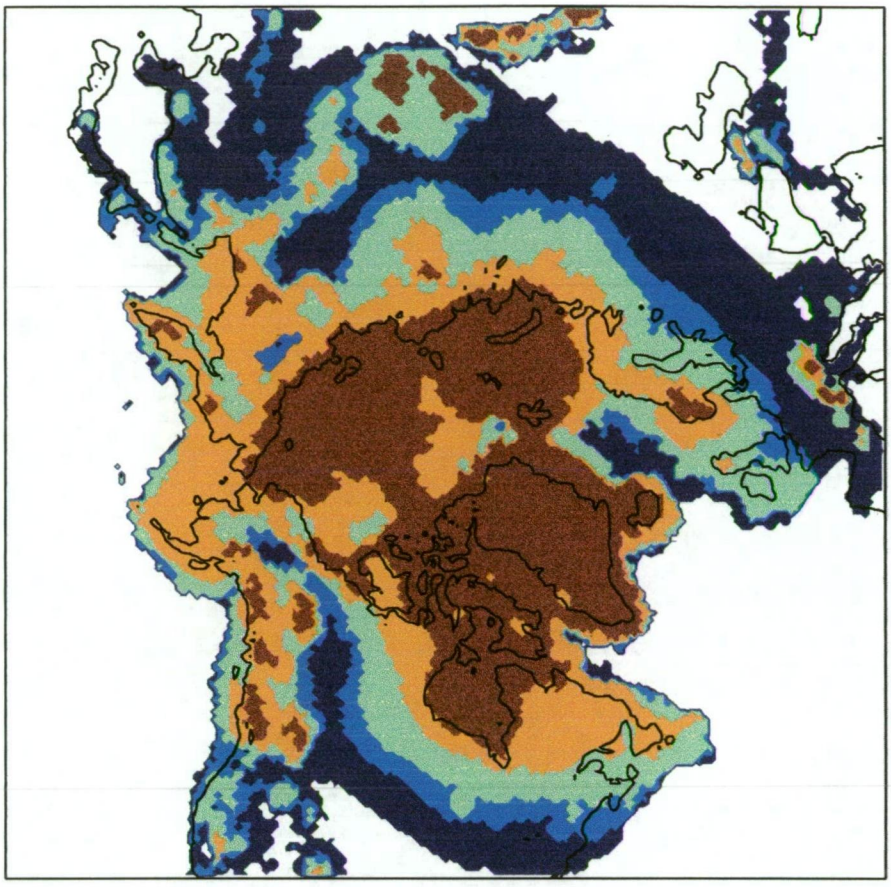

Figure 6.1: LGM ice sheet extent during glacial cycles with maximum temperature depressions of:5°C (brown), 10°C (orange), 13°C (green), 15°C (light blue), 20°C (dark blue). The present continental outlines are shown.

ice sheet extent at the LGM. Regionally, a difference of a degree or two from this value may more accurately place the margin. Location of the ice sheet margin may be affected by other factors such as altered accumulation rate or distribution. This is discussed in Section 6.4

Ice extent at the LGM has been used to find a best fit for the temperature change curve derived by Budd and Rayner (1993). From this best fit, the ice sheets of the last glacial cycle are now investigated in more detail through the entire period since the last interglacial.

6.2 Response of ice volume to temperature and sea level forcing

Figure 6.2 gives some illustration of the relationship between the variation in radiation due to changes in the Earth's orbit (at 65°N), glacial climate changes and the response of the northern ice sheets and underlying bedrock. As mentioned previously, the variation in temperature curve (Figure 6.2 (b)) was derived from the EBM study of Budd and Rayner (1993) which was partly driven by radiation forcing such as that shown in Figure 6.2 (a). The ice sheet area and volume (Figure 6.2 (c)-(e)) are in turn driven by that temperature forcing and the isostatic response is then driven by the overlying ice burden. The system components are thus related and the orbital signal can be seen to be transmitted throughout. The pattern of orbital variation is to some extent exhibited in all the Figure 6.2 plots, although there is a progressive lag as the inertia of the respective climatic components delays and damps the signal. There is a progressive weakening of the $\sim$ 20ka period which is clearly apparent in the first half of Figure 6.2 (a). The radiation minimum (the normalised radiation anomalies are inverted in Figure 6.2 (a)) at 92ka BP which corresponds to the isotopic substage 5b has all but disappeared from the pattern of bed response, and the radiation minimum at 42ka BP, which is weak even in the radiation curve, is non-existent in all the other responses.

Where the higher frequencies are the most damped, there is also the most delay in the response to the radiation forcing. The pattern of variation is so delayed in the total ice volume response and particularly in the bed depression response as to be completely out of phase with the initial radiation anomalies. At times when the orbit may have had a geometry optimal for warming, the bed was still approaching the depression maximum due to the thick ice sheets which resulted from the earlier pro-cooling orbital geometry. The lags of the various components at individual peaks and troughs are shown in Table 6.1.

It has been proposed that the more rapid response of ice area than ice volume to the forcing, through its influence on surface albedo, may have been an important feedback to the development of large ice sheets (Budd and Rayner (1993), see Section 2.4.1). Here it is shown that the ice area response does

Isotope stage	5d	5c	5b	5a	4	3			2	average lag
Δ radiation 65°N	114	102	92	82	70	56	42	36	22	0
Temperature	112	100	88	78	66	46			20	-4
Floating ice volume	109	98	89	77	57	42			19	-6.7
Ice area	108	97	89	76	60	38			19	-7.3
Total ice volume	106	97	87	76	58	40			17	-8.1
Bed depression	101	93	83	71	52	32			15	-13

Table 6.1: Timing of the peaks and troughs (in ka BP) in the; radiation anomalies at 65°N, the temperature forcing, floating ice volume, total ice area, total ice volume and volume of bed depression, as shown in Figure 6.2. The isotope stages associated with these maxima and minima are shown, as is the average lag (behind the radiation anomalies) of each climate component throughout the glacial cycle.

generally lead that of the total ice volume, although overall it lags that of the floating ice volume. At glacial maxima however the trend is for the ice area to react more quickly than either floating or total ice volume. Ice sheet advance tended to occur in the form of thin sheets which then became thicker (see Figure 6.6) and so especially during advance ice sheet area tends to lead volume. When it came to retreat, the ice sheets were generally thick up to their margins so a reduction in area would also produce a significant decrease in volume. Any early transmission of radiation driven climate change due to the relatively early response of the ice area would therefore have been more pronounced during episodes of glacial advance than during retreat.

The slow decrease in the volume of floating ice following the LGM is a result of a tendency in the model to preserve ice at high latitudes, even under the influence of a near-present temperature regime. Holocene retreat of floating ice in the Arctic was slow in the model as there was a positive balance at the surface and ice only gradually thinned due to ocean melting. This gradual decrease is also reflected in the ice area curve.

Figure 6.4 again shows the variation of total ice volume through the glacial cycle. Also shown are the volume of ice above buoyancy (the volume which contributes to sea level) and the total volume of ice in the individual northern hemisphere ice sheets (see Figure 6.3). The total volume maxima and minima are apparent and the times from which are taken the various distribution maps Figure 6.6 to Figure 6.9 are shown.

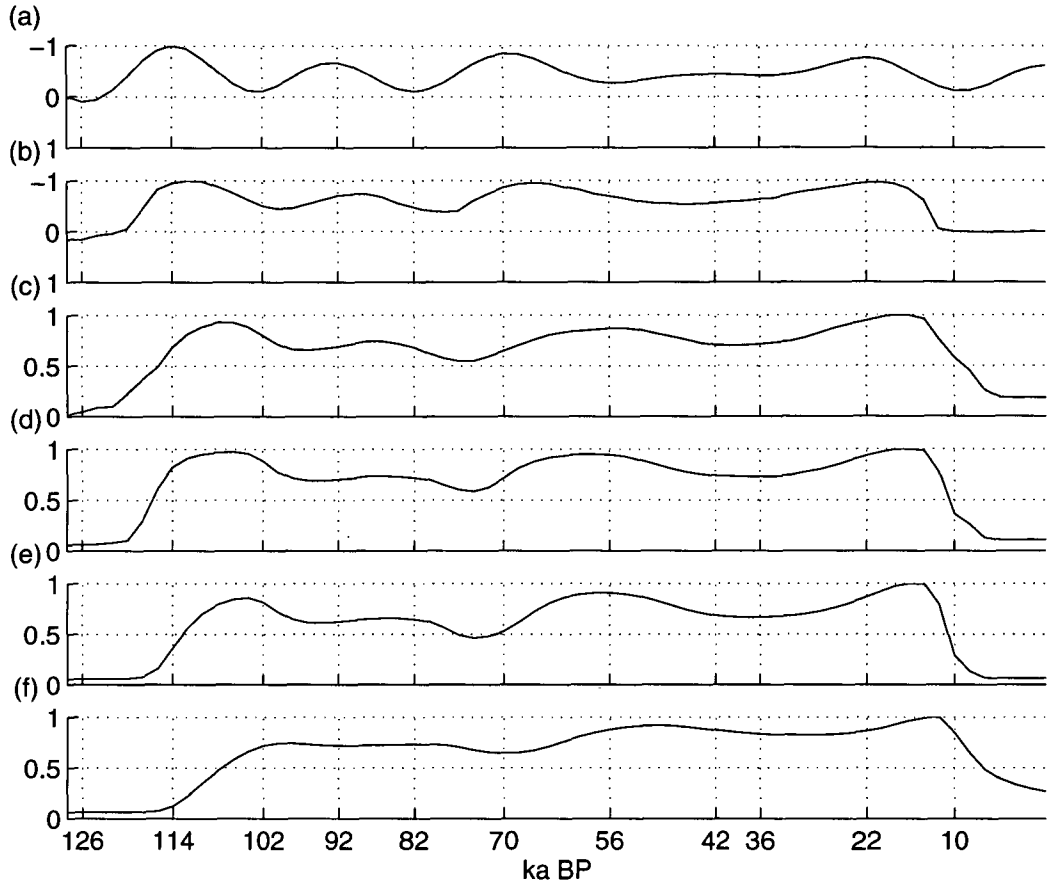

Figure 6.2: The transmission of the radiation anomaly signal through the system. The radiation anomaly at 65°N (a) is inverted, as is the temperature forcing curve (b). (c) shows the variation in floating ice volume through the glacial cycle, (d) shows that for the ice area, (e) gives the total volume change and (f) illustrates the total volume of bed depression. All curves are normalised.

Although the three main depressions in the temperature forcing, at 112ka BP, 66ka BP and 20ka BP were of almost the same amplitude, the volume of most of the ice sheets and the total volume tended to increase from one maximum to the next. The first glacial advance commenced from a virtually ice-free state (excepting Greenland), whereas the later ones grew from progressively larger pre-existing ice sheets and so were able to grow further. Also the increasing depression of the bed through the glacial cycle meant that for the same surface elevation, a greater thickness of ice could be maintained. For some regions however, the lower surface elevations resulting from the bed depression which followed the initial glacial advance led to increasing ablation

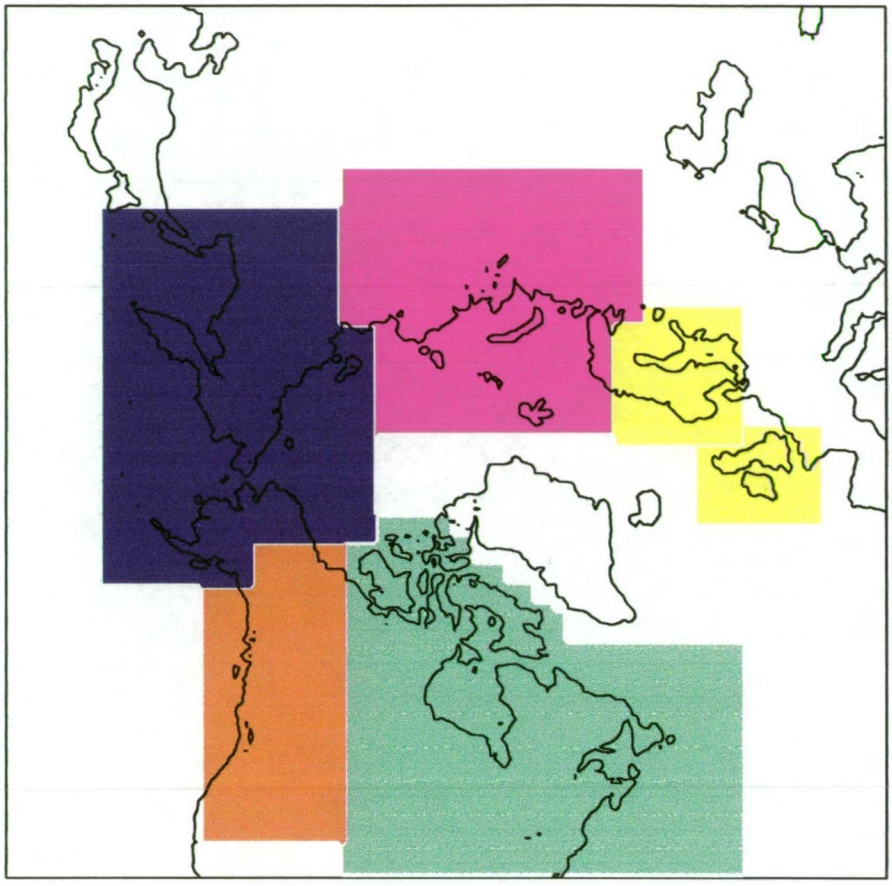

Figure 6.3: Individual ice sheet regions. The shaded regions define the areas allotted to the individual ice sheets for the calculation of their ice volume. The British and Fennoscandian Ice Sheets area is shaded yellow, Barents-Kara Ice Sheet - purple, Siberian Ice Sheet - blue, Cordilleran Ice Sheet - red, and the Laurentide Ice Sheet - green.

due to the warmer surface temperatures. In these cases (e.g. British - Fennoscandian), the ice sheet was less voluminous at subsequent glacial maxima.

6.2.1 Greenland

Figure 6.5 shows the glacial changes in the volume of the Greenland Ice Sheet and the thickness at the modelled summit. Qualitatively, this agrees reasonably with the modelling studies of Letréguilly et al. (1991) (see Figure 3.3) and Fabre et al. (1995). Their higher resolution models produced more than 30% less ice than found in this study, where the ice sheet margins advanced around the coastline. However, the trend from a small volume at the last interglacial,

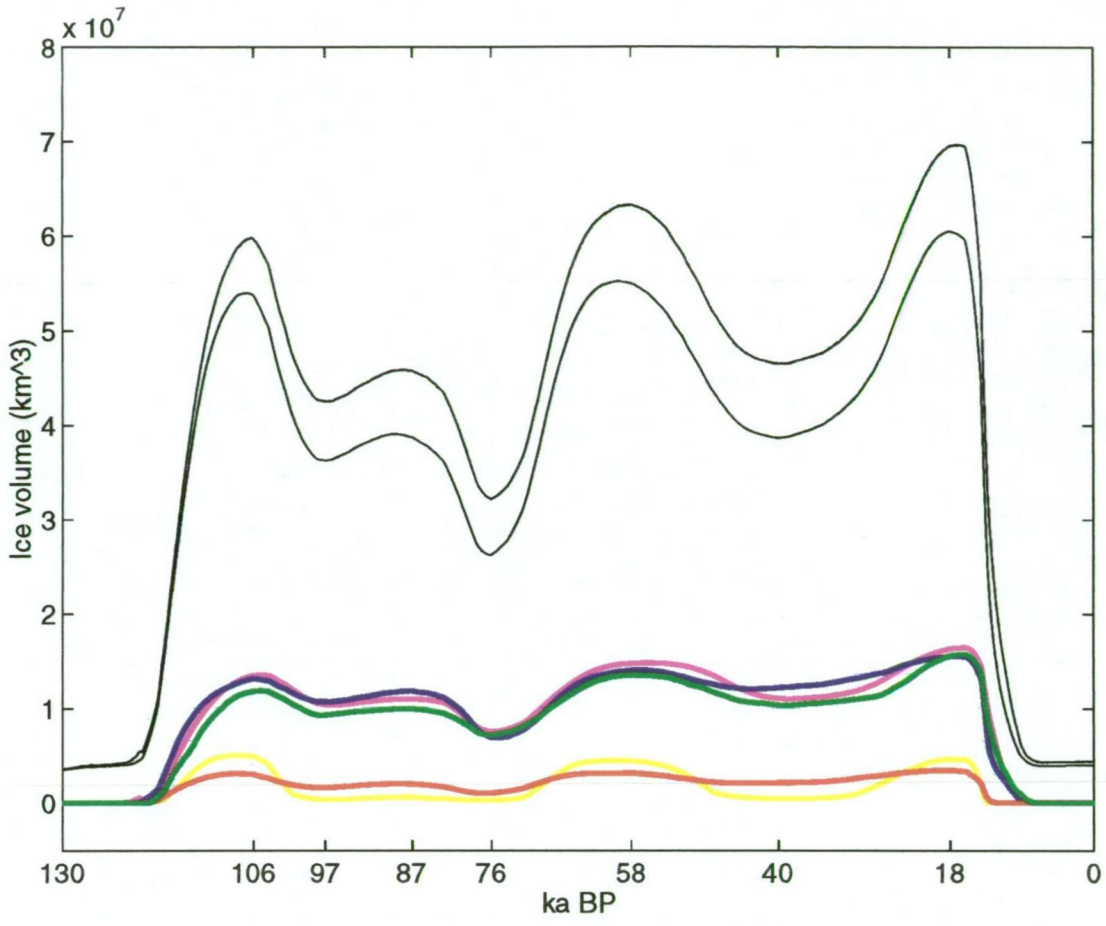

Figure 6.4: Ice volume change through the last glacial cycle. Shown are; total ice volume (top black line), volume of ice above buoyancy (lower black line), and the total volumes of the British and Fennoscandian Ice Sheets (yellow), Barents-Kara Ice Sheet (purple), Siberian Ice Sheet (blue), Cordilleran Ice Sheet (red), and Laurentide Ice Sheet (green). The timing of peaks and troughs for the total ice volume is also shown.

increasing to an early peak, then oscillating before approaching an LGM maximum and declining to a present ice sheet more voluminous than at the last interglacial is consistent with their results. Although accumulation forcing is not explicitly included here, the effect of changing sea level and ice thickness on the elevation leads to variation in the accumulation over Greenland and the temperature and sea level forcing appears to have produced a reasonable pattern of volume change in Greenland through the glacial cycle. The change in ice sheet thickness also compares favourably with the results of Letréguilly et al.

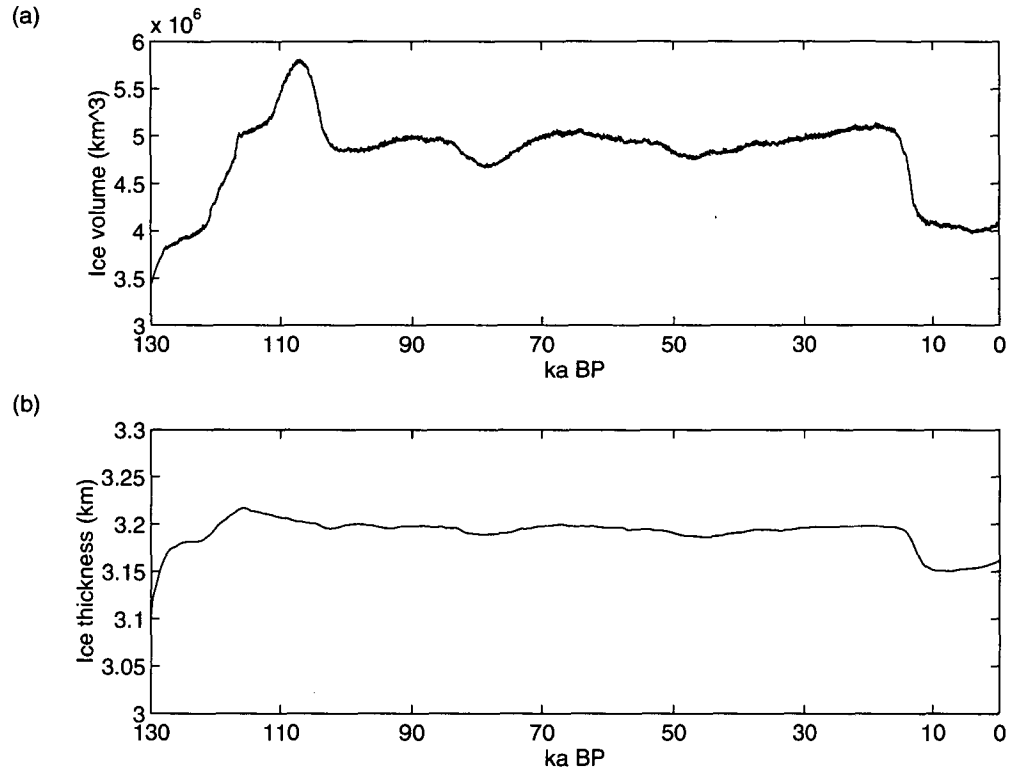

Figure 6.5: (a) Total ice volume change for Greenland through the glacial cycle. (b) Summit ice thickness change for Greenland through the cycle.

(1991) who also found a marked increase in thickness from 130ka BP to 120ka BP and decrease in thickness following the LGM.

6.3 Ice sheet changes prior to the LGM

6.3.1 From the last interglacial to first glacial maximum (5e-5d)

Figure 6.6 (a) shows the state of the ice and bedrock for the last interglacial, the initial state for the model. From this relatively unglaciated state, ice advanced into North America as temperatures depressed towards the low that produced the stage 5d maximum ice extent shown in Figure 6.7 (a). The nature of this advance is shown in the Figure 6.6 (b)-(d) sequence. This ice advance appears first as an expansion in the Greenland Ice Sheet and with the growth of ice on Baffin Island and the northern Canadian islands, is consistent with what

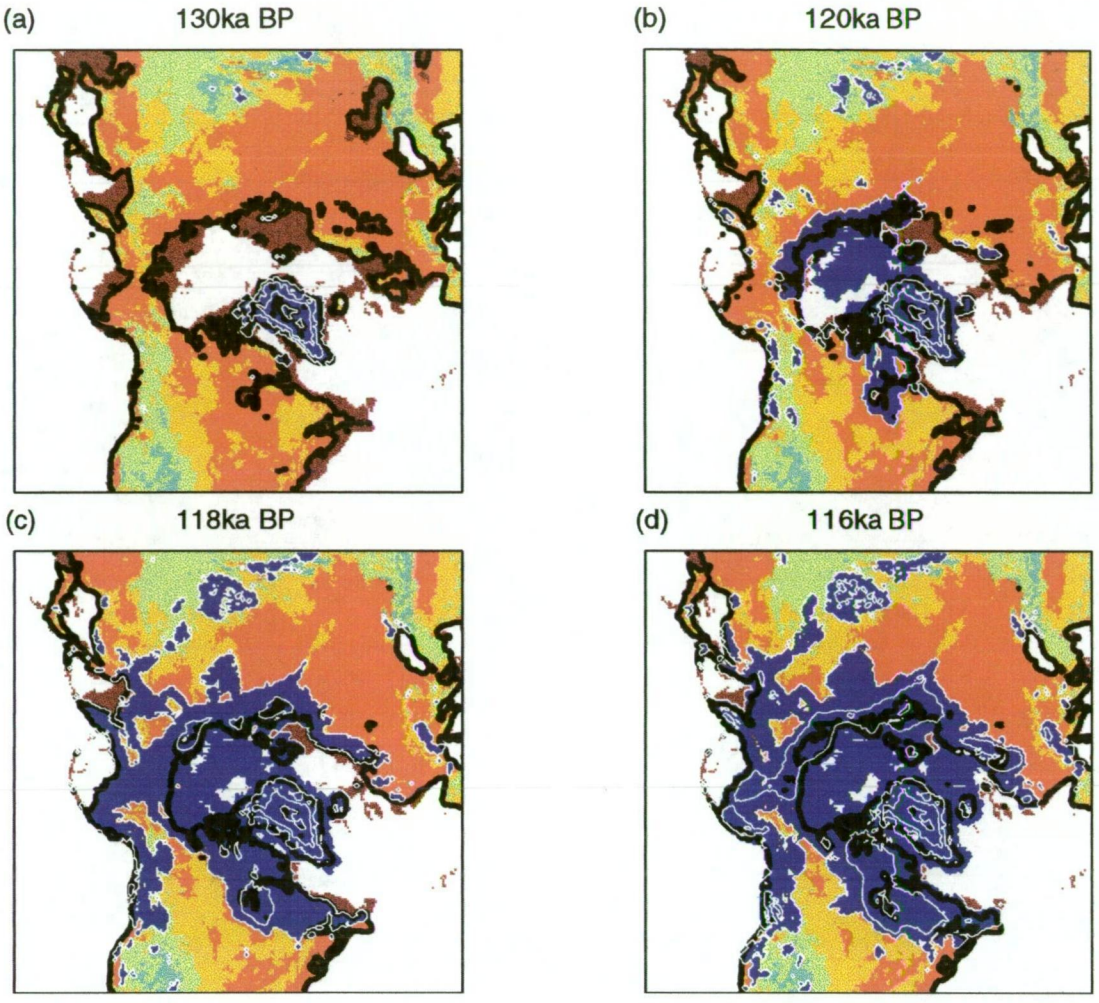

Figure 6.6: Ice and bedrock states during the initial advance. Iced regions are shown as dark blue with thickness contours in white. The contour interval is 1km. The black contour shows the modelled sea level at the time. Bed elevation colours are as for Figure 5.11.

is known of this early stage of glaciation. The Hudson Bay region remained largely above sea level at this early stage of the model run and so was readily open to glaciation also. The shape of this early Laurentide Ice Sheet appears to reflect the present day temperature distribution in the region. The present day summer temperatures in Hudson Bay are depressed relative to its surrounds (see Figure 5.3) and this bias remains in the temperature distribution even when the bed in the region is raised above sea level to its interglacial level. Now submerged, there is no available evidence relating to this early glacial history. Nevertheless, considering the recorded advance of ice in Keewatin and Quebec,

a simultaneous advance in the area between seems plausible.
Palaeo-reconstructions of the stage 5d Laurentide Ice Sheet agree well with the modelled maximum of Figure 6.7 (a), with the ice margin extending beyond the present day extent of Hudson Bay, perhaps arguing the case for the nature of the advance modelled here.

Consistent with the palaeo-record, glaciation commenced later in Europe and around the Arctic coast to Siberia. The onset of glaciation in Scandinavia occurred in the mountains of western Norway, but otherwise seeding largely took place on the Arctic islands, either as expansion of existing ice in Svalbard, Franz Josef Land, Severnaya Zemlya and Novaya Zemlya or the initiation of ice caps in the New Siberian Islands and on Wrangel Island.

From these Arctic islands, ice expanded out across regions of continental shelf either exposed by the fall in sea level or where the water depth was shallow. In this way the marine Kara and Siberian Ice Sheets were formed. Even when sea level change was not included in the model, both these ice sheets readily formed, grounding on the continental shelf without impinging on land above sea level inland of the Arctic coast. This is consistent with the interpretation of Grosswald and Hughes (1995) who suggested that the evidence indicated that marine ice sheets formed in these regions before expanding into continental areas. These marine ice sheets modelled here developed earlier and more quickly than the land based European ice, with no ice sheet occurring in Britain until 118ka BP.

However, the ice cap in Scandinavia did continue to expand and was joined by a second cap further north on the Norwegian coast, although the model failed to produce as much ice in Europe as is generally thought to have existed. There was expansion of ice caps in mountain ranges from the European Alps to the Mid-Siberian Plateau and the extensive ranges in eastern Siberia. These eastern Siberian mountain ice caps grew and eventually coalesced with the marine Siberian Ice Sheet to form the large Siberian Ice Sheet seen in Figure 6.7 (a). Similarly the ice cap on the Mid-Siberian Plateau was the continental source of the Kara Ice Sheet and ice in the Ural Mountains became part of the Barents Ice Sheet.

Some reconstructions have suggested that there may at some stage have

been extensive glaciation in the eastern Siberian ranges, although the maximum produced here and in later advances seems excessive. Advancing ice from the Siberian mountains, as well as from the marine ice sheets in the Arctic and the Bering Sea all contributed to this large ice mass.

Evidence suggests that the first significant glaciation of the Cordilleran Ice Sheet region came later than occurs here. In fact, as seen in other mountain ranges, the Rocky Mountains were very sensitive to glaciation when temperatures decreased in the model. A large Cordilleran Ice Sheet was augmented by the encroachment of the marine Barents Sea Ice Sheet into Alaska. Ice advancing predominantly from the marine ice sheet to the west left Alaska ice bound but for an ice-free Yukon Valley.

The growth of ice in Scandinavia and the inland components of the Siberian, Kara and Barents Ice Sheets coincided with the development of an ice sheet in Britain which merged with that in Scandinavia, producing an almost continuous ring of ice around the Arctic Ocean. A narrow channel in the Greenland Sea and another between Iceland and northern Britain allowed the only connection between the Arctic and the rest of the worlds oceans.

A large shelf of floating ice developed roughly synchronous with the advance of the grounded ice. From the ice caps on Arctic islands, the ice shelf spread and connected with grounded ice as that grounded ice extended around the Arctic coast. This large ice shelf appears to have been sensitive to the accumulation rate, with 'holes' developing in regions of low accumulation. These holes are also dependent on the non-existence of icebergs in the model. When ice calves from ice shelves in the model, it is no longer considered. But with no way of escaping these ice shelf 'holes' except through melting, it is expected that calved icebergs would re-attach to the ice shelf which would become continuous to its southern, open ocean boundary. It was also found that the nature of the floating ice cover in the Arctic Ocean was dependent on the oceanic melt rate. In the absence of any oceanic melt, it was found that the fast flowing ice shelf quickly converged, thickened and eventually grounded in the Arctic Ocean. This grounding initially occurred on the relatively shallow Harris Ridge and then quickly spread throughout the Arctic Ocean. Once this grounding occurred, it was found that subsequent climatic warming was not

sufficient to remove the mass of grounded ice. As discussed in Section 4.3.2, the model includes the effects of oceanic melt on floating ice which ranges from no melt during the coldest glacial periods to 0.5 $m\,a^{-1}$ for the present.

Generally this initial glacial advance is characterised by a tendency to increase in extent before becoming thicker. Large areas became covered in relatively short times by extensive, thin sheets of ice. This is suggestive of the 'instantaneous glacierization' mechanism of glacial advance suggested by Fulton and Prest (1987). Something close to the maximum areal extent was reached (~109ka BP) some time before maximum thicknesses (and volume) were achieved (106ka BP).

It may be noted in Figure 6.6 and similar figures that bedrock elevations appear to change even in ice-free regions. This may be as a result of the bed continuing to uplift even after the overlying ice has disappeared. The long response times of the bed response mean that the bed may remain out of equilibrium with its burden for many thousands of years and so may continue to adjust in the absence of a load, in response to the removal of an earlier burden. The bedrock elevations may also appear to change in these figures due to the change in sea level. As discussed in Section 4.2, sea level change is effected in the model by altering the bed elevations. A lower sea level is produced by raising the bed in the model and this is relfected in the bed elevation contours in the figures.

6.3.2 Substages 5d-5a

Following the maximum reached around 106ka BP, there was a degree of deglaciation as temperatures warmed. A local minimum was reached by 97ka BP for which the bed elevation and ice thickness distribution is shown in Figure 6.7 (b). The deglaciation mirrored the previous advance in as much as the British Ice Sheet and European ice in general, retreated more readily than that in Siberia or North America. A small ice cap remained in the Scandinavian mountains where the Fennoscandian Ice Sheet was initiated. Retreat of the Barents Ice Sheet was largely confined to its western margin where the diminution of the Fennoscandian ice was accentuated by the eastward retreat of the Barents Ice Sheet.

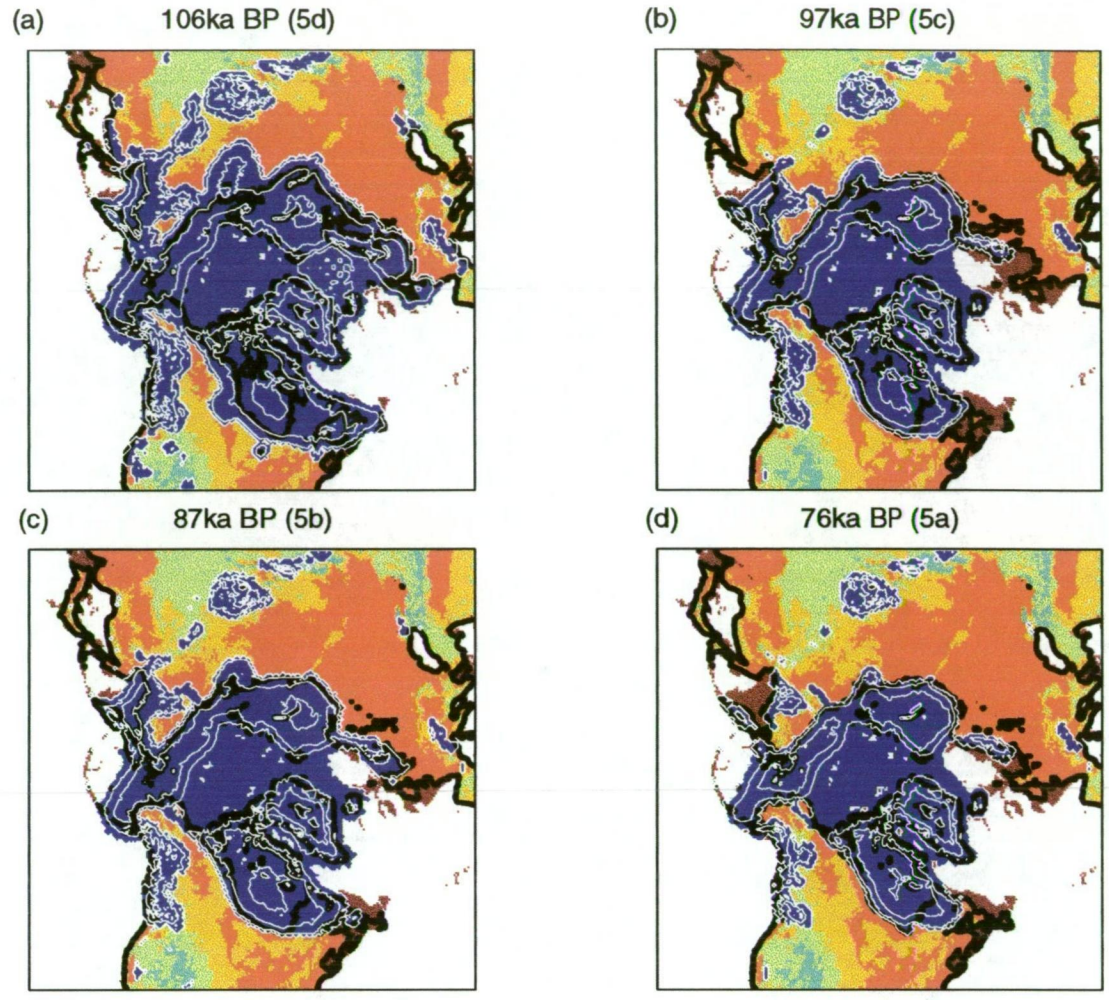

Figure 6.7: Ice and bedrock states at volume peaks and troughs corresponding to isotopic substages 5d-5a. Iced regions are shown as dark blue with thickness contours in white. The contour interval is 1km. The black contour shows the modelled sea level at the time. Bed elevation colours are as for Figure 5.11.

In the model, the Kara and particularly the Siberian Ice Sheet remained virtually intact. There was significant deglaciation in the mountains in southern Russia but only a small retreat in the mountains further north. The marine based ice sheets in these regions were virtually unaffected by the warming. The Siberian Ice Sheet continued to extend to the edge of the continental shelf and into Alaska and maintained a strong connection with ice extending up the western North American coast. The Cordilleran Ice Sheet contracted to some degree along its southern margin, but was otherwise stable.

As pointed out in Section 6.2 the duration of the cooling period in stage

5b was too short for the ice sheets to react strongly. The volume curve shows this stage as more of an interruption to a warming trend which culminated at stage 5a, rather than as a significant volume peak. This is reflected in the ice distribution. Figure 6.7 (c) shows the ice and bed distribution at this point and it can be seen that there has been minimal readvance from Figure 6.7 (b). Some expansion can be seen in the Scandinavian and the eastern Laurentide Ice Sheets and some of the southern mountain ranges such as the Caucasus, but otherwise there is little discernible change.

Retreat again set in and by 76ka BP ice volume had reached its lowest point between the interglacials, as shown in Figure 6.7 (d). The modelled Laurentide Ice Sheet remained robust throughout stage 5, and at stage 5a is only reduced by slight contraction in the east, south and west from its stage 5d distribution. Palaeo-evidence suggests that retreat was in reality more significant than this, although the scarcity of observations from Hudson Bay limit the accuracy of locating the extent of retreat. In the Canadian Arctic islands, reconstructions based on observations also suggest that after the early glacial maximum extent, ice retreated and never again advanced so far, even at the LGM. This is not the case in the modelled reconstruction where the northern margin of the Laurentide Ice Sheet remains virtually unchanged. For the same change in temperature, the method of calculating ablation used here will produce a far greater change in ablation at warmer temperatures than colder ones. Hence in comparison to southern margin migration, northern margins are not expected to react so strongly to the temperature forcing.

Figure 6.7 (d) shows that some contraction in the Cordilleran Ice Sheet and in northern Alaska left Alaska more ice-free and similarly retreat in the mountains of Siberia reduced the size of the land based Siberian Ice Sheet. The Scandinavian Ice Sheet also retreated to the point of just separating from ice in the Barents Sea which contracted slightly to the east. That the Fennoscandian Ice Sheet survived in some form through this period, before readvancing, is consistent with observations. Elsewhere the ice remained relatively intact.

The Arctic ice shelf reached its maximum extent for the entire glacial cycle by 106ka BP, when it extended to the northern British coast and reached thicknesses of over 1km, although the model retained ice shelf 'holes' in some

areas. At this time grounded ice covered the Barents Sea to Svalbard and the only connection between the Arctic Ocean and the rest of the world's oceans was through the Greenland Sea. While at some points in the Greenland Sea the model found that the ice sheet was within hundreds of metres of grounding, the minimum water gap across this channel was found to be about 1.6km, ensuring that ice shelf grounding and the consequent complete oceanic isolation of the Arctic Ocean was not imminent. After this time, the modelled ice thinned and retreated so that the ice edge was in a position close to the present day maximum limit of drift ice, where it remained until after the LGM.

6.3.3 Stages 4 and 3

By 60ka BP a new maximum was reached (Figure 6.8 (a)) resembling that which occurred at 106ka BP in both total volume and distribution of ice. Generally, the distribution of ice at these two peaks is similar, with perhaps slightly greater grounded ice extent at 60ka BP than at the earlier maximum. Possibly due to greater bed depression, all the large ice sheets are thicker at the later peak. This is compensated in the total volume curve by the larger ice shelf at substage 5d, and the total volume at the 60ka BP maximum is only slightly greater than at 106ka BP, despite there being larger ice sheets at the stage 4 maximum. A similar sized Laurentide Ice Sheet at stages 5d and 4 is consistent with palaeo-evidence (Clark et al. 1993). A significant Cordilleran Ice Sheet is also thought to have appeared by, or probably before this time, and indeed the Cordilleran Ice Sheet did peak slightly prior to its North American neighbour and was beginning to recede by the time the Laurentide Ice Sheet peaked.

From 60ka BP to 40ka BP (Figure 6.8 (b)) retreat again set in, following a similar pattern to earlier retreats. The effects of the bed being depressed beneath old ice sheets allowed a greater thickness of ice to exist within the same margins than in earlier periods when the bed was not so depressed. Decreasing accumulation rate with elevation makes it difficult for ice sheets to exceed a certain altitude but with the bed sinking, a thicker ice sheet may exist beneath the same elevation.

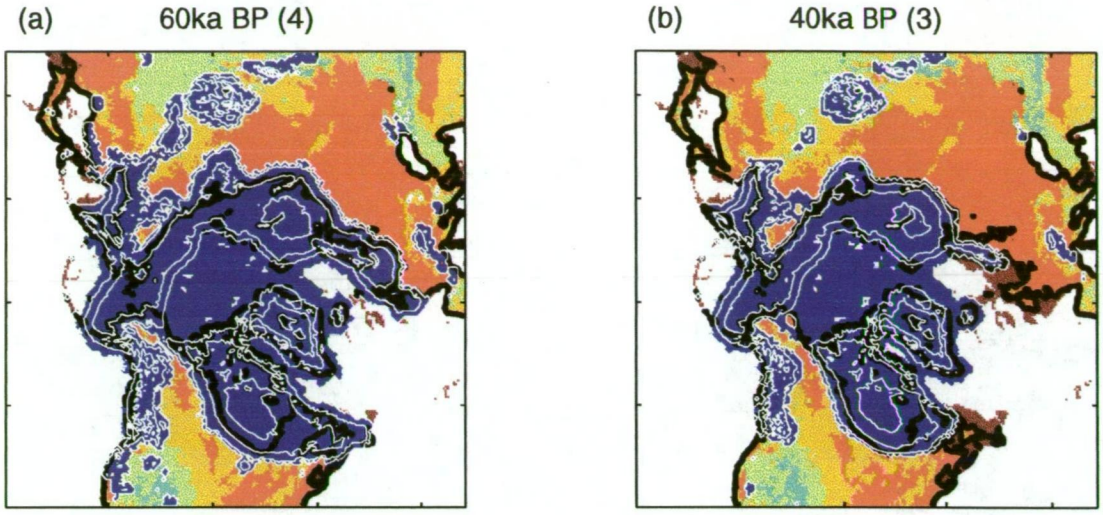

Figure 6.8: Ice and bedrock states at the volume peak during isotopic stage 4 and the volume trough in stage 3. Iced regions are shown as dark blue with thickness contours in white. The contour interval is 1km. The black contour shows the modelled sea level at the time. Bed elevation colours are as for Figure 5.11.

6.4 Last Glacial Maximum

The modelled LGM was not reached simultaneously in all regions, but maximum thickness and extent were attained in most places by 18ka BP (Figure 6.9) and everywhere by 16ka BP. This represents a lag behind the forcing of 2-4ka.

Reconstructions of the Laurentide Ice Sheet based on observations indicate that the southern margin reached its maximum extent at the LGM, with lobes progressing some distance south of the extent reached at the earlier maxima, so that the ice sheet covered the present location of the Great Lakes. Melt water from along this southern margin is thought to have drained into the Gulf of Mexico via the Mississippi River. The maximum modelled southern extent of the Laurentide Ice Sheet for the glacial cycle occurred at the LGM, although this margin is not quite as extensive as is thought to have existed in reality (e.g. Grosswald (1988)). This is also the case for the western margin which some consider to have merged with the Cordilleran Ice Sheet as far north as Alaska. While palaeo-evidence supports the separation between the North American ice sheets in Alaska, that the separation continued to the southern margins of the ice sheets is less clear (Mayewski et al. 1981). Despite being slightly less

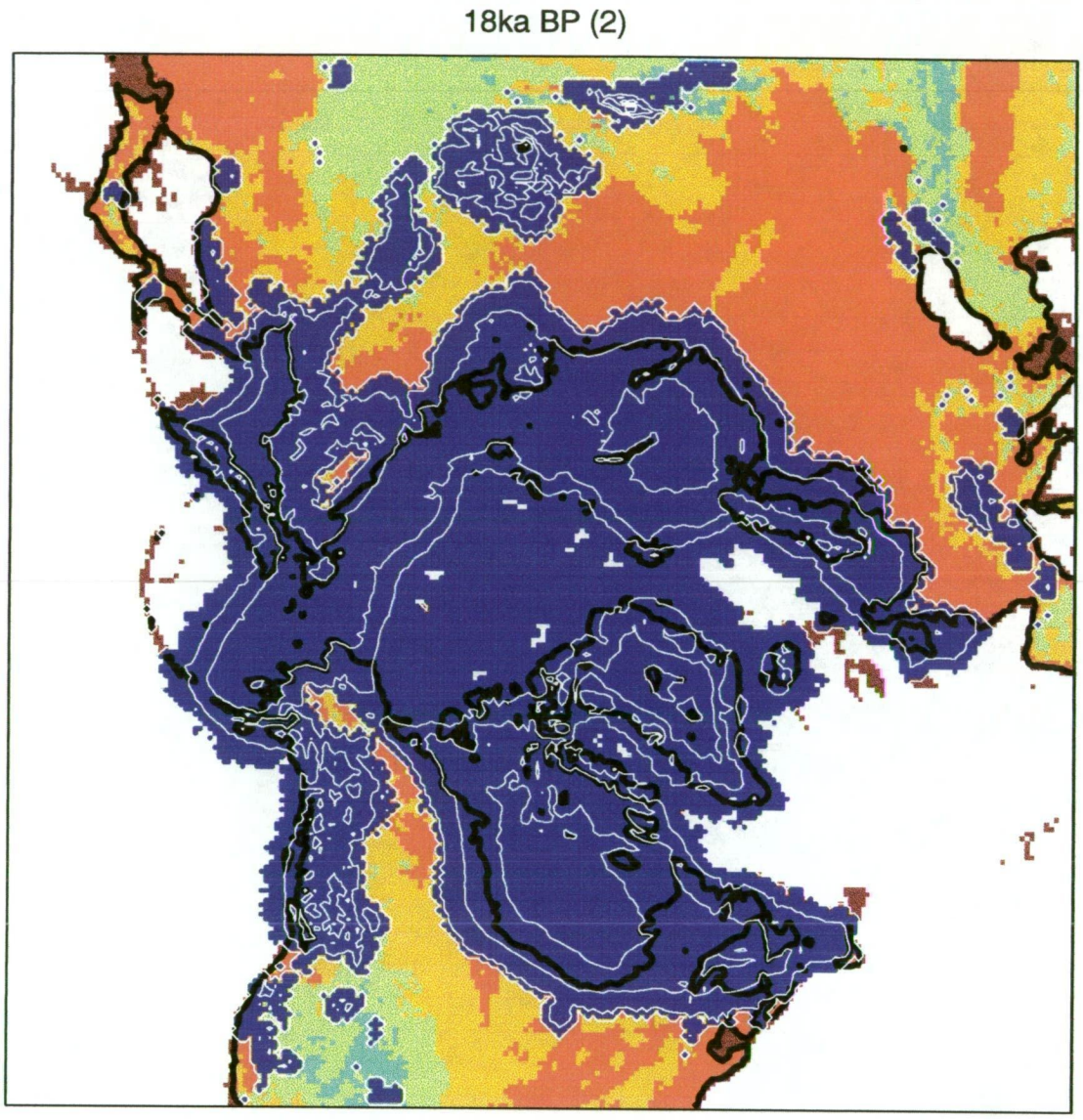

Figure 6.9: Modelled ice and bedrock states at the Last Glacial Maximum (stage 2 maximum). Iced regions are shown as dark blue with thickness contours in white. The contour interval is 1km. The black contour shows the modelled sea level at the time. Bed elevation colours are as for Figure 5.11.

extensive than palaeo-reconstructions, the modelled Laurentide Ice Sheet reached thicknesses of over 3km, in agreement with other estimates, both modelled (Peltier and Marshall 1995) and observation based (Peltier 1994). Some suggest that the ice sheet may have been made up of 2 major domes (Dyke and Prest 1987) and here the model produces two such domes, in the depressed basins of Hudson Bay and near the Gulf of St. Lawrence, in Labrador. The separate domes are clear in the thickness distribution (Figure 6.9) but their distinction is less pronounced in the elevation distribution (Figure 6.10) where the two peaks are separated by a saddle only $\sim$ 30m below them.

Notwithstanding the complete separation from the Laurentide Ice Sheet, the LGM Cordilleran Ice Sheet is well represented by the model. Two main domes, a northern and a southern, are produced. Their location and thicknesses are in good agreement with observation (Grosswald 1988). The margin in the north east of the modelled ice sheet is too extensive, but elsewhere resembles palaeo-reconstructions. In the south, the ice sheet thins rapidly with distance from the southern dome, with a few small isolated ice caps appearing in the mountains further south. In the north, ice extends to the West Alaskan coast and up the Alaskan peninsula, where it becomes indistinguishable from the Siberian ice further west.

As in previous advances, the expansion of Siberian mountain ice caps until they extensively coalesced produced a large land based ice sheet in the modelled eastern Siberia. All that remains that is suggestive of the separation of the ice caps of different ranges are the ice-free Kolyma lowlands. While this reconstruction is excessive compared to what is apparent from sparse observation, there is evidence in the palaeo-record of extensive glaciation in these mountain ranges which was not far short of a significant connection (Hughes 1998). Given the resolution of the model is 50km, the reproduction of these features is reasonable.

The marine section of the Siberian Ice Sheet extended to the edge of the continental shelf in the Laptev, East Siberian, Chukchi and Bering Seas in the model from 118ka BP and that margin remained very stable throughout the glacial cycle until after the LGM. The only expansion of this ice sheet at the LGM was in the form of a thickening due to the growth of the inland ice and

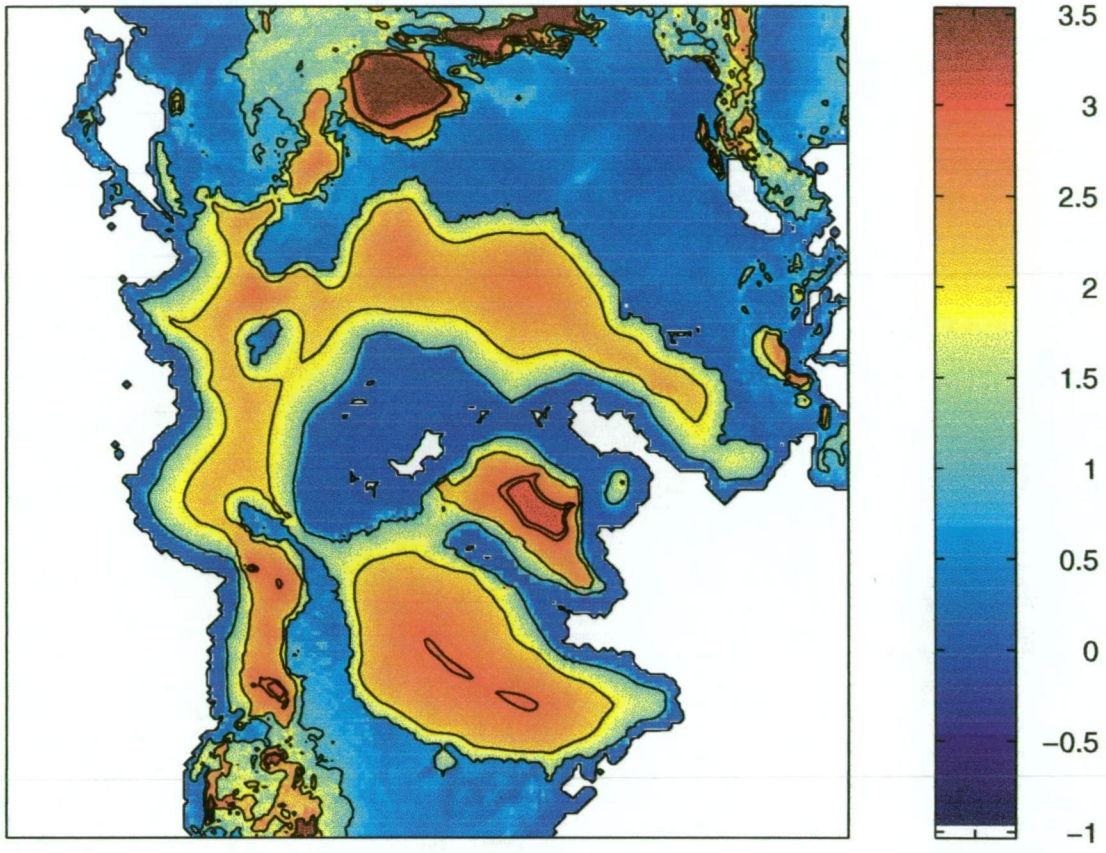

Figure 6.10: Modelled surface elevation at the Last Glacial Maximum. The scale is in km and the contour interval is 1km, but there is also a contour at 2.93km to highlight the separate domes in the Laurentide Ice Sheet. The associated ice distribution is that shown in Figure 6.9.

bedrock depression. But for the extension of this modelled ice sheet into the Bering Sea it is a good reproduction of the marine Siberian Ice Sheet which is thought to have existed at the LGM. Even in the Bering Sea there is a suggestion in the palaeo-record that there was some glaciation of the continental shelf edge and the Aleutian Islands, so the eastward extent of the Siberian Ice Sheet produced in the model may be thought of as excessive rather than unsubstantiated. Other models have produced similar, if not larger Siberian Ice Sheets (Lindstrom and MacAyeal 1989; Peltier and Marshall 1995; Huybrechts and T'siobbel 1995; Calov and Marsiat 1998). This suggests that either further understanding of the glacial climate in the region is required or that the reliability of geological palaeo-reconstructions there needs to be assessed, and

indeed some more recent reconstructions tend to have more ice in this region, with a distribution similar to that produced by this model (e.g. Hughes (1998)).

The model produces an LGM Barents-Kara Ice Sheet in good agreement with palaeo-evidence. Inlandward expansion into the Mid-Siberian Plateau and the Urals produced an expansive ice sheet with a single dome centred south of Novaya Zemlya. The northern margin again extends to near the continental shelf edge but is thinner than its southern counterpart. The northern, marine margins of all the Arctic Ice Sheets tend to be less steep than the inland southern margins due to the effect of the low bedrock on the thickness above buoyancy of the ice. At the northern margins where the bed is below sea level, the consequent increase in buoyancy leads to higher sliding (and total) velocities (Figure 6.11) and thinner ice.

There is a considerable amount of data locating the margin of the Fennoscandian Ice Sheet at the LGM. At that time ice extended well into present day Germany and Poland (e.g. Andersen (1981)). While the modelled reconstruction does not exhibit such southward extent, a significant ice sheet has formed in the region.

Further west the ice in Britain all but covers the present extent of the British Isles, leaving only a small southern region ice free. Considering the limitations due to the resolution of the model, this result agrees fairly well with palaeo-reconstructions of the LGM in the region which maintain a slightly larger portion of southern England as having been free of ice.

6.4.1 Variation in the accumulation rate

Discrepancies in the location of the ice sheet margin can also be compensated by adjustment of the accumulation rate. The influence of accumulation rate is investigated by comparing the LGM ice distribution produced above to those produced when the accumulation rate is halved or doubled and when the Jaeger present accumulation distribution (see Section 5.2.1) is used as the initial accumulation pattern (Figure 6.12). The amplitude of the temperature forcing remained at $\Delta T_{max} = -13°C$ for these model runs.

From Figure 6.12 it is clear that variation in accumulation rate did not exert a strong influence on determining the extent of the grounded ice sheets.

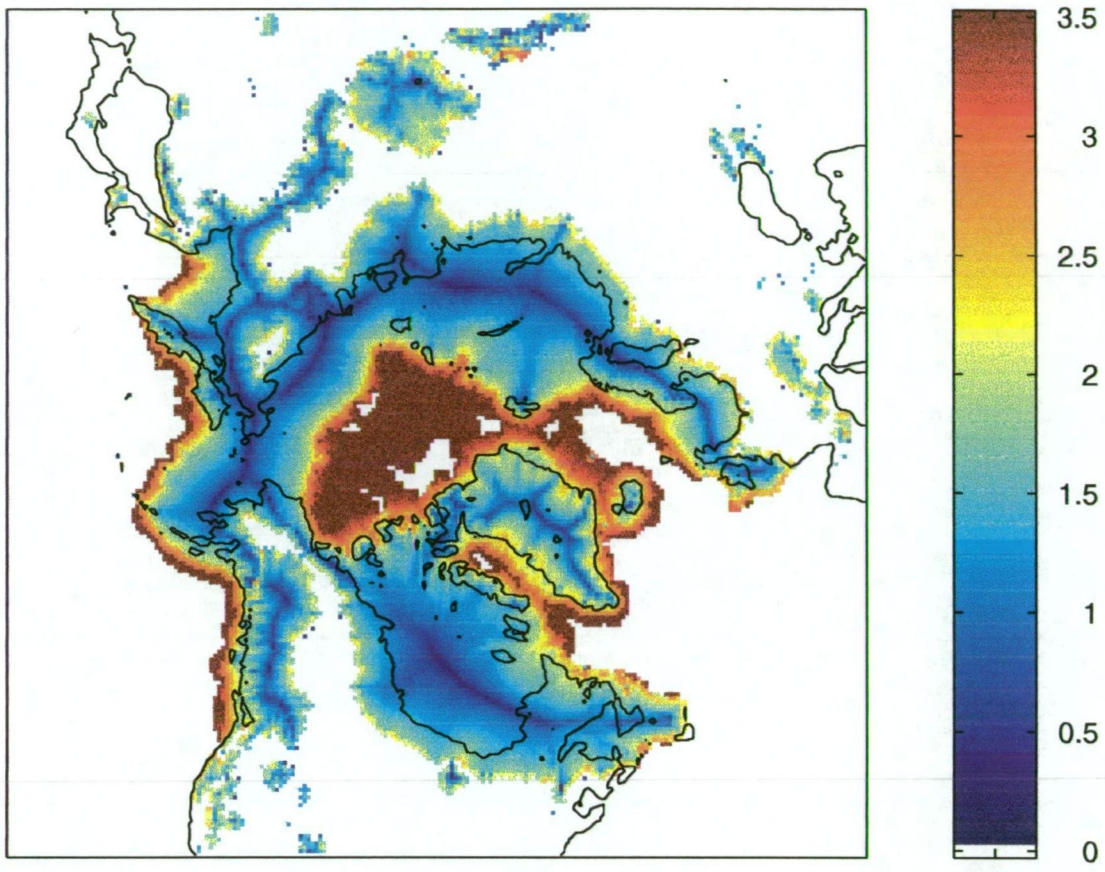

Figure 6.11: Ice velocities at the LGM ($\log(m\,a^{-1})$). Marine margins are characterised by higher velocities due to the increased sliding where the ice is grounded below sea level. The majority of the ice shelf is at the threshold velocity of $5000m\,a^{-1}$.

Doubling the accumulation rate led to only slightly greater advance along the southern grounded ice sheet margins and halving the accumulation produced marginally less extensive ice sheets. A 100% increase in the applied accumulation rate extended the ice sheet margins by about the same amount as a 13% change in the maximum amplitude of the temperature forcing (see Figure 6.1). There was also very little reduction in the southern extent of the ice sheets, at least along the grounded margins, when the base accumulation rate was halved. Although, as discussed below, the lower rate had a significant effect on the Arctic ice shelf and grounding in the Barents Sea, its effect on the southward extent of the grounded ice sheets was approximately equivalent to that of a 1°C change in the maximum amplitude of the temperature forcing.

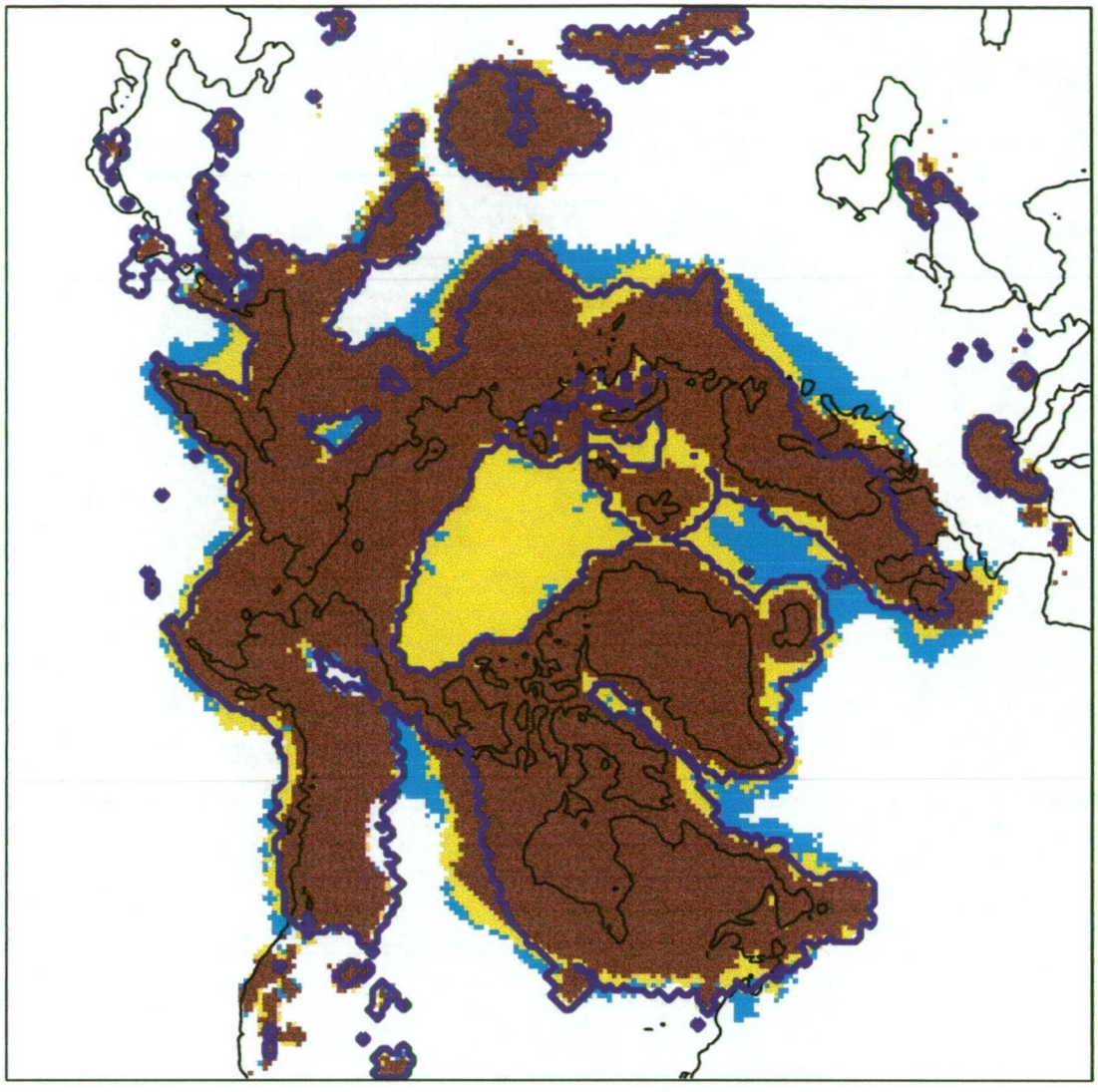

Figure 6.12: Variation in LGM ice extent due to changes in the accumulation rate. The yellow shading illustrates the iced area when the present (GCM) accumulation rate is used. The light blue area is for a doubling of this rate and the brown is for a halving of this rate. The dark blue line indicates the ice extent when the Jaeger accumulation data is used rather than the GCM data.The present coastline is shown.

Similarly, the use of the Jaeger accumulation data resulted in generally slightly less extensive grounded ice than that obtained using the GCM accumulation data. The accumulation rate applied will affect the ice sheet thickness, but over the ice sheets the accumulation rate is dominated by the 'elevation-desert' effect (see Figure 6.13), which largely limits the elevations the ice sheets may attain.

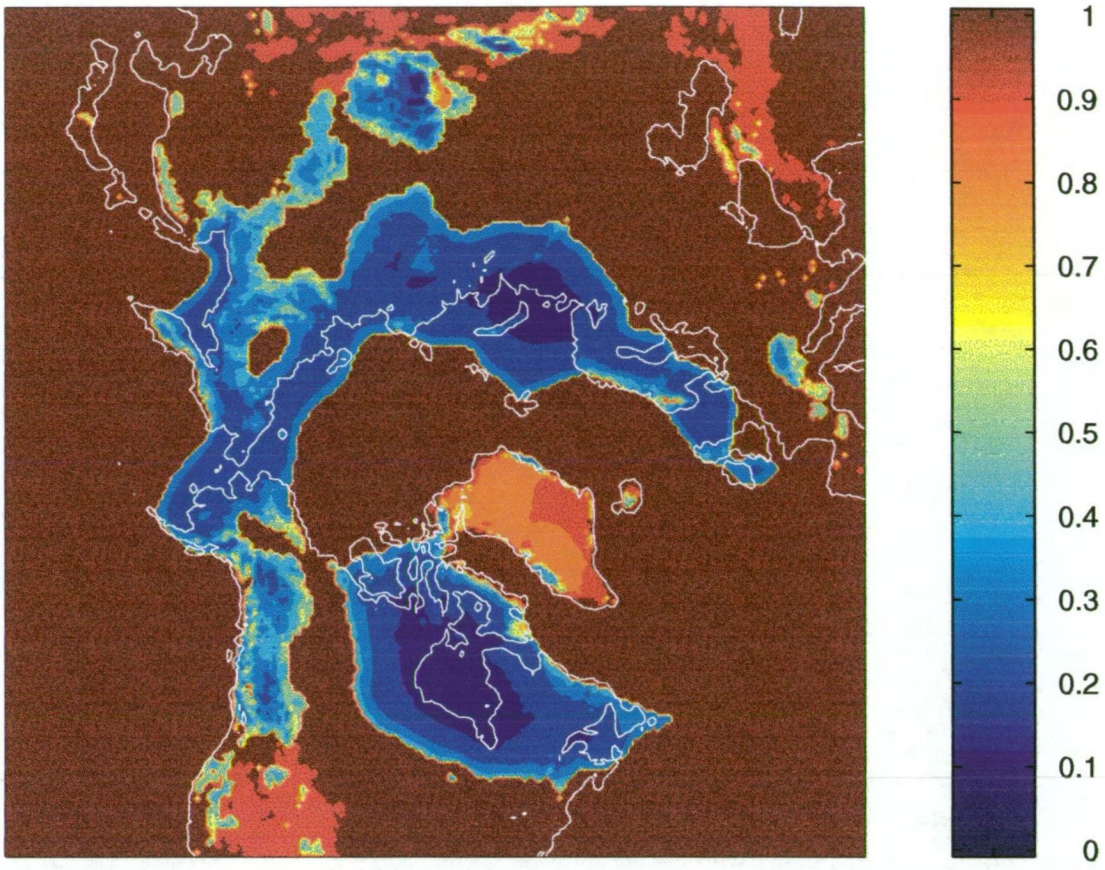

Figure 6.13: The influence of the elevation-desert effect. Precipitation rate at the LGM as a proportion of the base accumulation rate. Over much of the ice sheets the LGM accumulation rate is less than 30% of the base accumulation rate. Over Greenland, where there has been less height variation, the change in the accumulation rate is much smaller. Present coastline is shown.

Furthermore, there is generally great uncertainty in reconstructions of LGM ice sheet thickness and it is felt that in assessing the accuracy of a reconstruction, comparison of ice sheet extents is far more meaningful.

On the other hand, it was found that the extent and even the existence of an Arctic ice shelf was strongly dependent on the accumulation rate applied. The low elevations of floating ice exclude the influence of the elevation-desert effect and the change in thickness which resulted from the different amounts of accumulation determined the ability of the ice to remain thicker than the calving criterion. Doubling the accumulation rate produced an ice shelf extending across the Norwegian Sea and showed no signs of the 'holes' which

appeared in the ice shelf produced under the present accumulation regime, while halving the rate resulted in virtually no ice shelf at all. The Jaeger data give less precipitation over the Arctic Ocean than the GCM data set, and this low accumulation rate was also unable to sustain an extensive ice shelf there.

It is notable also that in the low accumulation scenarios, when no significant Arctic ice shelf was produced, the extent of glaciation in the Barents Sea was greatly reduced. The water depth there is greater than for the rest of the Arctic submarine continental shelf and it appears that, without an ice shelf, it would have been more difficult for ice to ground in this region. It was thought that given this sensitivity in the Barents Sea region, the formation of a grounded ice sheet there might also be dependent on a sea level decrease in glacial times. However, when the model was run without sea level forcing, but with the present GCM accumulation distribution, the Barents Sea was still filled with a grounded ice sheet similar to that which formed when sea level forcing was included. A decrease in sea level effectively raises the surface elevations in the model, leading to generally colder temperatures and lower ablation rates. The main effect of not including the sea level change was found to be a slight reduction in the southern extent of the ice sheets due to the effectively warmer temperatures compared to those of the model which included glacial sea level lowering.

Given the uncertainty in glacial accumulation rates and distributions, it appears that in modelling the grounded ice sheets of the last glacial cycle, it is wise to concentrate primarily on the temperature forcing, which appears to dominate, as suggested by Hostetler and Clark (1997). A change in the maximum amplitude of the temperature forcing of $\pm 1°C$ would generally be enough to account for discrepancies between model output and observations in establishing the position of the ice sheet southern margins, whereas given the dominance of the elevation-desert effect in the model, a much larger and unrealistic change in the accumulation rate and distribution would be required to produce the same effect. The comparatively minor influence of variation in the base accumulation rate on ice sheet extent also justifies the lack of consideration paid to the solid accumulation percentage. However, the question of the existence of an Arctic ice shelf may be closely tied to accumulation rates

over the Arctic Ocean in glacial times.

6.5 Deglaciation

In some ways the retreat of the northern hemisphere ice sheets after the LGM mirrored the early glacial advance. In general, the regions which were last to be glaciated at the beginning of the glacial cycle were places where the ice first retreated, and the earliest forming ice sheets were the last to disappear. After only small losses of ice immediately following the LGM, the retreat became rapid with entire ice sheets almost completely collapsing in a few thousand years, just as during glacial advance, large areas became ice covered in a relatively short period once some threshold had been attained. However, where extensive, thin ice sheets formed during glaciation, the retreat was characterised by the erosion of ice from the edges while, to a large extent the ice sheets maintained their thickness while they survived.

The ice distribution at 14ka BP is shown in Figure 6.14 (a). Retreat from the 18ka BP to 14ka BP mainly took the form of minor contraction along the ice sheet southern margins. After this time however, retreat accelerated (see Figure 6.17) and was especially noticeable in the British and Fennoscandian Ice Sheet. By 13.5ka BP (Figure 6.14 (b)) the British Ice Sheet was gone and the Fennoscandian as well as the Cordilleran Ice Sheet were reduced to small, isolated ice caps. Elsewhere, inland margins began to retreat more rapidly but marine margins remained stationary. This continued to be the case around the Arctic Ocean continental shelf where the marine ice sheets were the last to disappear. The marine ice sheet in the Bering Sea however had commenced retreat at its southern margin by 13ka BP (Figure 6.14 (c)). During this period of rapid deglaciation of the grounded ice, the Arctic ice shelf remained relatively stable. A 'hole' developed in the ice shelf along the north coast of Greenland and spread around the North American Arctic coast, but elsewhere the shelf remained intact.

By this time inland ice was confined to a few mountainous regions and the vast majority of the transient (i.e. excluding Greenland and the small Arctic ice caps) northern hemisphere ice was marine based. The ice sheets retreated to

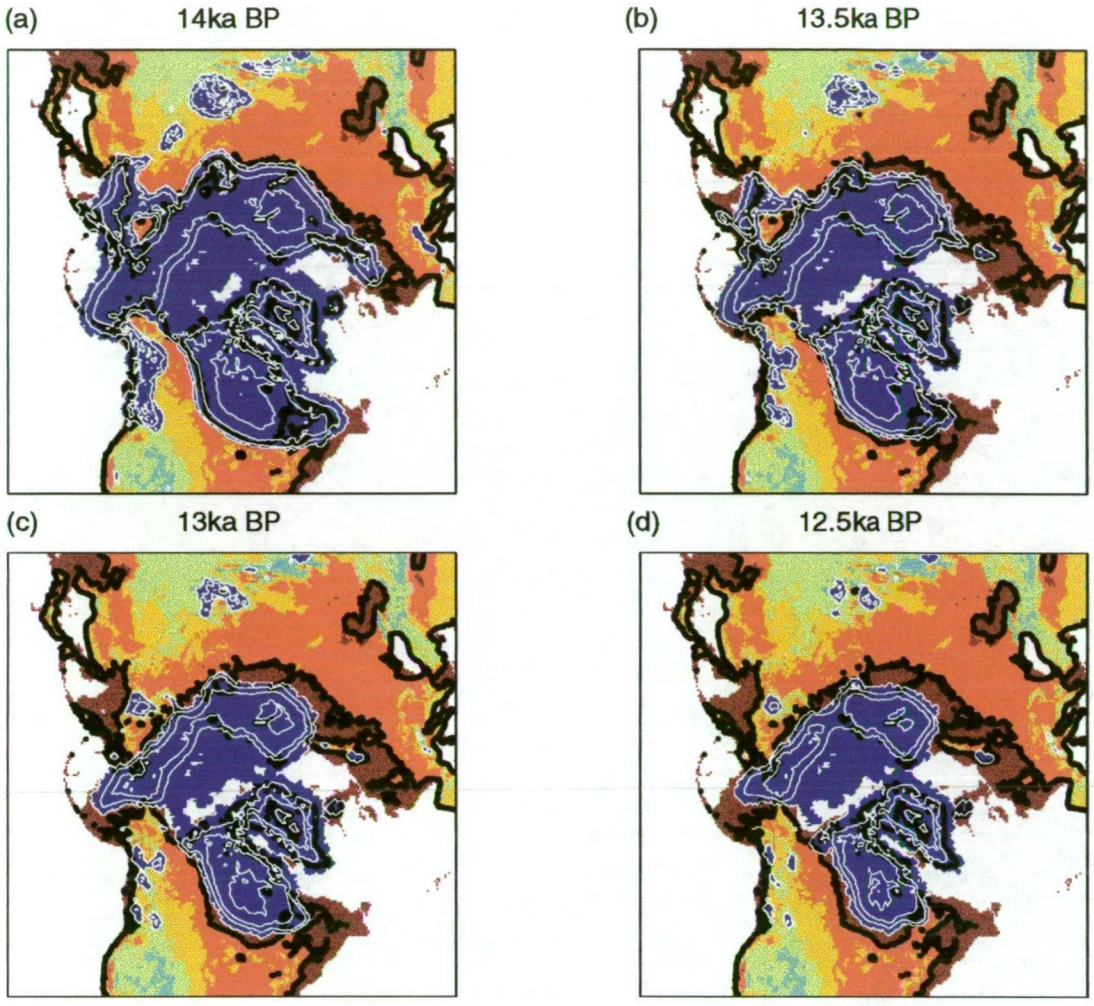

Figure 6.14: Ice and bedrock states during deglaciation following the LGM, 14-12.5ka BP. Iced regions are shown as dark blue with thickness contours in white. The contour interval is 1km. The black contour shows the modelled sea level at the time. Bed elevation colours are as for Figure 5.11.

regions where the bed was depressed below sea level. The isostatic rebound of the bed did not occur quickly enough to raise the bases of the ice sheets above sea level, a situation exacerbated by the rising sea level. Even at the same latitude, marine based ice was more robust than that grounded above sea level, as the ice in the Bering Sea retreated later than neighbouring Alaskan and Siberian ice. This agrees well with the conclusions of Dyke and Prest (1987) who found that often marine margins retreated more slowly than did those grounded above sea level and that marine based parts of an ice sheet were often the last to disappear. This evidence appears contrary to the theory of the

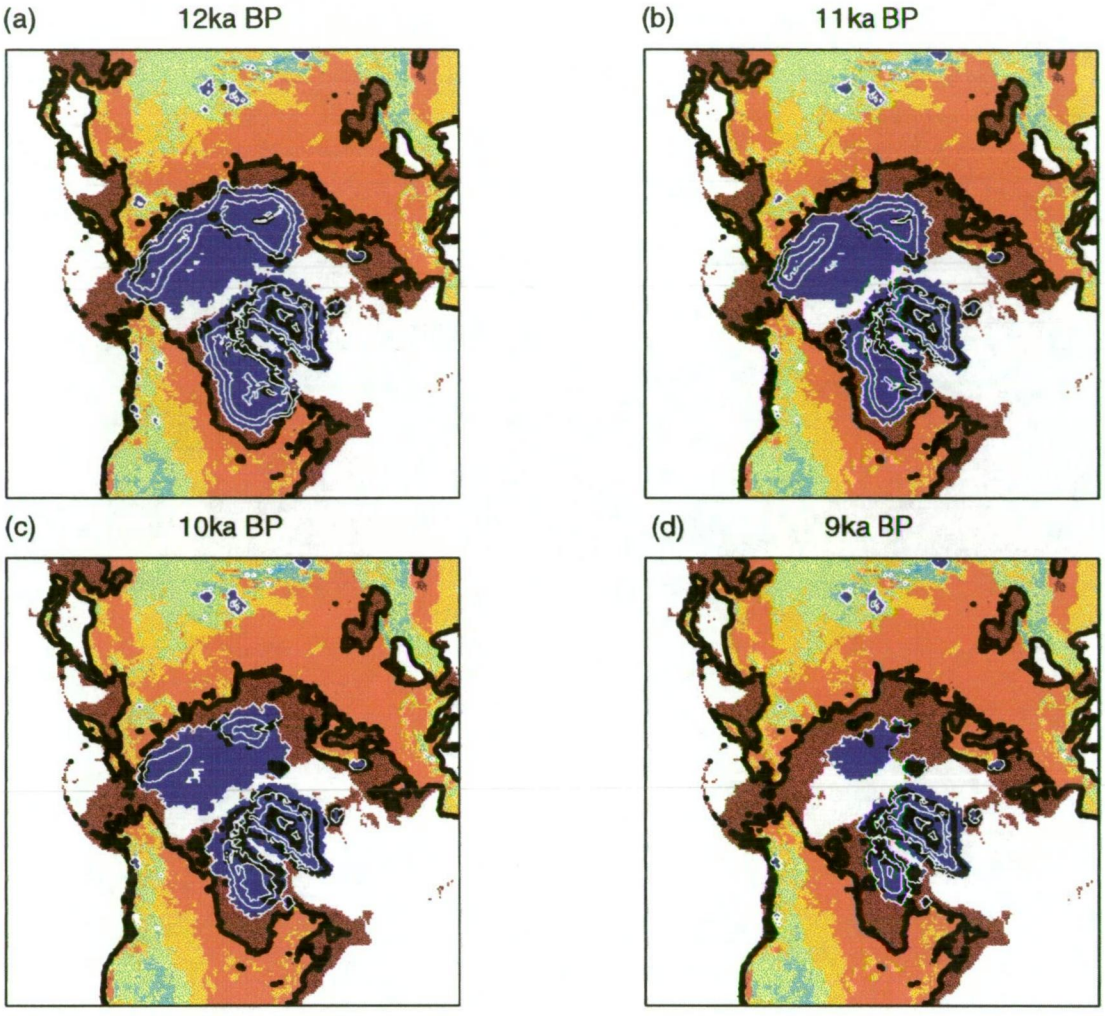

Figure 6.15: Ice and bedrock states during deglaciation following the LGM, 12-9ka BP. Iced regions are shown as dark blue with thickness contours in white. The contour interval is 1km. The black contour shows the modelled sea level at the time. Bed elevation colours are as for Figure 5.11.

inherent instability of the marine ice sheets and the likelihood that calving at marine margins was central to the retreat of some northern hemisphere ice sheets (Hughes et al. 1977). The late retreat of the Arctic ice shelf however, may have contributed to the stabilising of the marine margins. Some of the modelled marine ice sheets were also in relatively shallow water, and in considering the instability of the ice sheet, the depth below sea level at which it is grounded may have to be considered. Generally, ice sheets grounded in deep water should be more vulnerable than those grounded in shallow water or above sea level.

This pattern of retreat continued but around 12ka BP the rate of retreat

decreased (Figure 6.17). Grounding line retreat commenced about this time along the northern Siberian Ice Sheet margin and over the next few thousand years grounded ice there contracted to the Arctic islands, although this ice tended to remain connected by the remnant ice shelf which contracted into this region (Figure 6.15). At the same time the Laurentide Ice Sheet also contracted into the Canadian Arctic.

Figure 6.16 shows the model representation of the present. All ice sheets except that in Greenland have disappeared but for small remnant ice caps on some Arctic islands and in various mountain ranges. Although the extent is slightly excessive, the retention of these small ice caps on Baffin and Ellesmere Islands, as well as in Iceland, Svalbard and the Russian Arctic islands is consistent with reality. Ice has also survived in the Rocky Mountains in North America, the Altai Mountains in Asia and the European Alps. In some cases the amount of ice remaining in the model is exaggerated by the limited (50km) resolution of the model. This is the case for the Greenland ice sheet which, although exhibiting summit thicknesses similar to observed values (Budd et al. 1982), showed an increased extent in the modelled present state than that which is observed to exist. The nature of the ablation calculation in the model appears to allow an excessive ice extent to remain under present conditions around the Greenland coastline (and some other northern Arctic regions). This ice was not produced when the previous interglacial distribution was being generated and in part appears to be remnant ice dependent on earlier glacial advance for its existence.

All else being equal, the temperature forcing should produce temperatures at the end of the run slightly colder than at the last interglacial. However, the present bedrock being depressed to lower elevations than assumed here to have existed at the last interglacial leads to lower surface elevations and effectively slightly warmer temperatures in some locations. Because of these contrasting influences, ice distributions at the initial and final states are similar.

6.5.1 Ice volume changes

The climate forcing reached its maximum amplitude at around 20ka BP. The individual ice sheets lagged that by between 1.8ka and 3.7ka BP with peak

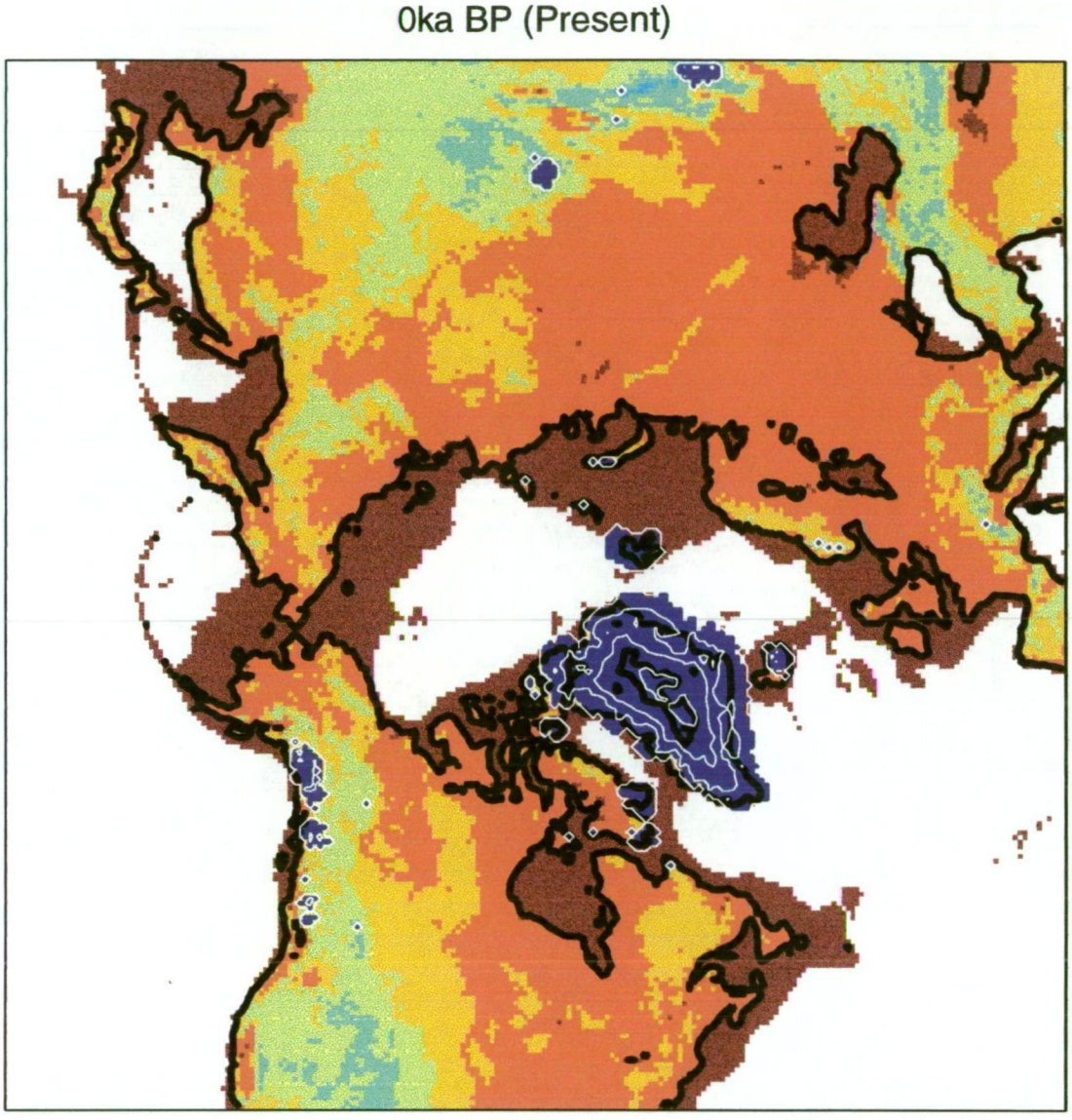

Figure 6.16: Ice and bedrock states at the end of the glacial cycle. Modelled ice and bed distributions are reasonable representations of present day conditions within the limitations of the model resolution. Iced regions are shown as dark blue with thickness contours in white. The contour interval is 1km. The black contour shows the modelled sea level at the time. Bed elevation colours are as for Figure 5.11.

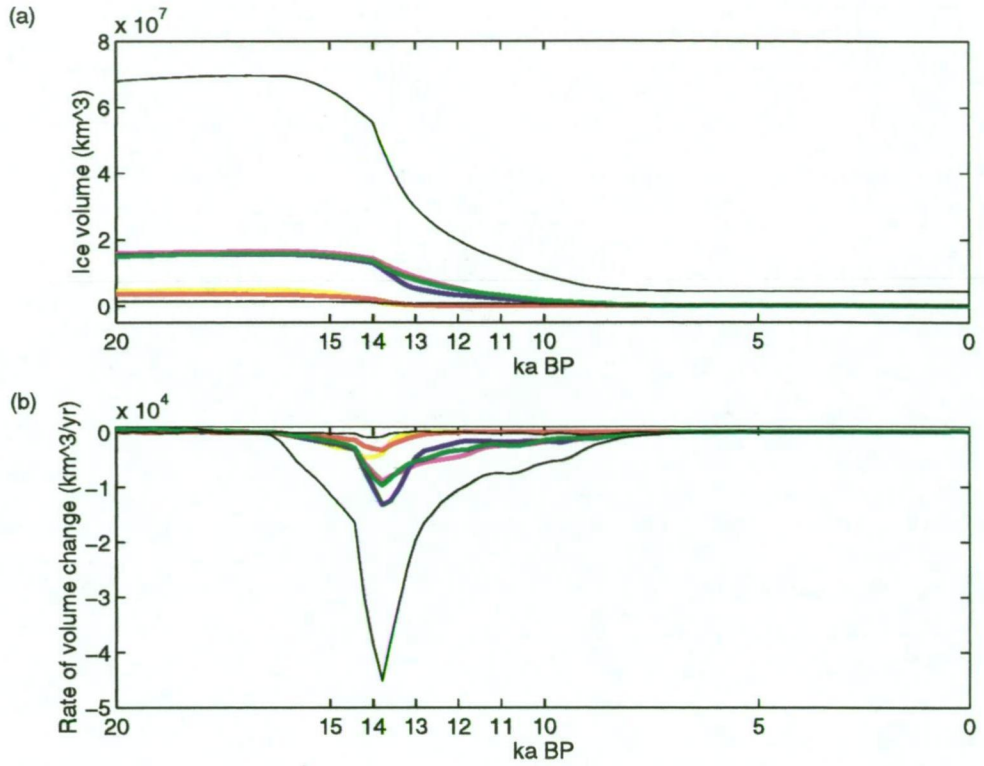

Figure 6.17: (a) Change in the ice volume for the northern hemisphere since 20ka BP. The top black line represents the total ice volume, the lower black line is the volume of floating ice, primarily in the Arctic Ocean ice shelf. The other lines represent the total volume changes for the different ice sheets. (b) The rate of change with time of the ice volume. The maximum rate of ice melt is at 13.8ka BP, coinciding well with the beginning of the Younger Dryas cooling period.

volumes for each ice sheet at: 18.2ka BP (Cordilleran and Siberian), 17-18ka BP (British-Fennoscandian), 16.5ka BP (Laurentide) and 16.3ka BP (Barents-Kara). Following this peak, the rate of ice loss increased to a maximum at 13.8ka BP (Figure 6.17), although ice loss from the British-Fennoscandian system peaked at 14.2ka BP.

At the LGM the southern margins of the large ice sheets were generally grounded above sea level and may have supported large ice dammed lakes (Grosswald 1988). These lakes are thought to have drained southward through the Mississippi to the Gulf of Mexico for the southern Laurentide lakes and through various rivers such as the Volga and Dnepr to the Caspian, Black and eventually the Mediterranean Sea in Eurasia (Grosswald 1988). At this time, ice

south of ice sheet divides which fed into these lakes (see Figure 6.18 (a)) was effectively part of the catchment for these drainage paths and this ice, when melted, would have to a large extent been removed from the Arctic region. With the exception of Cordilleran ice and some eastern Siberian ice, ice north of the ice sheet divides would have flowed into the Arctic Ocean, with nowhere else then to go, while the Bering Strait remained closed (until $\sim$ 11ka BP), but the North Atlantic Ocean. As the ice sheets diminished though, the southern margins retreated in many cases to below sea level and the drainage of meltwater from the southern margins would have been much more into the Arctic or directly into the North Atlantic Ocean (Figure 6.18 (b)). After 14ka BP then, it may be considered that a large percentage of the melting ice in the model would have flowed into the Arctic and eventually the North Atlantic Ocean. It has been proposed that the change in drainage along the southern margin of the Laurentide Ice Sheet from the Mississippi to the Gulf of St.Lawrence could have produced freshening of the North Atlantic, having a significant climatic influence in the region (Broecker et al. 1988).

6.5.2 Freshwater flow into Atlantic Ocean

As discussed in Section 2.4.4, the influx of freshwater to the North Atlantic may have been a cause for climate cooling in the region, and around the world. The Younger Dryas period of climatic cooling is thought to have some climate effects worldwide, but particularly in the North Atlantic region between about 14.5ka BP and 11.5ka BP (Dansgaard et al. 1993; Mayewski et al. 1996). As can be seen in Figure 6.17, this corresponds well with the timing of modelled maximum ice loss, or freshwater influx, from the northern hemisphere ice sheets. Radio-thorium dating of Barbados corals have also indicated that there was a rapid sea level rise at around 14ka BP (Bard et al. 1990), closely corresponding to the timing of the maximum rate of sea level rise modelled here. The magnitude of the freshwater influx may be compared to the amount of freshwater which entered the region through precipitation. Table 6.2 shows the volume of freshwater entering the Arctic catchment area per year due to accumulation (in $10^4 km^3 a^{-1}$) within a range of latitude bands and at different times during deglaciation. Also shown are the rates of meltwater discharge at

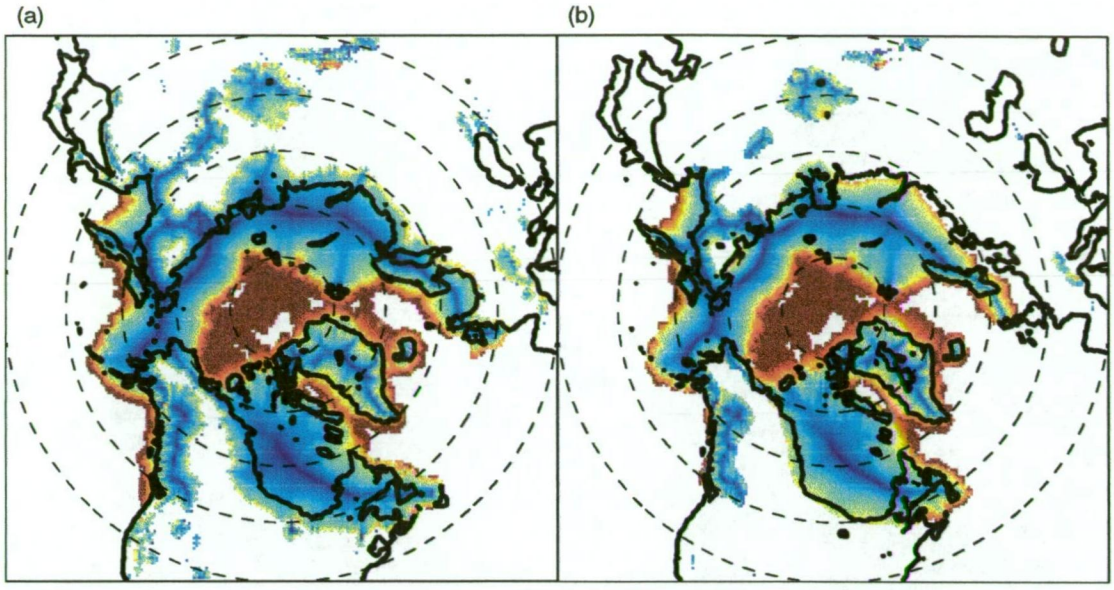

Figure 6.18: Ice velocity at (a) LGM, and (b) 14ka BP. The southern ice sheet margins have largely retreated to below sea level by 14ka BP, so that except for ice in the southern Bering Strait and Cordilleran Ice Sheet, even ice south of the divide will tend to flow into the Arctic or North Atlantic Oceans. Colour shading is as for Figure 6.11. Latitudes bands are shown every 10°from 40°N in dashed lines.

these times, calculated as the rate of ice volume loss multiplied by the ratio of the densities of ice and water.

Depending on how much of the ice is draining into the Arctic Ocean, the catchment area for the Arctic Ocean may vary with time. Also, since the ice sheets are not perfectly concentric around the pole, estimating the catchment area as being bound by a single latitude is very approximate. Hence the volume of accumulation per year is shown for a range of areas. While acknowledging this limitation, the rate of volume accumulation within the 65 ° parallel was chosen for comparison with the meltwater rate resulting from the retreating ice sheets. If the ice sheets are in steady state, the meltwater contribution will be zero - it is the change in net volume of ice which is considered. At steady state the volume of ice melting is assumed to match the volume of ice accumulating and so the rate at which freshwater is released under steady state conditions is equal to the volume of accumulation per year. Whatever the meltwater contribution, it must be added to the volume of accumulation to get the total

	18ka BP	16ka BP	14ka BP	12ka BP	10ka BP	8ka BP
50°N	3.22	3.26	3.6	4.16	4.26	4.27
60°N	1.01	1.03	1.17	1.52	1.61	1.62
65°N	0.6	0.61	0.66	0.9	0.96	0.97
70°N	0.39	0.4	0.42	0.51	0.56	0.56
80°N	0.12	0.12	0.12	0.12	0.12	0.12
Meltwater	0.05	0.28	3.33	0.905	0.48	0.07

Table 6.2: Total accumulation per year ($\times 10^4 km^3 a^{-1}$) in the area bounded by the latitude band shown. The rate increases with time because the accumulation rate increased as the ice sheets thinned and the elevation-desert effect diminished. Also shown is the rate of meltwater produced by the retreat of the ice sheets (also $\times 10^4 km^3 a^{-1}$).

freshwater contribution to the Arctic Ocean.

The accumulation rate values generally increase through the deglaciation as the thinning ice sheets led to a reduced surface elevation and a diminished elevation-desert effect. The rate of meltwater contribution varies simply due to the rate of diminution of the ice sheets. At 18ka BP the freshwater contribution from the meltwater was small compared to that from the accumulation. The meltwater contribution increased and was at least comparable to the accumulation contribution from ~16ka BP until ~10ka BP. The meltwater rate remained above $2 \times 10^4 km^3 a^{-1}$ (~3 times the accumulation contribution) from 14.4ka BP until 13.2ka BP and peaked at 13.8ka BP when it had a value of $3.89 \times 10^4 km^3 a^{-1}$, which is about 6 times the estimated contribution due to accumulation. The deglaciation modelled here suggests that a significant influx of freshwater into the Arctic and North Atlantic Oceans occurred at around 14ka BP, approximately the time of the Younger Dryas cooling. Coupled ocean-atmosphere models have been able to reproduce conditions representative of the Younger Dryas using a freshwater influx of only $\sim 0.315 \times 10^4 km^3 a^{-1}$ over 500 years (Manabe and Stouffer 1997) and $\sim 2 \times 10^4 km^3 a^{-1}$ over a similar period (Schiller et al. 1997). Even considering that not all the melted ice would have reached the North Atlantic Ocean at the same time, or even at all, there appears to be ample freshwater provided by the collapsing ice sheets to the North Atlantic Ocean to account for this proposed cause of the Younger Dryas cold episode, particularly as the potential contribution from the release of ice

dammed lakes has not been considered here.

There is observational evidence that there were in fact two pulses of meltwater into the North Atlantic Ocean during deglaciation (Fairbanks 1989), the first possibly originating from Fennoscandian Ice Sheet melt, the second from elsewhere (Birchfield et al. 1994). While results here do indicate an early meltwater pulse may have come from the early deglaciation of the Fennoscandian and British Ice Sheets, there is only one clear peak in the total meltwater flux. Fairbanks (1989) suggested that the pulses occurred at ~14-13ka BP and ~11-10ka BP, with a combined meltwater flux about half the peak produced in this model. The rate of ice volume loss during deglaciation produced by this model appears to be greater than that suggested by the palaeo-record, but the timing of the deglaciation corresponds well with the initial meltwater influx suggested by observations.

6.5.3 Comparison with the $\delta^{18}O$ record

Variation in the concentration of the ^{18}O isotope in sea sediment records has long been regarded as a record of global ice volume (e.g. Emiliani (1955)). It has also been suggested though that change in global ice volume alone cannot explain the ^{18}O variation in the sea sediment record and that changes in the temperature of the deep ocean must also be considered (Chappell and Shackleton 1986). The concentration of the isotope in ice cores is also indicative of the surface temperature of the ice sheet when the snow fell, and variations in this concentration are used to reconstruct palaeo-temperature records (e.g. Jouzel et al. (1987)) As the northern hemisphere ice sheets grew, and temperatures became colder, the depletion of ^{18}O there would have increased. Records from cores in the southern Greenland Ice Sheet indicate that the depletion of the isotope there is $\delta^{18}O \approx -30^{o}/_{oo}$ (Dansgaard et al. 1982). If we assume there was a similar degree of depletion in the other northern hemisphere ice sheets during the last ice age, an estimate of the total depletion due to the ice sheets can be made, using the change in total ice volume from LGM ($\sim 70 Mkm^3$) to present ($\sim 4.5 Mkm^3$). As this depletion must have been balanced by an enrichment in the ocean, an estimate for the change in the oceanic ^{18}O concentration can also be made, which may then be compared to

measured values from sea sediment cores.

$$\delta^{18}O_o = -\delta^{18}O_i \frac{V_i}{V_o} \tag{6.1}$$

where V is volume and i and o indicate ice and ocean values.

$$\delta^{18}O_o = 30\frac{(70-4.5)Mkm^3}{1400Mkm^3} = 1.4^o/_{oo}$$

Analyses of sea sediment cores based on planktic foraminifera (see Imbrie et al. (1992)) indicate that the ^{18}O enrichment at the LGM compared to present was $\delta^{18}O \approx 1.5^o/_{oo}$. Given the uncertainties in estimating the average isotopic depletion in the glacial ice sheets, the agreement between sea sediment $\delta^{18}O$ and the value obtained here seems reasonable. This tentatively indicates that the entire variation in sea sediment ^{18}O concentration since the LGM may be accounted for by the decay of the transient northern hemisphere ice sheets. No Antarctic contribution or deep sea temperature variation effects need be considered. The contribution of the Arctic ice shelf produced by the model, is also small ($\sim 1.15Mkm^3$) and its contribution to the total ^{18}O depletion in the cryosphere is calculated as less than 2%.

6.6 Contribution to sea level

The collapse of most of the northern hemisphere ice sheets following the LGM led to a rise in sea level. The melting of the ice released water back into the ocean and the consequent change in load on the bed beneath the ice sheets and beneath the ocean also influenced relative sea level.

Floating ice is not considered in the calculation of sea level change as it is in hydrostatic equilibrium with the ocean and so its melting will not contribute to eustatic sea level. Similarly, where ice is grounded below sea level, the proportion of that ice which contributes to the ice buoyancy makes no contribution to sea level (Figure 5.9). The change in volume of ice above buoyancy for the modelled glacial cycle is shown in Figure 6.19. For comparison, the time series for total ice volume and total grounded volume of ice are also shown. The sea level equivalent volumes are marked for LGM and present as the eustatic sea level change following the LGM will be dependent on

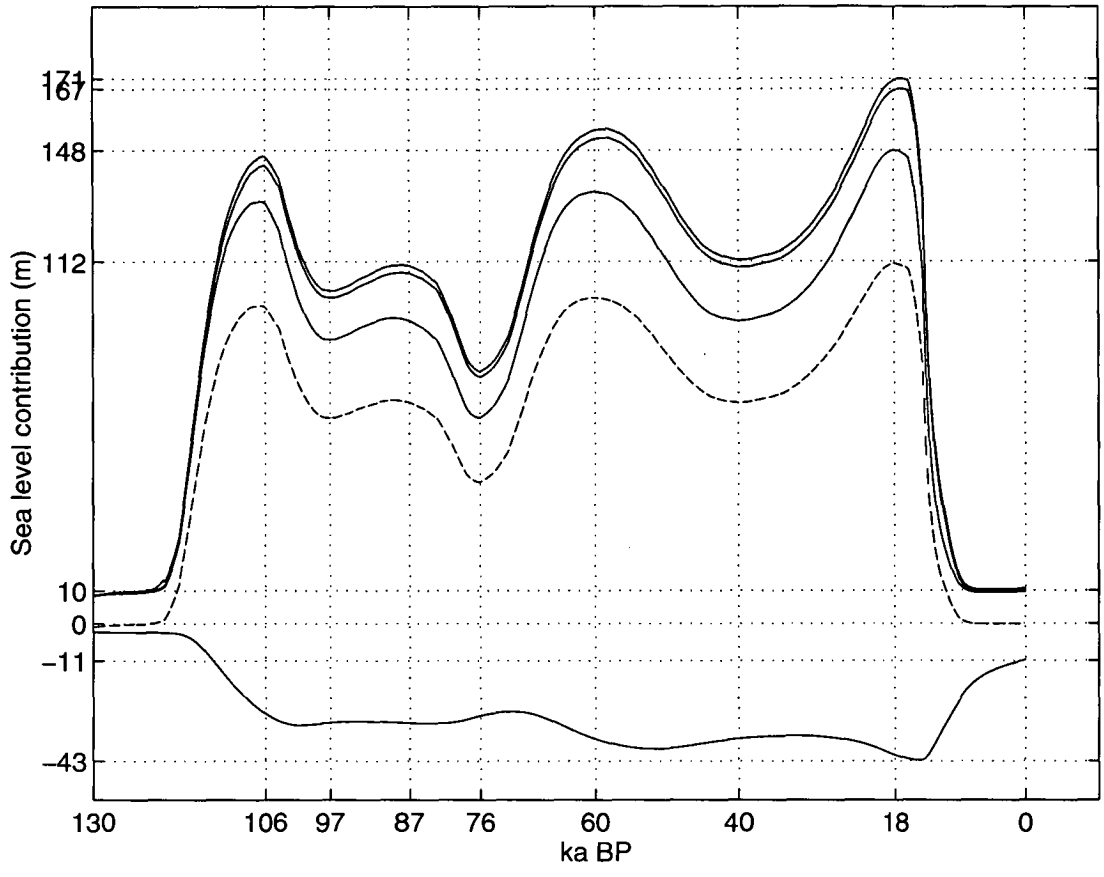

Figure 6.19: Time series for ice volume. The top three solid lines correspond to total (top), grounded and grounded above buoyancy ice volumes. The dashed line gives sea level change if basic bed depression beneath the ocean is included (see text). The bottom solid line is the volume of bed depression beneath the ice sheets. The units are metres of sea level equivalent.

the difference between these values. The volume of bed depression beneath the ice sheets is also shown and its contribution to sea level is discussed below.

While lithospheric stiffness is not directly accounted for in the isostatic calculations in this model, in reality when the bed is depressed in one region it will tend to cause uplift in another. Hence the depression of the bed beneath the ice sheets may be expected to lead to uplift in other areas, particularly in the vicinity of the ice sheets. The model produced a volume of bed depression beneath the ice sheets at the LGM equivalent to 43m of sea level change, and there was an 11m residue at the end of the run, giving a modelled change in

volume of bed depression from the LGM to present of 32m. It is difficult to estimate how this uplift would have been distributed as bed subsidence over the globe and what proportion would have contributed to a relative sea level decrease (ocean bed subsiding) or increase (bed above sea level subsiding). Regardless, the direct influence of the sub-ice sheet bed uplift on the surrounding bedrock response would have been relatively local. However, a resulting gravitational anomaly at low latitudes could have led to a high in the oceanic geoid there (Mitrovica and Peltier 1991).

The isostatic response of the bed to the increased load due to eustatic sea level rise following the LGM however, may have been more global. The increased water load due to the 138m increase in eustatic sea level (see Table 6.3) would have depressed the bed by an amount proportional to this increased burden. The bed beneath the ice sheets was found to have depressed to ~73% of its equilibrium position. It is unlikely that the ocean will have responded to this extent to the eustatic sea level rise since the LGM but as an estimate it is assumed the bed may have reached 60% of its post-LGM equilibrium level by the present. Taking the density of ocean water as 1027 $kg\,m^{-3}$ and that of the athenosphere to be 3300 $kg\,m^{-3}$ (Le Meur and Huybrechts 1996) the equilibrium depression should be ~0.31 of the load. This leads to an estimate of the subsidence of the ocean bed following the LGM of:

$$\Delta B_o = -(0.6 \times 0.31 \times 138)$$

$$\approx -26m$$

where B_o is the bed elevation beneath the ocean.

This ocean bed depression may of course have caused uplift over the land, further affecting relative sea level. Other influences such as thermal expansion, tectonic movement of the bed, variations in the Earth's spin axis due to the changing distribution of mass over the globe during deglaciation and the possible draining of ice dammed lakes would also have influenced relative sea level change from the LGM to present. The calculation of a global relative sea level curve is at the very least problematic as some global reference point must be established to which sea level may be relative. In reality, relative sea level

	Sea level equivalent	$\Delta s.l._e$	$\Delta s.l._r$
LGM total ice volume	171	-	-
LGM grounded ice volume	167	-	-
LGM volume above buoyancy	148	-	-
Residual volume above buoyancy	-10	138	-
Ocean bed depression	-26	138	112

Table 6.3: Ice volume and sea level changes from LGM to present. $\Delta s.l._e$ is the eustatic sea level change and $\Delta s.l._r$ is the relative sea level change. Units are metres. The volume of ice above buoyancy is the volume of ice which contributes to sea level. The change in the volume of ice above buoyancy from LGM to present is 138m. If the simple estimate of the isostatic response of the ocean bed is included (see text), relative sea level change is 112m from LGM to present.

change varies considerably between locations dependent on numerous factors. Correct treatment of these influences would require a comprehensive global isostatic model, which is beyond the scope of this thesis.

Table 6.3 shows the contribution to post-LGM sea level change from the modelled northern hemisphere ice sheets. The total and grounded LGM ice volumes are also shown. The eustatic contribution to sea level is 138m. This translates to a 'global' relative sea level change of 112m when the simple estimate of ocean bed depression is included.

The calculation of the response of the ocean bed to increased loading following the LGM performed here is extremely rudimentary and only included for the sake of comparison with the estimate of the eustatic sea level change. The eustatic curve in Figure 6.19 agrees reasonably with palaeo-reconstructions of sea level (see Figure 3.14). The modelled curve is to a degree sawtoothed, with subsequent maxima becoming progressively larger. The ice sheet volume at the 106ka BP peak appears too large when compared with the sea level record but the record does indicate that there must have been significant glaciation after about 60ka BP. Extensive glaciation prior to the LGM was produced by the model although it appears that the modelled ice sheet volume is larger than that estimated by the sea level record. The record suggests that sea level was ~80m below present at that time, while the model estimates that sea level was somewhat lower than this (ignoring the possible contribution of the Antarctic Ice Sheet to sea level). Nevertheless, the amplitude and overall shape of the

modelled sea level curve is not dissimilar to that of the palaeo-record.

While the modelled sea level curve here does not vary greatly during the Holocene, the bed elevations in the locations of the former ice sheets can be seen to be increasing (shown as the volume of bed depression becoming less negative in Figure 6.19). As the formerly ice covered land uplifted during this time, a decrease in relative sea level should result, while in the surrounding ocean regions it is expected that there will be an increase in relative sea level as the bed there subsides. Observations have found that the relative sea level in the regions of the former ice sheets have in fact behaved in this manner over the last 6000 years (Clark et al. 1978).

6.7 Summary

Using a simple, uniform application of temperature change through the last glacial cycle, a good reproduction of the location of ice sheet margins at the LGM and their subsequent retreat has been produced. A temperature depression amplitude of 13 °C resulted in LGM ice sheet margins close to estimates based on palaeo-evidence. Excepting Siberia and the Bering Sea, most discrepancies between the model output and observation can be accounted for by differences of $\pm$ 1°C or an altered base level accumulation rate. In Siberia, the modelled ice sheet was found to be larger than that of some palaeo-reconstructions. However, palaeo-evidence in this region is still scarce and reconstructions of the Siberian Ice Sheet are perhaps the least reliable of all the northern ice sheets of the last glacial cycle.

The degree of temperature depression, through its control over the ablation rate, was found to be more important in determining ice margin positions than was the base accumulation rate. Excepting over the ice shelf, where the accumulation rate was found to be an important factor in determining ice extent, halving or doubling the base accumulation rate had about as much influence on the ice sheet margins as did a $\pm$1°C temperature change. It appears that the control of the elevation-desert effect over the accumulation rate is dominant over grounded ice sheets, and variation in the base accumulation rate had minimal effect in these regions.

A good representation of present conditions for both ice distribution and bed elevation was also obtained after the model had completed a glacial cycle. Results also compared reasonably with what little is known about ice sheet extent prior to the LGM and with the success in reproducing both present and LGM ice extent, model estimates of ice distribution earlier in the glacial cycle may perhaps be considered a good guide for comparison with further field observations. However, comparison with sea level change reconstructions suggests that the pre-LGM ice sheets modelled here were of greater volume than may have existed in reality.

Initial bed conditions were found to be crucial to model accuracy. In order to arrive by the end of a glacial cycle at a bed distribution close to that which currently exists, the initial bed had to be raised to allow for the depression which would subsequently occur over the cycle. Furthermore, without elevating the initial bed, ice could not have readily accumulated in certain important areas such as in Hudson Bay, and the nature of the ice sheets produced would have been significantly different. The initial bed was required to be such that i) the final bed condition would approach the present state after experiencing the changing burden of the overlying ice sheet and ii) that the rate of uplift and remaining depression produced by the model for the present state also match observations. As a result it was found that the derived bed adjustment also helped to grow a more realistic ice cover distribution. The effects of erosion beneath the ice sheets, which may be in the order of $1mm\,a^{-1}$ were not considered.

The shape of the temperature forcing signal, which arose from the variation in radiation due to changes in the Earth's orbit, was to some extent reproduced in the ice sheet and bedrock responses. Radiation anomalies led the temperature forcing, which led the ice area, which largely led the ice volume which led the bedrock response. The ice volume and bed depression lagged the radiation variation by so much as to be being close to completely out of phase.

Ice sheet volume lagged the forcing by between ~2ka and ~8ka and responded more strongly to the ~ 40ka period in the forcing than the ~20ka period. The total ice volume of the northern hemisphere ice sheet system reached its maximum at ~18ka BP but the timing varied between individual ice

sheets from 18.2ka BP to 16.3ka BP. Following this there was slow retreat until about 14ka BP when the ice sheets retreated rapidly, releasing large quantities of freshwater into the ocean. The timing of this melt is consistent with the timing of the Younger Dryas cold event and the freshening of North Atlantic water resulting from rapid ice sheet retreat may have contributed to this.

Due to the strongly latitudinal nature of the temperature forcing, ice formed first and melted last at high latitudes. The paths followed by the growth and retreat of the ice sheets were similar. However, during retreat the ice sheets tended to be thicker as the ice ablated from the margins while when the ice sheets were initiated large thin ice sheets formed quickly. Although the ice sheets tended to be initiated at high points, much of their early growth appeared to follow an 'instantaneous glaciation' pattern. The Barents-Kara and East Siberian Ice Sheets were found to form predominantly as marine ice sheets and then expand southward onto the continent.

The marine margins of ice sheets tended to be more stable than inland margins. This was largely because marine margins were generally further north, but even at similar latitudes, marine margins were relatively stable. This does not support the theory that calving from marine margins was central to the collapse of the northern hemisphere ice sheets, although the model was not able to establish the stability or instability of the margins which were grounded well below sea level.

The model produced a large ice shelf in the Arctic Ocean, providing the accumulation rate was high enough. The existence of the ice shelf was a significant factor in determining the extent to which the ice grounded in the Barents Sea. However, grounding in this region was found not to be sensitive to whether sea level change through the glacial cycle was included in the model.

The total ice volume change of the northern ice sheets produced by the model from the LGM to present was enough to account for the $\delta^{18}O$ variation observed in sea sediment cores, assuming an average depletion in the glacial ice sheets of $\delta^{18}O = -30^{o}/_{oo}$.

By tracking the volume of grounded ice (both total and that above buoyancy), through the glacial cycle, the contribution of the northern hemisphere ice sheets to sea level change could be calculated. Estimating the

effects of the isostatic response of the ocean bed to the sub ice sheet bed variation and to a changing water load could lead to further refinement of post-LGM relative sea level change but would require complex global isostatic modelling. It was found that the decay of the LGM ice sheets produced here would have led to a change in eustatic sea level of 138m. Relative sea level change over this period could have been 10's of metres less than this due to isostatic influences.

Due to the subsidence of the bed beneath the ice sheets, thicker ice sheets developed at later maxima despite similar temperature regimes existing at the different times. This resulted in a trend towards gradually increasing ice volume before the rapid collapse after the LGM, resulting in a slightly sawtoothed shape in the calculated sea level curve.

The sea level change estimated by the change in the volume of ice above buoyancy gave a reasonable match to palaeo-sea level reconstructions. That results also compared satisfactorily with the geomorphological, $\delta^{18}O$, isostatic and cryospheric record in modelling the glacial cycle is perhaps indicative of the general robustness of these results.

Chapter 7

Changes in the Antarctic Ice Sheet through the last glacial cycle

The present state of the Antarctic is a product of its past history. In particular the Antarctic Ice Sheet has responded to variations in external climate control factors such as precipitation and also to sea level change and its effect on the buoyancy and dynamics of ice grounded below sea level. The sea level changes through the last glacial cycle were largely dependent on the growth and decay of the northern hemisphere ice sheets, as discussed in the previous chapter. Changes in sea level would have been relatively global in nature and so the Antarctic Ice Sheet would have been affected by a similar sea level change pattern as that which was associated with the northern ice sheet changes. By forcing the Antarctic Ice Sheet through a glacial cycle with the same sea level curve as was used to drive the the northern hemisphere ice sheets, it is possible to model some of the connection between northern and southern hemisphere ice during that cycle. A variable accumulation rate derived from EBM results (Budd and Rayner 1993) and ice core records, is also applied to the model and its effects investigated.

Considering sea level and accumulation rate changes to be the most important external factors in determining the state of the Antarctic Ice Sheet, this ice sheet has been modelled through the last glacial cycle. Although large temperature variations also occurred through the glacial cycle, as discussed in Section 4.1.4 the influence of these changes on ice temperature was greatly

delayed and damped out as it passed through the thick interior ice sheet. The thinner coastal ice would have been more strongly affected by the temperature changes and these possible secondary effects are examined through sensitivity studies (with varied flow rates) superimposed on the the results from the primary forcing. The modelled change in the Antarctic Ice Sheet since the LGM may be compared to observations. By modelling the ice sheet through its past history to reproduce the present ice distribution, surface elevation pattern and the surface mass balance, an estimate of the present state of the Antarctic Ice Sheet may be obtained. As was the case for the northern hemisphere modelling, by finding the nature of the change in the Antarctic since the LGM, estimates of the Antarctic contribution to sea level change since then, as well as the current contribution of the Antarctic to sea level change, can be made.

7.1 Setup of the simulations

Although the state of the Antarctic Ice Sheet at the last interglacial is not accurately known, it is thought to have been similar to the present configuration or perhaps a little smaller (see Section 3.1.6). As discussed in Section 5.5.2, the Antarctic model was started from a steady state condition, then run through a complete glacial cycle (with sea level and accumulation forcing) to a state which was then considered representative of the ice sheet at the last interglacial. The surface elevations of this ice sheet is shown in Figure 7.1 (a), and may be compared to the present day observed elevation distribution shown in Figure 7.1 (b). It can be seen that the West Antarctic Ice Sheet is intact and the overall distribution of ice is somewhat similar to that which currently exists, but with a slightly less advanced grounding line in West Antarctica. It will be shown that the model was highly sensitive to certain parameters, particularly those relating to the sliding. In order to explore the effects of these parameters, a large number of model runs was required, and so a relatively coarse model resolution of 100km was used to reduce model run-time. Some additional model runs were then performed with 20km resolution, but the differences between results from the high resolution model and the lower resolution model were small.

From this initial condition, the model was forced through another cycle,

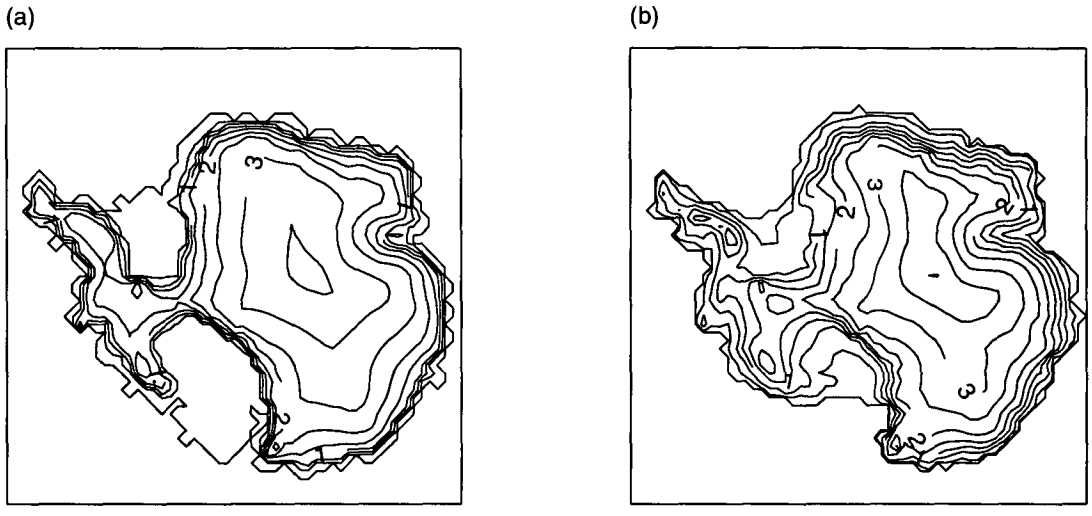

Figure 7.1: (a) Surface elevations for the start of the run. (b) Present observed surface elevations. For both figures, contours are at 0m, 100m, 500m, then every 500m.

representing the last glacial cycle. The climate forcing was made up of sea level forcing and accumulation forcing as described in Chapter 5. These were applied both separately and in unison so that there were three main forms of experiment:

1) Sea level forcing only;

2) Accumulation forcing only; and

3) Sea level and accumulation forcings combined.

As discussed in the previous chapter and in Section 4.4, due to the internal 'elevation-desert' effect in the model, accumulation may vary even when no external forcing is applied. As ice sheet elevation varies, the model may alter the accumulation rate due to the change in atmospheric moisture content, which it is considered would have accompanied the elevation change. Because of this, changes in sea level, which directly affect the ice sheet surface elevation (see Section 4.2), may also result in an altered accumulation rate. Similarly, any isostatic response of the bed due to a change in load will cause an effective change in bed elevation which may affect surface elevation and the level of the

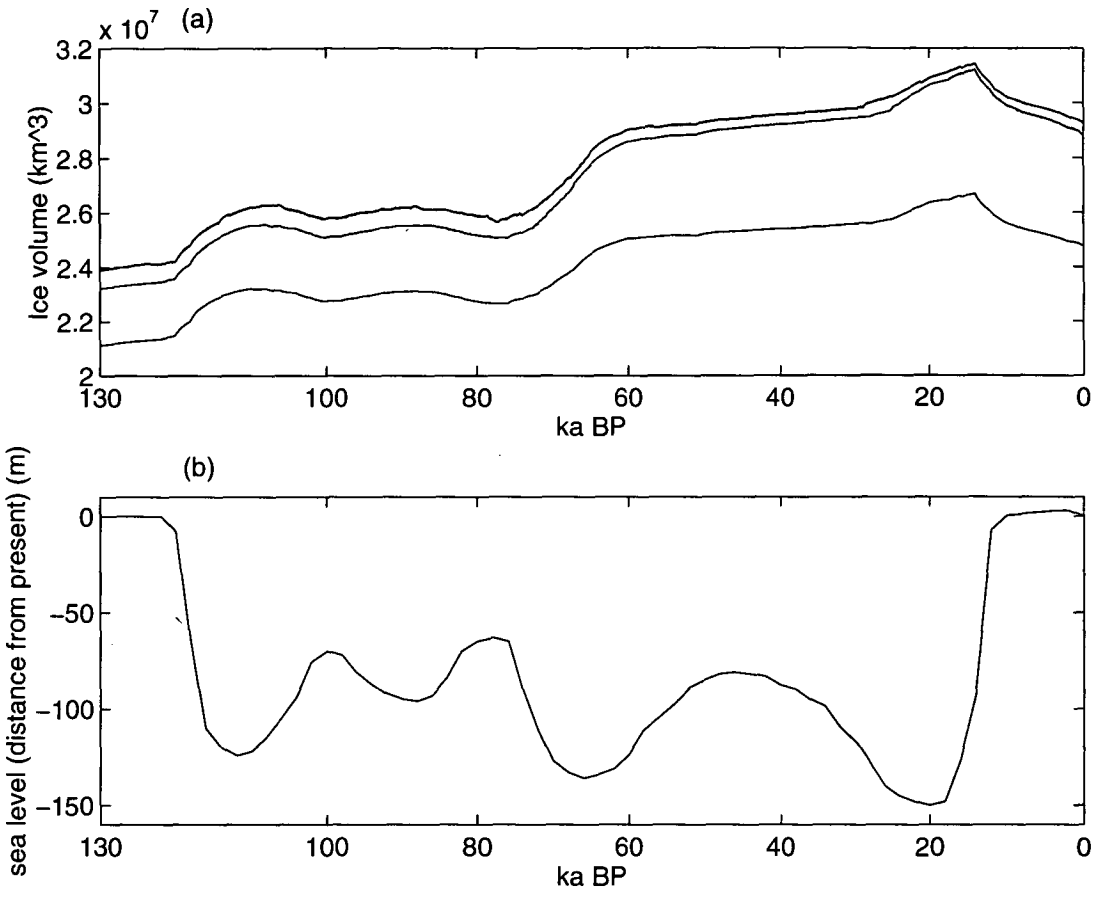

Figure 7.2: (a) Ice volume (total - top line, grounded - middle line, and above buoyancy - lower line) changes through the glacial cycle for a model run with sea level forcing only. (b) Sea level forcing from EBM study of Budd and Rayner (1993), shown as the difference in sea level from present.

ice in relation to sea level.

7.2 Sea level forcing

The change in total ice volume, grounded ice volume and the volume of ice above floating are shown in Figure 7.2 (a) for the 'sea level forcing only' case. The sea level forcing curve (Figure 7.2 (b)) is also shown. This is the same sea level forcing that was applied to the modelling of the northern hemisphere ice sheets discussed in the previous chapter.

In general, the Antarctic Ice Sheet volume increased with sea level lowering and decreased as sea level came up, but the relationship between ice

volume and sea level is clearly not linear. Ice volume responded more readily to sea level lowering than to increasing sea level. Local sea level peaks at ~96ka BP and ~74ka BP are weakly reflected in the ice volume curve, but the ~46ka BP sea level maximum appears to have virtually no impact on the Antarctic ice volume and while the final and initial sea levels are the same, the ice volume at the end of the run is considerably greater than at the beginning. In the model, the less the thickness above buoyancy at the grounding line, the greater the sliding velocity response to sea level change will be (see Section 4.5.2). When ice near the grounding line becomes thicker as a result of a reduced flow rate due to lower sea level, the effect of sea level change on the flow of that ice is reduced and so subsequent sea level rise may be expected not to have the same degree of influence as did the initial lowering of sea level. Thicker ice therefore tends to respond less to sea level change than does thinner ice. This causes a lesser, or at least delayed, reaction to sea level rise in comparison to sea level lowering.

The grounding line around the western Ronne Ice Shelf in particular, was found to be sensitive to a decrease in sea level. The ice shelf grounded in the Weddell Sea to near the edge of the continental shelf (Figure 7.3) and did not retreat even when sea level returned to its interglacial level. Grounding line advance also occurred early in the glacial cycle beneath the Amery Ice Shelf and again the post LGM sea level rise did not produce any grounding line retreat. In the Ross Sea there was also some grounding line advance during the glacial cycle, as well as a degree of retreat following the LGM.

The advance of the grounding line in the Weddell Sea to near the edge of the continental shelf by the LGM is consistent with observation, although of course observations also indicate that there has been significant retreat there since the LGM, as today the Ronne Ice Shelf comes afloat much further south than this. While the 'sea level only' experiment has not produced this retreat to the present grounding line position, the model did produce substantial grounding line advance. It is interesting then to investigate the nature of this advance to near the continental shelf edge.

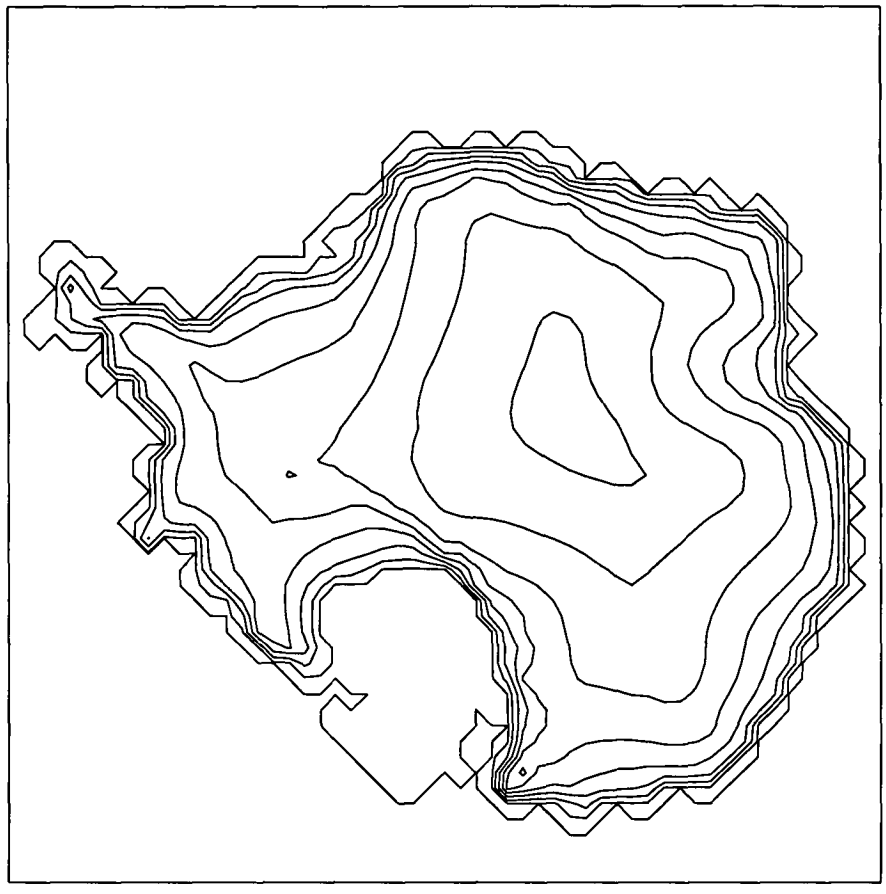

Figure 7.3: Surface elevations at the end of the run (sea level forcing only). Contours are at 0m, 100m, 500m, then every 500m.

7.2.1 Grounding line advance in the Weddell Sea

Figure 7.4 illustrates the nature of the modelled grounding line advance in the Weddell Sea. It shows that initially advance occurred around the perimeter of the ice shelf but after this, the dominant direction of advance was from the west. As sea level decreased, ice began to ground on points in the interior of the ice shelf, forming ice rises which acted as pinning points to the ice shelf and slowed the shelf velocity. Widespread grounding quickly followed as the grounding line advanced to capture these points. This pattern of isolated grounding, followed by general grounding line advance, continued throughout the advance in the Weddell Sea. Eventually the ice shelf narrowed to a channel in the east, before that also grounded. Most of the advance shown occurred over a period of 16ka.

There was some grounding line movement in other regions, particularly

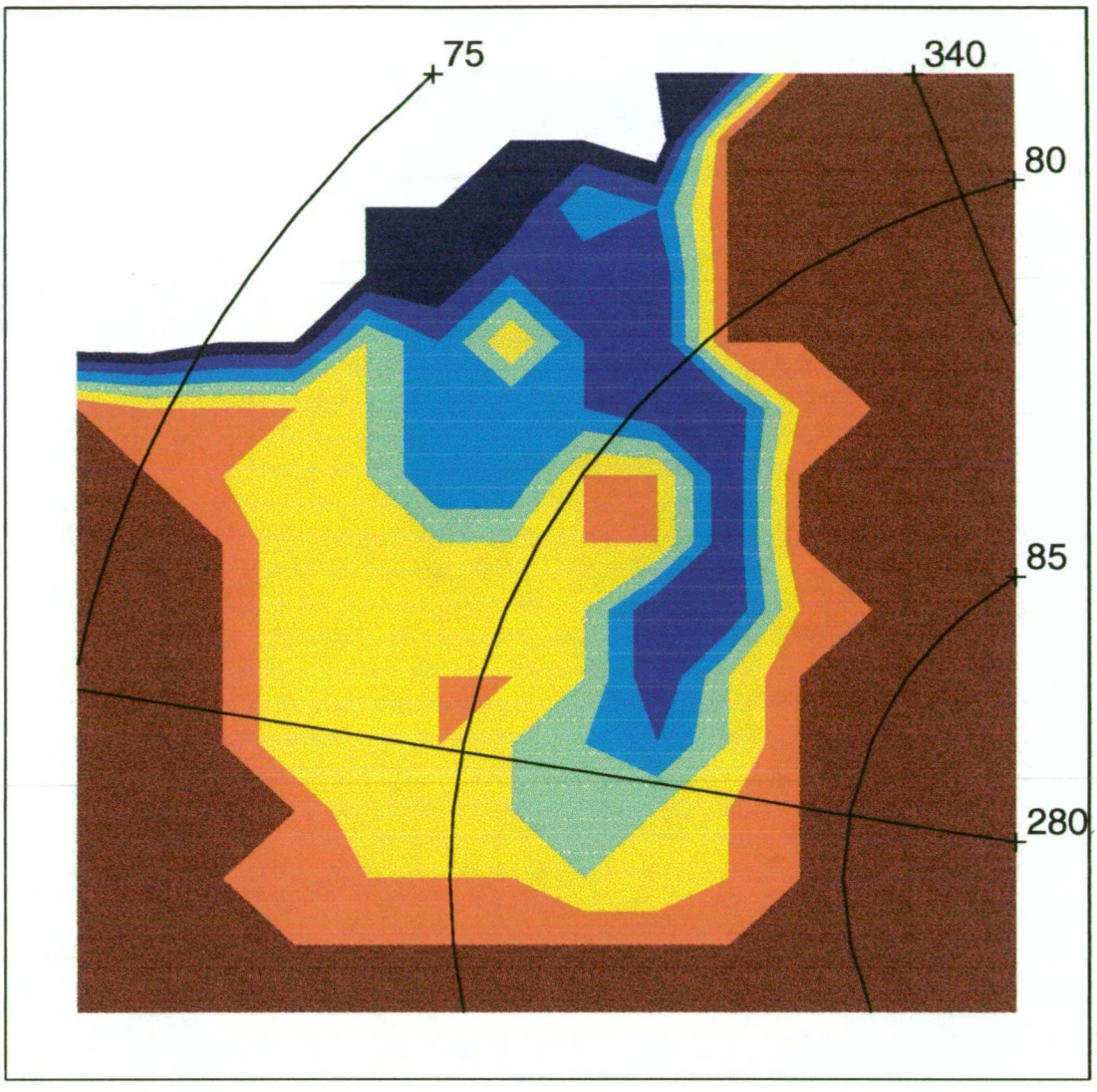

Figure 7.4: Grounding line advance in the Weddell Sea. Grounding line positions are shown for 120ka BP (brown),100ka BP (red), 98ka BP (orange), 96ka BP (green), 92ka BP (light blue), 88ka BP (blue) and 60ka BP (dark blue).

beneath the Amery Ice Shelf, as mentioned above. Some points around the coast of East Antarctica exhibited minor advance and retreat also. Beneath the Ross Ice Shelf, the model produced grounding line advance by the LGM which was not too dissimilar to that suggested by some palaeo-reconstructions (Licht et al. (1996) and see Figure 3.9). Significant thickness changes since the LGM in Antarctica have been attributed to the influence of grounding line retreat in West Antarctica during this time.

7.2.2 Thickness change from LGM to present

The change in thickness from LGM to present is shown for the 'sea level only' experiment in Figure 7.5, along with the associated LGM and present grounding line positions. The figure shows that but for some relatively small regions at the seaward edge of some floating ice, under the 'sea level only' conditions the ice thinned from LGM to present. This was particularly the case in the Ross Sea where grounding line retreat led to substantial thinning. Even inland of the final grounding line position in this region, there was significant thinning as sliding increased with the decrease in thickness above buoyancy induced by the sea level rise. By comparison, there is little evidence of thinning at the ice margin in the Weddell Sea where the ice became so well grounded that the effects of sliding were greatly reduced and so sea level rise exerted little influence on the flow.

The depth of the ocean bed in the Weddell Sea, where there is a large expanse of relatively shallow water near the continental shelf edge, is generally less than in the Ross Sea. The shallowness of the Weddell Sea at the margin of the advanced ice sheet may be responsible for the extent of the grounding there. The bed topography in this region is in fact shallower than much of the bed beneath the current West Antarctic Ice Sheet, suggesting that it may be more difficult to initiate retreat in a West Antarctic Ice Sheet such as that shown in Figure 7.3 than for the present ice sheet in the West Antarctic.

Other modelling studies have also found that grounding line advance occurred readily in the Weddell Sea when sea level decreased, but that subsequent retreat when sea level increased was not so easily achieved (Oerlemans 1982; Huybrechts 1992). While the lack of retreat in the Weddell Sea may not correspond well with observations, it does suggest the possibility that different steady states are possible for the same climatic conditions. Once grounded, the modelled ice effectively became too thick to sufficiently respond to ensuing sea level rise. To unground the ice in the Weddell Sea in these model runs with sea level forcing alone, the sea level was required to rise to some level higher than present sea level before the grounding line would begin to retreat significantly towards its initial position.

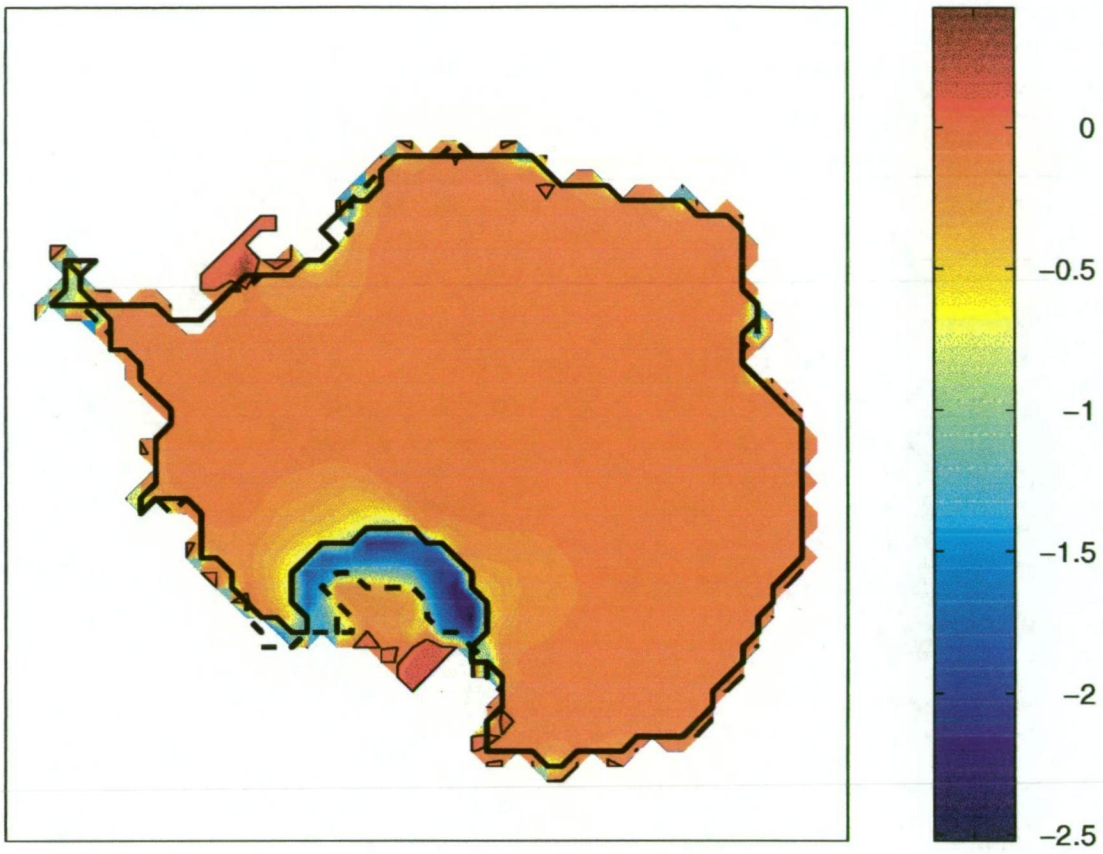

Figure 7.5: Thickness change from LGM to present (Present - LGM), for 'sea level only' model (km). Grounding line positions are shown for LGM (thick dashed) and present (thick solid). The only notable grounding line migration has occurred in the Ross Sea. Zero thickness change is shown by a thin black contour.

7.3 Accumulation forcing

The accumulation forcing curve (Figure 7.6(b)) is characterised by high accumulation rates at the last interglacial and at present, with generally somewhat lower rates between these times. Because of this, ice volume was also low between the interglacials when the accumulation forcing was the only forcing applied to the model (Figure 7.6(a)). The shape of the ice volume change curve closely resembles that of the accumulation forcing curve throughout the run, with the exception that following the volume minimum at the LGM, ice volume does not rise to previous interglacial levels when the accumulation rate is returned to its present value.

The lower accumulation rate over the ice sheet led to thinning of the ice,

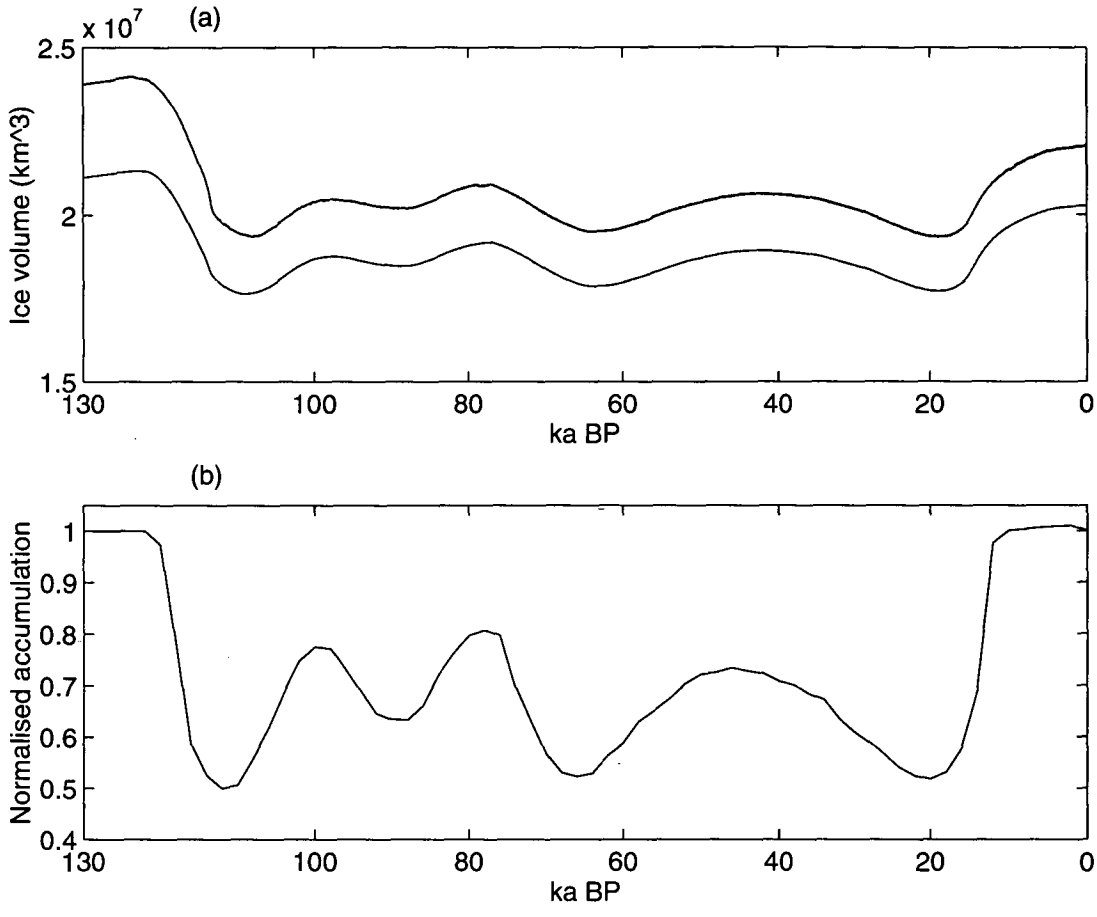

Figure 7.6: (a) Ice volume (Total - top line, above buoyancy - lower line) changes through the glacial cycle for a model run with accumulation forcing only. (b) Accumulation forcing. Accumulation rate as a proportion of the present accumulation rate. The minimum accumulation rate during the glacial cycle is half the present rate.

which in West Antarctica resulted in significant grounding line retreat and the collapse of much of the West Antarctic Ice Sheet. The West Antarctic Ice Sheet then became characterised by large regions of thin, floating, fast flowing ice Figure 7.7. Once collapsed, the modelled West Antarctic Ice Sheet became resistant to subsequent increases in thickness resulting from inreased accumulation, as the high velocity of the ice reduced the ability of increased accumulation to produce thickening of the ice. The increased quantity of accumulation at the end of the glacial cycle was removed too quickly by the fast flowing ice to produce sufficient thickening to induce significant grounding line advance. So it can be seen that when a decreased accumulation rate leads to

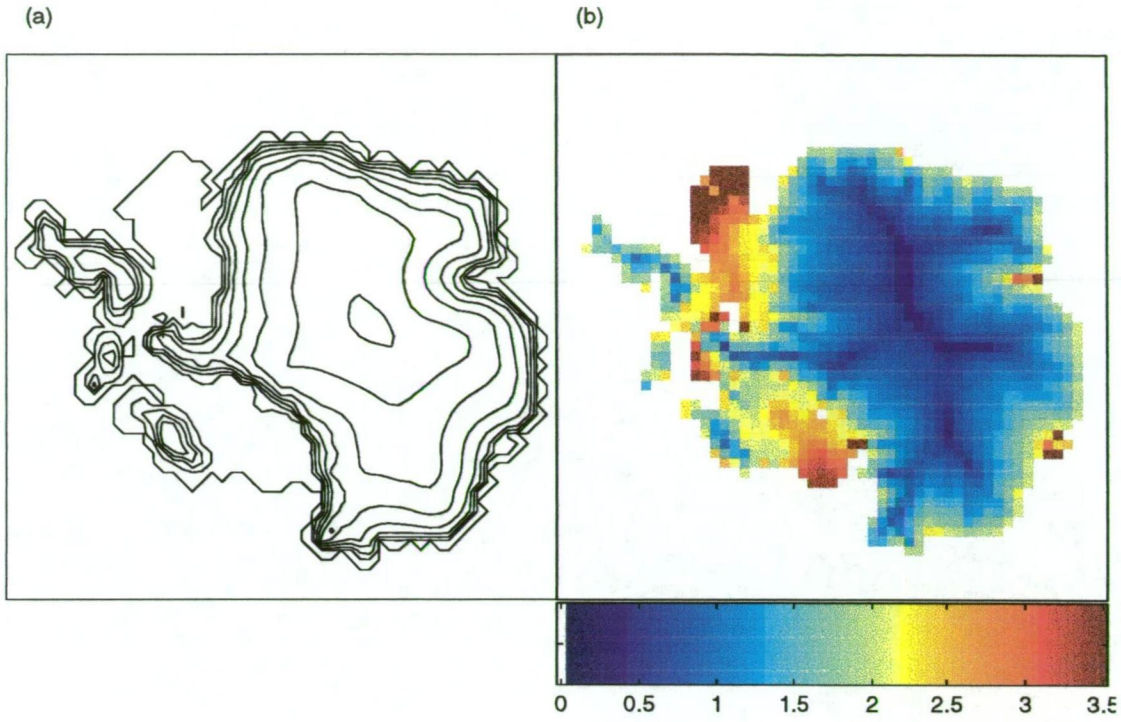

Figure 7.7: (a) Surface elevations at the end of the run (accumulation forcing only). Contours are at 0m, 100m, 500m, then every 500m. (b) Ice velocity ($\log(m\,a^{-1})$) at this time. Note the high velocities corresponding to the floating ice in the collapsed West Antarctic Ice Sheet.

ungrounding, returning the accumulation rate to its former value will not necessarily result in a similar return in the grounding line position. For the same accumulation distribution, different flow modes are possible, and while the modelled ice sheet has not yet achieved steady state at the end of the glacial cycle, it is clear in Figure 7.6 that the ice volume is not approaching the level of the previous interglacial.

A significant assumption has been made by applying the same rate of change in the accumulation rate to the entire ice sheet. The accumulation rate is generally higher at lower altitudes (see Figure 5.8). By applying the same percentage change to all regions, regions of lower elevation such as around the coast and in much of West Antarctica, experience a considerably larger change in the actual accumulation rate.

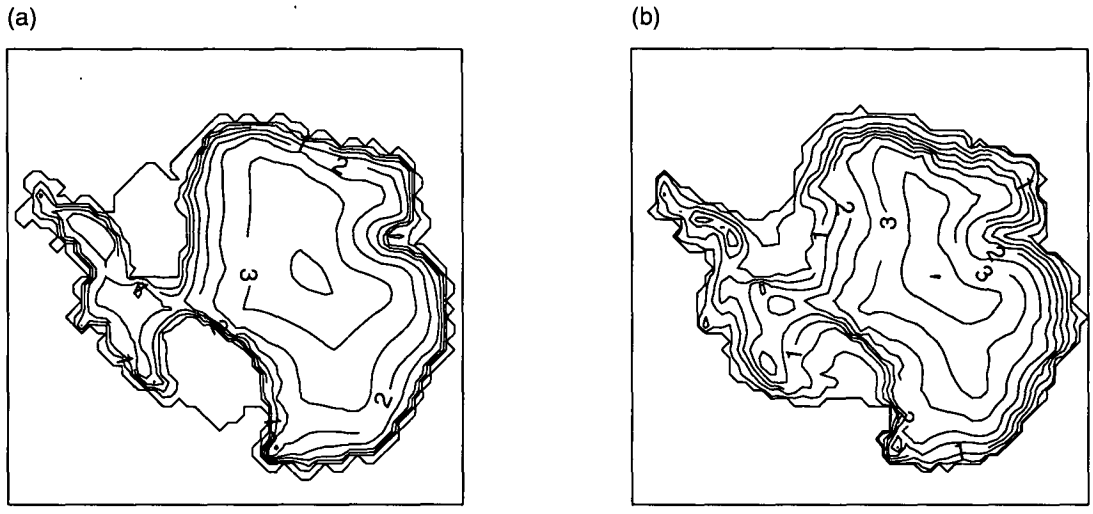

Figure 7.8: (a) Surface elevations at the end of the run (sea level and accumulation forcing). (b) Present observed surface elevations. For both figures, contours are at 0m, 100m, 500m, then every 500m.

7.4 Combined sea level and accumulation forcing

Figure 7.8 (a) shows the surface elevations of the modelled ice sheet at the end of a run where the ice sheet was forced by both sea level and accumulation changes. Although comparison to observed present day elevations (Figure 7.8 (b)) indicates that the modelled ice sheet produced here from the combined forcing differs from the observed elevations in some regions, the modelled distribution gives a reasonable approximation of the present ice distribution in Antarctica. The modelled grounding line beneath the large West Antarctic ice shelves is generally inland of its observed positions, leading to a thinner West Antarctic Ice Sheet between the Ross and Ronne Ice Shelves. A thicker than observed Antarctic Peninsula is also produced by the model. This has also occurred in other studies and has been attributed to poor bedrock data in this region (Huybrechts 1992).

The mass balance of the ice sheet is affected by changes in both sea level and accumulation rate. A comparison of Figure 7.2 and Figure 7.6 shows that where the sea level forcing tended to lead to greater ice volume through the glacial cycle, the accumulation forcing led to generally decreasing volume.

While the two processes (sea level change and accumulation rate change) do not exert influence on ice sheet mass balance through the same processes, to some extent their respective effects on total ice volume appear to be directly opposed. Decreasing sea level tends to produce thicker ice and a greater volume while decreasing accumulation rate causes the ice to thin and the volume to decrease.

Although the sea level and accumulation rate forcing curves are not identical in shape, they are closely related and the timing of the peaks and troughs in both forcings are very similar. Given that the respective forcings exert their influence on the ice sheet through different processes which may have different time responses, the effects of the changes in sea level and accumulation rate are not expected to be completely synchronous. Nevertheless, these timing differences should be compensated by the comparatively low frequencies observed in the forcing curves and when the two climate forcings are applied to the model in unison, it may be expected that the changes to the ice sheet will lie somewhere between those produced when the forcings were applied separately.

Figure 7.9 compares the total ice volume changes for the experiment which included sea level and accumulation rate variation, to the the total ice volume time series for the experiments when the forcings were applied in isolation. Generally, there is less variation in the ice volume for this experiment than when the sea level and accumulation forcings were applied individually. There is no pattern suggesting the consistent dominance of either accumulation or sea level forcing, and the fact that the volume remains relatively constant suggests that each moderates the influence of the other. That the modelled ice volume remained relatively constant does not mean that there were not significant regional thickness changes. Opposing signs of thickness change in grounding line regions and in the interior may have led to little net volume change despite large local changes in ice thickness (e.g. Figure 7.11).

Given the uncertainty in the assumption that the accumulation rate changed by the same proportion throughout the Antarctic, a further investigation was made into the effect of reducing the amplitude of accumulation variation. Using the same shape curve as shown in Figure 7.6 (b), but with only 1/3 the amplitude of that curve, a second accumulation rate curve was obtained with a minimum accumulation rate of $\frac{5}{6}$ the present rate.

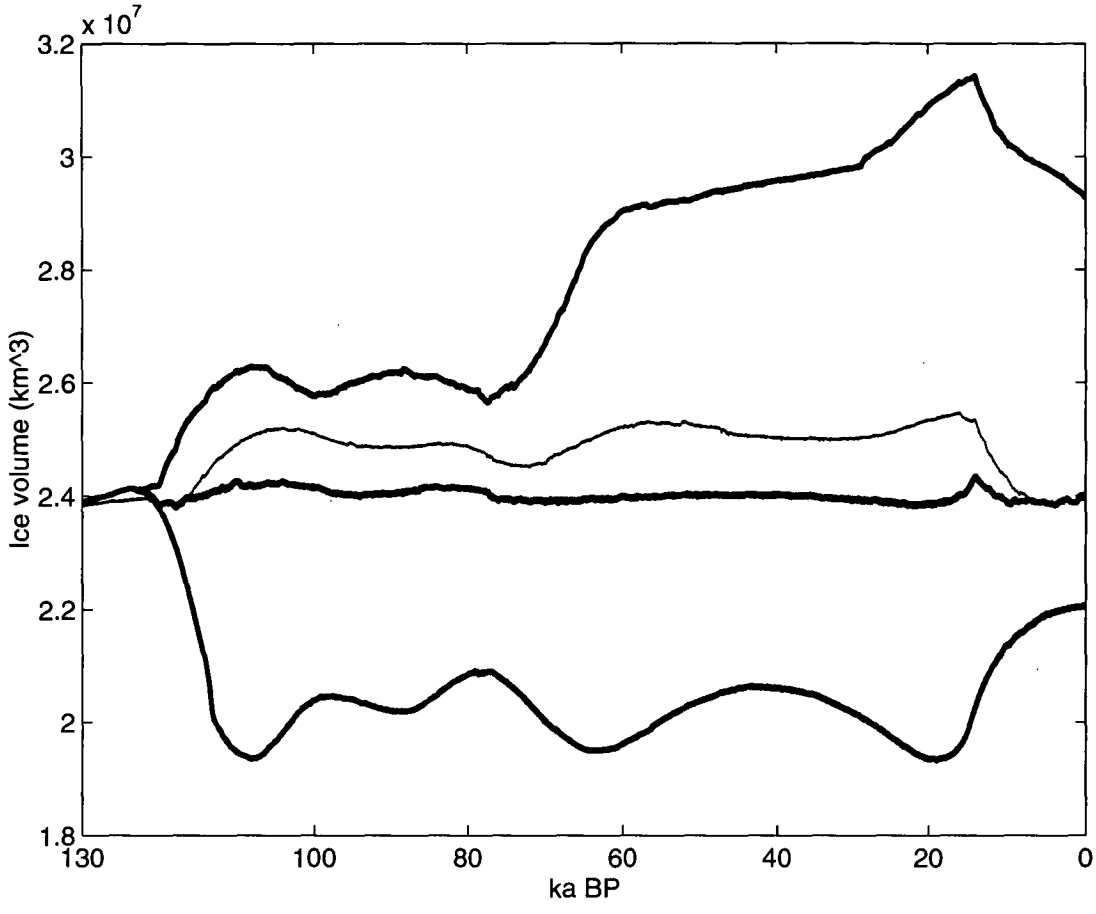

Figure 7.9: Comparison of total ice volume through a glacial cycle for: sea level forcing only (top thick line), sea level and accumulation forcing (middle thick line), and accumulation forcing only (bottom thick line). The total volume variation for a run with sea level forcing and a reduced amplitude accumulation forcing (minimum accumulation rate of $\frac{5}{6}$ the present accumulation rate) is shown as a thin line.

This accumulation forcing was applied in conjunction with the full sea level forcing and run through two glacial cycles. The total ice volume changes for the second cycle is shown as a thin line in Figure 7.9. Not surprisingly, when the accumulation rate did not decrease by as much, the influence of the sea level forcing was more dominant, with the ice volume curve strongly reflecting the sea level changes. However, while the reduced amplitude in the accumulation forcing allowed stronger response to the sea level changes, there was little or no grounding line migration in the West Antarctic for this experiment. When the accumulation forcing amplitude was sufficiently reduced to allow grounding line

migration, there tended to be grounding line advance, particularly in the Weddell Sea, but no subsequent retreat, and ice volume followed a similar pattern to that produced by the 'sea level forcing only' experiment.

7.4.1 Changes in ice volume

The change in total ice volume through the glacial cycle for the sea level and full accumulation forcing case is again shown in Figure 7.10 along with the grounded ice volume and volume of ice above buoyancy time series. In this experiment, the sea level minimum corresponding to the LGM led to a subsequent volume maximum, followed by a volume decrease as sea level began to rise again. By about 9ka BP, the influence of the increasing accumulation rate began to dominate and ice volume again began to increase, a trend which continued until the end of the run (see Section 7.4.8).

The most recent volume peak was reached in this model run at around 14ka BP, sometime later than for the northern hemisphere ice sheets. This appears to be due to the delayed response of the ice sheet to the changing sea level. When the sea level forcing acted in isolation, ice volume change lagged the forcing by a similar amount (~6ka). The onset of rapid decrease in ice volume following the peak coincides with the timing of maximum ice volume loss from the modelled northern hemisphere ice sheets and the period of most rapid sea level rise in the sea level forcing.

7.4.2 Post LGM sea level rise

The modelled net decrease in volume of ice above buoyancy from LGM to present is $3.5 \times 10^5 km^3$ corresponding to a eustatic sea level contribution of less than a metre. At the ~9ka BP volume minimum the amount of ice above buoyancy had decreased by $1.3m$ sea level equivalent. Other estimates of the Antarctic contribution to post-LGM sea level have been generally considerably greater than that produced here (Tushingham and Peltier 1991; Huybrechts 1992). The small contribution found here in comparison to these other studies is largely due to the minimal advance and retreat of the West Antarctic Ice Sheet produced by this model. Other reconstructions have had the LGM West

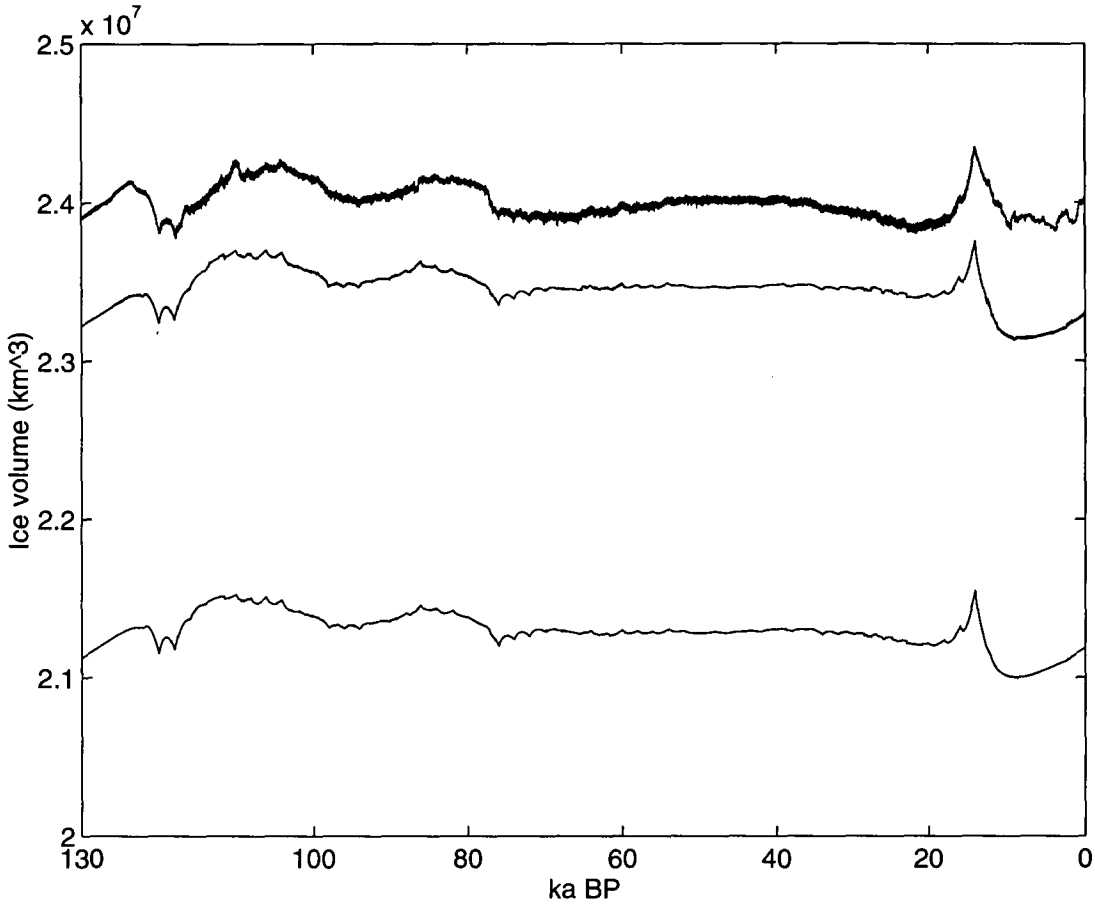

Figure 7.10: Ice volume (total - top line, grounded - middle line, above buoyancy - lower line) changes through the glacial cycle for a model run with combined sea level and accumulation forcing.

Antarctic Ice Sheet grounded to near the edge of the continental shelf in the Weddell and Ross Seas, supporting a much greater thickness of ice in West Antarctica, so that subsequent retreat in these regions produced a significant loss of ice, resulting in a substantial contribution to sea level rise during deglaciation. This model produced minimal grounding line movement in these regions due to the counteracting influences of changes in accumulation rate and in sea level and so the estimated contribution to sea level is diminished.

7.4.3 Thickness change since the LGM

Figure 7.11 shows the modelled change in total thickness from LGM to present. The inland East Antarctic Ice Sheet in the model is shown to have increased in

thickness from LGM to present, whereas around the coast and where the ice is grounded in West Antarctica the ice sheet has thinned. As discussed in Section 4.5.2, the ice shelves are relatively dynamically uncoupled from the grounded ice and variation in sea level does not dramatically affect floating ice compared to its effect on ice vulnerable to sliding. Hence there is a marked transition from inland of the grounding line, where sea level effects dominate, to the ice shelves which have become thicker in response to the increase in accumulation after the LGM.

Evidence suggests that at the site of the Byrd ice core in West Antarctica (80°S 119.5°W), the ice sheet surface may have been thinner by 200-250m at the LGM, compared to present (Raynaud and Whillans 1982). As can be seen in Figure 7.11 the model has in fact produced a thinning over the majority of West Antarctica from the LGM to present. However, the grounding line produced by the model in this region, particularly along the Siple Coast is generally inlandward of its observed position, consequently the thickness of much of the West Antarctic Ice Sheet is reduced. The modelled inland regions in the West Antarctic exhibit only a small amount of thinning after the LGM and if the ice there were thicker, and so more heavily grounded and less susceptible to the effects of sea level change, it would have been more likely to have thickened since the LGM in response to the increased accumulation rate.

7.4.4 Grounding line sensitivity

The extent to which the actual LGM grounding line was advanced from its present position in West Antarctica is still unclear, with some reconstructions suggesting it was well advanced, particularly in the Weddell Sea (Figure 3.8) while others indicate the possibility that this was not the case and that the LGM grounding lines in the West Antarctic were not much advanced on their present position (Figure 3.9). The model dynamics respond to sea level change largely through the influence it has on the the sliding velocity by affecting the thickness of ice above buoyancy. The dependence of the sliding velocity on thickness above buoyancy is shown in equation 4.12. The factor k_s in this equation is dependent on the basal temperature and bed roughness (see Section 4.1.4) but not well known and a range of values of this parameter were

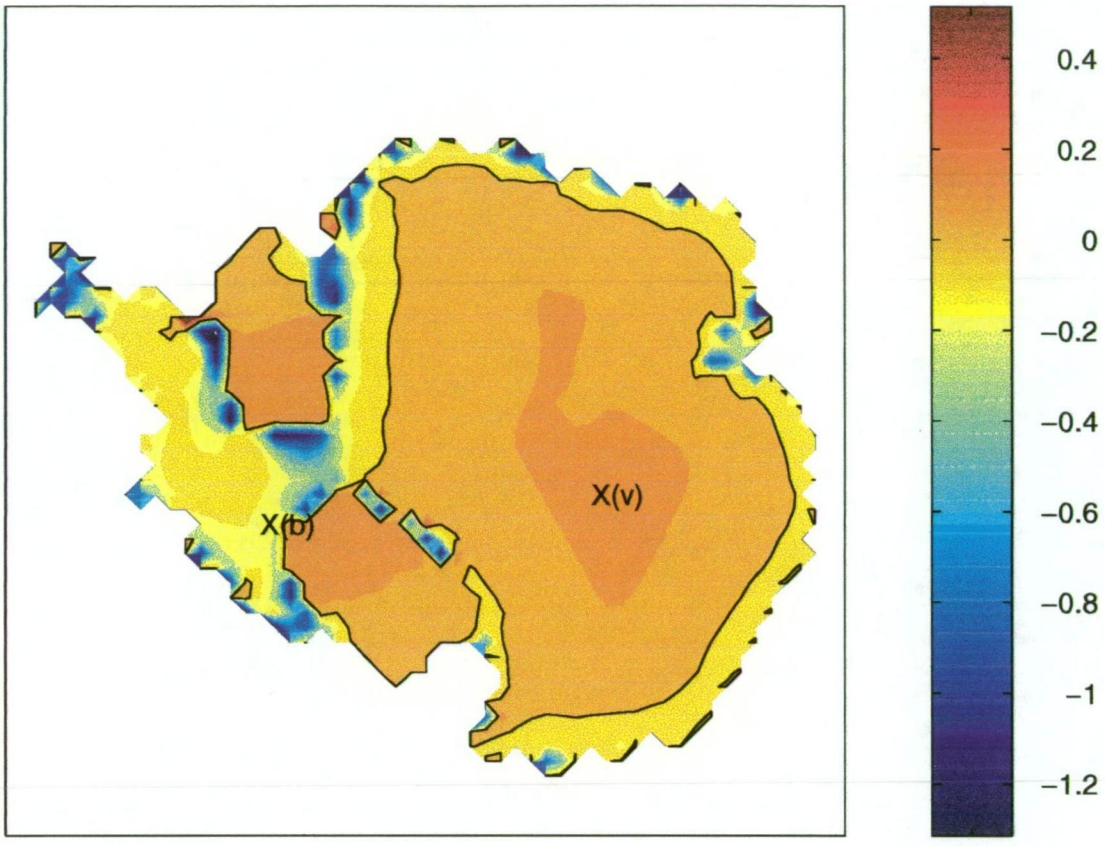

Figure 7.11: Thickness change from the volume maximum after the LGM, to present (km). Vostok (v) and Byrd (b) sites are marked.

tested to find that which produced the best fit to the present Antarctic Ice Sheet. During this process it was found that the grounded extent of the West Antarctic Ice Sheet was very sensitive to changes in this parameter and that this sensitivity was highly non-linear.

Figure 7.12 illustrates the variation in LGM grounding line for different values of k_s. A 10% increase in the value of k_s from that used to produce the ice sheet shown in Figure 7.8 led to the collapse of the West Antarctic Ice Sheet, whereas by reducing the value of k_s by 2% the grounding line advanced to the continental shelf edge in the Weddell Sea. From a condition which produced the advanced grounding line in the Weddell, but not the Ross Sea, a further 10% reduction led to similar advance in the Ross Sea. These changes in the modelled grounding line positions occurred when these threshold changes in k_s were made. For smaller changes than those mentioned there was virtually no change

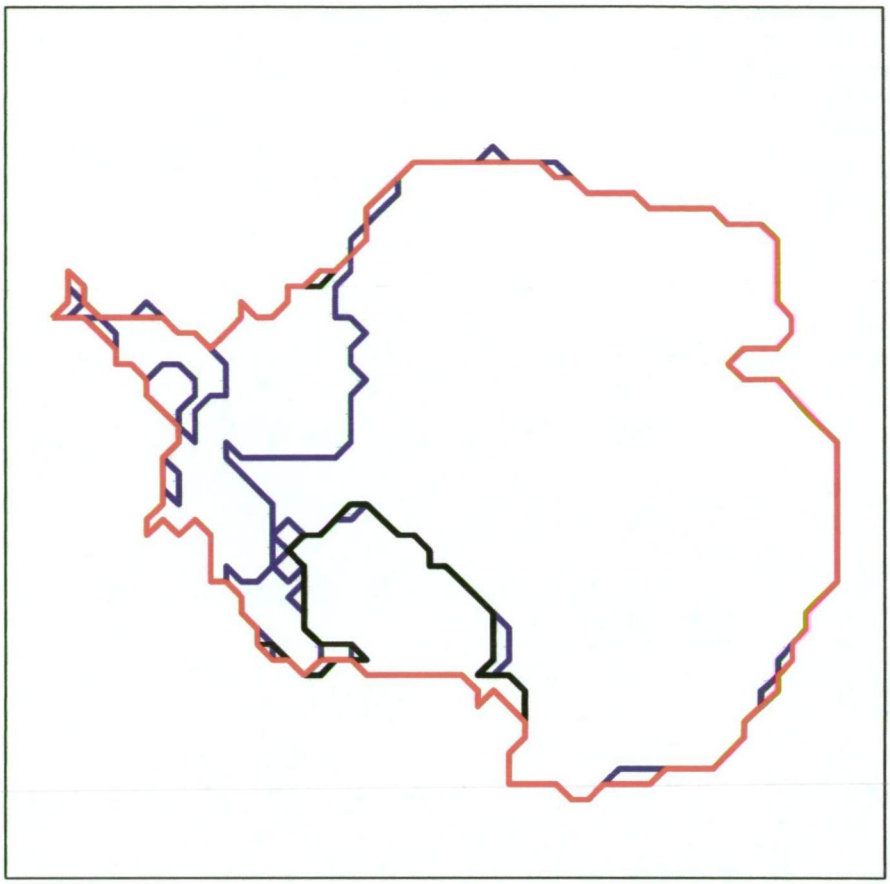

Figure 7.12: LGM grounding line positions for changes in k_s: 10% increase (blue), 2% decrease (black), a further 10% decrease (red). Where the grounding lines occupy the same points, red overlies black which overlies blue contours.

in the modelled grounding line position, but once these threshold values were applied, large grounding line changes resulted.

Grounding line position in the West Antarctic and particularly in the major embayments there, was highly sensitive to changes in the sliding parameter k_s in the model. In particular, the location of the grounding line was found to be dependent on threshold k_s values being obtained, beyond which there would be significant advance (to the edge of the continental shelf) or retreat (large scale collapse of the West Antarctic Ice Sheet) over a glacial cycle. The model had great difficulty producing limited grounding line migration to positions which lay between these states, which to a large extent correspond to the end states for the sea level forcing only and the accumulation forcing only

runs. If the West Antarctic grounding lines retreated, they tended to retreat extensively, and if there was advance in the Weddell Sea it tended to be to the continental shelf edge. However, as is seen in Figure 7.5, limited advance and subsequent retreat was achievable in the Ross Sea.

Although the model was found to be capable of producing grounding line advance in line with some estimates of its LGM position, subsequent retreat in response to sea level rise during deglaciation was not readily achieved. As discussed in Section 4.5.2 the response of the grounding line to changes in sea level is complex. The high sensitivity of the grounding line dynamics to sliding and bed conditions as well as to the changes in sea level means that the model changes near the grounding line may not be very reliable and further work is still needed to improve the ice shelf dynamics and the sliding formulation to match the observed dynamics. A further influence on the grounding changes is the effect of erosion and bedrock elevation change during the glacial which were not explicitly included in the model but are considered in a simple way below.

7.4.5 Possible greater ice sheet extent for previous glaciations

If ice was grounded much further out into the Ross and Weddell Seas as suggested by palaeo-evidence, the flow of the ice there would have strongly affected the underlying bed topography through erosion. Drewry (1986) collated data on estimated rates of erosion beneath glaciers and found that these estimates varied between $0.073 mm\,a^{-1}$ and $30 mm\,a^{-1}$, although the more reliable estimates were closer to the lower end of this range. Larsen and Mangerud (1981) estimated the rate of erosion beneath a Younger Dryas glacier in western Norway as around $0.6 mm\,a^{-1}$.

There is evidence that the ice sheet in the West Antarctic was at some time grounded to near the continental shelf edge and higher mountains were overridden by ice but were ice free at the LGM. The extent of the grounded ice sheet in the West Antarctic appears to be strongly dependent on the bed topography beneath sea level. If an erosion rate of $1 mm\,a^{-1}$ is assumed, the lowering of the bed by $\sim$100m over a glacial cycle is possible. Hence it may be speculated that the bed could have been considerably higher during previous

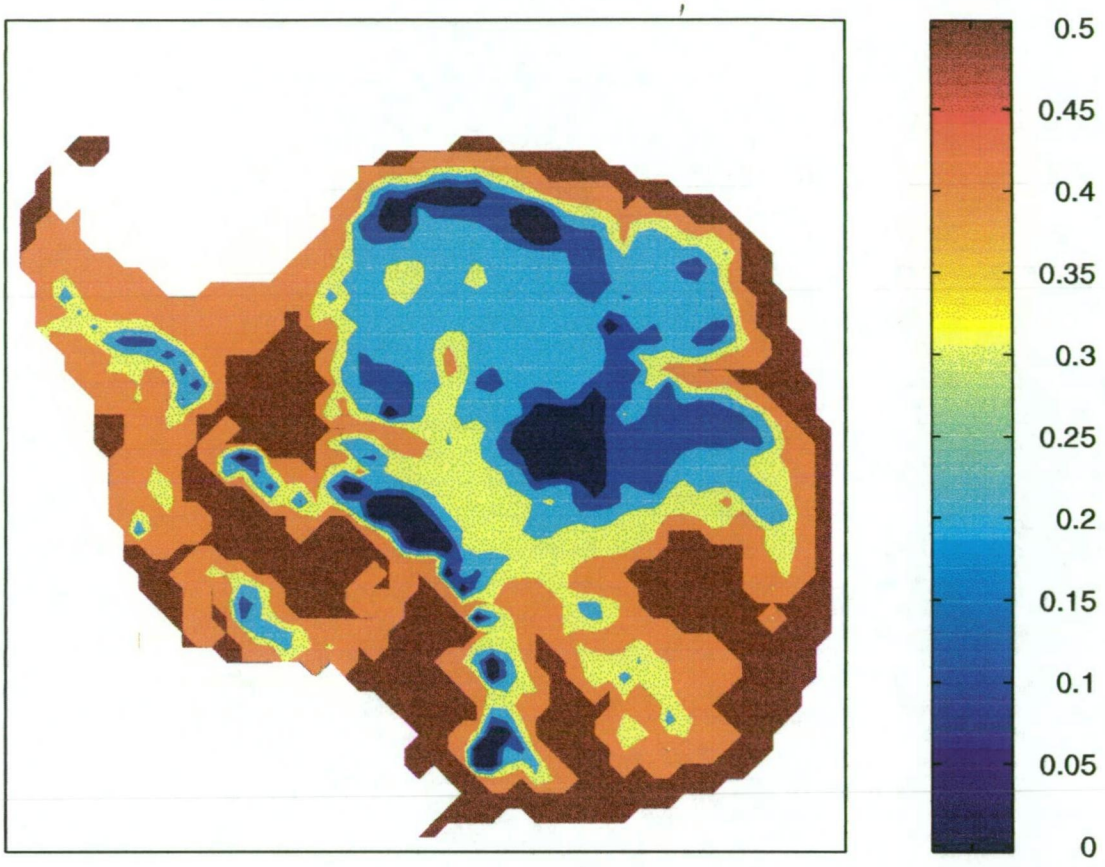

Figure 7.13: The increase in bed elevation for the raised bed experiment.

glacial cycles.

A crude attempt to model a glacial cycle from earlier in the Quaternary was made by raising the present bed distribution to a state which might represent the bed at an earlier time. The bed was raised by an amount which varied from 500m for the bed below sea level, tapering to no change in the bed topography at elevations greater than 1km as shown in Figure 7.13.

The surface elevations after two glacial cycles with accumulation rate and sea level forcing on this elevated bedrock are shown in Figure 7.14. The resulting ice sheet is grounded to near the continental shelf edge at all margins. This sensitivity result suggests that glacial extent prior to the last glacial cycle may have been well advanced in comparison to its present distribution. This result stresses the importance of obtaining reliable dating of the evidence for a more extensive ice sheet in the Weddell Sea, a position which is often attributed

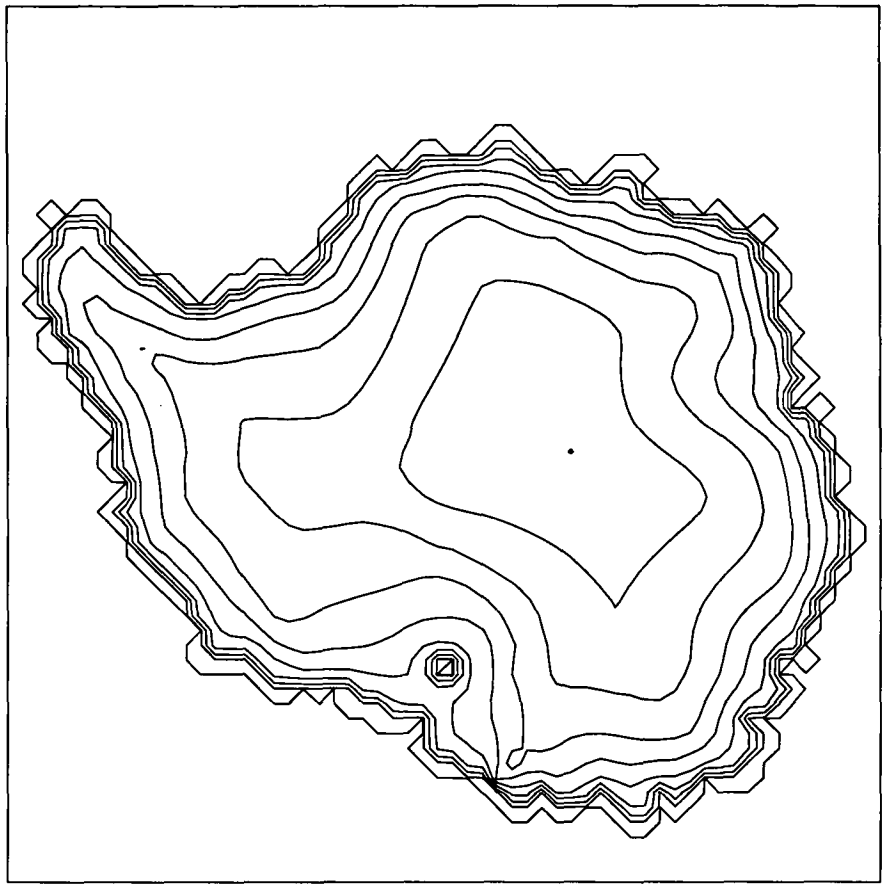

Figure 7.14: Surface elevations for the raised bed experiment (sea level and accumulation forcing). Contours are at 0m, 100m, 500m, then every 500m.

to the LGM.

7.4.6 Model resolution

To investigate the limitations of the relatively coarse 100km model, some experiments were performed at a resolution of 20km. Figure 7.15 shows the Antarctic Ice Sheet elevations at the end of a modelled glacial cycle with sea level and accumulation forcing, produced by the 20km resolution model.

At the higher resolution the model was able to produce a more advanced grounding line in the West Antarctic than that produced by the 100km grid model. In fact, even though for the higher resolution model a 50% larger value of k_s (4.12) was employed, the West Antarctic grounding line produced was generally advanced on its present observed position. For values of k_s larger than

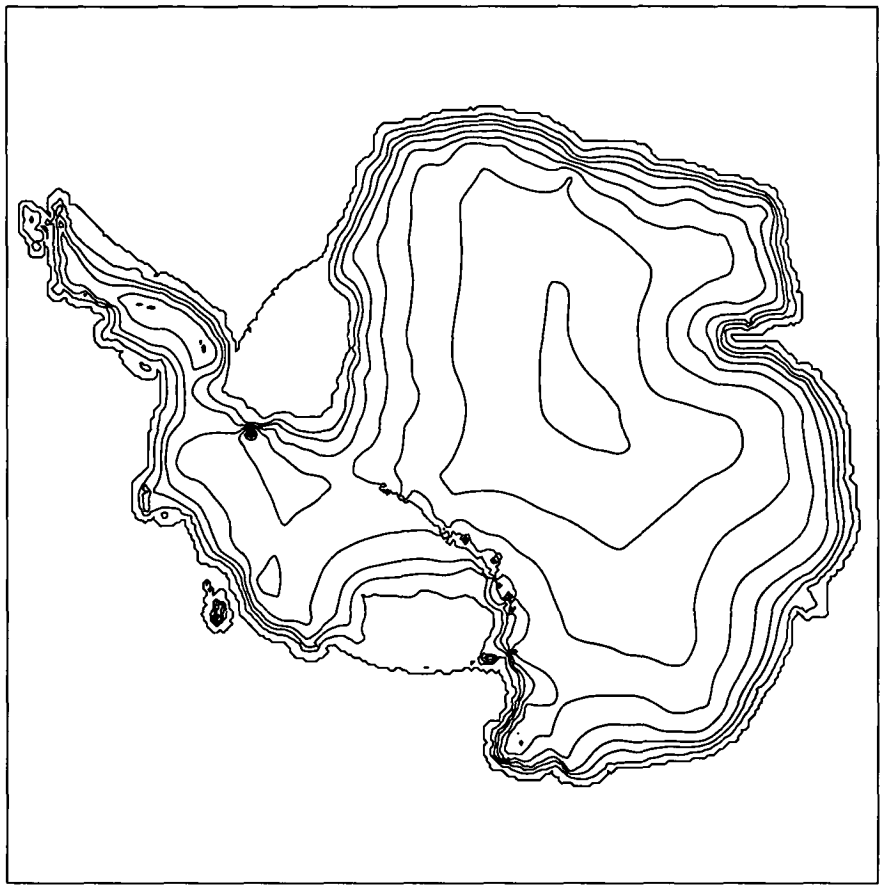

Figure 7.15: Surface elevations at the end of the run for the 20km grid model (sea level and accumulation forcing). Contours are at 0m, 100m, 500m, then every 500m.

this, there was significant ice loss from regions of the East Antarctic such as George V Land and Wilkes Land.

Throughout the glacial cycle however, the 20km resolution model grounding line location was found to be very static for the combined sea level and accumulation forcing experiment, as was the case for the 100km grid version. Where there was some very small grounding line migration from LGM to present in the 20km grid model, this tended to be in the form of advance, as changes in the West Antarctic Ice Sheet in particular, were dominated by the variation in accumulation rate more than by the sea level changes. The dominance of the accumulation forcing was stronger for the higher resolution model than for the lower resolution model.

While the results, particularly in regions near the grounding line, were

found in some ways to be sensitive to differences in resolution, for much of the grounding line response this was apparently not the case. The general resistance to grounding line movement in response to sea level change was similar for both versions of the model. It was also found that for the higher resolution model, when the application of a small value of k_s did lead to grounding line advance in the West Antarctic in response to sea level lowering, subsequent sea level rise did not induce any noticeable grounding line retreat. This was particularly the case for the grounding line in the Weddell Sea, and this behaviour strongly resembled that of the lower resolution model.

While the results obtained here using a 100km grid spacing would be enhanced in some ways through the use of a finer grid, the amount of time required to perform model runs at the higher resolution was prohibitive. Given that in many ways the results from both model versions were very similar, it was considered that the use of the 100km grid model for most of the experiments was preferable, because it allowed a large range of scenarios to be investigated, and the sensitivity to various factors to be tested. As more powerful computers become available, a higher resolution approach to this investigation will be possible.

7.4.7 East Antarctica

While there is some doubt over the models response to sea level change and its influence on grounding line migration, in East Antarctica, particularly inland, ice thickness changes are less influenced by the effect of sea level change on ice dynamics, and may be considered to be more realistic. The minor grounding line advance and small thickness change around the coast of East Antarctica produced by the model is also compatible with the palaeo-reconstructions of that region (Goodwin 1995).

Figure 7.16 shows the modelled variation in surface elevation at a location near Vostok (Vostok Station is at 78.3°S 106.5°E), the site of the ice core from which the amplitude of the accumulation forcing curve is derived. Climate records from ice cores will be affected by changes in the surface elevation history of the ice sheet as change in the surface elevation will lead to different surface temperatures and accumulation rates, even if the climate is otherwise

unchanged. Model results suggest that variation in the glacial surface elevation at Vostok due to changes in thickness and isostatic effects was around 145m (Figure 7.16). This variation was mainly a result of thickness changes in response to the varied accumulation rate. If elevation is considered to be the height above sea level, sea level change directly affects the surface elevation. When this effect was included in the Vostok surface elevation profile there was a significantly reduced amplitude of elevation change, as the periods when the ice thinned due to the low accumulation rate generally corresponded to low sea level episodes and these effects were found to largely cancel. Throughout the glacial cycle, the height above sea level at Vostok varied over about 90m, although most of this variation was in the last 20ka when sea level quickly rose to near present levels, while the ice thickened more gradually, so that for the last ~10ka the height above sea level was the same as the elevation resulting from thickness and isostatic changes. Elevation changes such as these could influence surface temperatures by as much as ~1°C, but were not considered when the Vostok surface temperature history was derived. Without being directly influenced by the effect of sea level on ice dynamics, well grounded, low sliding regions of Antarctica may still be affected by sea level change through the influence of this change on surface climate.

There is an indication of a period of slight cooling, or reduced warming at about 13ka BP in the Vostok ice core record (Jouzel et al. 1987). The results here suggest that a rapid decrease in the rate of sea level rise, after the peak in the rate of deglaciation of the northern hemisphere ice sheets at around 14ka BP, could have allowed the ice sheet elevation around Vostok to suddenly begin to rise. This may have produced a sudden change towards cooling at Vostok, which was dependent only on sea level change. It is speculated that the small cooling signal found in the Vostok ice core, may result from a reduced rate of sea level increase following the LGM and not from an actual cooling of the atmosphere due to a global Younger Dryas event. If the apparent cooling event in the Antarctic were due directly to sea level changes, while in the North Atlantic the Younger Dryas phenomenon were dependent on changes in ocean and atmospheric circulation resulting from a freshwater influx, there may be some explanation for the apparent leading of the Antarctic response.

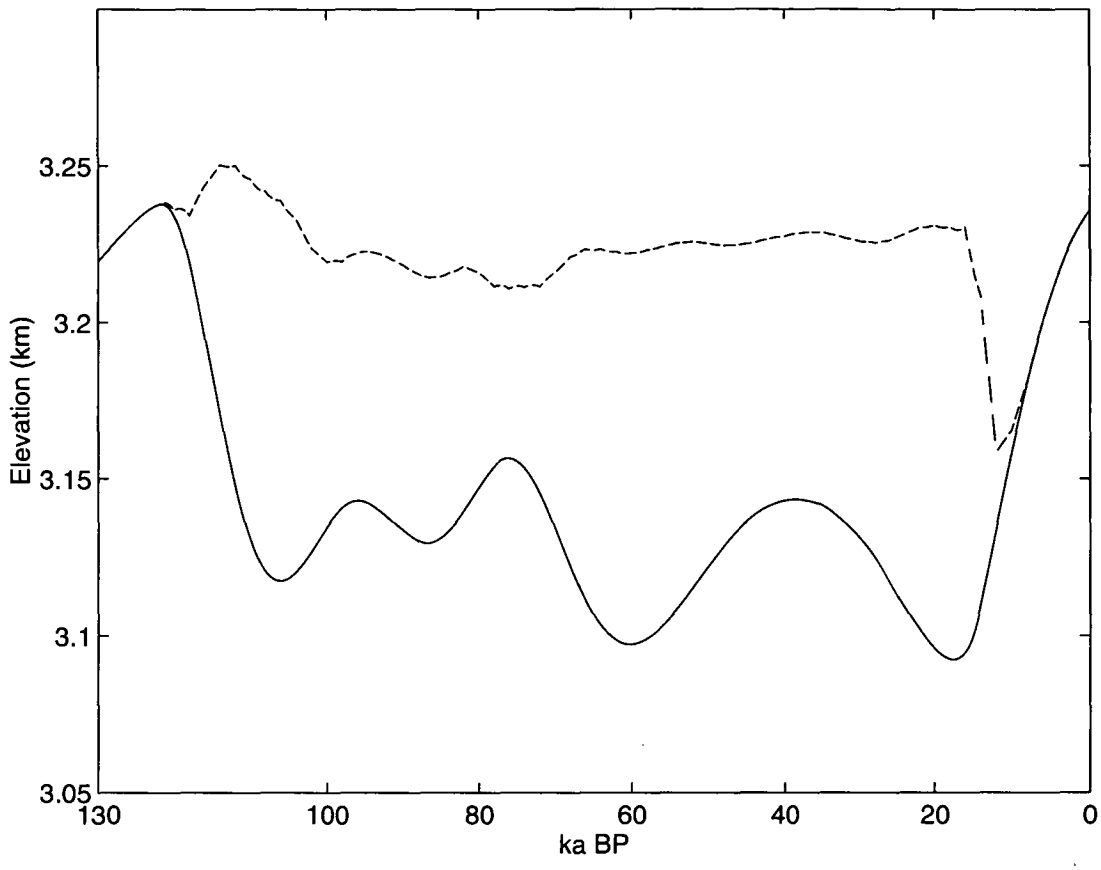

Figure 7.16: Variation in the surface elevation at Vostok (78.3°S 106.5°E). The solid line gives the change in elevation due to variation in thickness and bed elevation only. The dashed line gives the total change in elevation above sea level (i.e. sea level variation is included).

7.4.8 Deglaciation

The accumulation rate and sea level forcings reached their minima at about 20ka BP, then began to increase before levelling out at about 10ka BP. The ice sheet gradually reacted to these changes in the climate forcing. Rising sea level led to increased velocities in regions where there was sliding, which tended to produce ice thinning. Increasing accumulation however tended to cause the ice to become thicker, particularly at low elevations where the accumulation rate was higher, and the change in the accumulation rate greater.

Figure 7.17 illustrates the effects of the sea level and accumulation forcing on the pattern of thickness change in the Antarctic. Only the changes in grounded ice are shown. The accumulation forcing minima was attained at

around 20ka BP, but by 18ka BP (Figure 7.17 (a)) there was little change in the ice volume (see Figure 7.10). The ice sheet had started to become thicker at lower elevations, particularly in the east. In the central East Antarctic region however, the ice sheet was still thinning slightly in response to the earlier, lower accumulation rate. By the time of maximum volume at 14ka BP (Figure 7.17(b)) virtually the entire East Antarctic Ice Sheet was gaining thickness (although still more so at lower elevations), as was the inland West Antarctic Ice Sheet, but the greater rate of thinning in coastal regions was then balancing this and there was no longer a net increase in volume. The margin thinning then began to dominate the mass balance as the ice sheet adjusted to the increase in accumulation. The sea level rise induced margin thinning continued to dominate over the increasing thickness inland for about 4ka until by about 10ka BP (Figure 7.17 (f)) the increasing area of positive thickness change was able to balance the ice loss in the diminished region of thinning at the ice sheet margin. Again the higher elevations were slowest to respond to the accumulation forcing, with the greatest thickness increases occurring inland at this time. The rapid change in the forcing was largely complete by this time and grounding line thinning continued to become less pronounced and the ice sheet mass balance once again became dominated by the accumulation rate. By about 9ka BP, the ice sheet was gaining volume as the ice sheet continued to progress towards balance with the high accumulation rate.

The timing of the deglaciation in Antarctica produced by the model agrees reasonably with palaeo-estimates. Peltier (1988) suggested that the onset of deglaciation in Antarctica corresponded to the maximum rate of deglaciation in the northern hemisphere. In Section 6.5 it was found that the maximum northern hemisphere deglaciation occurred around 14ka BP, about the same time that deglaciation commenced in the Antarctic model. Other observations indicate that the deglaciation of the Antarctic commenced around 15-14ka BP and continued until ~8-6ka BP (see Section 3.1.6), in broad agreement with the timing displayed here.

The ice sheet reacts in different ways to the different forcings. Sea level changes affect coastal regions where significant sliding occurs. Altered accumulation rate is felt throughout the ice sheet, but its influence is also

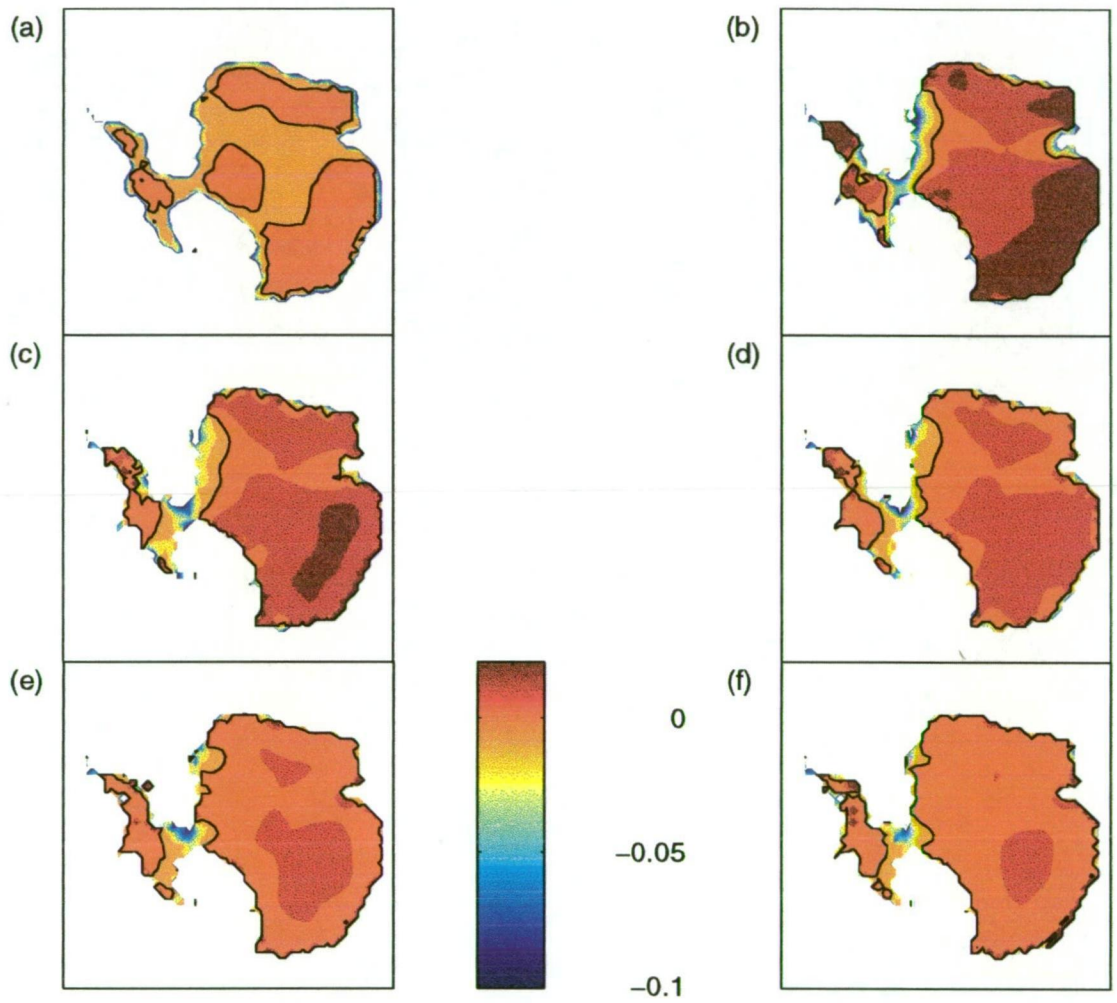

Figure 7.17: Rates of thickness change ($m\,a^{-1}$) at (a)18ka BP, (b) 14ka BP, (c) 13ka BP, (d) 12ka BP, (e) 11ka BP, (f) 10ka BP. The zero contour is marked.

particularly strong at low elevations where the accumulation rate is relatively high. The timing of these responses also differs and total response of the ice sheet to the climate forcing is complex with first one aspect of the climate dominating the mass balance, then the other.

7.4.9 Present state of balance of the ice sheet

Once the climate forcing became more stable over the last 10ka, the ice sheet began to approach a state more in balance with its environment. The present rate of thickness change and degree of imbalance derived from the model are shown in Figure 7.18. The degree of imbalance is given by the ratio of thickness change to accumulation rate:

$$B = \frac{\delta D}{\delta t} \frac{1}{P} \tag{7.1}$$

where B is the imbalance as a proportion of the accumulation rate, P is the accumulation rate and D is the ice thickness at time t.

From the changes in the modelled ice sheet over the last 2ka ($\delta t = 2ka$), it was found that most of the ice sheet is in a state of slightly positive mass balance due to the post ice age accumulation increase. Some grounding zone regions are still thinning due to the effects of sea level rise, but elsewhere the ice sheet is becoming thicker. The ice sheet is out of balance by ~20-30% in central East Antarctica, where the ice dynamics have not fully adjusted to the high interglacial accumulation rate. The low ice velocities (see Figure 7.19) and low accumulation rate there cause the response to the increased accumulation rate to be the most delayed in this region. The result that the model produced a positive balance in the Lambert Glacier basin is in agreement with recent observations in that area (Phillips 1999). Towards the coast, the ice sheet is closer to balance, the thickness change being generally less than 2-3% of the accumulation rate. In these areas, the dynamics have largely adjusted to the increased sea level and are also close to being in balance with the increased accumulation.

It is important to note that these simulated changes represent computed changes up to the time before possible recent anthropogenic changes to climate

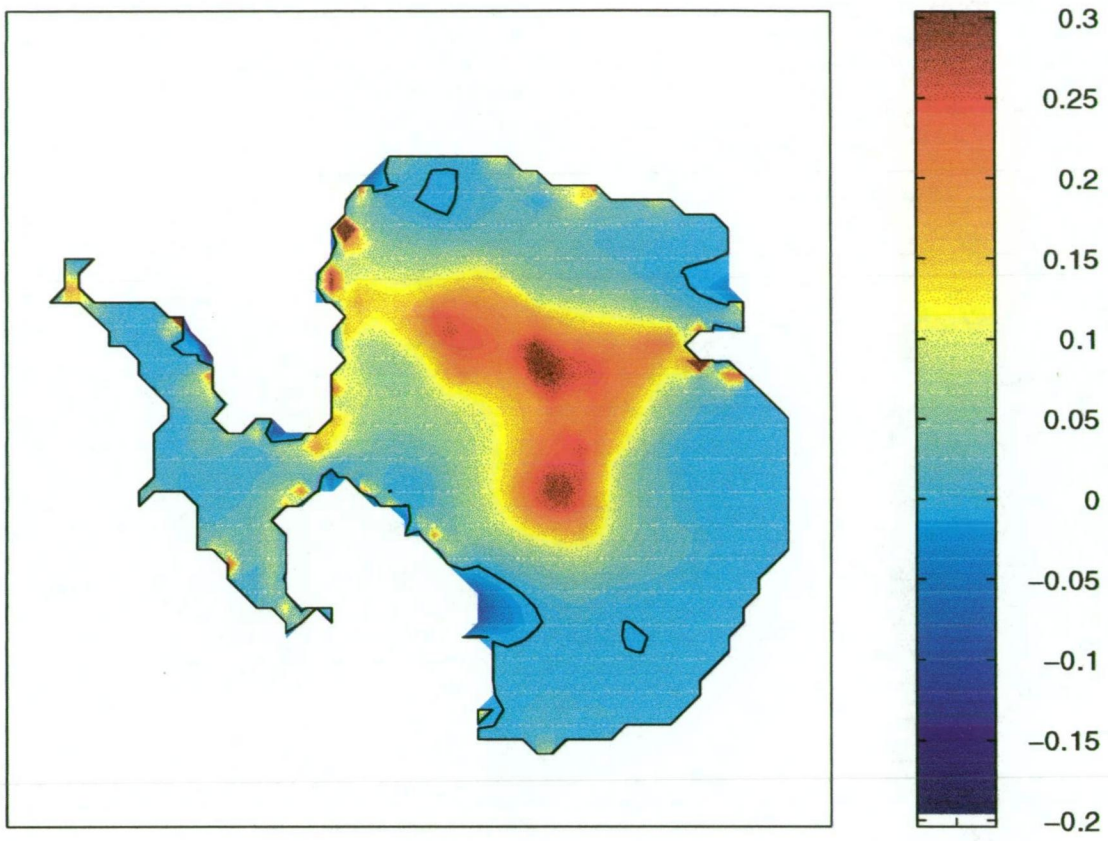

Figure 7.18: The degree of mass imbalance for the Antarctic Ice Sheet. The present rate of thickness change as a proportion of the present accumulation rate. The zero contour is marked and it can be seen that most of the ice sheet is in a state of positive mass balance.

over the last century may have taken place. The results from Smith et al. (1998) indicate that since last century an additional 5-10% increase in net accumulation rate may have taken place. This would need to be added to the post-glacial responses derived here to give the present state of balance.

The present contribution of the Antarctic Ice Sheet to sea level changes from its continuing postglacial adjustment can be calculated from the change in the volume of ice above buoyancy over the last few hundred years. The slight positive mass balance of the ice sheet has its contribution to sea level as $-0.07mm\,a^{-1}$, i.e. a sea level lowering of less than $0.1mm\,a^{-1}$. This compares reasonably with other estimates of the Antarctic contribution to sea level which consider the ice sheet as close to balance (King and Turner 1997), although recent estimates that the net accumulation in the Antarctic may be higher than

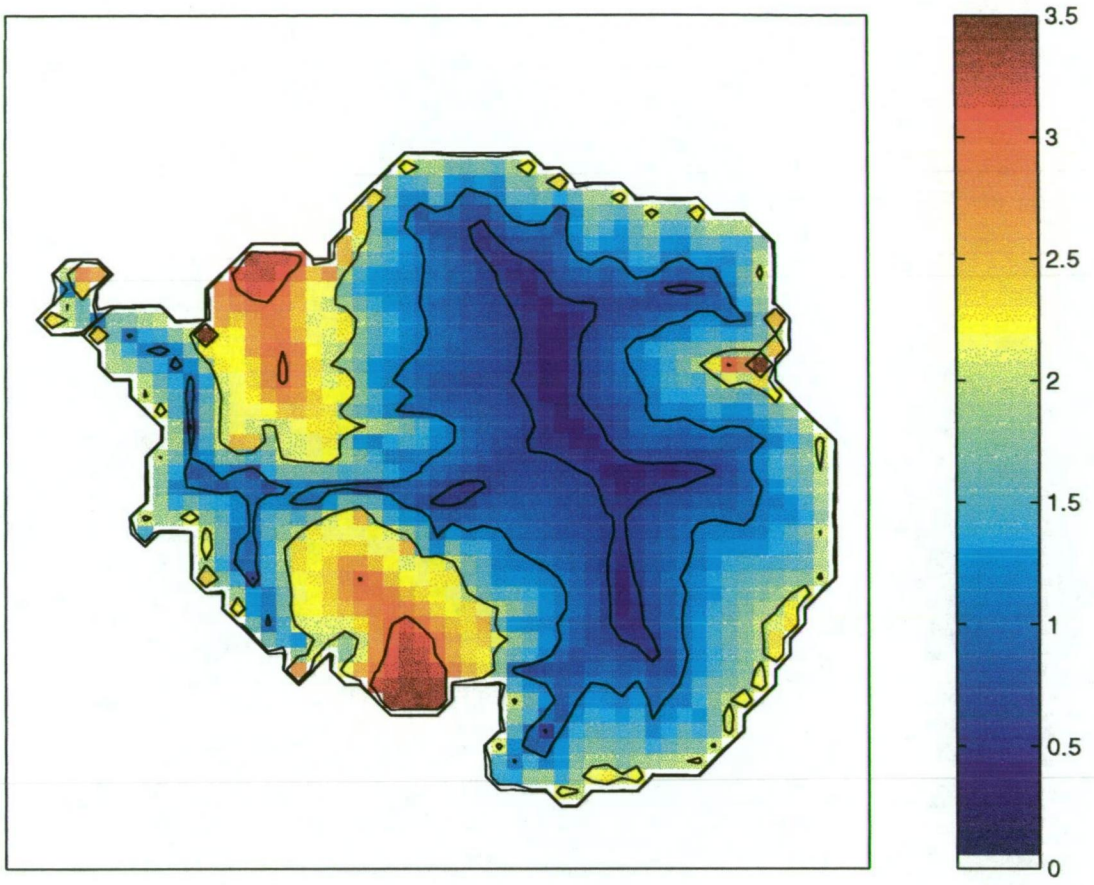

Figure 7.19: Model velocities for the present Antarctic Ice Sheet ($\log(m\,a^{-1})$). Contours are at $2m\,a^{-1}$, $10m\,a^{-1}$, $100m\,a^{-1}$ and $1000m\,a^{-1}$.

previously thought (Vaughan et al. in press) suggest that there may be a slight positive mass balance. Negative Antarctic contributions to present sea level of less than $1mm\,a^{-1}$ have also been suggested by other studies (see Section 3.1.6).

7.5 Summary

The influences of accumulation rate and sea level change on the Antarctic Ice Sheet through the last glacial cycle have been investigated. Grounding lines and ice volume tended to respond more strongly to decreasing sea level than to increasing sea level so that in the absence of any accumulation forcing, the grounding line in the Weddell Sea readily advanced to the edge of the continental shelf. Once the ice became heavily grounded there, subsequent sea level rise was unable to initiate any significant grounding line retreat.

Grounding line advance in the Weddell Sea in the 'sea level forcing only' case was found to be largely from the West. When the ice shelf grounded upstream, causing pinning points, the the influence on the shelf flow was such that the grounding line quickly advanced out to capture those points. Advance to near the continental shelf edge was largely completed over a period of ~16ka.

When grounding line advance was produced in the Weddell Sea, either due to sea level change, changes in the nature of the sliding employed by the model or variation in the bed elevation, the advance was found to be extensive and to some extent irreversible. The relatively shallow depth of water at the continental shelf edge in the Weddell Sea allowed ice to become well grounded there, to the extent that basal sliding became small and the ice did not respond strongly to subsequent sea level rise.

In the Ross Sea however, grounding line advance and retreat were achieved, providing the accumulation forcing was not applied. Under these conditions, a grounding line advance and post LGM retreat of similar magnitude to that estimated by some palaeo-reconstructions was produced. When the accumulation rate did vary through the glacial cycle however, there was virtually no grounding line migration produced by the model, although ice thickness change was still dominated by the influence of sea level in regions of high basal sliding and further inland of these regions.

Applying the accumulation forcing in isolation caused the ice sheet to thin under the influence of the low glacial accumulation rates. This led to a collapse of the deep marine part of the West Antarctic Ice Sheet. When the accumulation rate increased again to interglacial levels, the high velocities of the then floating ice in the West Antarctic did not allow the ice to thicken to the extent where it would ground again, and the West Antarctic Ice Sheet remained as a few isolated ice caps connected by a large ice shelf.

By imposing the two types of climatic forcing separately, two different end states were achieved. Where the sea level forcing acted alone, a heavily grounded, stable West Antarctic Ice Sheet formed. When the changing accumulation rate was the only applied forcing, the West Antarctic Ice Sheet largely collapsed to a point where small ice caps were only connected to each other and to the East Antarctic Ice Sheet by a large ice shelf.

The largely opposing influences of sea level and accumulation forcing when combined, produced an ice sheet fairly representative of the present Antarctic Ice Sheet, with the modelled state of the West Antarctic Ice Sheet in the 'combined' run being something between those produced by the 'sea level alone' and 'accumulation alone' runs, making a third possible end state for this marine ice sheet. For this experiment, elevation changes at Vostok were calculated to have varied by as much as 145m which may have significant consequences for the climatic interpretation of the Vostok ice core. This analysis also offers a possible explanation for the early occurrence of the cooling event in the Antarctic which is associated with the Younger Dryas cooling found in sea sediment and ice cores in the North Atlantic region.

While the match with the present was satisfactory when all the forcing was applied however, the model failed to produce significant LGM grounding line advance in the Weddell and Ross Seas where some palaeo-reconstructions suggest such advance occurred. This resulted in an estimate of the Antarctic's contribution to post glacial maximum sea level rise of $\sim 1m$, considerably less than some other estimates. Nevertheless, the timing of the deglaciation agrees well with observation as does the modelled present state of balance of the Antarctic Ice Sheet. It was found that while there is still some ice thinning at some grounding zone locations, generally the ice is becoming thicker due to the high interglacial accumulation rate. This is particularly the case in the central East Antarctic Ice Sheet where the low accumulation rate and ice velocity lead to a greater lag of the forcing. It was estimated that the growth of the Antarctic Ice Sheet contributes $< 1mm\,a^{-1}$ to sea level lowering.

Chapter 8

Conclusions

Evidence is strong that recent glacial cycles at least, stem primarily from changes in insolation resulting from variations in the Earth's orbital parameters. Although the radiation anomalies caused by these orbital changes vary seasonally and latitudinally, the feedback and amplification of the radiation changes by the ice sheets and the climate make the ice ages essentially global phenomena. In this study, the influence of the orbitally driven insolation changes as calculated by an energy balance model which included ice sheet feedback was used as the primary forcing for the ice sheet modelling (including bedrock adjustment and floating ice shelves) of the large ice sheets of the last glacial cycle in the northern hemisphere and Antarctica. This global approach allowed some of the interaction between individual ice sheets to be simulated, particularly for the ice sheets of the northern hemisphere but also between hemispheres. Palaeo-evidence and model output were compared to estimate the validity of model results and aid in the interpretation of palaeo-observational data. It was intended that this modelling would give some insight not only into past ice distributions but also into climate, sea level and bedrock histories. Through better understanding these changes, knowledge of present conditions is enhanced.

8.1 Northern hemisphere

8.1.1 Palaeo-climate

The model for the northern hemisphere was primarily driven by temperature and sea level forcing. The influence of the precipitation rate on the ice sheets produced by the model was also investigated. It was found that temperature, through its control over the ablation rate, was the dominant climatic influence in determining the southern margins of the ice sheets. The modelled Last Glacial Maximum southern margins of the northern hemisphere ice sheets compared reasonably with the margin locations suggested by palaeo-reconstructions when a maximum temperature depression amplitude of -13°C was applied to the temperature forcing. In some locations this match with observations was better for temperatures 1°C warmer or cooler than this, suggesting that temperatures in the ablation zone at the southern margins of the ice sheets at the LGM were in the vicinity of 13°C below their present values. It is expected that temperatures would have warmed quickly with distance south of this region while further north over the ice sheets, temperatures would have been considerably lower. This allows only a narrow ablation zone at the southern ice sheet margin, which is not at all resolved in present global climate models.

Variation in the base accumulation rate had only a small impact on the location of the southern margins of the ice sheets. Doubling, or halving the base accumulation rate influenced southern extent of the ice sheet by about the same amount as a 1°C change in the temperature forcing. This was due in part to the dominance of ablation on the ice sheet mass balance, but also to the strong influence of the 'elevation-desert' effect. The parameterisation of the dependence of the accumulation rate on elevation greatly diminished the effect of even large changes in the initial accumulation distribution as the generally high elevations over much of the iced area allowed only low accumulation rates there. Results indicated then that temperature was the dominant factor in determining the southern extents of the northern hemisphere ice sheets as suggested by Hostetler and Clark (1997).

In the Arctic Ocean however, it was found that the extent or existence of a floating ice shelf was strongly dependent on the base accumulation rate. Due

to the generally low surface elevations over floating ice, the 'elevation-desert' effect has no direct influence there. Of more concern is the way in which the Arctic basin accumulation may change with the size of the surrounding ice sheets. The generally low temperatures in the Arctic Ocean did not allow for much ablation and in this region ice thicknesses were determined by the balance between the accumulation, flux divergence, ocean melt and the calving of the ice shelf. Given the likelihood that the access of water vapour to the northern Arctic atmosphere may have been reduced by the existence of high ice sheets encircling the Arctic for much of the glacial cycle, a rain shadow effect may have significantly reduced the amount of precipitation there. When the base accumulation rate was halved, the model produced virtually no Arctic ice shelf.

The influence of sea level on the extents of the northern ice sheets was also found to be small in comparison to the effect of temperature change. Ice sheets tended to ground to the edge of the continental shelf whether or not sea level change was applied to the model. The retreat of the marine ice sheets in these locations also tended to be dominated by increased ablation at the southern margins rather than collapse at marine margins due to sea level rise. For the modelled northern hemisphere ice sheets the largest effect of sea level change did not occur through its influence on grounding line dynamics so much as through the accompanying effective change in surface elevations and temperature.

8.1.2 Ice sheet and bedrock reconstructions

Limitations such as the restricted range of carbon dating have resulted in a preponderance of palaeo-data relating to the time since the LGM. Because of this, validation of model results was based primarily on the results produced for this period. As mentioned previously, the model had some success in matching observational estimates of the LGM ice sheet extent. The ability of the model to also produce a final state representative of the present as well as giving a reasonable match with what is known about the deglacial time between LGM and present, is considered to give some credibility to the northern hemisphere results in general.

The modelled East Siberian Ice Sheet was larger than that which is currently thought to have existed during the last glacial cycle. While not being

in complete agreement with observational reconstructions for this region however, model results do concur with some other modelled reconstructions. The apparently excessive amount of ice produced by models in this area may be explained by a much lower than present accumulation rate there during glacial times or, given the dominant influence of temperature on ice sheet extent discussed above, conditions there must have cooled considerably less than in other places at the same latitude. Palaeo-data from Eastern Siberia are relatively scarce however and more evidence may establish the cause of the smaller than modelled ice sheets and/or the accuracy of the palaeo-reconstructions of those ice sheets. Applied in this way, model results may provide information on palaeo-climate conditions and in assessing the available evidence for palaeo-ice sheet extents.

Just as model results may be of use in places where observations are limited, so too may they be valuable for times when there is little observational data. With very little known about the history of the bed topography in the region of the northern hemisphere ice sheets, modelling offers a method of estimating palaeo-bed topographies. As well as the requirement that the overlying ice sheets should match palaeo-reconstructions of ice sheet extent, the model was also constrained by the requirement that the final modelled bed positions match present observed bed elevations and the residual uplift in the model reflect observations of the present day uplift rate and the amount of uplift which has occurred since the ice disappeared. It was found that in order to meet these requirements, an initial bedrock distribution which was considered to be representative of conditions at the last interglacial, was considerably higher than present in some locations. Ignoring the effects of erosion over the glacial cycle it is assumed that the present bed is 'attempting' to return to elevations similar to this initial distribution, with consequences for relative sea level change in coastal regions where rebound continues to occur.

It was also found that an elevated initial bed distribution was not only significant in matching the final state of the bed to observations but was also a crucial factor for the initiation of ice sheet growth in some regions. If the initial bed elevation did not exceed some threshold in these places, ice sheet growth was limited. It appears that the ability to allow the growth of realistic ice sheets

may constrain estimates of palaeo-bedrock elevations, particularly in northern North America, where the growth of the Laurentide Ice Sheet was found to be sensitive to initial bed conditions. This sensitivity highlights the fact that while glacial cycles may have been driven by external orbital influences, the terrestrial nature of those cycles is heavily dependent on the state of the Earth and its climate system.

Initial ice advance tended to occur as the expansion of thin sheets of ice. Following seeding at higher altitudes these sheets spread to lower and more southerly regions as temperatures decreased and some continental ice sheets only developed when northern marine ice sheets expanded southward. While the extent of the ice sheets increased rapidly, the ice sheets only approached maximum thicknesses sometime later, as ice area was found to lead ice volume during glacial advances, although area and volume tended to be closer to synchronous during retreat. Ice sheet retreat was found to follow a similar path to the advance (but in reverse), but as the margins were considerably thicker at the time of retreat, a greater volume of ice was lost in the retreat of an ice sheet over a certain distance than was gained during its advance. For the same rate of margin migration, ice will be lost from an ice sheet more quickly than it is gained. Some of the 'sawtooth' nature found in sea sediment records of ice volume may therefore be explained by the different thicknesses of the ice sheets during advance and retreat.

8.1.3 Other glacial phenomena

Modelling the northern hemisphere ice sheets through the glacial cycle allowed an estimate of the eustatic contribution to sea level of these ice sheets. Without a global approach to the isostatic modelling, it was difficult to determine the relative sea level changes which resulted from the northern hemisphere glacial changes but the 138m change in eustatic sea level from LGM to present resulting from deglaciation was in approximate agreement with that required for relative sea level estimates based on observation. An estimate of the ^{18}O anomaly which would have resulted from the total volume of ice in the northern hemisphere ice sheets was also found to be comparable to those found in sea sediment cores without the need for recourse to an Antarctic Ice Sheet

contribution to ice volume change or the influence of ocean temperature on $\delta^{18}O$. Also, even if an ice shelf did cover the Arctic Ocean during the glacial cycle, it appears that it would not have been voluminous enough to significantly influence the degree of isotopic depletion in the ocean. The general agreement of modelled and observed sea level and $\delta^{18}O$ further supports the ice sheet modelling results obtained here.

The sea level change estimated by the model exhibited a degree of the sawtoothed character of slow decrease followed by a rapid rise. This may have been in part due to the different natures of ice sheet advance and retreat described earlier but it also appears that the progressively increasing depression of the bed beneath the ice sheets contributed to a trend of increasing ice volume through the ice age. The 'elevation-desert' effect placed an effective ceiling on the elevations of the ice sheets but with increasing bed depression the ice sheets were able to thicken beneath this ceiling leading to an increase in ice volume. For two glacial maxima with similar climatic conditions, the succeeding one tended to be of greater volume. While the derived sea level changes did not feedback directly into the ice sheet model, it is expected that the sawtooth nature of the sea level change which resulted from the progressively increasing volume of ice would be amplified by the response of the ice sheets to the sea level change. Although it was found that sea level change did not strongly affect the ice sheets, whatever influence it did have would have fed back positively to the sea level change as progressively lower sea levels should encourage progressively more advanced ice sheets.

The orbitally driven radiation forcing was transmitted through all the components of the modelled system. However, the signal was damped and transmuted along this passage. For example, total ice sheet volume and total bed depression were almost completely out of phase with the insolation changes and climate forcing. At times when temperatures were decreasing, the bed was depressing, bringing the overlying ice to warmer elevations. While the radiation and primary climate forcing signals are apparent in model output it is once again apparent that the internal mechanics of the ice sheet system exert a considerable influence of their own on the nature of the glacial cycle. The out of phase relationship between the radiation anomalies and some components of the

ice sheet system, particularly the total ice volume and isostatic depression means that the system never reaches a steady state balance with its forcing.

As well as altering the nature of the external temperature and precipitation forcing, changes in the ice sheets may have produced other important climatic variation as well. The timing of the Younger Dryas cold reversal during deglaciation was found to have some correspondence with the timing of the peak rate of deglaciation of the northern hemisphere ice sheets, supporting the theory that a large influx of fresh water into the North Atlantic at this time may have altered the climate, not only in that region, but possibly extending around the globe.

8.2 Antarctic

8.2.1 Balance of accumulation and sea level forcing

It was assumed that ablation is negligible for the Antarctica, particularly when considering the generally colder glacial conditions and so temperature was not explicitly used to force the Antarctic Ice Sheet model. However, the change in accumulation rate derived from EBM results and the Vostok ice core was applied to the model as a proportional change to the base accumulation rate. Sea level change like that used for the northern hemisphere modelling was also applied as forcing to the Antarctic model. This curve was similar to the sea level change curve derived from the northern hemisphere ice sheet modelling.

The reaction of the modelled grounding line to changes in sea level was found to be complex. While in general grounding lines tended to advance when sea level decreased and retreat during sea level rise episodes, the extent of this response depended on the ice thickness, buoyancy and thickness profile as well as the profile of the bed. Consequently, the reaction of the Antarctic model to sea level change was also non-linear. In the absence of accumulation forcing, the lowering of sea level during the glacial cycle did indeed lead to grounding line advance in the model, particularly in the Weddell Sea. However, the ice at the advanced grounding line tended to become too thick to then respond adequately to subsequent sea level rise.

Inspection of the modelled large scale advance of the grounding line in the

Weddell Sea suggested that advance over large areas was preceded by isolated grounding of the ice shelf. The pinning of the ice shelf away from the grounding line apparently allowed the ice shelf to thicken and ground out to the pinning points.

In the Ross Sea the model produced grounding line advance and retreat approximately in line with that which is thought to have occurred. This was only achieved however when the model acted without external accumulation forcing. Once the accumulation forcing was applied, although the dynamics and thicknesses of the ice in the grounding zone where there was significant basal sliding were still affected by sea level changes, the effect was moderated by the changes in accumulation rate and little grounding line movement resulted. In fact, the respective influences of changing accumulation rate and sea level largely cancelled each other in terms of change in total ice volume and grounding line movement.

Applying the accumulation forcing in isolation (i.e. no sea level forcing) resulted in the collapse of the West Antarctic Ice Sheet as the low glacial accumulation rates could not support the ice sheet there. The thin, fast flowing ice sheet-ice shelf system which remained there survived even when accumulation rates returned to interglacial levels. The fast flowing ice continued to remove the accumulation too quickly to allow any significant grounding line advance.

So, when the two types of external forcing were applied in isolation, two different but stable, ice distributions resulted in the West Antarctic. In one case the ice in the Weddell Sea became too thick to respond to the applied sea level rise, and in the other West Antarctic ice became too fast flowing to respond greatly to increased precipitation. Between these two states lay a third which was achieved when all the forcing was applied simultaneously to produce an Antarctic Ice Sheet not too dissimilar from that which presently exists. Much of the modelled grounding line response to the climate forcing was found to be largely independent of model resolution, with similar responses produced by 100km and 20km grid spacing versions of the ice sheet model.

It is considered that the uniform application of the percentage change (derived partly from the Vostok ice core from central East Antarctica) in the

accumulation rate across the entire Antarctic continent was far from an ideal approximation of what must have occurred during the glacial cycle. This approach produced large changes in the amount of accumulation at lower coastal areas, regions where basal sliding and the response to sea level change was generally strong. More information on the nature of the change in accumulation rate in West Antarctic regions, for example, may have produced a different relationship between the response of the grounding line to sea level change and to change in the accumulation rate.

8.2.2 Last Glacial Maximum and deglaciation

In the absence of any significant grounding line advance and retreat in the major West Antarctic embayments, the model produced only a small change in the volume of Antarctic ice above buoyancy from LGM to present. While some other model and observation based reconstructions suggest that the change in the extent of the grounded ice through deglaciation would have been larger than this, the timing of the deglaciation produced in this study agrees reasonably well with other estimates. It has been suggested that deglaciation in the Antarctic would have corresponded with the time of maximum rate of deglaciation in the northern hemisphere. As part of the global approach to the modelling of the last glacial cycle, the Antarctic Ice Sheet model was driven by the same sea level forcing as was applied to the northern hemisphere ice sheets, and modelled deglaciation in the Antarctic corresponded closely with the peak rate of deglaciation of the modelled northern hemisphere ice sheets.

The influence of erosion was not explicitly included in this model. The bed under the grounded ice may have been considerably higher during earlier ice age cycles before being reduced by erosion. In a sensitivity test, an extremely advanced Antarctic Ice Sheet was produced when modelled through a glacial cycle on a bed distribution possibly representative of earlier glacial cycles. The dating of evidence for significant glacial advance in the West Antarctic therefore is considered crucial to evaluating reconstructions of the LGM, to which much of this evidence is attributed.

It may be possible to estimate the magnitude of the erosion from the amount of deposited glacial sediments off shore. The relatively high bed at the

continental shelf edge in the Weddell Sea, which made it difficult for the model to unground once the ice had advanced there, may be a result of sediment deposition. The model with an erosion formulation included could assist in defining the sources and distribution of sediment and so help our understanding of palaeo-bed elevations.

8.2.3 Present state of the Antarctic

The final state of the modelled Antarctic Ice Sheet gives a reasonable representation of the present observed ice distribution. Deglaciation is considered to have been largely complete by 5ka BP and so the present state of the Antarctic Ice Sheet should be fairly independent of any large scale grounding line retreat which may have occurred during that deglaciation.

These model results suggest that while there may be a very small degree of thinning around the margins of the grounded ice in Antarctica and in the coastal regions in general, the ice sheet is in a state of slightly positive mass balance. Further inland, in central East Antarctica, the ice sheet is still responding to the present higher accumulation rate which coincided with the end of the ice age, and is out of balance with the accumulation by as much as $\sim$20%. The consequent net state of slightly positive mass balance for the present Antarctic places the Antarctic Ice Sheet's current contribution to sea level lowering at less than $0.1 mm\, a^{-1}$. This represents the modelled state of the ice sheet up to the time before any recent anthropogenic effects may have developed since last century.

8.3 Future work

An attempt has been made to model the ice sheets of the last glacial cycle using forcing derived, in part, from the Earth's orbital variations. The simplicity of the climate forcing employed to force the model suggests that benefit may be gained through coupling the ice sheet model with a GCM, theoretically producing more realistic glacial climate conditions. Previous GCM investigations into glacial climates have tended to produce similar results to each other, possibly due to their common use of CLIMAP (1976) or CLIMAP

(1981) ice sheet reconstructions as boundary conditions. There is apparently a strong climatic dependence on the distribution of ice, just as there is a strong dependence of ice sheet extent on temperature and ablation. To best model the glacial ice sheets, climate and ice sheet modelling should be performed as interactively as possible. The interaction between the ocean circulation and the ice sheets and climate was only briefly contemplated in this study but it is likely that ocean dynamics and other factors such as sea ice extent played a crucial role in determining glacial conditions and ideally should be included in any attempt to model the ice sheets and conditions of the last glacial cycle.

The inclusion of full three dimensional thermodynamics in the ice sheet model may also improve model results but the importance of complete thermodynamics in palaeo-climatic simulations, particularly for the northern hemisphere ice sheets, is not yet clear (Calov and Marsiat 1998). Given the dominance of ablation in establishing the (southern) margins of these ice sheets, and the dependence of an Arctic ice shelf on the accumulation rate, it appears that improved climate modelling is a higher priority than improvement in the ice sheet model.

The inclusion of a more sophisticated global isostatic model would enable modelling of relative sea level changes throughout the planet in response to the ice and sea water loading and unloading. Erosion and deposition of sediment should also be included.

The results for the West Antarctic Ice Sheet in this study suggest that a more complete approach to the modelling of grounding line dynamics would be of benefit. The application of the same sliding relation at all locations and for all bedrock conditions may be unrealistic and a more smooth transition from grounded to floating in the stress transition zone may also improve the models response to sea level change. The modelling of the ice shelves and the grounding line may also benefit from a more complete approach to the ice shelf dynamics. Although the 100km resolution modelling of the Antarctic used here was found to be satisfactory, the possibility of modelling at higher resolutions as more powerful computers become available will allow greater precision in the results.

Having established the present state of the Antarctic and Greenland Ice Sheets by modelling their evolution over a glacial cycle, prognostic studies may

be performed to test the response of these ice sheets to possible future climates. However, the results presented here for the Antarctic Ice Sheet suggest that as it is so close to balance, the assumption of steady state as an initial condition for modelling the ice sheet into the future, as was done by Coutts (1992) and Budd et al. (1994), may be satisfactory.

References

Abe-Ouchi, A., H. Blatter and A. Ohmura, 1994: How does the Greenland Ice Sheet geometry remember the ice age?, *Global and Planetary Change*, **9**, 1133–1142.

Adams, J., and N. Petit-Maire, 1992: Methane and Milankovitch cycles, *Nature*, **355**, 214.

Ahlmann, H., 1948: Glaciological Research on the North Atlantic Coasts, *RGS Research Series 1*, , Royal Geographic Society.

Ambach, W., 1989: Effects of climatic perturbations on the surface-ablation regime of the Greenland Ice Sheet, West Greenland, *Journal of Glaciology*, **35 (121)**, 311–316.

Andersen, B., 1981: Late Weichselian Ice Sheets in Eurasia and Greenland, in *The Last Great Ice Sheets*, edited by G. Denton, and T. Hughes, pp. 3–65, Wiley, NY.

Andersen, E., T. Dokken, Elverhøi, A. Solheim and I. Fossen, 1996: Late Quaternary sedimentation and glacial history of the Western Svalbard continental margin, *Marine Geology*, **133**(3-4), 123–156.

Andrews, J., and R. Barry, 1978: Glacial inception and disintegration during the last glaciation, *Ann. Rev. Earth Planet. Sci.*, **6**, 205–228.

Arkhipov, S., J. Ehlers, R. Johnson and H. Wright, 1995: Glacial drainage towards the Mediterranean during the Middle and late Pleistocene, *Boreas*, **24**, 196–206.

Bard, E., B. Hamelin, R. Fairbanks and A. Zindler, 1990: Calibration of the ^{14}C timescale over the past 30,000 years using mass spectrometric U-Th ages from Barbados corals, *Nature*, **345**, 405–410.

Barnola, J.-M., P. Pimenta, D. Raynaud and Y. Korotkevich, 1991: CO_2-climate relationship as deduced from the Vostok ice core: a re-examination based on new measurements and on a re-evaluation of the air dating, *Tellus*, **43B**, 83–90.

———, D. Raynaud, Y. Korotkevich and C. Lorius, 1987: Vostok ice core provides 160,000-year record of atmospheric CO_2, *Nature*, **329**, 408–414.

Bartlein, P., T. Webb III and E. Fleri, 1984: Holocene Climatic Change in the Northern Midwest: Pollen-derived, *Quaternary Research*, **22**, 361–374.

Baumann, K.-H., K. Lackshewitz, J. Mangerud, R. Spielhagen, T. Wolf-Welling, R. Henrich and H. Kassens, 1995: Reflection of Scandinavian Ice Sheet Fluctuations in Norwegian Sea Sediments during the Past 150,000 Years, *Quaternary Research*, **43**(2), 185–197.

Bender, M., T. Sowers, M. Dickson, J. Orchardo, P. Grootes, P. Mayewski and D. Meese, 1994: Climate correlations between Greenland and Antarctica during the past 100,000 years, *Nature*, **372**, 663–666.

Bentley, C., 1997: Rapid sea-level rise from a West Antarctic ice-sheet collapse,

Science, **275**, 1077–1078.

Bentley, M., and J. Anderson, 1998: Glacial and marine geological evidence for the extent of grounded ice in the Weddell Sea-Antarctic Peninsula Region during the last glacial maximum, *Antarctic Science*, **10**(3), 309–325.

Berger, A., 1978: Long-term variation of caloric insolation resulting from the earth's orbital elements, *Quaternary Research*, **9**, 139–167.

———, 1979: Long-term variation of daily insolation and Quaternary climatic change, *Journal of the Atmospheric Sciences*, **35**, 2362–2367.

Berger, A., 1993: Glaciation and deglaciation mechanisms in a coupled two dimensional climate-ice-sheet model, *Journal of Glaciology*, **39**(131), 45–49.

———, H. Gallée, X. Li, A. Dutrieux and M. Loutre, 1996: Ice-sheet growth and high-latitudes sea-surface temperature, *Climate Dynamics*, **12**, 441–488.

Bills, B., and T. James, 1996: Late Quaternary variations in sea level due to glacial cycle polar wander, *Geophysical Research Letters*, **23**(21), 3023–3026.

Birchfield, G., H. Wang and J. Rich, 1994: Century/millenium internal climate oscillations in an ocean-atmosphere-continental ice sheet model, *Journal of Geophysical Research*, **99**(C6), 12,459–12,470.

———, J. Weertman and A. Lunde, 1982: A model study of the role of height, latitude and topography in the climate response to orbital insolation anomalies, *Journal of the Atmospheric Sciences*, **39**, 71–87.

Biryukov, V., M. Faustova, P. Kaplin, Y. Pavlidis, E. Romanova and A. Velichko, 1988: The paleogeography of Arctic shelf and coastal zone of Eurasia at the time of the last glaciation (18,000 yr BP), *Palaeogeogr. Palaeoclim. Palaeoecol.*, **68**, 117–125.

Bischof, J., and D. Darby, 1997: Mid- to Late Pleistocene Ice Drift in the Western Arctic Ocean: Evidence for a Different Circulation of the Past, *Science*, **277**, 74–78.

Bloom, A., W. Broecker, J. Chappell, R. Mathews and K. Mesolella, 1974: Quaternary sea level fluctuations on a tectonic coast: new Th^{230}/U^{234} dates from the Huon Peninsular New Guinea, *Quaternary Research*, **4**, 185–205.

Bond, G., ———, S. Johnsen, J. McManus, L. Labeyrie, J. Jouzel and G. Bonani, 1993: Correlations between climate records from North Atlantic sediments and Greenland ice, *Nature*, **365**, 143–147.

Borzenkova, I., 1992: *The changing climate during the Cenozoic*, p. 247, Hydrometeoizdat, Saint Petersburg.

———, V. Zubakov and A. Lapenis, 1992: Global climate changes during the warm epochs of the past, *Meteorol. Gidrol.*, **8**, 25–37.

Boulton, G., and C. Clark, 1990: A highly mobile Laurentide Ice Sheet revealed by

satellite images of glacial lineations, *Nature*, **346**, 813–817.

———, and A. Jones, 1979: Stability of temperate ice caps and ice sheets resting on beds of deformable sediment, *Journal of Glaciology*, **24**(90), 29–43.

Boyle, E., 1995: Last-Glacial-Maximum North Atlantic Deep Water - On, Off or somewhere in between, *Philosophical Transactions of the Royal Society of London - Series B: Biological Sciences*, **348**(1324), 243–253.

———, 1988: Vertical oceanic nutrient fractionation and glacial/interglacial CO_2 cycles, *Nature*, **331**, 55–56.

Bradley, R., 1985: *Quaternary Paleoclimatology*, Chapman and Hall.

Braithwaite, R., 1990: A simple energy balance model to calculate ice ablation at the margin of the Greenland Ice Sheet, *Journal of Glaciology*, **36 (123)**, 222–228.

———, 1993: Seasonal variation of ice ablation at the margin of the Greenland Ice Sheet and its sensitivity to climate change, Qamanârssûp sermia, West Greenland, *Journal of Glaciology*, **39 (132)**, 267–274.

Bray, J., 1979: Surface albedo increase following massive Pleistocene explosive eruptions in western North America, *Quaternary Research*, **12**, 204–211.

Broccoli, A., and S. Manabe, 1987a: The Effects of the Laurentide Ice Sheet on North American Climate During the Last Glacial Maximum, *Geographie Physique et Quaternaire*, **41**(2), 291–299.

———, and ———, 1987b: The influence of continental ice, atmospheric CO_2, and land albedo on the climate of the last glacial maximum, *Climate Dynamics*, **1**, 87–99.

Broccoli, A., and E. Marciniak, 1996: Comparing Simulated Glacial Climate and Paleodata - A Reexamination, *Paleoceanography*, **11**(1), 3–14.

Broecker, W., 1992: The glacial world according to Wally, Lamont-Doherty Geological Observatory of Columbia University, Palisades, NY 10964.

———, M. Andree, W. Wolli, H. Oeschger, G. Bonani, J. Kennett and D. Peteet, 1988: A case in support of a meltwater diversion as the trigger for the onset of the Younger Dryas, *Paleoceanography*, **3**, 1–19.

Broecker, W., and G. Denton, 1989: The role of ocean-atmosphere reorganizations in glacial cycles, *Geochimica et Cosmochimica Acta*, **53**, 2645–2501.

———, and ———, 1990: What Drives Glacial Cycles?, *Scientific American*, pp. 43–50.

Broecker, W., M. Klas, E. Clark, G. Bonani, S. Ivy and W. Wolffi, 1991: The influence of $CaCO_2$ dissolution on core top radiocarbon ages for deep-sea sediments, *Paleoceanography*, **6**, 593–608.

———, and T. Peng, 1989: The cause of the glacial to interglacial atmospheric CO_2 change: A polar alkilinity hypothesis, *Global Biogeochemical Cycles*, **3**, 215–239.

Broecker, W., D. Peteet and D. Rind, 1985: Does the ocean-atmosphere system have more than one stable mode of operation?, *Nature*, **315**, 21–26.

Brooks, C., 1926: *Climate Through the Ages*, Yale University Press.

Budd, W., 1969: The dynamics of ice masses, *Scientific Report 108*, , ANARE.

———, 1981: The importance of ice sheets in the long term changes of climate and sea level, in *Sea Level, Ice and Climatic Change*, number 131 in IAHS Publ., pp. 441–471.

Budd, W., 1991: Antarctica and Global Change, in *Climatic Change*, pp. 271–299, Kluwer Academic Publishers.

———, and I. Allison, 1975: An empirical scheme for estimating the dynamics of unmeasured glaciers, in *Snow and Ice Symposium*, number 104 in International Association of Hydrological Sciences, pp. 246–256.

Budd, W., B. Coutts and R. Warner, 1998: Modelling the Antarctic and northern hemisphere ice sheet changes with global climate during the glacial cycle, *Annals of Glaciology*, **27**, 153–160.

———, and T. Jacka, 1989: A review of ice rheology for ice sheet modelling, *Cold Regions Science and Technology*, **16**, 107–144.

Budd, W., ———, D. Jenssen, U. Radok and N. Young, 1982: Derived physical characteristics of the Greenland Ice Sheet, *Tech. Rep. 23*, , The University of Melbourne Meteorology Department, Parkville, VIC. 3052, Australia.

———, T. Jacka and V. Morgan, 1980: Antarctic ice berg melt rates derived from size distributions and movement rates, *Annals of Glaciology*, **1**, 103–112.

Budd, W., and D. Jenssen, 1989: The dynamics of the Antarctic Ice Sheet, *Annals of Glaciology*, **12**, 16–21.

———, ———, E. Mavrakis and B. Coutts, 1994: Modelling the Antarctic Ice Sheet changes through time, *Annals of Glaciology*, **20**, 291–297.

Budd, W., D. Jenssen and U. Radok, 1970: The extent of basal melting in Antarctica, *Polarforschung*, **6**(39), 293–306.

———, ——— and ———, 1971: Derived physical characteristics of the Antarctic Ice Sheet, *Interim Reports Series A 120*, , ANARE.

Budd, W., P. Keage and N. Blundy, 1979: Empirical studies of ice sliding, *Journal of Glaciology*, **23**(89), 155–170.

———, and P. Rayner, 1990: Modelling globale ice and climate through the ice ages, *Annals of Glaciology*, **14**, 23–27.

Budd, W., and ———, 1993: Modelling ice sheet and climate changes through the ice ages, in *Ice in the Climate System*, edited by W. Peltier, pp. 293–317,

Springer-Verlag.

———, and I. Smith, 1981: The growth and retreat of ice sheets in response to orbital radiation changes, in *Sea Level, Ice and Climatic Change*, number 131 in IAHS Publ., pp. 369–409.

Budd, W., and ———, 1982: Large-scale numerical modelling of the Antarctic Ice Sheet, *Annals of Glaciology*, **3**, 42–49.

———, and I. Smith, 1985: Glaciers, ice sheets, and sea level: Effect of a co_2-induced climatic change, *Tech. Rep. DOE/ER/60235-1 Dist. Category UC-11*, , United States Department of Energy, Washington, D.C. 20545.

Budd, W., and ———, 1987: Conditions for growth and retreat of the Laurentide Ice Sheet, *Geographie Physique et Quaternaire*, **41(2)**, 279–290.

———, and R. Warner, 1996: A computer scheme for rapid calculations of balance-flux distributions, *Annals of Glaciology*, **23**, 21–27.

Budd, W., and ———, 1998: Modelling the long-term response of the Antarctic Ice Sheet to global warming, *Annals of Glaciology*, **27**, 161–168.

Caldeira, K., and M. Rampino, 1992: Mount Etna CO_2 may affect climate, *Nature*, **355**, 401–402.

Calder, N., 1974: *The Weather Machine*, BBC Publications.

Calov, R., and I. Marsiat, 1998: Simulations of the Northern Hemisphere through the last glacial-interglacial cycle with a vertically integrated and a three-dimensional thermomechanical ice-sheet model coupled to a climate model, *Annals of Glaciology*, **27**, 169–176.

Chappell, J., A. Omura, T. Esat, M. McCulloch, J. Pandolfi, Y. Ota and B. Pillans, 1996: Reconciliation of late Quaternary sea levels derived from coral terraces at Huon Peninsula with deep sea oxygen isotope records, *Earth Planet. Sci. Letters*, **141**(1-4), 227–236.

———, and N. Shackleton, 1986: Oxygen isotopes and sea level, *Nature*, **324**, 137–140.

Chappellaz, J., J. Barnola, D. Raynaud, Y. Korotkevich and C. Lorius, 1990: Ice-core record of atmospheric methane over the past 160,000 years, *Nature*, **345**, 127–131.

Charles, C., and R. Fairbanks, 1992: Evidence from Southern Ocean sediments for the effect of North Atlantic deep-water flux on climate, *Nature*, **355**, 416–419.

———, D. Rind, J. Jouzel, R. Koster and R. Fairbanks, 1994: Glacial-Interglacial Changes in Moisture Sources for Greenland: Influences on the Ice Core Record of Climate, *Science*, **263**, 508–511.

Chen, B., D. Bromwich, K. Hines and X. Pan, 1995: Simulations of the 1979-88 polar climates by global climate models, *Annals of Glaciology*, **21**, 83–90.

Clark, J., W. Farrell and W. Peltier, 1978: Global changes in postglacial sea-level: a numerical calculation, *Quaternary Research*, **9**, 265–278.

———, M. Hendriks, T. Timmermans, C. Struck and K. Hilverda, 1994: Glacial isostatic deformation of the Great Lakes region, *Geological Society of America Bulletin*, **106**, 19–31.

Clark, P., J. Claque, B. Curry, A. Dreimanus, S. Hicock, G. Miller, G. Berger, N. Eyles, M. Lamothe, B. Miller, R. Mott, R. Oldale, R. Stea, J. Szabo, L. Thorliefson and J.-S. Vincent, 1993: Initiation and development of the Laurentide and Cordilleran Ice Sheets following the last interglacial, *Quaternary Science Reviews*, **12**, 79–114.

CLIMAP, 1976: The surface of the ice-age earth, *Science*, **191**, 1131–1137.

———, 1981: Seasonal reconstructions of the Earth's surface at the last glacial maximum, *Tech. Rep. Map and Chart series MC-36*, , Geological Society of America, Boulder, Colorado.

COHMAP, 1988: Climatic Changes of the Last 18,000 Years: Observations and Model Simulations, *Science*, **241**, 1043–1052.

Coutts, B., 1992: Incorporation of simple thermodynamics into a transient ice sheet model, *Honours thesis*, , Meteorology Department, University of Melbourne.

Croll, J., 1864: On the physical cause of the change of climate during geological epochs, *Philosophical Magazine*, **28**, 121–137.

Crowley, T., 1992: North Atlantic Deep Water cools the southern hemisphere, *Paleoceanography*, **7**(4), 489–497.

———, 1993: Climate change on tectonic time scales, *Tectonophysics*, **222**(3-4), 277–294.

Crowley, T., and G. North, 1991: *Paleoclimatology*, p. 349, Oxford University Press.

Cuffey, K., G. Clow, R. Alley, M. Stuiver, E. Waddington and R. Saltus, 1995: Large Arctic Temperature Change at the Wisconsin-Holocene Glacial Transition, *Science*, **270**, 455–458.

Dansgaard, W., H. Clausen, N. Gundestrup, C. Hammer, S. Johnsen, P. Kristinsdottir and N. Reeh, 1982: A new Greenland deep ice core, *Science*, **218**, 1273–1277.

———, S. Johnsen, H. Clausen, D. Dahl-Jensen, N. Gundestrup, C. Hammer, C. Hvidberg, J. Steffensen, A. Sveinbjörnsdottir, J. Jouzel and G. Bond, 1993: Evidence for general instability of past climate from a 250-kyr ice-core record, *Nature*, **364**, 218–220.

De Angelis, M., N. Barkov and V. Petrov, 1987: Aerosol concentrations over the last climate cycle (160 kyr) from an Antarctic ice core, *Nature*, **325**, 318–321.

Deblonde, G., W. Peltier and W. Hyde, 1992: Simulations of continental ice sheet

growth over the last glacial-interglacial cycle: experiments with a one level seasonal energy balance model including seasonal ice albedo feedback, *Global and Planetary Change*, **6**(1), 37–55.

Denton, G., J. Bockheim, S. Wilson and M. Stuiver, 1989: Late Wisconsin and early Holocene glacial history, Inner Ross Embayment, Antarctica, *Quaternary Research*, **31**, 151–182.

———, and C. Hendy, 1994: Younger Dryas age advance of Franz Josef Glacier in the Southern Alps of New Zealand, *Science*, **264**, 1434–1437.

Denton, G., and T. Hughes, 1981: The Arctic Ice Sheet: An Outrageous Hypothesis, in *The Last Great Ice Sheets*, edited by G. Denton, and T. Hughes, pp. 440–468, Wiley, NY.

———, ——— and W. Karlén, 1986: Global Ice-Sheet System Interlocked by Sea Level, *Quaternary Research*, **26**, 23–26.

Dome-F Ice Core Research Group, 1998: Preliminary investigation of palaeoclimate signals recorded in the ice core from Dome Fuji station, east Dronning Maud Land, Antarctica, *Annals of Glaciology*, **27**, 338–342.

Dong, B., and P. Valdes, 1995: Sensitivity Studies of Northern Hemisphere Glaciation Using an Atmospheric General Circulation Model, *Journal of Climate*, **8**(10), 2471–2496.

Dredge, L., and L. Thorliefson, 1987: The middle-Wisconsinan history of the Laurentide Ice Sheet, *Geographie Physique et Quaternaire*, **41**(2), 215–235.

Drewry, D., 1983: *Antarctica: glaciological and geophysical folio*, Cambridge, University of Cambridge. Scott Polar Research Institute.

———, 1986: *Glacial Geologic Processes*, p. 274, Edward Arnold Ltd, London.

Drewry, D., 1979: Late Wisconsin reconstruction of the Ross Sea region, *Journal of Glaciology*, **24**(90), 231–244.

Dwyer, G., T. Cronin, P. Baker, M. Raymo, J. Buzas and T. Correge, 1995: North Atlantic deepwater temperature change during late Pliocene and late Quaternary climatic cycles, *Science*, **270**(5240), 1347–1351.

Dyke, A., and V. Prest, 1987: Late Wisconsinan and Holocene history of the Laurentide Ice Sheet, *Geographie Physique et Quaternaire*, **41**(2), 237–263.

Eiriksson, J., L. Simonarson, K. Knudsen and P. Kristensen, 1997: Fluctuations of the Weichselian ice sheet in SW Iceland - a glaciomarine sequence from Sudurness, *Quaternary Science Reviews*, **16**(2), 221–240.

Ekberg, M., T. Lowell and R. Stuckenrath, 1993: Late Wisconsin glacial advance and retreat patterns in southwestern Ohio, USA, *Boreas*, **22**(3), 189–203.

Elverhøi, A., W. Fjeldskaar, A. Solheim, M. Nyland-Berg and L. Russwurm, 1993:

The Barents Sea Ice Sheet - A model of its growth and decay during the last ice maximum, *Quaternary Science Reviews*, **12**, 863–873.

Emiliani, C., 1955: Pleistocene temperatures, *J. Geol*, **63**, 538–578.

England, J., 1985: The late Quaternary history of Hall Land, northwest Greenland, *Canadian Journal of Earth Sciences*, **22**(9-12), 1394–1408.

Epstein, S., R. Sharp and A. Gow, 1970: Antarctic Ice Sheet: Stable isotope analyses of Byrd station cores and interhemispheric climate implications, *Science*, **168**, 1570–1572.

Ewing, M., and W. Donn, 1956: A theory of ice ages, *Science*, **123**, 1061–1066.

Eyles, N., 1993: Earth's glacial record and its tectonic setting, *Earth Science Reviews*, **35**, 1–248.

Fabre, A., A. Létreguilly, C. Ritz and A. Mangeney, 1995: Greenland under changing climates: sensitivity experiments with a new three-dimensional ice-sheet model, *Annals of Glaciology*, **21**, 1–7.

Fairbanks, R., 1989: A 17,000-year glacio-eustatic sea level record: Influence of glacial melting rates on Younger Dryas event and deep-ocean circulation, *Nature*, **342**, 637–642.

Fichefet, T., S. Hovine and J.-C. Duplessy, 1994: A model study of the Atlantic thermohaline circulation during the Last Glacial Maximum, *Nature*, **372**(6503), 252–255.

Flint, R., 1971: *Glacial and Quaternary Geology*, Wiley, NY.

Forsström, L., 1996: Comment on "Reflection of Scandinavian Ice Sheet Fluctuations in Norwegian Sea Sediments during the Past 150,000 Years" by Karl-Heinz Baumann, Klas, S. Lackshewitz, Jan Mangerud, Robert F. Spielhagen, Thomas, C. W. Wolf-Welling, Rüdger Henrich and Heidemarie Kassens, *Quaternary Research*, **46**(2), 84–85.

Franzén, L., 1994: Are wetlands the key to the ice-age cycle enigma?, *Ambio*, **23**(4-5), 300–308.

Fulton, R., and V. Prest, 1987: The Laurentide Ice Sheet and its significance, *Geographie Physique et Quaternaire*, **41**(2), 181–186.

Funder, S., C. Hjort and J. Landvik, 1994: The last glacial cycles in East Greenland, an overview, *Boreas*, **23**(4), 283–293.

Gallée, H., J. van Ypersele, T. Fichefet, I. Marsiat, C. Tricot and A. Berger, 1992: Simulations of the Last Glacial Cycle by a Coupled, Sectorially Averaged Climate-Ice Sheet Model 2. Response to Insolation and CO_2 Variations, *Journal of Geophysical Research*, **97**(D14), 15,713–15,740.

———, ———, ———, C. Tricot and A. Berger, 1991: Simulations of the Last Glacial

Cycle by a Coupled, Sectorially Averaged Climate-Ice Sheet Model 1. The Climate Model, *Journal of Geophysical Research*, **96**(D7), 13,139–13,161.

Gallimore, R., and J. Kutzbach, 1996: Role of orbitally induced changes in tundra area in the onset of glaciation, *Nature*, **381**, 503–505.

Gates, W., 1976: The numerical simulation of ice-age climate with a general circulation model, *Journal of the Atmospheric Sciences*, **33**, 1844–1873.

Genthon, C., J. Barnola, D. Raynaud, C. Lorius, J. Jouzel, N. Barkov, Y. Korotkevitch and V. Kotlyakov, 1987: Vostok ice core: Climatic response to CO_2 and orbital forcing changes over the last 2 climatic cycles, *Nature*, **329**, 414–418.

Gibson, J., P. Kållberg, S. Uppala, A. Hernandez, A. Nomura and E. Serrano, 1997: ECMWF Re-Analysis Project Report Series, *Tech. rep.*, , European Centre for Medium-Range Weather Forecasts.

Glen, J., 1955: The creep of polycrystalline ice, *Proc. R. Soc. London*, **A228**(2-4), 519–538.

Goodwin, I., 1995: On the Antarctic contribution to Holocene sea-level, Ph.D. thesis, University of Tasmania.

Gornitz, V., 1995: Monitoring sea level changes, *Climatic Change*, **31**(2-4), 515–544.

Greischer, L., and C. Bentley, 1980: Isostatic equilibrium grounding line between the West Antarctic inland ice sheet and the Ross Ice Shelf, *Nature*, **283**, 651–654.

Greve, R., 1997: Application of a Polythermal Three-Dimensional Ice Sheet Model to the Greenland Ice Sheet: Response to Steady-State and Transient Climate Scenarios, *Journal of Climate*, **10**, 901–918.

———, unpublished: A polythermal Ice-Sheet Model using orthogonal coordinates on the surface of the Earth and its application to northern hemisphere glaciation.

Gribbin, J., 1978: The search for cycles, in *Climatic Change*, pp. 139–148, Cambridge University Press.

Grosswald, M., 1980: Late Weichselian ice sheet of northern Eurasia, *Quaternary Research*, **13**(1), 1–32.

———, 1988: Antarctic-style ice sheet in the Northern Hemisphere: toward the new global glacial theory, *Data of Glaciological Studies 63*, pp. 3–25, USSR Academy of Science.

Grosswald, M., 1993: Extent and melting history of the late Weichselian ice sheet, the Barents-Kara continental margin, in *Ice in the Climate System*, edited by W. Peltier, pp. 1–20, Springer-Verlag.

———, and T. Hughes, 1995: Paleoglaciology's grand unsolved problem, *Journal of Glaciology*, **41**(138), 313–332.

Guiot, J., A. Pons, J. de Beaulieu and M. Reille, 1989: A 140,000-year continental climate reconstruction from two European pollen records, *Nature*, pp. 309–313.

Hall, N., P. Valdes and B. Dong, 1996: The Maintenance of the Last Great Ice Sheets: A UGAMP GCM Study, *Journal of Climate*, **9**(5), 1004–1019.

Ham, N., and J. Attig, 1996: Ice wastage and landscape evolution along the southern margin of the Laurentide Ice Sheet, north-central Wisconsin, *Boreas*, **25**(3), 171–186.

Harmon, R., L. Land, R. Mitterer, P. Garrett, H. Schwarcz and G. Larson, 1981: Bermuda sea level during the last interglacial, *Nature*, **289**, 481–483.

Harrison, S., J. Kutzbach, I. Prentice, P. Behling and M. Sykes, 1995: The response of northern hemisphere extratropical climate and vegetation to orbitally induced changes in insolation during the last interglaciation, *Quaternary Research*, **43**, 174–184.

Harvey, L., 1988: Climatic impact of ice-age aerosols, *Nature*, **334**, 333–335.

Hays, J., J. Imbrie and N. Shackleton, 1976: Variations in the Earth's Orbit: Pacemaker of the Ice Ages, *Science*, **194 (4270)**, 1121–1132.

Hebbeln, D., T. Dokken, E. Andersen, M. Hald and A. Elveroi, 1994: Moisture supply for northern ice-sheet growth during the last glacial maximum, *Nature*, **370**(6488), 357–360.

Heinze, C., E. Maier-Reimer and K. Winn, 1991: Glacial pCO_2 reduction by the world ocean - experiments with the Hamburg carbon cycle model, *Paleoceanography*, **6**, 395–430.

Hemleben, C., D. Meischner, R. Zahn, A. Almogilabin, H. Erlenkeuser and B. Hiller, 1996: Three hundred eightythousand year long stable isotope and faunal records from the Red Sea - Influence of global sea level on hydrography, *Paleoceanography*, **11**(2), 147–156.

Hoffert, M., and C. Covey, 1992: Deriving global sensitivity from palaeoclimate, *Nature*, **360**, 573–576.

Honda, M., K. Yamazaki, Y. Tachibana and K. Takeuchi, 1996: Influence of Okhotsk sea-ice extent on atmospheric circulation, *Geophysical Research Letters*, **23**(24), 3595–3598.

Hostetler, S., and P. Clark, 1997: Climatic controls of western U.S. glaciers at the last glacial maximum, *Quaternary Science Reviews*, **16**(6), 505–511.

Houghton, H., 1985: *Physical Meteorology*, MIT, Cambridge, MA.

Houghton, J., L. Meira Filho, B. Callander, N. Harris, A. Kattenberg, and K. Maskell (eds.), 1996: *Climate Change 1995, The Science of Climate Change*, Cambridge University Press.

Hughes, B., and T. HughesTransgressions: Rethinking Beringian glaciation, *Palaeogeography, Palaeoclimatology, Palaeoecology.*

Hughes, T., 1996: Can ice sheets trigger abrupt climatic change?, *Arctic and Alpine Research*, **28**(4), 448–465.

———, G. Denton and M. Grosswald, 1977: Was there a late Würm Arctic Ice Sheet?, *Nature*, **266**, 596–602.

Hughes, T., 1998: *Ice Sheets*, p. 343, Oxford University Press, NY.

———, ———, B. Andersen, D. Schilling, J. Fastook and C. Lingle, 1981: The Last Great Ice Sheets: A Global View, in *The Last Great Ice Sheets*, edited by G. Denton, and T. Hughes, pp. 275–317, Wiley, NY.

Hutter, K., 1983: *Theoretical Glaciology*, p. 510, D. Reidel (Dordrecht).

Huybrechts, P., 1990: The Antarctic Ice Sheet during the last glacial-interglacial cycle: A three-dimensional experiment, *Annals of Glaciology*, **14**, 115–119.

———, 1992: The Antarctic Ice Sheet and environmental change: a three-dimensional modelling study, *Reports on Polar Research 99*, , Alfred Wegner Institute for Polar and Marine Research.

Huybrechts, P., 1994: The present evolution of the Greenland Ice Sheet: an assessment by modelling, *Global and Planetary Change*, **9**, 39–51.

———, and S. T'siobbel, 1995: Thermomechanical modelling of the Northern Hemisphere ice sheets with a two-level mass-balance parameterization, *Annals of Glaciology*, **21**, 111–116.

Imbrie, J., E. Boyle, S. Clemens, A. Duffy, W. Howard, G. Kukla, D. Kutzbach, D. Martinson, A. McIntyre, A. Mix, B. Molfino, J. Morley, L. Peterson, N. Pisias, W. Prell, , M. Raymo, N. Shackleton and J. Toggweiler, 1992: On the Structure and Origin of Major Glaciation Cycles 1. Linear Responses to Milankovitch Forcing, *Paleoceanography*, **7**(6), 701–738.

———, ———, ———, A. Duffy, W. Howard, G. Kukla, D. Kutzbach, D. Martinson, A. McIntyre, A. Mix, B. Molfino, J. Morley, L. Peterson, N. Pisias, W. Prell, , M. Raymo, N. Shackleton and J. Toggweiler, 1993: On the Structure and Origin of Major Glaciation Cycles 2. The 100,000-year cycle, *Paleoceanography*, **8**(6), 699–735.

Imbrie, J., and J. Imbrie, 1980: Modelling the Climatic Response to Orbital Variations, *Science*, **207**, 943–953.

———, and K. Imbrie, 1979: *Ice Ages: Solving the mystery*, Enslow Publishers, Hillside, NJ.

Imbrie, J., H. J.D., D. Martinson, A. McIntyre, A. Mix, J. Morley, N. Pisias, W. Prell and N. Shackleton, 1984: The orbital theory of Pleistocene climate: Support from

a revised chronology of the marine δO^{18} record, in *Milankovitch and Climate*, edited by A. Berger, J.Imbrie, J.Hays, G.Kukla, and B.Saltzman, pp. 269–305, D.Riedel, Hingham, Mass.

Ingólfsson, O., C. Hjort, P. Berkman, S. Björck, E. Colhoun, I. Goodwin, B. Hall, K. Hirakawa, M. Melles, P. Möller and M. Prentice, 1998: Antarctic glacial history since the last glacial maximum: an overview of the record on land, *Antarctic Science*, **10**(3), 326–344.

Ives, J., J. Andrews and R. Barry, 1975: Growth and decay of the Laurentide Ice Sheet and comparisons with Fenno-Scandinavia, *Naturwissenschaften*, **62**, 118–125.

Jaeger, L., 1976: Monatskarten des Niederschlags für die ganze Erde, *Ber. Deutschen Wetterdienstes 139*, p. 38.

Jenssen, M., and U. Radok, 1961: Transient temperature distributions in ice caps and ice shelves, in *IUGG. IASH Symposium of Helsinki*, p. 112.

Jezek, K., R. Alley and R. Thomas, 1989: Rheology of glacier ice, *Science*, **227**(4692), 1335–1337.

Jones, G., K. Elder and A. Gagnon, 1994: The use of AMS ^{14}C dating to solve the central Arctic Ocean chronology problem, *EOS*, **75**, 198.

Joussaume, S., 1993: Paleoclimatic tracers: An investigation using an atmospheric GCM under ice age conditions, *Journal of Geophysical Research*, **98**(D2), 2767–2805.

Jouzel, J., C. Lorius, J. Petit, C. Genthon, N. Barkov, V. Kotlyakov and V. Petrov, 1987: Vostok ice core: A continuous isotope temperature record over the last climatic cycle (160,000 years), *Nature*, **329**, 403–408.

Kamb, B., and E. LaChappelle, 1964: Direct observation of the mechanism of glacier sliding over bedrock, *Journal of Glaciology*, **5**(38), 145–158.

Kapsner, W., R. Alley, C. Shuman, S. Anandakrishnan and P. Grootes, 1995: Dominant influence of atmospheric circulation on snow accumulation in Greenland over the past 18,000 years, *Nature*, **373**, 52–54.

Keffer, T., D. Martinson and B. Corliss, 1988: The position of the Gulf Stream during Quaternary glaciations, *Science*, **241**, 440–442.

Kennett, J., 1977: Cenozoic evolution of Antarctic glaciation, the circum-Antarctic ocean and their impact on global palaeoceanography, *Journal of Geophysical Research*, **82**(27), 3843–3860.

———, 1982: *Marine Geology*, p. 812, Prentice-Hall, Englewood Cliffs.

Kennett, J., and R. Thunell, 1975: Global increase in Quaternary explosive volcanism, *Science*, **187**, 497–503.

Kheshgi, H., and A. Lapenis, 1996: Estimating the accuracy of Russian

paleotemperature reconstructions, *Palaeogeogr. Palaeoclim. Palaeoecol.*, **121**, 221–237.

King, K., and J. Turner, 1997: *Antarctic Meteorology and Climatology*, p. 410, Cambridge University Press, Cambridge.

Klein, J., J. Lerman, P. Damon and E. Ralph, 1982: Calibration of radiocarbon dates, *Radiocarbon*, **24**, 103–150.

Koerner, R., 1989: Ice Core Evidence for Extensive Melting of the Greenland Ice Sheets in the Last Interglacial, *Science*, **244**, 964–968.

Krishnamurthy, R., K. Syrup, M. Baskaran and A. Long, 1995: Late Glacial Climate Recordof Midwestern United States from the Hydrogen Isotope Ratio of Lake Organic Matter, *Science*, **269**, 1565–1567.

Kutzbach, J., and P. Guetter, 1986: The influence of changing orbital parameters and surface boundary conditions on climate simulations for the past 18,000 years, *Journal of the Atmospheric Sciences*, **43**, 1726–1759.

Lambeck, K., 1993: , *Geophysical Journal International*, **115**(3), 960–990.

———, 1995: Constraints on the late Weichselian ice sheet over the Barents Sea from observations of raised shorelines, *Quaternary Science Reviews*, **14**, 1–16.

Lambeck, K., 1997: Sea-level change along the French Atlantic and channel coasts since the time of the Last Glacial Maximum, *Palaeogeogr. Palaeoclim. Palaeoecol.*, **129**(1-2), 1–22.

Larsen, E., and J. Mangerud, 1981: Erosion rate of a Younger Dryas cirque glacier at Kråkenes, western Norway, *Annals of Glaciology*, **2**, 153–158.

Le Meur, E., and P. Huybrechts, 1996: A comparison of different ways of dealing with isostasy: examples from modelling the Antarctic Ice Sheet during the last glacial cycle, *Annals of Glaciology*, **23**, 309–317.

Ledley, T., and S. Chu, 1995: The initiation of ice sheet growth, Milankovitch solar radiation variations and the 100ky ice age cycle, *Climate Dynamics*, **11**, 439–445.

Lee, W., 1970: On the global variations of terrestrial heat flow, *Physics of the Earth and Planetary Interior*, **2**(5), 332–341.

Lehman, S., G. Jones, L. Keigwin, E. Andersen, G. Butenko and S.-R. Østmo, 1991: Initiation of Fennoscandian ice-sheet retreat during the last deglaciation, *Nature*, **349**, 513–516.

———, and L. Keigwin, 1992: Sudden changes in North Atlantic circulation during the last deglaciation, *Nature*, **356**, 757–762.

Lestringant, R., 1994: A two-dimensional finite-element study of flow in the transition zone between an ice sheet and an ice shelf, *Annals of Glaciology*, **20**, 67–72.

Letréguilly, A., N. Reeh and P. Huybrechts, 1991: The Greenland Ice Sheet through the last glacial-interglacial cycle, *Global and Planetary Change*, **4**, 385–394.

———, and C. Ritz, 1993: Modelling of the Fennoscandian Ice Sheet, in *Ice in the Climate System*, edited by W. Peltier, pp. 21–46, Springer-Verlag.

Levesque, A., L. Cwynar and I. Walker, 1997: Exceptionally steep north-south gradients in lake temperatures during the last deglaciation, *Nature*, **385**, 423–426.

Licht, K., J. Jennings and K. Williams, 1996: Chronology of the Late Wisconsin ice retreat from the Western Ross Sea, Antarctica, *Geology*, **24**(3), 223–226.

Lindstrom, D., 1990: The Eurasian ice sheet formation and collapse resulting from natural atmospheric CO_2 concentration variations, *Paleoceanography*, **5**(2), 207–227.

———, and D. MacAyeal, 1989: Scandinavian, Siberian, and Arctic Ocean glaciation: Effect of Holocene atmospheric CO_2 variations, *Science*, **245**, 628–631.

Liu, X., T. Rolph, J. Bloemendal, J. Shaw and T. Liu, 1995: Quantitative estimates of palaeoprecipitation at Xifeng, in the Loess Plateau of China, *Palaeogeogr. Palaeoclim. Palaeoecol.*, **113**(2-4), 243–248.

Lliboutry, L., 1963: Regime thermique et deformation de la base des calottes polaires, *Annales de Geophysique*, **19**(2), 149–156.

———, 1965: *Traité de Glaciologie*, vol. 2, p. 1040, Masson, Paris.

Lorius, C., J. Jouzel, D. Raynaud, J. Hansen and H. Le Treut, 1990: The ice-core record: climate sensitivity and future greenhouse warming, *Nature*, **347**, 139–145.

———, ———, C. Ritz, L. Merlivat, Y. Barkov, N.I. Koretkevich and V. Kotlyakov, 1985: A 150,000-year climatic record from Antarctic ice, *Nature*, **316**, 139–145.

Lorius, C., G. Raisbeck, J. Jouzel and D. Raynaud, 1989: Long-term Environmental Records from Antarctic Ice Cores, in *The Environmental Record in Glaciers and Ice Sheets*, edited by H. Oeschger, and C. Langway, pp. 343–361, Wiley, NY.

Lowell, T., C. Heusser, B. Anderson, P. Moreno, A. Hauser, L. Heusser, C. Schlüchter, D. Marchant and G. Denton, 1995: Interhemispheric Correlation of Late Pleistocene Glacial Events, *Science*, **269**, 1541–1549.

MacAyeal, D., 1994: Lessons in Ice-Sheet Modelling, Department of Geophysical Sciences, University of Chicago, Chicago Illinois.

Manabe, S., 1989: Studies of Glacial Climates by Coupled Atmosphere-Ocean Models: How Useful Are Coupled Models?, in *Global Changes of the Past*, pp. 421–448.

———, and A. Broccoli, 1985: The influence of continental ice sheets on the climate of an ice age, *Journal of Geophysical Research*, **90**(D1), 2167–2190.

Manabe, S., and K. Bryan, 1985: CO_2-Induced Change in a Coupled

Ocean-Amosphere Model and Its Paleoclimatic Implications, *Journal of Geophysical Research*, **90**, 11,689–11,707.

———, and R. Stouffer, 1997: Coupled ocean-atmosphere model response to freshwater input: Comparison to Younger Dryas event, *Paleoceanography*, **12**(2), 321–336.

Mangerud, J., 1991: The Last Interglacial/Glacial Cycle in Northern Europe, in *Quaternary Landscapes*, edited by L. Shane, and E. Cushing, pp. 38–77, Belhaven Press, London.

Markussen, B., R. Zahn and J. Thiede, 1985: Late Quaternary sedimentation in the eastern Arctic Basin: Stratigraphy and depositional environment, *Palaeogeogr. Palaeoclim. Palaeoecol.*, **50**, 271–284.

Marsiat, I., 1995: The waxing and waning of the Northern Hemisphere ice sheets, *Annals of Glaciology*, **21**, 96–102.

Martinson, D., N. Pisias, H. J.D., J. Imbrie, T. Moore and N. Shackleton, 1987: Age dating and teh orbital theory of the ice ages: Development of a high-resolution 0 to 300,000-year chronostratigraphy, *Quaternary Research*, **27**, 1–30.

Matteucci, G., 1993: Multiple Equilibria in a Zonal Energy Balance Climate Model: The Thin Ice Cap Instability, *Journal of Geophysical Research*, **98**(D10), 18,515–18,526.

Mavrakis, E., 1989: Derived physical characteristics of the Wilkes-Vostok region, *Honours thesis*, , Meteorology Department, University of Melbourne.

———, 1992: Time dependent, three dimensional, modelling of the dynamics and thermodynamics of large ice masses, Master's thesis, Meteorology Department, University of Melbourne.

Mayewski, P., G. Denton and T. Hughes, 1981: Late Wisconsin Ice Sheets in North America, in *The Last Great Ice Sheets*, edited by G. Denton, and T. Hughes, pp. 67–178, Wiley, NY.

———, M. Twickler, S. Whitlow, L. Meeker, Q. Yang, J. Thomas, K. Kreutz, P. Grootes, D. Morse, E. Steig, E. Waddington, E. Saltzman, P.-Y. Whung and K. Taylor, 1996: Climate Change During the Last Deglaciation in Antarctica, *Science*, **272**, 1636–1638.

McCrea, W., 1975: Ice ages and the galaxy, *Nature*, **255**, 607–609.

McInnes, B., and W. Budd, 1984: A cross-sectional model for West Antarctica, *Annals of Glaciology*, **5**, 95–99.

Meese, D., A. Gow, P. Grootes, P. Mayewski, M. Ram, M. Stuiver, K. Taylor, E. Waddington and G. Zielinski, 1994: The Accumulation Record from the GISP2 Core as an Indicator of Climate Change Throughout the Holocene, *Science*, **266**, 1680–1682.

Mellor, M., and J. Smith, 1966: Creep of snow and ice, *CRREL Research Report 220*, , U.S. Army.

Mercer, J., 1978: Glacial development and temperature trends in the Antarctic and in South America, in *Antarctic glacial history and world Paleoenvironments*, edited by E. van Zideren Bakker, pp. 73–93, A.A. Balkema (Rotterdam).

Mesolella, K., R. Mathews, W. Broecker and D. Thurber, 1969: The astronomical theory of climate change: Barbados data, *J. Geol*, **77**, 250–274.

Milankovitch, M., 1941: *Canon of Insolation and the Ice Age Problem*, p. 633, Royal Serbian Academy, Belgrade, Translation, Israel Program for Scientific Translation, Jerusalem, 1969.

Mitrovica, J., and W. Peltier, 1991: On postglacial geoid subsidence over the equatorial oceans, *Journal of Geophysical Research*, **96**(B12), 20,053–20,071.

Mix, A., 1987: Hundred-kiloyear cycle queried, *Nature*, **327**, 370.

———, and W. Ruddiman, 1984: Oxygen-isotope analyses and Pleistocene ice volumes, *Quaternary Research*, **21**, 1–20.

Morgan, V., and T. Jacka, 1981: Mass balance studies in East Antarctica, *IAHS*, **131**, 253–260.

Muller, R., 1994: Glacial cycles and orbital inclination, *Tech. Rep. LBL-35665*, , Lawrence Berkeley Laboratory Report.

———, and G. MacDonald, 1997: Glacial Cycles and Astronomical Forcing, *Science*, **277**, 215–218.

Nakada, M., and K. Lambeck, 1988: The melting history of the late Pleistocene Antarctic ice sheet, *Nature*, **333**(6168), 36–40.

Neumann, A., and P. Hearty, 1996: Rapid sea-level changes at the close of the last interglacial (substage 5e) recorded in Bahamian island geology, *Geology*, **24**(9), 775–778.

Newell, R., 1973: Changes in the poleward energy flux by the atmosphere and ocean as a possible cause for ice ages, *Quaternary Research*, **4**, 117–127.

Nikolayev, V., and D. Mikhalev, 1995: An Oxygen-Isotope Paleothermometer from Ice in Siberian Permafrost, *Quaternary Research*, **43**(2), 14–21.

Nisbet, E., 1990: The end of the ice age, *Canadian Journal of Earth Sciences*, **27**, 148–157.

North, G., J. Mengel and D. Short, 1983: Simple Energy Balance Model Resolving the Seasons and the Continents: Applications to the Astronomical Theory of the Ice Ages, *Journal of Geophysical Research*, **88**(C11), 6576–6586.

Oerlemans, J., 1982: A model of the Antarctic Ice Sheet, *Nature*, **297**, 550–554.

Olsen, P., 1986: A 40-million-year lake record of early mesozoic orbital climate forcing, *Science*, **234**, 842–848.

Paillard, D., 1998: The timing of Pleistocene glaciations from a simple multiple-state climate model, *Nature*, **391**, 378–381.

Paterson, W., 1981: *The Physics of Glaciers, 2nd edition*, Pergamon.

———, 1994: *The Physics of Glaciers, 3rd edition*, p. 480, Pergamon.

Pearce, F., 1997: Southern oceans hold key to climate, *New Scientist*, **154**, 21.

Peltier, W., 1988: Lithospheric thickness, Antarctic deglaciation history, and ocean basin discretization effects in a global model of postglacial sea level change: A summary of some sources of non-uniqueness, *Quaternary Research*, **29**, 93–112.

———, 1994: Ice age paleotopography, *Science*, **265**, 195–201.

Peltier, W., and W. Hyde, 1984: A model of the ice age cycle, in *Milankovitch and Climate*, edited by A. Berger, J.Imbrie, J.Hays, G.Kukla, and B.Saltzman, pp. 565–580, D.Riedel, Hingham, Mass.

———, and S. Marshall, 1995: Coupled energy-balance/ice-sheet model simulations of the glacial cycle: A possible connection between terminations and terriginous dust, *Journal of Geophysical Research*, **100**(D7), 14,269–14,289.

Peterson, G., T. Webb III, J. Kutzbach, T. van der Hammen, T. Wijmstra and F. Street, 1979: The Continental Record of Environmental Conditions at 18,000 yr B.P.: An Initial Evaluation, *Quaternary Research*, **12**, 47–82.

Phillips, H., 1999: Applications of ERS satellite radar altimetry in the Lambert Glacier - Amery Ice Shelf system, East Antarctica, Ph.D. thesis, University of Tasmania.

Pisias, N., and T. Moore, 1981: The evolution of Pleistocene climate: A time series approach, *Earth Planetary Science Letters*, **52**, 450–458.

Punkari, M., 1995: Glacial flow systems in the zone of confluence between the Scandinavian and Novaya Zemlya Ice Sheets, *Quaternary Science Reviews*, **14**, 589–603.

Radok, U., R. Barry, D. Jenssen, R. Keen, G. Kiladis and B. McInnes, 1982: Climatic and Physical Characteristics of the Greenland Ice Sheet, *Tech. rep.*, , Cooperative Institute for Research in Environmental Sciences, University of Colorado.

———, D. Jenssen and B. McInnes, 1987: On the surging potential of polar ice streams, *Tech. rep.*, , United States Department of Energy.

Rampino, and Self, 1992: Volcanic winter and accelerated glaciation following the Toba super-eruption, *Nature*, **359**, 50–52.

Raymo, M., and W. Ruddiman, 1992: Tectonic forcing of late Cenozoic climate,

Nature, **359**, 117–122.

———, ———, J. Backman, B. Clement and D. Martinson, 1989: Late Pliocene variations in northern hemiephere ice sheets and North Atlantic Deep Water circulation, *Palaeoceanography*, **4**, 413–446.

Raynaud, D., and I. Whillans, 1982: Air content of the Byrd core and past changes in the West Antarctic Ice Sheet, *Annals of Glaciology*, **3**, 269–273.

Rial, J., 1995: On the origin of the long period sawtooth shape of the late Pleistocene paleoclimate records: The first derivative of the earth's orbital eccentricity, *Geophysical Research Letters*, **22(15)**, 1997–2000.

Rind, D., 1986: The dynamics of warm and cold climates, *Journal of the Atmospheric Sciences*, **43**(1), 3–24.

Ritz, C., 1987: Time dependent boundary conditions for calculation of temperature fields in ice sheets, in , number 170 in IAHS Publ., pp. 207–216.

Roush, W., 1997: Upstart ice age theory gets attentive but chilly hearing, *Science*, **277**, 183–184.

Ruddell, A., 1994: Recent glacier and climate change in the New Zealand Alps, Ph.D. thesis, University of Melbourne.

Ruddiman, W., and J.-C. Duplessy, 1985: Conference on the Last Deglaciation: Timing and Mechanisms, *Quaternary Research*, **23**, 1–17.

———, and J. Kutzbach, 1989: Forcing of Late Cenozoic Northern Hemisphere Climate by Plateau Uplift in Southern Asia and the American West, *Journal of Geophysical Research*, **94**(D15), 18,409–18,427.

Ruddiman, W., and A. McIntyre, 1981: Oceanic mechanism for amplification of the 23,000-year ice-volume cycle, *Science*, **212**, 617–627.

———, M. Raymo and A. McIntyre, 1986: Matuyama 41,000 year cycles; North Atlantic Ocean and northern hemisphere ice sheets, *Earth Planet. Sci. Letters*, **80**, 117–129.

Ruddiman, W., ———, D. Martinson, B. Clement and J. Backman, 1989: Pleistocene evloution: Northern hemisphere ice sheets and North Altantic Ocean, *Paleoceanography*, **4**(4), 353–412.

Russell-Head, D., 1980: The melting of free-drifting ice bergs, *Annals of Glaciology*, **1**, 119–122.

Schaferneth, C., and K. Stattegger, 1997: Meltwater pulses in the northern North Atlantic - Retrodiction and forecast by numerical modelling, *Geologische Rundschau*, **86**(2), 492–498.

Schiller, A., U. Mikolajewicz and R. Voss, 1997: The stabillity of the North Atlantic thermohaline circulation in a coupled ocean-atmosphere general circulation model,

Climate Dynamics, **13**, 325–347.

Schneider, S., and S. Thompson, 1979: Ice ages and orbital variations: some simple theory and modeling, *Quaternary Research*, **12**, 188–203.

Sclater, J., C. Jaupart and D. Galson, 1980: The heat flow through oceanic and continental crust and the heat loss of the earth, *Rev. Geophys. Space Phys.*, **18**, 289–311.

Sejrup, H., H. Haflidason, S. Aarseth, E. King, C. Forsberg and D. Long, 1994: Late Weichselian glaciation history of the northern North Sea, *Boreas*, **23**(1), 1–13.

Shabalova, M., 1996: Universal pattern of changes - on what spatial scale?, *Climatic Change*, **35**, 133–135.

Shaffer, G., and J. Bendtsen, 1994: Role of the Bering Strait in controlling North Atlantic ocean circulation and climate, *Nature*, **367**, 354–357.

———, and J. Sarmiento, 1995: Biogeochemical cycling in the global ocean 1. A new, analytical model with continuous vertical resolution and high-latitude dynamics, *Journal of Geophysical Research*, **100**(C2), 2659–2672.

Sharma, M., and L. Owen, 1996: Quaternary glacial history of NW Garwhal, Central Himalayas, *Quaternary Science Reviews*, **15**(4), 335–365.

Shaw, G., 1989: Aerosol transport from sources to ice sheets, in *The Environmental Record in Glaciers and Ice Sheets*, pp. 13–27, Wiley, NY.

Shinn, R., and E. Barron, 1989: Climate sensitivity to continental ice sheet size and configuration, *Journal of Climate*, **2**, 1517–1537.

Shreve, R., 1984: Glacier sliding at subfreezing temperatures, *Journal of Glaciology*, **30**(106), 341–347.

Siegert, M., and J. Dowdeswell, 1995: Numerical modelling of the Late Weichselian Svalbard Barents Sea Ice Sheet, *Quaternary Research*, **43**, 1–13.

Sigmundsson, F., 1991: Post-glacial rebound and aesthenosphere viscosity in Iceland, *Geophysical Research Letters*, **18**, 1131,1134.

Simmonds, I., G. Trigg and R. Law, 1988: The Climatology of the Melbourne University General Circulation Model, *Department of Meteorology Publication 31*, , The University of Melbourne.

Smith, I., 1984: Numerical modelling of ice masses, Ph.D. thesis, University of Melbourne.

———, W. Budd and P. Reid, 1998: Model estimates of Antarctic accumulation rates and their relationship to temperature changes, *Annals of Glaciology*, **27**, 246–250.

Souchez, R., and H. Lorraine, 1991: *Ice Composition and Glacier Dynamics*, Springer-Verlag, Berlin.

St.Onge, D., 1987: The Sangamonian stage and the Laurentide Ice Sheet, *Geographie Physique et Quaternaire*, **41**(2), 189–198.

Stuiver, M., G. Denton, T. Hughes and J. Fastook, 1981: History of the marine ice sheet in West Antarctica during the last glaciation: a working hypothesis, in *The Last Great Ice Sheets*, edited by G. Denton, and T. Hughes, pp. 319–436, Wiley, NY.

Stute, M., J. Clark, P. Schlosser, W. Broecker and G. Bonani, 1995: A 30,000 year Continental Paleotemperature Record Derived from Noble Gases Dissolved in Groundwater from the San Juan Basin, New Mexico, *Quaternary Research*, **43**(2), 209–220.

Suarez, M., and I. Held, 1976: The sensitivity to an energy balance climate model to variations in orbital parameters, *Nature*, **263**, 46–47.

Thomas, R., S. Stephenson, R. Bindschadler, S. Shabtaie and C. Bentley, 1988: Thinning and grounding line retreat on Ross ice shelf, Antarctica, *Annals of Glaciology*, **11**, 165–172.

Toggweiler, J., and B. Samuels, 1992: Is the magnitude of the deep outflow from the Atlantic Ocean actually governed by southern hemisphere winds?, in *The Global Carbon Cycle*, edited by M. Heimann, Springer-Verlag.

Tushingham, A., and W. Peltier, 1991: Ice-3G: A new global model of the Late Pleistocene deglaciation based upon geophysical predictions of post-glacial relative sea level change, *Journal of Geophysical Research*, **96**(B3), 4497–4523.

Vaughan, D., J. Bamber, M. Giovinetto, J. Russell and P. Cooper, in press: Reassessment of net surface mass balance in Antarctica.

Vernekar, A., 1972: Long-period global variations of incoming solar radiation, *Meteorological Monogr.*, **12**, 34pp.

Vincent, J.-S., and V. Prest, 1987: The early Wisconsinan history of the Laurentide Ice Sheet, *Geographie Physique et Quaternaire*, **41**(2), 199–213.

Vogt, P., K. Crane and E. Sundvor, 1994: Deep Pleistocene iceberg plowmarks on the Yermak Plateau - sidescan and 3.5 kHz evidence for thick calving ice fronts and a possible marine ice sheet in the Arctic Ocean, *Geology*, **22**(5), 403–406.

Walcott, R., 1973: Structure of the earth from glacio-isostatic rebound, *Ann. Rev. Earth Plan. Sci.*, **1**, 15–37.

Walin, G., 1985: The thermohaline circulation and the control of ice ages, *Palaeogeogr. Palaeoclim. Palaeoecol.*, **50**, 323–332.

Warner, R., and W. Budd, 1998: Modelling the long-term response of the Antarctic Ice Sheet to global warming, *Annals of Glaciology*, **27**, 161–168.

Warrick, R., and J. Oerlemans, 1990: Sea level rise, in *Climate Change, the IPCC*

Scientific Assessment, edited by J. Houghton, G. Jenkins, and J. Ephraums, pp. 257–282, Cambridge University Press.

Webb, P., D. Harwood, B. McKelvey, J. Mercer and L. Stoff, 1984: Cenozoic marine sedimetation and ice-volume variation on the East Antarctic craton, *Geology*, **12**, 287–291.

Webb, T., P. Bartlein and J. Kutzbach, 1987: Climatic change in eastern North America during the past 18,000 years; Comparisons of pollen data with model results, *The Geology of North America*, **K-3, North America and adjacent oceans during the last deglaciation**, 447–462.

———, T. Crowley, B. Frenzel, A.-K. Gliemeroth, J. Jouzel, L. Labetyrie, I. Prentice, D. Rind, W. Ruddiman, M. Sarntheim and A. Zwink, 1993: Group report: use of paleoclimatic data as analogs for understanding future global changes, in *Global Change and the Perspective of the Past*, pp. 50–71, Wiley, NY.

Weertman, J., 1957: On the sliding of glaciers, *Journal of Glaciology*, **3**(21), 33–38.

———, 1964: Rate of growth or shrinkage of nonequilibrium ice sheets, *Journal of Glaciology*, **5**, 145–158.

Weertman, J., 1974: Stability of the junction of an ice sheet and an ice shelf, *Journal of Glaciology*, **13**, 3–11.

———, 1976: Milankovitch solar radiation variations and ice age ice sheet sizes, *Nature*, **261**, 17–20.

Weertman, J., 1979: The unsolved glacier sliding problem, *Journal of Glaciology*, **23**(89), 97–115.

Weller, G., 1968: The heat budget and heat transfer processes in Antarctic plateau ice and sea ice, *Scientific Report 102*, , ANARE.

Weyl, P., 1968: The role of the ocean in climatic change: A theory of the ice ages, *Meteorol. Monogr.*, **8**, 37–62.

Wigley, T., and S. Raper, 1992: Implications for climate and sea level of revised IPCC emissions scenarios, *Nature*, **357**, 293–300.

Wingham, D., A. Ridout, R. Scharoo, R. Arthern and C. Shum, 1998: Antarctic elevation change from 1992 to 1996, *Science*, **282**(5388), 456–458.

Wollin, G., W. Ryan and D. Ericson, 1977: Paleoclimate, paleomagnetism and the eccentricity of the Earth's orbit, *Geophyscial Research Letters*, **4**, 267–270.

World Atlas of Snow and Ice Resources, 1997: Russian Academy of Sciences.

Yiou, F., G. Raisbeck, D. Bourles, C. Lorius and N. Barkov, 1985: ^{10}Be in ice at Vostok Antarctica during the last climatic cycle, *Nature*, **316**, 616–617.

Zweck, C., 1997: Coupled Models of Glacial Isostasy and Ice Sheet Dynamics, Ph.D.

thesis, University of Tasmania.

Appendix A

Calculation of basal temperatures

Ice sheets have various sources of heat. Heat may come from the surface or geothermally. Regelation, enhanced plastic flow at the ice base and basal friction are all sources of heat at the ice base. The ice base and indeed the entire ice column can be supplied heat by internal heating resulting from deformation of the ice and from the advection of heat from upstream. The vertical motion of the ice within the column also influences the distribution of heat through the column.

The steady state heat conduction equation may be expressed as (Budd et al. 1971):

$$\frac{\delta\theta}{\delta t} = \kappa\frac{\delta^2\theta}{\delta z^2} - u_z\frac{\delta\theta}{\delta x} - \omega\frac{\delta\theta}{\delta z} + q \qquad \text{(A.1)}$$

where θ is the temperature, t time, κ the thermal diffusivity, u_z the horizontal velocity at depth z, ω the vertical velocity, x the horizontal coordinate and q represents the effects of internal heating.

The second and third terms on the right hand side of A.1 represent the horizontal and vertical advection of heat in the ice. Temperature becomes especially dependent on the horizontal velocity when the vertical velocity is calculated as a function of horizontal velocity as it should be. Here however, the vertical velocity is determined by the accumulation and melt rates only. At the surface ω is equal to the accumulation rate P while at the base it is equal to the melt rate M, and it varies linearly between these surface and base values.

Radok et al. (1982) gave a solution of A.1 for basal temperatures:

$$\theta_b = \theta_s + \frac{\gamma_0 D\sqrt{\pi}}{2P\beta} erf\,(P\beta) - \frac{2\epsilon D}{P} H\,(P\beta) \tag{A.2}$$

where θ_b is the basal temperature, θ_s the surface temperature, γ_0 the base temperature gradient, ϵ the warming due to internal heating and advection, D the ice thickness, and erf and H are the error function and the integral of Dawson's integral respectively. These can be modelled to a high degree of accuracy through the use of simple polynomial expressions (Mavrakis 1989). The value of β is given by:

$$\beta = \sqrt{\frac{D}{2\kappa\,(P+M)}} \tag{A.3}$$

Surface temperature is required to satisfy A.2. Surface temperature is here considered to be a function of position in that it is calculated from a theoretical mean sea level temperature as well as being a function of elevation. Assuming a standard atmospheric lapse rate of $\gamma = -6.5°/100m$, new surface temperatures can be calculated as the ice grows or thins:

$$\theta_s = \theta_{msl} + \gamma E_s \tag{A.4}$$

where θ_s and E_s are the surface temperature and elevation and θ_{msl} is the theoretical temperature at mean sea level. Mean sea level temperatures have been calculated from present surface temperatures and applying the above lapse rate.

A.1 Basal temperature gradient

The basal temperature gradient is considered here to be determined by the geothermal heat flux and the heat generated by basal sliding, and was expressed by Budd et al. (1970) as:

$$\gamma_0 = \Gamma_g + \frac{\tau_b u}{JK} \tag{A.5}$$

where Γ_g is the geothermal temperature gradient, τ_b the basal shear stress, u the horizontal velocity, J the mechanical equivalent of heat and K the thermal

conductivity. The geothermal temperature gradient is defined by the geothermal heat flux G, described by Budd et al. (1971) as:

$$\Gamma_g = \frac{G}{K} \tag{A.6}$$

There is large uncertainty in the value of the geothermal heat flux in Antarctica. Estimates have been made based on the geological structure of the continent (Lee 1970; Sclater et al. 1980), and based on these investigations a value of $G = 1.78 J.m^{-2}.a^{-1}$ appears broadly representative of the geological structure in Antarctica, although it is recognised that this probably varies throughout the continent, particularly from East Antarctica (a typical Precambrian shield) and West Antarctica (a product of mountain building since Cambrian times). Basal temperatures are sensitive to the value of the geothermal heat flux which is poorly known however and it is estimated that if a value of G 20% greater than the value employed here were applied it would be enough to produce basal melting throughout the Antarctic Ice Sheet (Coutts 1992). Uncertainty in the value of G has led some to question the effectiveness of thermodynamics in ice sheet models in comparison to simpler, non-thermodynamic models (Calov and Marsiat 1998).

Using $\tau_b = \rho g D \alpha$, Jenssen (unpublished) made an approximation of the influence of sliding on the geothermal temperature gradient so that the basal temperature gradient becomes:

$$\gamma_0 = \Gamma_g + 0.0127 \alpha D u \tag{A.7}$$

As the ice flow in the model is columnar, advective warming need only be calculated once at each grid point. Budd et al. (1971) showed that horizontal advection, internal heating and surface warming may be simply approximated by:

$$\epsilon = u \alpha \gamma \tag{A.8}$$

where α is the surface slope and γ is the standard atmospheric lapse rate used in A.4.

Significant assumptions and approximations have been made in this approach to solving the heat conduction equation. Any inaccuracy in the calculated velocities these may cause however, is minimised by the nature of the way the temperature dependent velocities are calculated. As the value of ν in 4.22 is only 0.1, the effect of basal temperature errors is greatly diminished and a base temperature error of 10°C may only affect the calculated velocity by less than 5%.

Regardless, comparison of fully thermodynamic steady state basal temperatures for the Antarctic with those produced by the above approach Coutts (1992) found that the method described here gives a good approximation of the more rigorous approach to the calculation of steady state basal temperatures (as described by Mavrakis (1992)).

Appendix B

A picture by Mateus

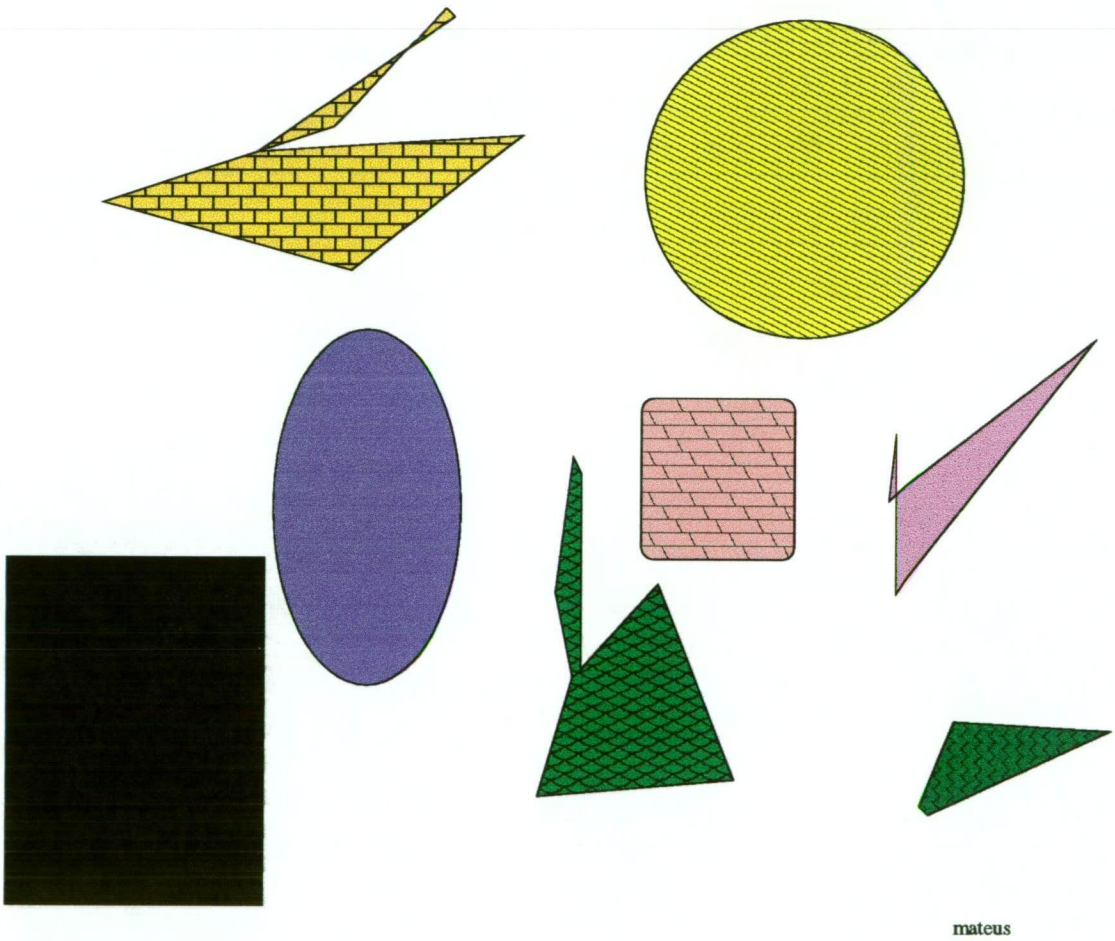

Appendix C

A dream I once had

This one was about a young boy who lived with his father in a sort of old world town. The father was a cobbler, but he was more than that - he was a shoe making genius. When he made a shoe, he made it for the sake of the shoe. Each cut, each stitch, every tap of the hammer was made with absolute focus. The smallest task he performed as if that were all that mattered but somehow a shoe would gradually come into existence and when the final stitch had been sewn, the old cobbler would stand back from it and realise that he had made a shoe. And then he would remember that that is what he had been doing all along. And even though he had made thousands of shoes, at the completion of each one he would have the same reaction and he would smile to himself and his extreme absent mindedness that even as he made a shoe he would forget he was doing so.

Anyway, the thing was these shoes were absolutely fantastic. They fitted like they were a part of your foot that you'd been missing all your life, and they lasted so long that often they outlived their owners. And as the old cobbler asked only a reasonable price for his shoes, he didn't exactly make a shitload of money and he and his son lived in a very modest home attached to his workshop. But the old cobbler was happy. He had all he needed - his son, a roof over their heads and enough money to feed them, with a little left over for small indulgences and occasional outings into the countryside.

In an abridged form, the story went that there was another guy in the town who was incredibly rich and successful and who had perhaps grown up with the cobbler and who originally had been a shoe maker too and who, despite all his worldly riches, success, and the respect of the community, was consumed

with jealousy at the simple contentedness of the old cobbler with his son, and also by the quality of the shoes the old cobbler made. He just couldn't cope with it. I think his jealousy went berserk and he ends up having the old cobbler killed and takes the boy. But that wasn't enough for him and he realised that to kill the old cobbler had been a mistake because there was no further focus for his vengence - or was there? Of course there was still the boy who he now had completely under his 'protection' (control). So he started toying with the son, who had been of course apprentice to his father, and asked what his father has taught him. Until then the son had just been getting to know his stuff and had just been making nails and thread and softening leather - but all this had been done to incredible extents so that his understanding of the tools and stuff of the trade would become inuititively part of him. So he tells the evil guy what he had been doing and the evil guy thinks about it for a while and decides to take it to a new level and makes the boy start licking his boots, ostensibly because that would give the boy a greater understanding of the boots but of course all he really wanted to do was degrade the boy who represented all the failure he saw in himself. And so it went so that the boy was licking dog shit off his boots and eventually he didn't worry with the boots at all - he would just summon the boy to him, crap on the floor and make the boy kneel there and eat it up. In the dream the evil guys pinnacle of 'success' was sitting there and watching, while the boy ate up a pile of shit. In those moments he approached being at ease with himself and seemed sooo close to being completely content.

But increasingly the rest of his life was devalued and all his work, position and wealth meant less and less to him and more and more frequently he would call the boy to him to satisfy what was becoming his only and all consuming need. If he went out, he would surely see someone wearing a pair of the old cobblers boots and he would rush back home and take a hit. But sometimes it still wasn't enough and he would have to make the boy do it twice or add further degradation to the ritual.

And so it went, oh, but - fuck there was so much to this dream that I can't really get it all down here - it also happened that the boy became obsessed with the tasks he was set and he would try harder and harder to satisfy his new father. He didn't actually enjoy eating piles of turd but he really NEEDED the

approval of the evil guy and his life was governed by a constant awareness of not giving enough; of never being able to quite satisfy this being that had become his entire source of self image or whatever. Sometimes when he ate up that shit like he was loving it, and he picked it up in his hands and wiped it all over his body, the evil guy would seem almost at peace and the boy would be similarly close to that sense of achievement that he seemed to be forever closing in on but not quite reaching - this time. But maybe next time....But anyway, thats how intertwined the evil guy and the boys obsessions were. Two sides of the same coin and getting stronger and stronger the more they tried to appease them. Their souls demanded something and they both believed that the boys complete, perfect debasement would bring satisfaction - if only it could be achieved.

So - then one day, a guy comes to see the boy. This guy had worn out some shoes that the old cobbler had made and just hadn't been able to lower his standards to the other shoes that were available and so he hunted down the old cobblers son and apprentice. He persuaded the boy to make him another pair of shoes and he would sneak in the materials the boy needed. The boy began slowly, his skill had never matured and had faded since his shoemaking lessons had been replaced by the powerful but difficult apprenticeship he had undertaken with the evil guy. But it came back to him and began to improve and his client was patient because he knew this was his only chance of getting another pair of shoes. So, he built on his shoemaking knowledge and all he could remember of his father but there came a point when this wasn't enough - to complete the shoes the boy had to take some risks and develop techniques he had never seen. He ruined many shoes this way. And sometimes he was extremely discouraged and came to the brink of depair. But somehow the patient client would be there, and say 'Don't make the shoes for me. Make them for yourself and when you are happy with them you will happily give them to me.' And he would calmly draw the boy back from the brink (where all in front of him was as dark as the Hobart rivulet in the middle of the night and he would be looking everywhere for the right path, but all there was was the complete darkness of infinite possibility), and draw him back, and draw him back....to the shoe. And the boy would start again.

And all this time the shit eating continued. Sometimes, when the boy was fresh from a failed shoe all would go well and the boy would perform with renewed vigour. But gradually, he came to need it less and less. Where once the call to his master filled him with expectation and he would rush there to satisfy their needs, the feeling became bittersweet and eventually he was filled with loathing when THAT knock at the door came. But strangely, the less and less ardent he became the more and more frequent and frenzied became his masters demands. And also strange was that though increasingly he feared those encounters and they became more and more sickening to him - he was becoming happier. Conversely, increasing doses could not drive away a terrible, underlying and growing distress in the evil guy.

But, do you know what? I don't know how it finished. I imagine the boy made a pair of shoes that was at once similiar and different to those his father had made but which, in terms of quality, suffered nothing in comparison. I think he would have held them proudly for a minute and happily given them over to his client who he would not have seen again. He would have left the care of his master and gone elsewhere, probably to make shoes of astonishing quality. His master, become slave - I just don't know how it turned out for him.